Aus dem
Institut für Anatomie und Zellbiologie III der Universität Heidelberg
Abteilung Neuroanatomie
Abteilungsleiter Prof. Dr. med. Thomas Skutella

über

Combination of Prox1/NeuroD1 Transcription Factor Overexpression Boosts Generation of Dentate Gyrus Granule Neurons from Pluripotent Stem Cells

Inauguraldissertation
zur Erlangung des medizinischen Doktorgrades

Dr. sc. hum.

an der
Medizinischen Fakultät Heidelberg
der Ruprecht-Karls-Universität
vorgelegt von

Maryam Hatami

aus

Teheran, Iran

2017

Dekan: Prof. Dr. med. Wolfgang Herzog
Doktorvater: Prof. Dr. med. Thomas Skutella

Contents

The List of Abbreviations 6
1. Introduction 10
1.1 Stem Cells 10
1.2 Embryonic and reprogrammed stem cells 11
1.3 Development of the DG: Molecular Mechanism, Transcription factors, Growth factors .. 13
1.4 Aims of this study 28
2. Materials and Methods 30
2.1 Technical Equipment 30
2.1.1 Instruments 31
2.1.2 Software 32
2.2 The Culture Media 33
2.2.1 Bacterial Culture Medium 33
2.2.2 Cell Culture Reagents and Material 33
2.2.3 Cell Lines and Primary Cell Culture Stocks 37
2.2.3.1 Media and Solutions 37
2.2.3.1.1 Cell Culture medium 37
2.2.3.1.1.1 Mouse Embryonic Fibroblast Medium 37
2.2.3.1.1.2 Mouse Embryonic Stem Cell Culture Medium 38
2.2.3.1.1.3 Freezing Medium for Manipulated Mouse ES Cell Clones 39
2.2.3.1.1.4 HEK293 NT Medium 39
2.2.3.1.1.5 Differentiation medium I 39
2.2.3.1.1.6 Differentiation medium II 40
2.2.3.1.1.7 Differentiation medium III 40
2.2.3.1.1.8 Astrocyte Medium 41
2.2.3.1.1.9 Astrocyte Freezing Medium 41
2.2.3.1.1.10 Immunocytochemistry Reagents 42
2.2.3.1.1.11 Buffers 42
2.2.3.1.1.12 Enzymes, Buffers, Kits and Transfection Reagents 43
2.3 Methods 44
2.3.1 Molecular Biological Approaches 44
2.3.1.1 Bacterial Plasmids 44
2.3.1.2 Isolation of Plasmid DNA (Plasmid Mini Preparation) 45
2.3.1.3 DNA Concentration Measurement 45

2.3.1.4 Plasmid Construct and Restriction Enzyme Digestion 47
2.3.1.5 Cloning of the Emx2 and Prox1-fragments into Tet-O-FUW-vector 50
2.3.1.6 Bacterial Transformation 51
2.3.1.7 DNA Sequencing 52
2.3.1.8 Gene Sequencing Allignment Data 54
2.3.1.9 Plasmid Mini & Maxi Preparation 58
2.4 Cell Culture Methods 58
2.4.1 Lentivirus Preparation, Titration and Usage 58
2.4.1.1 Lentiviral Plasmids and Packaging Constructs 58
2.4.1.2 HEK293 TN Cell Transfection 62
2.4.1.3 Determining Pseudo-viral Titration by Realtime PCR 63
2.4.1.4 Functional Titration 65
2.4.2 Mouse Feeder Embryonic Cells 69
2.4.2.1 MEF derivation and irradiation 69
2.4.2.1.1 Genotyping by X-gal staining 70
2.4.2.1.2 Mycoplasma Detection 71
2.4.2.1.3 Templates for PCR Analysis 71
2.4.2.1.4 Antibiotic Selection in mouse ESC Line 72
2.4.2.1.5 WST-1 Assay 73
2.4.3 ESC transduction 73
2.4.3.1 Transduction 74
2.4.3.1.1 Picking up 75
2.4.3.1.2 Clone Maintenance/Selection 75
2.4.3.1.3 Cryopreservation of Lt-Tet-EGFP-transduced ES cell clones 75
2.4.3.1.4 Fluorescence activated cell sorting (FACS) 76
2.4.3.2 Second transduction 78
2.4.3.3 Third transduction: 78
2.4.3.4 PCR: 78
2.4.3.5 Immunocytochemistry 80
2.4.3.6 Pilot studies 80
2.5 Astrocyte primary cell culture 80
2.5.1 The astrocyte freezing process 81
2.6 Differentiation 83
2.6.1 Embryoid body (EB) formation 83

2.6.1.1 Generation of EBs Using AggreWell™: 84
2.6.1.2. Ectodermal Induction: 86
2.6.1.3 Neuroectodermal Induction 86
2.6.1.4 Telencephalon induction 87
2.6.1.6 The full differentiation of DG neurons: 88
2.6.1.7 Immunofluorescence technique 88
2.6.1.8 DG Differentiation of mESCs by transcription factors induction 91
2.7 DNA preparation and PCR analysis 91
2.8 Gene expression analyses by Fluidigm Biomark system 92
3. Results 97
3.1 Preparatory work: 97
3.2 Neuronal Differentiation of Mouse ES Cells via EB Formation 99
3.3 Differentiation of mouse ES cell into DG precursors in a two-step culture method 100
3.3.1 Three-dimensional culture of neuroectodermal and telencephalic induction with growth factors treatment 100
3.3.2 Two dimensional culture of telencephalon progenitor cells astrocyte co-culture system 102
3.4 The hippocampal transcription factor induction and DG differentiation 108
3.5 Overall transcriptional profiling by nano-fluidic real–time PCR 119
4. Discussion 131
5. Summary 140
5.1 Zusammenfassung 142
6. References 144
7. Own Publications 158
8. CURRICULUM VITAE 162
9. ACKNOWLEDGEMENTS 165
10. Appendix 167

The List of Abbreviations

°C	Degree celsius
µm	Micrometer
µM	Micromolar
AA	Ascorbic acid
AD	Alzheimer's Disease
ATCC	American Type Culture Collection
ATP	Adenosine Triphosphate
Amp	Ampicillin
BLBP	Brain lipid binding protein
BMP	Bone morphogenetic protein
BSA	Bovine Serum Albumin
CH	Cortical Hem
ChAt	Choline Acetyltransferase
CMV	Cytomegalovirus
CMV	Cyto Megalo Virus
CNS	Central nervous system
CP	Cortical plate
D, d	Day
DAPI	4', 6-diamidino-2-phenylindole
DCX	Doublecortin
DKK	Dickkopf-related protein
DG	Dentate Gyrus
db-cAMP	Dibutyryl cAMP
DMEM	Dulbecco's Modified Eagle Medium
DMSO	Dimethylsulfoxid
DNA	Desoxyribonucleic acid
DnaseI	Deoxyribonuclease I
DMF	Dimethylformamide
dNTPs	Desoxynucleosid-triphosphate mix
DTT	Dithiotreitol
E	Embryonic day

EB	Embryoid body
E. coli	Escherichia coli
ECM	Extracellular matrix
EDTA	Ethylenediaminetetraacetic acid
EDTANa2	Ethylenediaminetetraacetic Acid, disodium
EGF	Epidermal growth factor
EGFP	Enhanced Green Fluorescent Protein
ELISA	Enzyme Linked Immunosorbent Assay
ESC	Embryonic stem cells
Emx2	Empty spiracles homolog 2
FACS	Fluorescence-activated cell sorting
FBS	Fetal Bovine Serum
FCS	Fetal calf serum
FGF	Fibroblast growth factor
Fig.	Figure
FoxG1	Forkhead box protein G1
g	Gram
G	Gravity
GCL	Granule cell layer
GDF	Growth differentiation factor
GFAP	Glial fibrillary acidic protein
h	Hour
HEK cells	Human Embryonic Kidney cells
HEPES	Hydroxyethylpiperazine Ethane Sulfonic acid
HES5	Hairy and Enhancer of Split 5
ICM	Inner cell mass
iPSC	induced Pluripotent Stem cells
iPS-DF	iPS-Derived Fibroblasts
ITSFn	Medium containing insulin, transferrin, sodium-selenite
Kan	Kanamycin
KO/SR	Knockout Serum Replacement
l	Liter
LB	Lysogeny Broth
LIF	Leukemia inhibitory factor

Lt	Lenti
Lt-Tet-EGFP	Lenti-Tet-EGFP
Lt-Tet-Emx2	Lenti-Tet-Emx2
Lt-Tet-NeuroD1	Lenti-Tet-Neurod1
M	Molar
MAP	Microtubule-associated protein
MEF	Mouse Embryonic Fibroblasts
MEM	Minimum Essential Media
mESC	Mouse embryonic stem cells
mL	Milliliter
mg	Milligram
min	Minute
MOI	Multiplicity of Infection
mM	Millimolar
ng	Nanogram
NeuroD1	Neurogenic differentiation 1
NeuN	Neuronal nuclei
NPC	Neuroprogenitor cell
ORF	Open Reading Frame
P	Posterior
P	Promoter
P	Postnatal day
Pax-6	Paired box protein
PBS	Phosphate Buffered Saline
PC	Pyramidal cell layer
PCR	Polymerase Chain Reaction
PCR	Polymerase chain reaction
PD	Parkinson's Disease
PFA	Paraformaldehyde
Prox1	Prospero-related homeobox 1
qPCR	quantitative PCR
qRT-PCR	quantitative Real Time PCR
RA	Retinoic acid
RE	Restriction Enzyme

RNA	Ribonucleic acid
ROCK	Rho-associated Kinase
rpm	Rounds per minute
RT	Room Temperature
RT-PCR	Reverse Transcription PCR
RtTAs	reverse tetracycline Transactivators
Sec	Second
SBI	System Biosciences
Sox1	Sex determining region Y-box 1
SV40	Simian virus 40
SVZ	Subventricular zone
tTAs	tetracycline Transactivators
TAE	Tris Acetate
Tbr2	T-box brain protein 2
TEA	Triethanolamine
tetR	tetracycline repressor
TGF	Transforming growth factor
tetO	tet operator sequence
TRE	Tetracycline Response Element
U	Unit
UV	Ultraviolet
VP16	Viral protein 16
VZ	Ventricular zone
V-SVZ	Ventricular-Subventricular Zone
WST	Water Soluble Tetrazolium
Wnt	Wingless type MMTV integration site family

1. Introduction

Over the past decade, the field of neural stem cell has witnessed a rapid development in many respects including embryonic development, cellular reprogramming and differentiation, and regenerative therapeutic techniques such as cell replacement, organoids and drug screening. Meanwhile, the basic and clinical research involving the human brain physiology and pathophysiology, as well as neuro-developmental diseases face several major challenges due to inaccessibility to the human brain from embryo to adult stage.

To tackle these problems, stem cell scientists have turned to the generation of in vitro biological models that capture some major aspects of the normal or abnormal human brain development, yet simpler, less variable and highly accessible. The differentiation of pluripotent stem cells (PSCs) towards specific glial and neuronal brain cells are used to improve our knowledge by providing mechanistic insights into human brain development, maturation and neurological diseases. In order to design the artificial architecture of the brain ex vivo, a fair control over directed neuronal differentiation of stem cell resembling critical events of brain development is a critical step for brain research.

1.1 Stem Cells

In 1868, the German biologist Ernst Haeckel coined the term “stem cell” to describe a fertilized oocyte. Twenty years later, a fellow of him, Theodor Boveri, refined the usage of the term stem cell to describe roundworm embryo cells capable of duplicating themselves (self-renewal) and of specializing (differentiating) into any other cells. Boveri’s description comprises the essential characteristics of an embryonic stem (ES) cell. In 1909, the Russian biologist Alexander Maximow theorized that a set of “stem cells” in bone marrow could differentiate into red and white blood cells. In effect, he described adult stem cells which renew themselves and serve as a means of repairing and maintaining tissues like the breast, brain, and bone marrow.

By some decades later, scientists made considerable progress in understanding how stem cells function. The functionality of stem cells was not fully understood but until 1981, when Gail Martin at the University of California in San Francisco, and Martin Evans at the University of Cambridge plucked the inner cell mass from a mouse embryo and coaxed it to grow in a petri

dish (Martin 1981). With a steady supply of mouse ES cells, scientists could provide a cellular platform for the study of development, maturation, and disease of these cells.

Another breakthrough was due to James Thomson and his colleagues at the University of Wisconsin in 1998, who employed a similar technique to grow human ES cells in the lab (Thomson, Itskovitz-Eldor et al. 1998). The scope of their progress was so promising that it was advertised by some as the means for an immediate treatment of most intractable degenerative diseases — and at the same time unleashed serious controversies involving moral issues such as the destruction of human embryo.

Stem cells are undifferentiated cells with the capacity of unlimited self-renewal and long-term viability. After cell division, the daughter cells can divide and form more precursor cells or cells that are functionally specialized matured cells. There are various types of stem cells based on their differentiation capacity: stem cells from zygotes (fertilized oocytes), stem cells isolated from embryo, stem cells isolated from adult body organs, and stem cells specified for a special organ or tissue.

The stem cells from zygotes are totipotent cells capable of differentiating into all kinds of cells which make up the embryo and cells necessary for the development of all tissues and organs in the adult body along with the placenta and umbilical cord.

The stem cells isolated from an embryo are pluripotent and can create all kinds of cells, except the umbilical cord and the placenta (Thomson, Itskovitz-Eldor et al. 1998); (Evans and Kaufman 1981).

The stem cells isolated from a particular tissue, organ, or physiological system are multipotent cells. An example of such are the hematopoietic stem cells which are also single cells. These cells can create all types of blood cells. The stem cells isolated from a specified tissue such as testis give rise to a single mature cell type (e.g., spermatogenic cells).

1.2 Embryonic and reprogrammed stem cells

ES Cells (hereafter ESCs) are either derived from the inner cell mass (ICM) of one blastocyst or early stage of morula, or they are generated by somatic cell reprogramming which is called iPSCs (an acronym for Induced Pluripotent Stem cell). The iPSCs can provide a potential source of cells for research, regenerative medicine or tissue bioengineering (Guo, Murthy et al. 2012). The term pluripotency has been assigned to different cell types with a wide range of functional capacities. Roughly speaking, pluripotency describes an aspect of a cell that can generate cell types from any of the three following embryonic germ layers: the endoderm, the mesoderm,

and the ectoderm. The exact definition for pluripotency, however, describes a cell that can create an entire organism, generating every cell type within that organism (Thomson, Itskovitz-Eldor et al. 1998); (Vallier and Pedersen 2005).

The study of ESCs seemed to offer unlimited possibilities, such as the understanding of early human development, tissue formation, and differentiation in vitro.

Moreover, this is particularly appealing to model previously untreatable conditions by uncovering the causing mechanisms which is eventually applicable to cell therapy (Niclis, Trounson et al. 2009); (Niclis, Trounson et al. 2009); (Vallier and Pedersen 2005); (Reubinoff, Pera et al. 2000). The derivation of embryonic stem cells from the human embryo, however, sparked a controversial ethical debate on the application of hESCs in clinical research. There are other limitations that must be overcome, such as the immune rejection as well as the technical obstacles concerning the use of human embryo as a source of ESCs for clinical application (Thomson, Itskovitz-Eldor et al. 1998); (de Wert and Mummery 2003); (Giacomini, Baylis et al. 2007); (Saric, Frenzel et al. 2008); (Elstner, Damaschun et al. 2009).

Although it is clear that functional neurons can be generated with the help of iPSCs, it remains a formidable task to stablish better differentiation strategies for generating more specific neurons and disease relevant neuronal subtypes. So far by iPSC technology, populations of ventral midbrain dopaminergic neurons for Parkinson disease (Perrier, Tabar et al. 2004); (Roy, Cleren et al. 2006); (Di Giorgio, Boulting et al. 2008); (Ma, Liu et al. 2011), spinal motor neurons for amyotrophic lateral sclerosis (Dimos, Rodolfa et al. 2008); (Marchetto, Muotri et al. 2008); (Kriks, Shim et al. 2011), cortical pyramidal neurons (Shi, Kirwan et al. 2012); (Vanderhaeghen 2012), and forebrain interneurons (Maroof, Keros et al. 2013); (Nicholas, Chen et al. 2013) could be achieved.

Recently, 3D culture models termed cerebral organoids have been developed which recapitulate some aspects of brain development such as the organization of discrete cortical regions (Lancaster, Renner et al. 2013); (Renner, Lancaster et al. 2017). These organoids include organized germinal zones, and both radial and tangential migration of cortical neuron subpopulations and cortical organizers such as the WNT secreting CH. The fact that they are not patterned by externally added growth factors or morphogens suggests that their development relies purely on self-organization by building neuronal microenvironments. Although the development of dorsal forebrain structures such as the hippocampus is still limited in these organoids, they build a foundation for designing the histological architecture of the hippocampus and the dentate gyrus (DG).

1.3 Development of the DG: Molecular Mechanism, Transcription factors, Growth factors

The DG formation is quite peculiar in its development. During development, the following zones can be distinguished:

1) Neuroephitelium (ventricular zone, primary matrix)
2) Subventricular zone
3) Radial migration path
4) Tangential migration path
5) Tertiary matrix (hilus and sub granule zone)
6) Granule cell layer (with ventral and dorsal striatum)

The neuroepithel and the subventricular zones together coin the term "germinative zone". The subventricular zone as well as the migration pathways form the secondary matrix. The adjacent structures of the CH and the hippocampal fissure with Cajal Retzius cells constitute important developmental regulations by the release of growth factors.

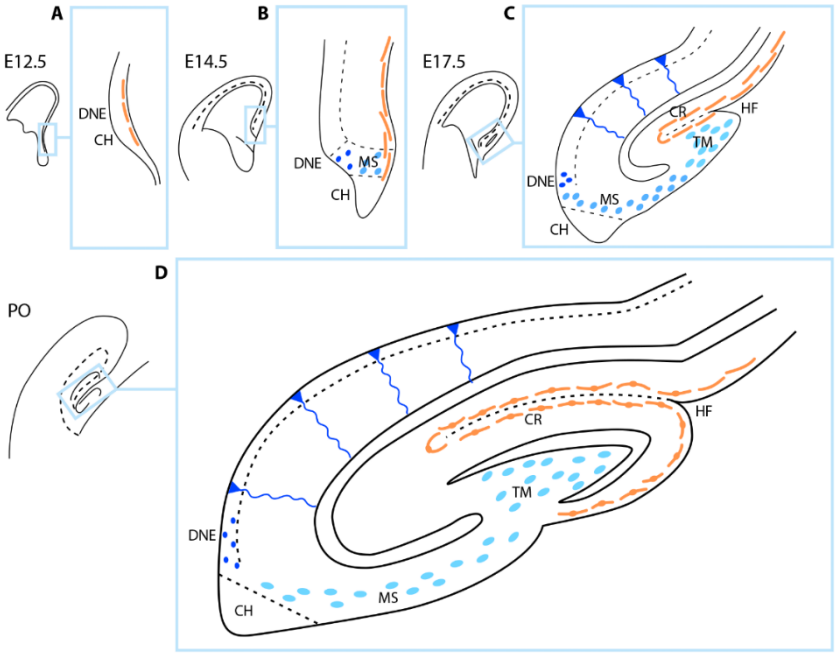

Fig. 1.1 Schematic representation of DG development from E12.5 up to postnatal stage.
DNE: Dentate Neuroepitelium; CH: Cortical Hem; MS: Migrational Stream;
CR: Cajal Retzius; TM: Tertiary Matrix; HF: hippocampal fissure
DG precursor cells (small dark blue) start to develop in DNE, adjacent to CH and migrate along MS (light blue) towards TM and build up granule cell layer. The migration and differentiation of granule cells is controlled by CH, glial scaffold and CR cells aligning the hippocampal fissure. Modified from Urban and Guillemot, 2014.

The dentate neuroepithelium (DNE)- also called primary matrix-belongs to the medial pallium VZ. This medial pallium immediately contacts the CH, can be perceived as early as embryonic day 14.5 and gives rise to the DG (Figs. 1.1A, B). The progenitor cells leave the DNE in the direction of medial cortex's pial side at the late-stages of gestation. This continuing development is subject to the Cajal-Retzius cells are originated from the hem and migrate to the hippocampal fissure (Rickmann, Amaral et al. 1987); (Del Rio, Heimrich et al. 1997). The DG progenitors are formed as a mixture of neuronal precursors and stem cells at distinct differentiation stages. They move towards the hippocampal fissure-away from the VZ and thus comprise a new migratory progenitor population, which is also named the secondary matrix (Figs. 1.1 B, C). The glial scaffold and bypasses simultaneously evolves from the fimbria to the pial side of the cortex and the hippocampal fissure. During DG development, glial scaffold and Cajal-Retzius cells stay in place and maintain all essential functions for migration and organization of dentate precursor cells and granule neurons. When arriving at the hippocampal fissure, neural progenitors gather and shape another junction of proliferating cells – the so-called tertiary matrix (Figs. 1.1 C, D). The GCL is generated by granule cells which are evolved during DG development from the precursors of all three matrices. Its contour with two blades is significant and predetermined by the Cajal-Retzius cells that encompass the hippocampal fissure and the pial surface (Fig. 1.1 D). The matrix becomes the only source of dentate progenitors and granule cells in early postnatal stages, while proliferation gets even more limited during postnatal week two. In the postnatal period, the extra proliferative zone continues to operate and grow to become SGZ, the site of adult hippocampal neurogenesis (Altman and Bayer 1990); (Bayer 1980) (Bayer 1980); (Khalaf-Nazzal and Francis 2013); (Pleasure, Collins et al. 2000); (Sugiyama, Osumi et al. 2013) (Fig. 1.2).

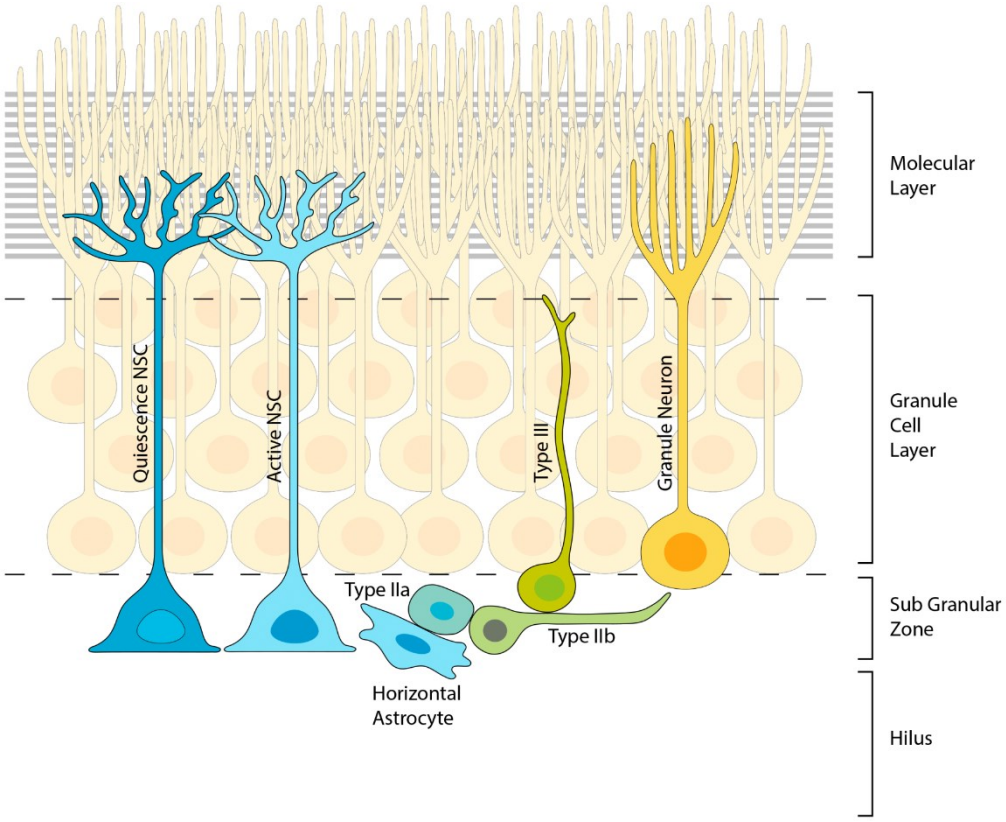

Fig. 1.2 Neurogenesis of DG granule cells from postnatal stage onwards. The neurogenic lineage of DG neurons consists of quiescent and active NSCs. Granule neurons form the granule cell layer with dentrites extending into the molecular layer and axons, building the Mossy fibre tract. (From Urban and Guillemot, 2014 with minor modifications).

The notch receptors and their ligands belong to molecules which generally participate in the cortical differentiation (Lee 1997). These molecules control the timely course of neurogenesis. The proteins connected after the notch receptors include a number of molecules with common motives, including basic transcriptional regulation domain and HLH-protein interaction domain. These proteins are called basic helix-loop-helix-proteins (bHLH). To this family belong anti-neurogenetic members, like the homologues to drosophila hairy and enhancer of split (Hes1 and Hes5) and extramacrochaete (Id1, Id2, Id3, Id4). Subsequent to the Notch activation, the Hes genes are upregulated and block the differentiation of precursor cells in their neuronal stage. These pro-neurogenetic bHLH genes contain homologues of drosophila atonal and are divided in two groups. The first group, referred to as the group of neuronal determination genes, is involved in the introduction of the neuronal differentiation process and includes genes like Neurogenin 1, 2 (Ngn1, Ngn2). The second group comprises neuronal differentiation genes and includes other atonal homologues, like NeuroD/BETA2, NeuroD2/NDRF, Meth2/Nex1 and Math3. It is assumed that this group regulates the later outcomes of neuronal differentiation.

Pleasure and his team (Pleasure, Collins et al. 2000) developed a model of sequential expression of transcription factors in the development of the DG. The DG neuroepithel is primarily characterized by the expression of the genes Id2, Id3, Hes5, and Mash1. In the sequence of expression and topography, the granule cells generating the neuroepithel of the DG primarily express the genes Ngn2, Hes5, Id2, and Id3. Subsequently, the expression of Mash1, Mash3, Notch1 and further Hes5, Id2, Id3 can be observed in the subventricular zone. It is generally known that Mash1 is expressed in mitotic precursor cells of the nervous system. After leaving the subventricular zone, the first granule cells express NeuroD. According to Pleasure et al., it is unclear whether NeuroD-positive cells emerge directly from the neuroepithel or via a precursor stage. It must be assumed that the cells involved in the migration towards the later DG consist of a mixture of precursor cells and newborn neurons with different molecular profiles. According to Pleasure et al., the genes Mash1, Notch1 and NeuroD1 are expressed in the migration pathway and in the tertiary matrix, whereas Prox1 and NeuroD2 are expressed in the developing granule layer of the DG. This means that cells which have reached their destination, express the granule cell specific homeobox protein Prox1, and NeuroD2 for final differentiation. Cells that have maintained their precursor stage continue to express Mash1 and form the tertiary matrix after reaching the DG anlage. In this tertiary matrix, further granule cells are being generated from Mash1 positive precursor cells within the sub-granular zone. These newborn granule cells then migrate radially to the inner segment of the granule layer,

thereby expressing first NeuroD, then NeuroD2, and at last Prox1. This common expression pattern is kept up in the adult system (Kunze, Grass et al. 2006).

Structures adjoining the DG

Structures adjacent to the DG, the CH, and the hippocampal fissure are of major importance for the normal development due to existing interdependencies and are thus outlined here.

Cortical hem signals: BMP and WNT

About embryonic day 14, the hippocampal formation is initiated in the mouse, reacting to signals that come forth from the cortical hem (CH). The CH is a dorsomedial structure of the telencephalon systematizing, the hippocampus, and the choroid plexus (Grove, Tole et al. 1998); (Mangale, Hirokawa et al. 2008). The active secretion of BMP and WNT molecules is a distinct feature of the hem, as it lacks TF Lhx2 expression. The function studies have made it evident that the hem has a decisive role in the hippocampal formation. A failure in hem's formation results in an improper development of the hippocampus (Yoshida, Assimacopoulos et al. 2006). The WNT signals of CH affect the proliferation of hippocampal neural precursor cells (Furuta, Piston et al. 1997); (Galceran, Farinas et al. 1999); (Lee, Tole et al. 2000); (Caronia, Wilcoxon et al. 2010). A number of WNT proteins like WNT2a, WNT2b, WNT3a, and WNT5a are generated in the embryonic CH, as these proteins are vital in their roles in systematizing the hippocampus. A disruption of WNT3a, for instance, would hinder the hippocampal formation, which is an obligatory step in the development of WNTs (Lee, Tole et al. 2000). Wnt3a is a gene, which is expressed very early and exclusively in CH (Grove, Tole et al. 1998); (Lee, Tole et al. 2000). Wnt3a mutants have a developmental disorder with a significant mediolateral and longitudinal gradient. At the medial border of the hippocampus formation, the DG is missing. CA3, CA1, and the subiculum, however, are missing rostral and are strongly reduced caudally. Severe defects of the hippocampus are also engendered by a disruption of the main downstream effector of canonical WNT signaling, Lef1, or a disruption of the WNT receptor Lrp6 (Galceran, Farinas et al. 1999); (Yoshida, Assimacopoulos et al. 2006). In LEF1-deficient embryos, the granule cells of the DG are missing (Galceran, Miyashita-Lin et al. 2000).

Furthermore, for characterizing specific hippocampal domains, the ectopic expression of Lef1 is adequate and it exhibits the sufficiency of WNT activation for conferring hippocampal

identity (Machon, Backman et al. 2007). In addition, the formation of the glial scaffold is vital for the neural precursor cell migration from the VZ into the medial pallium to their final hippocampal location. WNTs are instrumental in this glial scaffold formation (Zhou, Zhao et al. 2004).

At an early stage, the telencephalic roof plate generates multiple BMPs (BMP4, BMP5, BMP6 and BMP7), as does the CH at a later stage (Furuta, Piston et al. 1997); (Grove, Tole et al. 1998); (Hebert, Mishina et al. 2002). The total loss of BMP signaling causes a lack of medio-dorsal structures, the choroid plexus, and the CH, which again results in the absence of the hippocampus (Cheng, Hsu et al. 2006); (Fernandes, Gutin et al. 2007). Upon CH formation, BMPs appear not to be required any longer for defining characteristics of the hippocampal cells (Hebert, Mishina et al. 2002). The influence of BMPs on neural precursors is various, which might result from distinct type 1 BMP receptor activities (BMPR-I and BMPR-Ia). BMPR-Ia furthers embryonic telencephalon proliferation and BMPR-Ib induces cell cycle arrest and differentiation (Panchision, Pickel et al. 2001). BMPs are also vital in the adult DG for sustaining the quiescent condition of NSCs (Mira, Andreu et al. 2010). Granule neurons and NSCs themselves continually secret bone morphogenetic proteins (BMPs). In the hippocampal niche, also BMP inhibition by Noggin and Chordin exists (Scott, Steiglitz et al. 2000); (Fan, Xu et al. 2003); (Bonaguidi, McGuire et al. 2005); (Bonaguidi, Peng et al. 2008). When BMP signaling is lost due to destruction of the BMPR-Ia receptor subunit, there occurs an over-activation of adult NSCs, thus reducing their population (Mira, Andreu et al. 2010). The quiescence in NSCs in culture may as well be induced by BMPs, which supply a study model for detailed examination of molecular pathways that control stem cell behavior (Mira, Andreu et al. 2010, Sun, Hu et al. 2011, Martynoga, Mateo et al. 2013). BMPs are as well capable of furthering the astrocytic gene expression in vitro, thus making the induction of a selection of astroglial features of adult NSCs feasible (Gross, Mehler et al. 1996); (Sun, Hu et al. 2011). BMPs are vital for the quiescence of NSCs as well as granule cell differentiation and maturation (Bond, Peng et al. 2014). The differential expression of BMPR-I receptors can expound these two different roles of BMPs. BMPR-Ia, that is downregulated in IPCs, can be expressed by neural stem cells in the adult DG. On the contrary, BMPR-Ib is expressed by neuroblasts and neurons (Mira, Andreu et al. 2010). For this reason, neuroblasts and NSCs either receive BMP signals that each are explained as quiescence and differentiation cues. In the VSVZ, the results of BMP signaling on adult neurogenesis are comprehended poorly (Lim, Tramontin et al. 2000);(Colak, Mori et al. 2008). The role of BMPs in supporting the quiescence of V-SVZ stem cells is not transparently proven yet. The BMP inhibitor Noggin has no effect on the behavior

of V-SVZ-derived stem cells; however, it furthers the expansion of DG-derived stem cells in vitro (Bonaguidi, Peng et al. 2008).

Reelin is expressed by Cajal-Retzius cells and has an impact on the radial glia migration in the hippocampus. In Reelin mutants, the granule cells of the DG are formed morphologically; however, they do not generate a tightly packed granule layer and show a mal-positioning in the hilus area (Drakew, Deller et al. 2002). In these mice, a sharp demarcation between hilus and granule layer is missing. ApoER2/VLDR mutants have a similar phenotype. Furthermore, it could be proven that Reelin, disabled1, and β1-Integrin are involved in the formation of radial glia starting from the hilus in the DG marginal zone (Forster, Tielsch et al. 2002). Moreover, mutants of the genes Cdk5 (Ohshima, Ward et al. 1996), P35 (Chae, Kwon et al. 1997) and Pafah1b1/Lis1 (Hirotsune, Fleck et al. 1998) display a similar phenotype with abnormal neuronal cell migration and a thus result in the ectopic positioning of cells in CA and DG.

Transcription factors controlling the development of DG

The dorsomedial telencephalon embraces the dorsal pallium (isocortex) and the medial pallium (hippocampus proper or Cornu Ammonis (CA) and the DG). These morphologically and functionally distinct regions of the cortex are determined and differentiated during the development of a series of sub steps, starting with the growth of the open undifferentiated neural plate.

At the beginning of this process, signal molecules of the telencephalic centers of patterning are secreted (Rubenstein and Beachy 1998), which deliver positional information and regulate the regional growth in the cortex anlage. The interpretation of these signals by the cortex anlage gives rise to a species-specific proto-map (Fukuchi-Shimogori and Grove 2003). As of today, the following molecules are recognized for their involvement in patterning: “bone morphogenetic proteins” (BMPs), “growth differentiation factors” (GDFs), and “fibroblast growth factor” (FGF), “sonic hedgehog” (SHH), “epidermal growth factor” (EGF) and “wingless-type MMTV integration site family” (WNT) proteins (Tole, Christian et al. 1997, Grove and Tole 1999). So far, the anterior pole of the cortex anlage, the hem and the so-called Anti-Hem are defined as centers of patterning (Grove and Fukuchi-Shimogori 2003).

These signals activate or suppress the expression of transcription factors, which are regulating the further sequence of cortical regionalization, among others by controlling the cell proliferation (Rakic 1995), lamination, formation of radial glia, and the topographically limited evolving neuronal components of each specific area.

So far, a number of regulatory genes have been isolated and characterized, functioning in the constitution and maintenance of the identity of anterior telencephalon areas (Shimamura and Rubenstein 1997). Some of these genes are homeobox genes, which again belong to different gene families.

The transcription factors Gli3- a conserved zinc finger-transcription regulator- is responsible for the development of the dorsal telencephalon (Theil, Alvarez-Bolado et al. 1999). In XtJ/ XtJ mice, the complete hippocampus is missing, including the CA, the DG, and the plexus choroideus of the lateral ventricles. Furthermore, there is a loss of expression in Emx1 and Emx2 genes.

These two Emx genes define a certain region during telencephalon development, due to their limited expression in the dorsal prosencephalon (Simeone, Acampora et al. 1992). Emx2 is expressed in the dorsal and ventral neuro ectoderm of the forming prosencephalon, with a posterior demarcation within the diencephalon roof. The experiments with segment-specific hippocampal marker genes (Tole, Goudreau et al. 2000) hypothesized that Emx2 is responsible for normal growth and maturation of the hippocampus and the proximal medial neocortex, but not for cell specification of various hippocampal segments. This applies to the DG region as well. The DG cells exist in their appropriate anatomic position (neuroepithel migration path); however, they do not form a morphologically recognizable DG. The cortical neurogenesis in mice is normally completed at about E16.5 (Angevine 1965). For Emx2 mutants in contrast-at the same time-the marked ventricular zone still takes up a major part of the entire diameter of the embryonal cortex, similar to control animals about 2 – 3 days earlier. This could mean a delay of the cortical neurogenesis in Emx2 mutants, or that the cells do not leave the cell cycle on time, in order to be able to migrate to the ventricular zone. Accordingly, the incidence of another hippocampal region (CA3) in Emx2-/- mutants is delayed. In summary it can be stated that Emx2 is not only indispensable for the determination of the DG, but also for its differentiation.

Emx2 is not only expressed by proliferating cortical cells, but also by Cajal-Retzius cells of the marginal zone (Pellegrini, Mansouri et al. 1996, Yoshida, Suda et al. 1997, Mallamaci, Iannone et al. 1998). Cajal-Retzius cells are a transiently occurring cell population functioning in coordination with cortical neuron migration along the radial glia including the Reelin gene (Marin-Padilla 1998). In the cortex, there exist at least two populations of Cajal-Retzius cells, which can be differentiated due to their chronological occurrence. The later appearing Cajal-Retzius cells are missing in the cortex of Emx2 knockouts (Mallamaci, Iannone et al. 1998,

Mallamaci, Muzio et al. 2000). Consequently, the late development is influenced by radial glia, and thus, later born cells of the neuronal plate do not migrate through the earlier born ("inside-out layering"), so that the cortical laminating is disturbed (Mallamaci, Muzio et al. 2000). Furthermore, Bagri et al. could demonstrate the influence of the cytokine SDF-1-which is expressed by Cajal-Retzius cells-on the migration of granule precursor cells from the neuroepithel to the granule layer of the DG as a chemo attractive factor (Bagri, Gurney et al. 2002). In CXCR4-/- mutants, the DG is diminished and does not develop its typical horseshoe form. The number of proliferating cells in the migration path and in the DG is limited here, and the cells seem to differentiate too early. Thus, not enough precursor cells populate the developing DG, to ensure its normal formation (Lu, Grove et al. 2002). In Emx2-/- mutants, a morphologically identifiable DG is missing (Pellegrini, Mansouri et al. 1996); (Yoshida, Suda et al. 1997). At a closer observation, at E14.5 to E18.5 Emx2-/- mutants histologically display the ventricular zone-which gives rise to the hippocampus and the DG-is diminished, while the subventricular zone, a migration path, and a vestigial tertiary proliferation zone develop. At last, the granule layer of the DG is completely missing in mutants. Since homozygous embryos decease perinatal due to major changes of the urogenital system (lacking of kidneys, ureter, gonads and genital tract), see also (Miyamoto, Yoshida et al. 1997), however, as the complete development of the DG was achieved postnatally, it was yet impossible to examine the complete DG development in vivo.

(Tole, Goudreau et al. 2000) hypothesized, that the mutant DG is specified correctly, however, it suffers from a developmental problem that affects the whole medial cortex. Accordingly, the CA region of the Emx2-/- hippocampus, for example, shows a reduced and eventually immature hippocampal plate. It is indicated that this problem may be a defect in the cortical positional information-signal cascade, transmitted by Fgf8 (Fukuchi-Shimogori and Grove 2001); (Shimogori, Banuchi et al. 2004) and possibly by WNT proteins as well (Muzio, Di Benedetto et al. 2002); (Ligon, Echelard et al. 2003).

In Lhx5 knockout, the precursor cells for the hippocampal anlage are specified, but do not emerge from the cell cycle and differentiate. The disturbed migration of these cells causes a lack of DG granule cells (Zhao, Sheng et al. 1999). Lhx5-/- mutants display a broadened hippocampal neuro epithel with more proliferated cells at E18.5 as a wild type. Fimbria and hippocampal commissures are lacking.

As a bHLH TF with proneural activity in the embryonic brain, Neurog2 not only furthers the neuronal commitment of multipotent stem cells, but also induces the gene expression of other

neuronal differentiation genes like the NeuroD family of TFs (Seo, Lim et al. 2007, Wilkinson, Dennis et al. 2013). In the embryonic brain, it functions in a primary role characterizing glutamatergic neurons (Schuurmans, Armant et al. 2004, Berninger, Costa et al. 2007, Wilkinson, Dennis et al. 2013). Precursor cells in every proliferative matrix express Neurog2 while the DG evolves (Pleasure, Collins et al. 2000, Galichet, Guillemot et al. 2008). The analysis of Neurog2 in null mutant mice, which showed a severely atrophic DG at birth-a severely minimized upper blade and a lacking lower blade-, provided an evidence for the vital role of Neurog2 in DG formation (Galichet, Guillemot et al. 2008). Proliferation as well as differentiation defects are shown by progenitors in the Neurog2 mutant DG. Despite progenitor cells expressing Ascl1 during DG morphogenesis, Ascl1 does not make up for Neurog2 loss, compared with examinations in the embryonic telencephalon (Nieto, Schuurmans et al. 2001, Galichet, Guillemot et al. 2008). Moreover, the Neurog2 mutant DG has a disorderly glial scaffold, which implies a disrupted progenitor migration (Galichet, Guillemot et al. 2008). The atrophic DG and the disorganized glial scaffold remind of phenotypes found in WNT mutant embryos. It was stated that WNT signaling regulates Neurog2 expression in the embryonic brain, and thus, during the formation of DG, Neurog2 possibly functions as an effector of WNT signaling (Hirabayashi, Itoh et al. 2004, Zhou, Zhao et al. 2004, Galichet, Guillemot et al. 2008).

T-box TF Tbr2 is a further principal regulator of embryonic DG neurogenesis. In the cortex, it promotes the intermediate progenitors' generation and proliferation, which originate the pyramidal glutamatergic neurons in the cerebral cortex generation (Englund, Fink et al. 2005, Arnold, Huang et al. 2008, Sessa, Mao et al. 2008). In the emerging DG, proliferating progenitor cells express in all three matrices Tbr2 – like Neurog2 – (Hodge, Nelson et al. 2012). A deletion of Tbr2 hinders the IPC and granule neuron generation and increases the stem cell proliferation in the developing DG. This finding suggests that Tbr2 is vital for the transformation of stem cells into late differentiating IPCs. It was postulated that Tbr2 exerts its functions by directly down-regulating the stem cell TF Sox2 (Hodge, Nelson et al. 2012). Furthermore, the hem-derived Cajal-Retzius cells express Tbr2, as needed for their migration. A malfunctioning proliferation of Cajal-Retzius cells enhances defects in DG morphogenesis in Tbr2 mutant mice (Hodge, Garcia et al. 2013).

Various types of neuronal progenitors and post-mitotic cells express the transcription factor Prox1, including the newborn granule cells in the evolving DG's tertiary matrix (Oliver, Sosa-Pineda et al. 1993, Li, Kataoka et al. 2009). Despite its low expression in some hippocampal interneurons, Prox1 is often applied as a dentate granule neuron lineage marker (Rubin and Kessaris 2013). During the development of DG, Prox1 is vital for neuronal progenitor

proliferation and granule cell specification, as the examination of Prox1 null mutant mice made evident (Lavado, Lagutin et al. 2010). It is noticeable that knocking-out Prox1 especially in post-mitotic granule neurons causes a modification in cell identity – they become CA3 pyramidal neurons (Iwano, Masuda et al. 2012). During embryonic/postnatal hippocampal development in the adult DG, Tbr2 and Prox1 either function in an analogous manner in granule cell generation. This finding implies that, from DG development to adulthood, a similar genetic program, which includes the same key TFs (Neurog2 > Tbr2 > NeuroD1 > Prox1), furthers the differentiation of IPCs into glutamatergic DG cells (Hodge, Kowalczyk et al. 2008, Hodge, Nelson et al. 2012). Yet, this fact does not pertain to influential elements of the previous granule cell lineage, as described in the paragraph below.

The further differentiation of precursor cells depends on the NeuroD expression. Without this gene, no initial granule cell is synthesized. In the NeuroD knockout, the DG is lacking (Miyata, Maeda et al. 1999).

In the DG, proliferation of granule cells becomes limited to the tertiary matrix, which incrementally evolves into the SGZ, and the DG blades are already formed at postnatal day 14 (P14) (Pleasure, Collins et al. 2000, Sugiyama, Osumi et al. 2013). Simultaneously, the first presumptive GFAP- and Nestin-positive NSCs chose their specific location, while the nucleus remains in the SGZ and the basal prolongs extends through the GCL (Li and Pleasure 2005, Martynoga, Mateo et al. 2013). As lately proven, the NSCs need the transcription factor NFIX for adopting their exact location in the forming DG (Martynoga, Mateo et al. 2013). In two interesting mouse lines that carry null mutations in the CcnD2 and Tlx genes, explicit defects in adult neurogenesis are first observed about the ending of postnatal week two (Kowalczyk, Filipkowski et al. 2004, Shi, Chichung Lie et al. 2004, Ansorg, Witte et al. 2012). During embryonic and early postnatal life, these two mutants showed a quite normal DG formation and development; however, in their late postnatal stages and adulthood, the stem cells did not keep up their granule neuron production. The conditional deletion of the proneural gene Ascl1 caused a total hindrance of adult neurogenesis, although it is not imperative for embryonic and early postnatal neurogenesis in the DG (Galichet, Guillemot et al. 2008, Andersen, Urban et al. 2014). During development of the hippocampus, the transcription factors of the Nuclear Factor 1 (NFI) family have been implied to the neuronal and glial cell generation. More specifically, as early as E14, NFIX is strongly expressed in the DNE, the future DG primordium. Simultaneously, the DG formation of NFIX null mutant mice shows intense defects (Campbell, Piper et al. 2008, Heng, McLeay et al. 2014). In NFIX mutants, there is an impeded neuronal and glial differentiation. These animals show a reduced number of Prox1 granule neurons and have a

disordered glial scaffold and a DG morphogenesis defect (Heng, McLeay et al. 2014). NFIX mutant mice live through P20. By this time, NSCs are in place in the DG at an ordinary concentration; however, with misplaced cell bodies and misaligned basal processes their location is unusual (Martynoga, Mateo et al. 2013). An increased proliferation rate occurs simultaneously with their abnormal position of NFIX mutant NSCs. It is of great interest, that cell adhesion and motility, or the generation of an extracellular matrix, are controlled by an important fraction of NFIX-regulated genes (Martynoga, Mateo et al. 2013). For this reason, it might be necessary that NFIX trigger NSCs migration to the exact SGZ area and NSCs act reciprocally with various DG niche elements. NSCs may be unable to receive the needed signals for sustaining quiescence, if NFIX is lacking. The role of NFIX in adult neurogenesis has not been discovered yet.

The orphan nuclear receptor Tlx, also known as Nr2e1, functions in modelling the embryonic telencephalon and is expressed throughout the telencephalic VZ. Tlx is not expressed in the dorso-medial region in which the hippocampus has its origin. In late embryonic and postnatal stages, Tlx is less expressed in the neurogenic regions, and is upregulated merely during adult stages (Monaghan, Grau et al. 1995, Shi, Chichung Lie et al. 2004). The DG and olfactory bulbs of Tlx mutant mice are unusually undersized. This condition is the consequence of a disturbed adult neurogenesis from the SGZ and V-SVZ. Adult Tlx mutant mice DGs display an inadequate progenitor proliferation and new neuron generation. This defect is invertible through re-expression of Tlx in mutant NSCs (Shi, Chichung Lie et al. 2004, Zhang, Zou et al. 2008, Niu, Zou et al. 2011, Murai, Qu et al. 2014). A Tlx overexpression in wild-type mice DGs can not only excite neurogenesis but also intensify memory and learning performances (Murai, Qu et al. 2014). Tlx furthers the shift from quiescence to activation in NSCs, as implied in these studies. A few downstream pathways have been involved in this process, in the induction of WNT signaling, Ascl1 expression, and the downregulation of BMP signaling (Shi, Chichung Lie et al. 2004, Elmi, Matsumoto et al. 2010, Qu, Sun et al. 2010, Qin, Niu et al. 2014) .

As a key component of the cell cycle mechanism, CcnD2 (Cyclin D2) regulates cell cycle transition between G1- and S-phases in combination with the other Cyclin D proteins (CcnD1 and CcnD3) and the Cyclin-dependent kinases (CDKs) (Sherr 1994, Ekholm and Reed 2000). CcnD1 and CcnD2 further cell cycle progression during embryonic development; however, they also trigger the neural progenitors' neuronal differentiation (Lukaszewicz and Anderson 2011, Pauklin and Vallier 2013). CcnD genes are quite alike in their structure, yet they can generally replace each other in their functions, and their expression profiles. For the

proliferation and differentiation of distinct progenitor populations, a variety of CcnD genes are required. It was proven that CcnD2 is especially needed for the proliferation of intermediate precursors in the embryonic cerebral cortex (Komada, Iguchi et al. 2013). Important functions in progenitor proliferation such as neuronal commitment anddifferentiation are fulfilled by Ascl1, a proneural bHLH transcription factor (Bertrand, Castro et al. 2002, Castro, Martynoga et al. 2011, Imayoshi and Kageyama 2011). Its overexpression in astrocytes, fibroblasts, and other cell types renders the capability to re-program these cells into neurons (Berninger, Costa et al. 2007, Yang, Ng et al. 2011, Wapinski, Vierbuchen et al. 2013). Progenitor cells in the three matrices express Ascl1 during the development of the DG; however, Ascl1 is not essential in DG formation during embryonic stages (Pleasure, Collins et al. 2000, Galichet, Guillemot et al. 2008). Additionally, in early postnatal stages, a conditional Ascl1 abscission has no influence on stem cell proliferation. This finding implies that other factors can further progenitor proliferation in the emerging DG when Ascl1 is lacking (Andersen, Urban et al. 2014).

Table 1: Important genes affecting telencephalic including DG development. See also Appendix Figs. 10.1-10.6.

Gene / pathway	Effect during development
Wnt	Promotes proliferation and neuronal differentiation of neural precursors
BMPR-Ia	Promotes the proliferation of neural precursors
Gli3	Important for dorsal telencephalic development
Emx2	Important for dorsal telencephalic development
Notch	Maintains the NSC pool by preventing premature differentiation
Neurog2	Determines the glutamatergic differentiation of NSCs
Tbr2	Essential for the proliferation and differentiation of IPCs
Prox1	Promotes differentiation and determines granule cell identity
NeuroD	In NeuroD knockout DG is missing
NFIX	Required for correct positioning of NSCs in the postnatal DG
Tlx	Does not have an important role in development of the DG
CcnD2	Does not have an important role in development of the DG
Ascl1	Does not have an important role in development of the DG

Preliminary studies on the directed differentiation of telencephalic precursors and hippocampal/DG neurons from ESCs.

The subjects of telencephalic differentiation and hippocampus development have been motivating for a number of research teams across the world. The earliest attempts and accomplishments were carried out and reported by two independent teams led by Sasai and Gage to generate dorsal telencephalic neurons, including hippocampal, and DG-like neurons from ESCs (Watanabe, Kamiya et al. 2005); (Sakaguchi, Kadoshima et al. 2015); (Yu, Di Giorgio et al. 2014). Their ideas were based on manipulating the molecular signaling pathways in different stages of telencephalon and embryonic hippocampal development. In general, the EB and single culture systems with the addition of growth factors up to brain transplantation were used to differentiate these specific cell types.

Watanabe et al. from the Sasai group through an independent study in 2005 reported an optimized serum-free suspension culture by replacing KO/SR with the fetal bovine serum and treating with WNT antagonist DKK1 to induce efficient generation of FOXG1-positive telencephalic cells. The treatment with WNT3a during the late fate of culture lead to an increase of PAX6 and EMX1 positive typical dorsal telencephalic markers.

Later on, a member of the same lab (Sakaguchi, Kadoshima et al. 2015) produced FOXG1-positive from hESCs with suspension culture and reduced oxygen conditions immature NeuroD-, Prox1- and Tbr1-positive neurons with the addition of BMP and WNT growth factors. Here again, the method of self-organizing dorsal medial telencephalic organ cultures was implemented and a low number of Prox1 positive granule cells produced. Only a limited set of DG markers was used to characterize these cells, which weakened the results. These authors were unable to generate CA1 pyramidal neurons or recapitulate DG formation or any regionally specific hippocampal tissues. This would be necessary to reconstruct the primary hippocampal neuronal circuitry.

In parallel, Yu et al. (Yu, Di Giorgio et al. 2014) from the Gage's lab could produce small amounts of electrophysiologically more mature human functional Zbtb20/Prox1 positive granule and ZBtb20/K1 pyramidal-like neurons by trying to recapitulate key steps mimicking hippocampal development. Embryoid bodies generated from hESCs were initially treated with anti-caudalizing factors DKK1 (WNT antagonist), Noggin (BMP-antagonist), the ALK5 (TGF-β-pathway) inhibitor SB31432, and the sonic hedgehog inhibitor Cyclopamine followed by WNT3a plus BDNF and then co-cultured as a single cell suspension on hippocampal astrocytes.

Yu et al. also transplanted the DG-like precursor cells in the hippocampal formations in vivo and observed integration and further maturation of the cells. This group also performed no co-localization studies with DG markers to prove the final differentiation phenotype of the DG-like cells, which weakens the results as well.

Both groups have developed in vitro models to recapitulate hippocampal development with the production of limited amounts of hippocampal/DG-like neurons from ESCs. While the model by Sakaguchi et al. represents an early hippocampal developmental stage, the cultivation procedure of Yu et al. seems to gain electrophysiologically more mature neurons only after transplantation in vivo.

1.4 Aims of this study

The ultimate goal of stem cell research in tissue engineering and regenerative medicine is the creation of safe and functional biological models. These models can be applied to cell, tissue, and organ replacements, or be used in drug development and design of other therapeutic techniques. A key point in this field is the functional efficacy of tissues derived from iPSCs, for which a deeper understanding of the molecular singling pathways and involving factors during cell differentiation or tissue development is necessary.

The DG is a highly organized brain with several distinct types of cells underlying learning and memorizing. The ability to model DG development in vitro represents an important step in our study of developmental processes and neurological disorders such as AD.

Making tissues grow three dimensionally in the lab has been challenging across the board. This is especially problematic for structures in the nervous system. In addition to producing neuronal growth at all, the neurons must be connected in a very particular manner in order to function. A team from RIKEN Center for Developmental Biology in Japan have taken a substantial step forward on this front. They have successfully grown a 3D functional brain tissue which developed with proper patterning[1] .

In the present study, the major purpose was to establish new protocols by considering in vivo embryonic development processes for the generation of enriched DG neural cells from ESCs by applying both of growth and transcription factors.

The growth factors are involved in the differentiation of telencephalon embryonic development in different embryonic stages. The most famous ones are Noggin, which inhibits bone morphogenetic protein (BMP), SB431542, which inhibits the transforming growth factor-b (TGF-b), DKK1 and possibly DKK3, which block the WNT signaling pathway, and Cyclopamine, an antagonist of the Sonic Hedgehog pathway. The interaction of these several pathways in the telencephalon, contributes to obtaining telencephalic neural precursor cells and the enrichment of primordium medial progenitor cells.

The key transcription factors such as Emx2, Prox1, NeuroD1, when triggered by the growth factors, also push the cells to differentiate to specific neural progenitor cells belonging to the DG.

The aim of this study is the generation of ESC-derived neural DG precursor cells for basic research and presumably future transplantation approaches. For both applications, protocols

[1] http://www.riken.jp/en/pr/press/2015/20150130_1/

leading to highly enriched neural DG precursor cells are key prerequisites. For therapeutic approaches, neural precursors have promising capacities due to their ability to differentiate into granule cells.

For basic research, neural differentiation protocols performed under defined conditions offer various applications for the recapitulation of telencephalon (dorsomedial) developmental processes in the brain. To this end, strategies for the generation of enriched neural precursors were explored.

The first part of this study addresses the question whether growth factors play any roles in telencephalic differentiation induction protocols such as those established for murine ESCs could be developed for human ES cells, and whether cells generated by such an approach can differentiate upon transplantation into host CNS tissue.

The second part is dedicated to the establishment of ESCs which were manipulated with transcription factors under control of Tet inducible system and investigation of the role transcription factors in DG induction and granule neurons differentiation.

In what follows, we shall summarize one of the best-studied and most frequently modeled aspects of in vivo brain development in rodents and humans, the formation of the DG, and describing to which extent stem cell-derived cultures can reproduce the DG development in vivo.

2. Materials and Methods

Nearly all the cell culture devices and equipment including plates, gloves, dishes, flasks, pipettes, centrifugation tubes, cell strainer, filters and filter insert-ready to use and disposable-were obtained from the central storage at the facility center of Heidelberg University (Table 2.1).

2.1 Technical Equipment

Table 2.1: Technical Equipment

Material	Company
4, 6, 24, 48, 96 well-plates	RennerGmbH, Dannstadt-Schauernheim
AggreWell™ 400Plates EX	Stemcell™ Technologies
Cell Strainer (100 µm)	Easystrainer™
Cell Strainer (70 µm)	BD Falcon
Cell Strainer (70 µm)	Easystrainer™
Centrifugation tubes	Greiner bio-one GmbH, Frickenhausen
Coverslip	Manzel GmbH, Braunschweig
Cryo tubes 2mL	Greiner bio-one GmbH, Frickenhausen
DNAase / RNAase free tube 1.5 mL	nerbe plus GmbH
Eppendorf tubes0.2mL,0.5mL, 1.5 mL, 2 mL	Eppendorf AG, Hamburg
Filter Cups	Greiner bio-one GmbH, Frickenhausen
Filter Thininsert; Transparent,pore:0,4µm	Greiner bio-one
FlaskT75 cm	Renner GmbH, Dannstadt-Schauernheim
Microscope slides	Marienfeld GmbH, Germany
Pipettes 1 mL, 2 mL, 5 mL, 10 mL, 25 mL	Greiner GmbH, Frickenhausen
Sterile filter 0.2 µM	Millipore (USA)
Sterile Syringe Filter, CA membrane 0.2µm	Berrytec
Sterile Syringe Filter, MCE membrane 0.2µm	Millex®-GS
Sterile Syringe Filter, PES membrane, 0.45 µm	TPP,74995
Sterile syringe Filter, RC membrane 0.2µm	Corning Incorporated
Ultra centrifuge tube SW32	Beranke labour Seton secientific7052

2.1.1 Instruments

All of the instruments used in this study are listed in the following Table.

Table 2.2: Instruments

Material	Company
Balance	Sartorius AG, Göttingen
Bio photometer	Eppendorf AG
Biological Safety Cabinet	Thermo Scientific™ *Herasafe*™ KSP Class II
Biological Safety Cabinet	Thermo Scientific™ MSC-Advantage™ Class II
Biomark Realtime quantitative PCR (qPCR) system (Fluidigm)	Step One Plus
Centrifuge	Eppendorf 5415R
Centrifuge	Eppendorf 5415C
CO_2 Incubator	Heraeus D-6450,Series 6000 Gas Jacket
Confocal Microscope	Zeiss LSM700 AIM-System,2601000579
Electronic Scale Balance	Mettler Toledo PL601-S
Electrophoresis power supply	GiBCO, ST304
Electrophoresis Power Supply	Bio-Rad, PowerPac 300
Geltray UV-transparent	Renner GMBH Dannstadt
Incubator	Thermo Scientific, HERA Cell 150
Incubator	Heraeus instruments
Incubator	CERTOMAT ® BS-1,B.Braun.Biotech international
Incubator Shaker	B:Braun Biotch International Certomat BS1
Minispin	Eppendorf
Mr. Frosty Freezing Container	NALGENE™ Cryo 1˚C Freezing Container, Made in USA
Power Supply	Zeiss HB 0100
Power Supply HXP120	Kubler CODIX
Shaker	JANKE &KUNEL type VX7
Shaker	Heidolph Duomax 1030

Thermomixer Comfort	Eppendorf
Ultracentrifuge	Beckman Coulter ,Optima ™ LE-80K
UV System Fluorescent Tables	Renne GMBH
Vortex Gene 2	Scientific Industry
Water Bath	GFL, Burgwedel

2.1.2 Software

In this study, the following softwares were used in writing, word processing, and data analysis.

- EndNote web (Thomson Reuters)
- MS-Office2014 SP2 (Microsoft)
- GENEX
- MS-Oce2014 SP2 (Microsoft)
- GENEX
- Biomark Data Collection Software
- Real-time Analysis Software
- StepOnePlus Software
- LATEX Typesetting Software
- Brain Allen Atlas[2]
- Gene Paint Data Bank[3]
- Pubmed[4]
- ClustalW2[5]

[2] http://www.brain-map.org/
[3] http://www.genepaint.org/
[4] https://www.ncbi.nlm.nih.gov/pubmed
[5] http://www.ebi.ac.uk/Tools/msa/clustalw2

2.2 The Culture Media

The culture media used in this study are divided in two major groups of bacteria and mammalian cells which are explained in details in following tables.

2.2.1 Bacterial Culture Medium

For LB and Agar media preparation, the following components were used according to the manufacturer instructions. In each case, appropriate antibiotics were added after autoclaving of LB-medium. For long-term bacterial storage, Glycerol 87% (ROCH 4043.1) was used for bacterial stocks.

Table 2.3: LB and Agar Media Components

Component	Company	Catalog No.
Trypton/Pepton aus Casein Pankreatisch verdaut	ROTH	8952.3
Yeast extract	ROTH	2363.3
NaCl	SIGMA-ALDRICH	31434
Agar-Agar	ROTH	5210.2
Kanamycin	ROTH	T83201
Ampicilin	ROTH	K029.2

´

2.2.2 Cell Culture Reagents and Material

All the cell culture reagent media and components used in different stages of cell culture are listed below (Table 2.4).

Table 2.4: The List of Cell Culture Reagent and Media

Product	Company	Catalog No.
0.05% Trypsin/EDTA(1X)	gibco® by Life technologies™	25300-054
2-Mercaptoethanol	gibco® by Life technologies™	21985
Acutase Cell Detachment Solution	Capricorn scientific	ACC-18
B27 Supplement (50X)	gibco® by Life technologies™	17504-044
BrainPhys™ Neuronal Medium	Stemcell™ Technologies	05792
Collagenase VI	Sigma	C5138
Cyclopamine	Stemcell™ Technologies	72072
Deoxy Ribonuclease I (DNase I)	Sigma	D4527
Dimethyl Sulfoxide (DMSO)	Sigma	D1435
Doxycyclin Hydroclorid	Sigma	D-9891

Dulbecco's modified Eagle Medium (DMEM) high glucose	gibco® by Life technologies™	41965-039
Dulbecco's modified Eagle Medium F-12 Nutrient Mixture (Ham) DMEM/F-12 (1:1) (1X)	gibco® by Life technologies™	21331020
Dulbeco's Phosphate Buffered Saline (PBS^{+}) with Ca^{+2} and Mg^{+2}	gibco® by Life technologies™	14040-091
Dulbeco's Phosphate Buffered Saline (PBS) without Ca^{+2} and Mg^{+2}	gibco® by Life technologies™	14190-094
Fetal bovine serum	Capricorn Scientific	FBS-12A
Fetal Bovine Serum, Tetracycline Negative, Collected in South America	Capricorn Scientific	FBS-TET-12A
Fetal calf serum (FCS)	gibco® by Life technologies™	SH30072.03
GlutaMAX™ -I CTS™ (100X)	gibco® by Life technologies™	A12860-01
Human Recombinant Brain-Derived Neurotrophic Factor BDNF	Stemcell™ Technologies	78005
Knockout ™ DMEM (1X) GIBCO; Life technologies ™	gibco® by Life technologies™	10829-018
KnockOut ™ SR GIBCO; Life technologies ™	gibco® by Life technologies™	10828-028
Laminin	Sigma	L2020
L-Glutamine 200Mm (100X)	gibco® by Life technologies™	25030-024
Lipofectamine™ 2000 Reagent	Invitrogen™ Thermo Fisher Scientific	11668027
Minimum Essential Medium (MEM)	gibco® by Life technologies™	10829-018
Minimum Essential Medium Non-Essential Amino Acids(MEM- NEAA)100X	gibco® by Life technologies™	1140-035
Mouse Dkk-1 Protein (His Tag)	Sino Biological, Inc.	57248-M08H
Mouse Recombinant Noggin	Stemcell™ Technologies	78061
N-2 Supplement (100X)	gibco® by Life technologies™	17502-048
NeuroCult™ SM1 Neuronal Supplement	Stemcell™ Technologies	0571111
OPTI-MEM®I	gibco® by Life technologies™	31985-047
Penicillin/ Streptomycin	gibco® by Life technologies™	15140-122
Penicillin/ Streptomycin	gibco® by Life technologies™	15140-122
Poly –L–Ornithine	Sigma	P4957
Polybrene	Sigma	H9268

Poly-DL-ornithine hydrobromide	Sigma	P0671
Posphate Buffered Saline (PBS)	gibco® by Life technologies	14190-094
Recombinant Dkk3	Sino Biological, Inc.	50247-M08H
Recombinant Murine Wnt-3a	PeproTech	315-20
SB431542	Stemcell™ Technologies	72232
Tet System Approved FBS	A Takara Bio Company;	631106
Trypsin 2,5 %	gibco® by Life technologies™	15090046
Y-27632	Stemcell™ Technologies	72302

Table 2.5: Expression Plasmids used for Transfection of Cell Cultures.

Plasmid Vector	Size (bp)	Addgene ID	Resistance		Reference
			Prokaryotic	Eukaryotic	
FUW-M2rtTA	7979	20342	-	-	Rudolf Jaenisch,
pcDNA3.1-Emx2 cDNA	5752	-	Ampicillin	Zeocin	Invitrogen
pCMV-Sport6.1-Prox1		-	Ampicillin	-	Soruce bioscience
Tet-O-FUW-EGFP	9120	30130	Ampicillin	Zeocin	Marius Wernig
Tet-O-FUW-NeuroD1	9471	30129	Ampicillin	Zeocin	Marius Wernig

Table 2.6: 3rd generation lentiviral packaging plasmid.

Vector backbone	Backbone size w/o insert (bp)	Addgene ID	Resistance	Gene/Insert name	Reference
			Prokaryotic		
pRSV-Rev	4180	12253	Amp	Rev	Didier Trono
pMDLg/pRRE	8895	12251	Amp	HIV-1 GAG/POL	Didier Trono
pMD2.G	5824	12259	Amp	VSV-G; envelope expressing plasmid	Didier Trono

2.2.3 Cell Lines and Primary Cell Culture Stocks

During the project, several cell lines and animal sources were used. Below, some of their characteristics are listed in detail.

Table 2.7: Cell Lines and Primary Cell Culture Used in this Thesis.

Designation	Source	Organism/Tissue	Characteristics
E14 IVC	A gift from Austin Smith lab	Mouse Embryonic Stem Cells (P20)	Adherent Culture
HEK293	System Biosciences; Cat No. LV900A-1-GVO	TN Cell Line[6] (P8-12)	Adherent Culture, Genetically Modified Cell Line
Astrocytes	Heidelberg University, Animal Facility	Cortex of ZP Mouse Postnatal Cortex of ZP Mouse Line	Adherent Culture
Fibroblast cells	Heidelberg University, Animal Facility	E12.5-E13 ZP Mouse Line	Adherent Culture

2.2.3.1 Media and Solutions

All cell culture media and reagents were sterile-filtrated through a Millipore Filtration Unit (Millipore; Billerica, USA) before application.

2.2.3.1.1 Cell Culture medium

2.2.3.1.1.1 Mouse Embryonic Fibroblast Medium

The fibroblast medium was used for the expansion and culture of Mouse Embryonic Fibroblasts (MEFs) (E12.5-E13).

[6] The 293TN cells stably express the SV40 large T antigen and neomycin gene products.

Table 2.8: Mouse Embryonic Feeder (MEF) Expansion Medium

Medium	Concentration	Company
Knockout DMEM	87 %	Life Technology
L-glutamine	1%	Life Technology
Nonessential amino acids	1%	Life Technology
Penicillin-Sreptomycin	1%	Life Technology
2-mercaptoethanol	50 mM	Life Technology
Heat Inactivated FBS	10 %	Life Technology

2.2.3.1.1.2 Mouse Embryonic Stem Cell Culture Medium

Following the objective of this research and the genetic manipulation of ESCs by tetracycline inducible system, the normal ES Fetal Bovine Serum was replaced with tetracycline-free ES Fetal Bovine Serum or the Knockout-Serum replacement during cell culture and ESC expansion after ESC genetic manipulation. It is well known that one of the important factors for the maintenance of ESC in vitro cell culture is the mouse leukemia inhibitory factor (mLIF) which is added freshly to the cell culture media before use.

Table 2.9: ES Medium Culture

Medium and Supplement	Concentration	Company
DMEM High Glucose	77 %	gibco® by Life Technology
L-glutamine	1%	gibco® by Life Technology
Nonessential Amino Acids	1%	gibco® by Life Technology
Penicillin- Streptomycin	1%	gibco® by Life Technology
2-mercaptoethanol	50 mM	Life Technology
Heat Inactivated ES Fetal Bovine Serum (ES-FBS)[7]	20 %	Capricorn Scientific
Recombinant Mouse Leukaemia Inhibitory Factor (mLIF)	10^5 units per 100 mL	Cell Guidance System

[7] The ES-FBS was replaced by tetracycline-free serum.

2.2.3.1.1.3 Freezing Medium for Manipulated Mouse ES Cell Clones

Table 2.10: Freezing medium

Medium and Supplemet	Concentration (%)
mESC Medium Containing FBS-Tet-Free	50%
Heat Inactivated Tet negative Fetal Bovine Serum	40%
DMSO	10%

2.2.3.1.1.4 HEK293 NT Medium

Table 2.11: HEK 293 Medium

Medium and Supplement	Concentration	Company
DMEM High Glucose	88 %	gibco® by Life Technology
Nonessential Amino Acids	1%	gibco® by Life Technology
Penicillin-Streptomycin	1%	gibco® by Life Technology
Heat Inactivated FBS	10 %	Capricorn Scientific

2.2.3.1.1.5 Differentiation medium I

For the committed differentiation of stem cells, a particular cultivation medium is required. This medium has the capacity to conduct the differentiation potential of the cell towards a specified target. This specification is a step-by-step process, so that we implemented a medium which could induce neuro-ectodermal differentiation which is the primary step for a general neural differentiation. Moreover, since neural development and differentiation are progressive complex processes, some specific growth factors and inhibitors including Noggin, SB431542, Cyclopamine, Dkk1, and Dkk3 are required to more committed neuro-ectodermal lineages.

Table 2.12: Differentiation Medium I

Component	Concentration	Company
DMEM/F12	96 %	gibco® by Life Technology
GlutaMAX™-I CTS™ (100X)	1%	gibco® by Life Technology
Nonessential Amino Acids	1%	gibco® by Life Technology
N2 Supplement	1%	gibco® by Life Technology
B27 Supplement	1 %	gibco® by Life Technology
Mouse Recombinant Noggin	500 ng⁄mL	Stemcell™ Technologies
SB431542	10 mM	Stemcell™ Technologies
Cyclopamine	1 mM	Stemcell™ Technologies
Mouse Dkk-1 Protein (57248-M08H)	100 ng⁄mL	Sino Biological, Inc.
Recombinant Mouse Dkk-3 Protein (50247-M08H)	100 ng⁄mL	Sino Biological, Inc.

2.2.3.1.1.6 Differentiation medium II

For a deliberate differentiation of the neuro-progenitor cells, the differentiation medium II was applied. The main difference with the Medium I is the introduction of growth factors BDNF and WNT3a.

Table 2.13: Differentiation Medium II

Component	Concentration	Company
DMEM/F12	96 %	gibco® by Life Technology
GlutaMAX™ -I CTS™ (100X)	1%	gibco® by Life Technology
Nonessential Amino Acids	1%	gibco® by Life Technology
N2 Supplement	1%	gibco® by Life Technology
B27 Supplement	1 %	gibco® by Life Technology
Human Recombinant Brain-Derived Neurotrophic Factor (BDNF)	20 ng⁄mL	Stemcell™Technologies
Recombinant Murine WNT3a	20 ng/mL	PeproTech

2.2.3.1.1.7 Differentiation medium III

For a fully accomplished differentiation and the long-term maintenance of the neuronal culture, the differentiation medium III was utilized.

Table 2.14: Differentiation Medium III

Component	Concentration	Company
BrainPhys™ Neuronal Medium	96 %	Stemcell™ Technologies
L-Glutamax	1%	gibco® by Life Technology
Nonessential amino acids	1%	gibco® by Life Technology
N2 supplement	1%	gibco® by Life Technology
NeuroCult™ SM1 Neuronal Supplement	1 %	Stemcell™ Technologies
Human Recombinant Brain-Derived Neurotrophic Factor (BDNF)	20 ng/mL	Stemcell™ Technologies
Dibutyryl cAMP (db-cAMP)	1mM	Santa Cruz Biotechnology 16980-89-5
		Sigma; D0260
Ascorbic Acid (AA)	200 nM	Sigma; A92902
FBS	1%	Capricorn Scientific
Recombinant Murine WNT-3a	20ng/mL	PeproTech

2.2.3.1.1.8 Astrocyte Medium

The following medium was used for culture and expansion of the astrocyte culture

Table 2.15: Astrocyte Medium

Component	Concentration	Company
IMDM	87%	Stemcell™ Technologies
L-Glutamax	1%	gibco® by Life Technology
Nonessential amino acids	1%	gibco® by Life Technology
Heat Inactivated Fetal Bovine Serum	10%	Capricorn Scientific
Penicillin-Streptomycin	1 %	gibco® by Life Technology

2.2.3.1.1.9 Astrocyte Freezing Medium

Table 2.16: Astrocyte Freezing Medium

Medium	Company	Catalog No.
Cryostem Serum-Free Animal Components-Free Freezing Medium	Biological Industries	05-710-1E

2.2.3.1.1.10 Immunocytochemistry Reagents

Table 2.17: Immunocytochemistry Reagents

Product	Company	Catalog No.
Paraformaldehyde 4% in PBS	ChemCruz	SC-281692
Triton X-100	Merck, Darmstadt	10170
Goat Serum	Gibco	1621024
Donkey Serum	Sigma	D9663
Bovine Serum Albumin (Conzen, Conzen et al.)	Sigma	A9418
Alexa Fluor® 546 goat anti mouse IgG (H+L)	Thermofisher Scientific	A11018
Alexa Fluor® 568 goat anti rabbit IgG (H+L)	Thermofisher Scientific	A11011
Alexa Fluor® 568 goat anti mouse IgG (H+L)	Thermofisher Scientific	A11004
Alexa Fluor® 568 goat anti-chicken	Thermofisher Scientific	A-11041
Goat anti mouse chromeo™ 546	Abcam	Ab60316
Alexa Fluor® Donkey anti Rabbit 647	Thermofisher Scientific or Biolegend	A-31573 406414
4-6-diamidino-2-phenylindole (DAPI)	Sigma-Aldrich	D9542X

2.2.3.1.1.11 Buffers

Table 2.18: The List of the Used Buffers

Buffer	Contents	Concentration
6x loading dye	Tris-Hcl Bromphenolblue(Sigma-Aldrich) Xylene Cyanol (Sigma-Aldrich) Orange G (sigma-Aldrich) Glycerol EDT	10mM 0.03% 0.03% 0.15% 60% 60mM
50x TAE-buffer	Tris-Base or Trizma base EDTA (0.5 M, pH 8) Glacial acetic acid (100%) H2O	2M 10M 5.72%

Table 2.19: Wash Solution (0.1 M Phosphate Buffer, pH 7.3)

Component	Concentration	Amount
Sodium phosphate, monobasic, anhydrous	-	3.74 g
Sodium phosphate, dibasic, heptahydrate	-	10.35 g
MgCl2	2 M	1mL
Deoxycholate	10%	1 mL
NP-40	2%	10 mL
Total Vol.	-	q.s. to 1 L w/ H_2O

Table 2.20: X-gal (5-Bromo-4-chloro-3-indolyl-β-D-galactopyranoside) Stain (125 mL)

Chemical Component	Concentration	Concentration	Vol. (mL)
PBS		0.1M	107.875
X-Gal[8]	40mg/mL in Dimethylformamid (DMF)	1mg/mL	3.125
K3Fe (CN)6	100mM	5mM	6.25
K4Fe(CN)6	100mM	5mM	6.25
MgCl2	2M	2Mm	125
10%Deoxycholate	(0.01%)	0.01%	125
NP-40	2%	0.02%	1.25
Tot Vol.[9]	-	-	122.875 mL

2.2.3.1.1.12 Enzymes, Buffers, Kits and Transfection Reagents

Table 2.21: Enzymes, Buffers, Kits and Transfection Reagents

Product	Company	Catalog No.
Lipofectamine 2000 transfection reagent	Invitrogen™ | Thermo Fisher Scientific	11668027
Miniperp (250)	Qiagen	27106
Endotoxine free Maxi kit (Melief)	Qiagen	12362
GenElute™ Mammalian genomic DNA Miniprep Kits	Sigma	G1N70
RNeasy® Mini kit(50)	Qiagen	74104
DNA Clean & Concentrator™-5	Zymo Reaserh	D4014
Nucleospin250		740615.250
NucleoSpin® Plasmid quickPure	Macherey-Nagel	740615.250

[8] 40 mg/mL X-gal in DMF can be stored at -20˚C.
[9] The solution was sterilized by filtration through a 0.2 µm filter.

QIA quick Gel Extraction kit(50)	Qiagen	8704
Lenti-X ™ Gostix™	TaKaRa Clontech	631243
EcoRI	Biolabs	R0101S
AseI	Biolabs	R0526S
HindIII	Biolabs	R0104L
XmaI	Biolabs	R0180S
MLuI	Biolabs	R0198L
BglII	Biolabs	R0143L
PstI	Biolabs	R0140L
XbaI	Biolabs	R0145L
NheI	Biolabs	R0131L
EcoRI Buffer	Biolabs	B0101S
NEB buffer2.1	Biolabs	B7002S
NEB buffer3.1	Biolabs	B7203S
CutSmart	Biolabs	B7204S
Venor® GeM kit	Minerva Biolabs GmbH	Venor® GeM kit

2.3 Methods

The applied methods in our study include two major categories:

- The molecular biological methods
- The cell culture techniques

2.3.1 Molecular Biological Methods

To study the role of central transcription factors participating in the differentiation of hippocampus DG neurons, the mESCs were manipulated by applying the tetracycline inducible system. This system was primarily introduced by H. Bujard and M. Gossen in 1992 at Heidelberg University. The system has the ability to tightly control individual gene activities which would greatly facilitate the analysis of gene function, particularly in systems that are not prone to genetic dissection (Gossen, Freundlieb et al. 1995).

2.3.1.1 Bacterial Plasmids

We investigated a list of transcription factors contributing to the development of the embryonic DG by using Brain Allen Atlas and Gene Paint data bank. Subsequently, three of the most important transcription factors were selected. These are Emx2, Prox1, and NeuroD1. Some previous studies have proven the reduction in size or even the loss of DG in the absence of these transcription factors (Pellegrini, Mansouri et al. 1996); (Yoshida, Suda et al. 1997); (Miyata, Maeda et al. 1999); (Heng, McLeay et al. 2014).

For the genetic manipulation of the ESCs with the abovementioned transcription factors, the inducible tetracycline system was applied (Fig. 2.1).

The plasmids Tet-O-FUW-NeuroD1 (Fig. 2.2a), Tet-O-FUW-EGFP (Fig. 2.3), FUW-M2rtTA (Fig. 2.4a) were purchased from Addgene.org. The plasmid pCMV-Sport6-Prox1 was purchased from Source Bioscience, and pcDNA3.1-Emx2-cDNA from Invitrogen (Fig. 2.5).

In short, the bacterial plasmids were cultured overnight on an Agar plate containing Ampicillin 50μg/mL at 37° C. Three to five single colonies were picked up from each bacterial culture separately and inoculated into 5 mL LB medium containing Ampicillin early in the evening and were shaken overnight at 37° C.

2.3.1.2 Isolation of Plasmid DNA (Plasmid Mini Preparation)

The small-scale Bacterial DNA plasmid extraction was carried out utilizing Qiagen Mini Kit. according to manufacturer instructions.

2.3.1.3 DNA Concentration Measurement

The concentration of DNA was measured using a spectrophotometer. The absorbance of the nucleic acid solution was measured at the wavelength of $\lambda = 260$ nm.

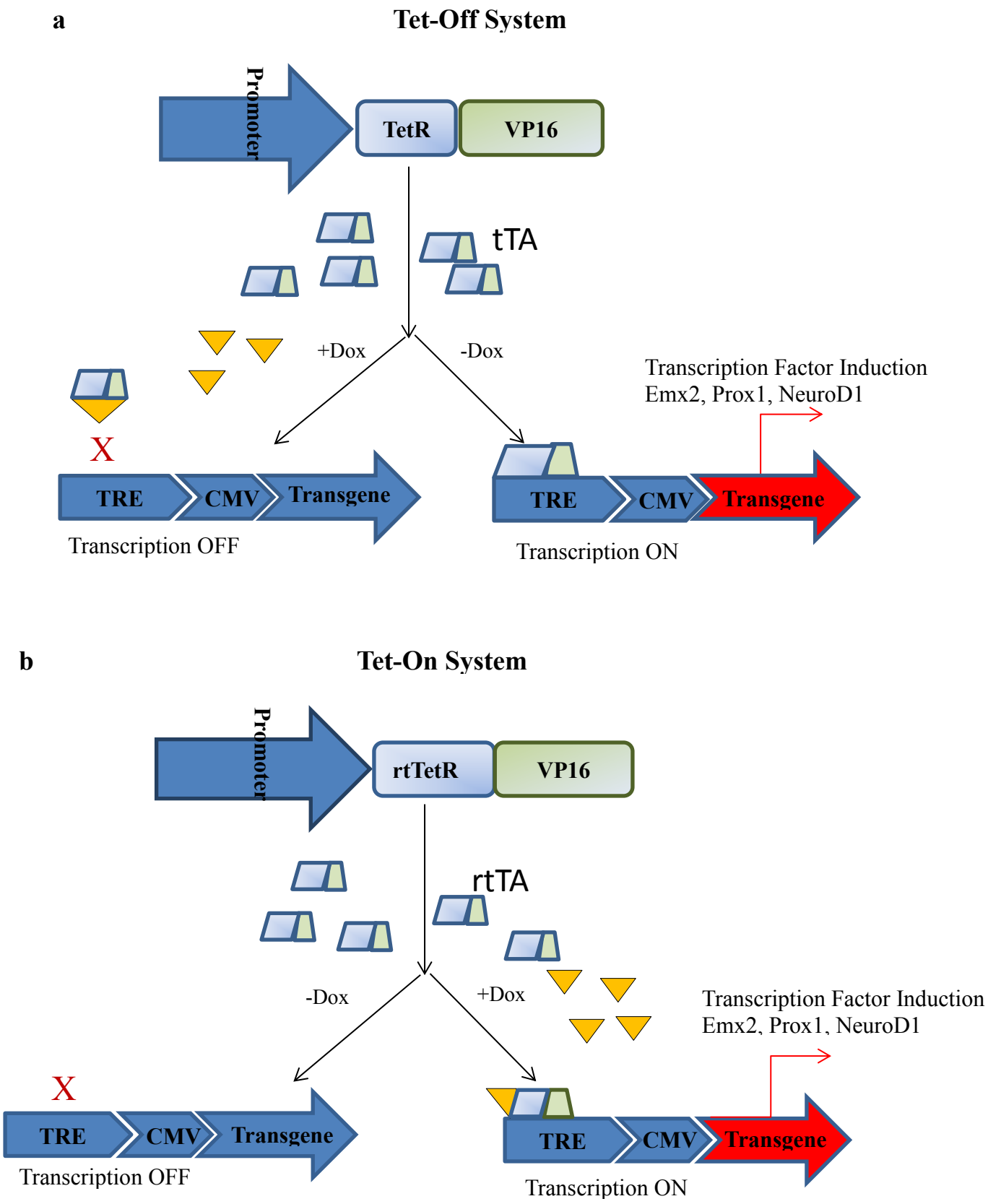

Fig. 2.1 The schematic Tet system. The Tet system can be used for conditional activate gene expression in the mouse. (**A)** the Tet-off system (tTA) will activate expression in the absence of its ligand doxycycline (DOX, shown as brown box). Upon addition of Dox, transcription of the gene of interest is extinguished. (**B)** in contrast, addition of Dox to the Tet-on system (rtTA) results in the transcriptional induction of the gene of interest. tTA, tetracycline-dependent transactivator; rtTA, reverse tetracycline-dependent transactivator; Dox, doxycycline (ligand); TRE, Tet-responsive element.

2.3.1.4 Plasmid Construct and Restriction Enzyme Digestion

To find out whether the plasmid construction map during the bacterial culture remained intact or not (no recombination), it is necessary that after bacterial mini-prep, the plasmid DNA extraction be digested using specific restriction enzymes, as recommended by the manufacturer. To check the correct orientation and length of the inserted DNA, a sample of 0.5 µg/µL plasmid DNA was digested with 5 units of restriction enzyme (purchased from New England BioLabs). The digests were normally incubated in the appropriate buffer (Table 2.22b and 2.23b) at 37° C for 1-1.5 hours. Finally, the digested DNA fragments were analyzed by 0.8% Agarose gel electrophoresis (Figs. 2.2b and 4.2b).

Table 2.22: The Overview of Tet-O-FUW-NeuroD1 restriction digestion

RE	Cutting Site 5′ to 3′	Fragment Size (bp)
AseI	30-5954,5955-6354,6355-7198, 7199-7257,7258-8492,8493-29	5925,400,844,59,1235,1008
BglII	624-2365,2366-4690,4691-5064, 5064-9255,9256-623	1742,2325,374,4191,839
EcoRI	2819-6304,6305-6500,	1090,8381
XmaI	2677-6304,6305-6500,6501-2676	3628,196,5647
SacI	8801-8800	9471

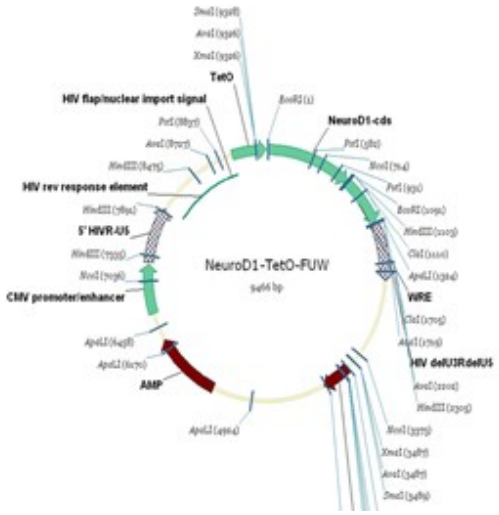

Fig. 2.2a Lentivirus Addgene Plasmid; Tet-O-FUW- NeuroD1.

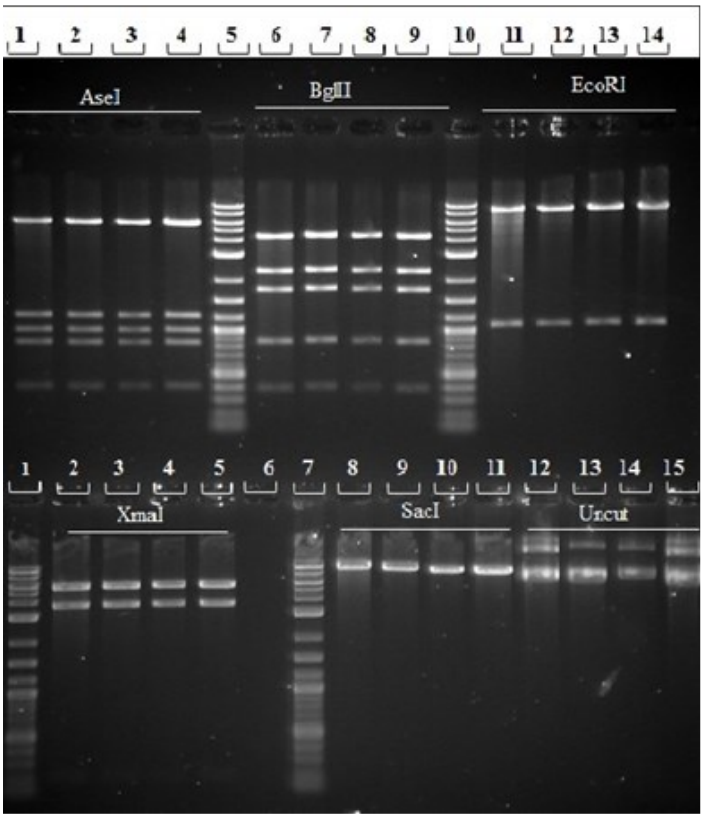

Fig. 2.2b Tet-O-FUW-NeuroD1 (19471 bp) clone 1-4 were digested with AseI, BglII, EcoRI, XmaI, SacI. **First Row AseI** (Line1-4), BglII (Line 6-9), EcoRI (Line 11-14)
Second Row XmaI (Line 2-5), SacI (Line 8-11), uncut(Line 12-15). 2-Log DNA Ladder.

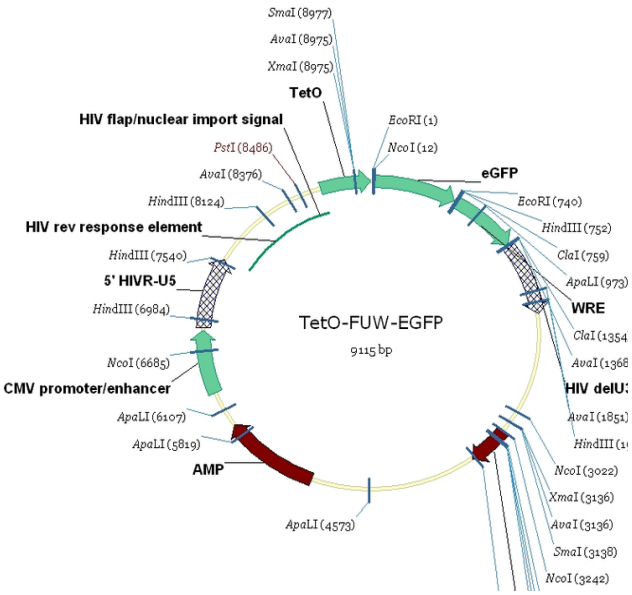

Fig.2.3 Lentivirus Addgene Plasmid; Tet-O-FUW-EGFP; Construction Map

Table 2.23: Overview of FUW-M2rtTA restriction digestion

RE	Cutting Site 5′ to 3′	Fragment Size
BglII	14-852, 853-2614, 2615-5401, 5402-5775, 5776-13	839, 1762, 2787, 374, 2217
AseI	259- 3850, 3851-7229, 7230-258	3592, 3379, 1008
XmaI	3843-459, 4599-3842	756, 7223

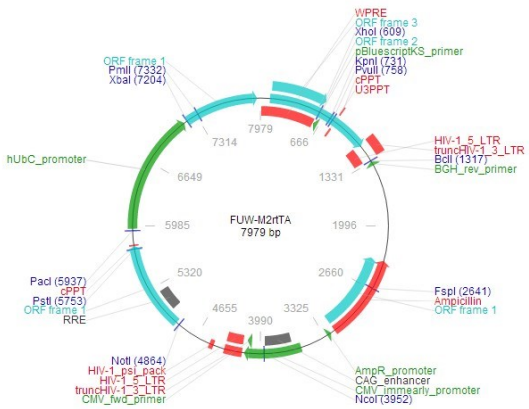

Fig. 2.4a Lentivirus Trans-activator Adgene Plasmid; FUW-M2rtTA Construction Map.

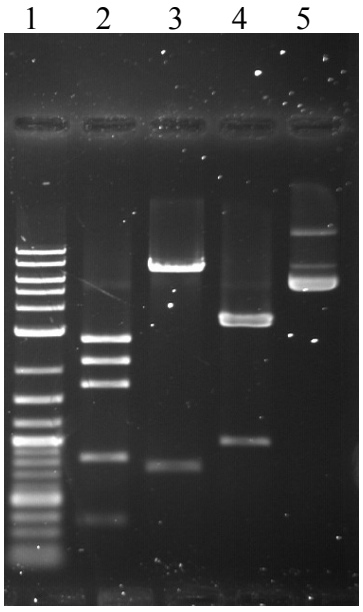

Fig. 2.4b FUW-M2rtTA were digested with, BglII (Lane 2), XmaI (Lane 3), AseI (Lane 4), uncut (Lane 5), 2-log DNA ladder (Lane 1).

2.3.1.5 Cloning of the Emx2 and Prox1-fragments into Tet-O-FUW-vector

Dr. Zhou, a postdoctoral scholar at the group of Prof. Skutella assisted the author to construct the new plasmids Tet-O-FUW-Emx2 and Tet-O-FUW-Prox1. These new plasmids were constructed by direct cloning of Emx2 (extracted from pcDNA3.1-Emx2) and Prox1 (extracted from CMV-Sport6-Prox1) into the backbone of Tet-O-FUW-NeuroD1.

In summary, Emx2 and Prox1 fragments were digested from the original plasmids, and were cut and extracted from 1.5 % Agarose gel. Then the target DNA plasmid was extracted from the gel and cleaned with clean-up-DNA-kit, according to the manufacturer instruction.

Subsequently, the extracted DNA was amplified by PCR (Table 2.24). The molecular manipulations such as extraction, purification, digestion, and ligation as well as the bacterial culture and transformation were performed according to standard methods.

Table 2.24: Primer Sequences for Emx2 and Prox1-fragment Cloning

Oligo Name	Sequence (5'-3')
AgeI_Prox1-f	AACCGGTGCCACCATGCCTGACCATGACAGC
MLuI_Prox1-r	CGACGCGTCTACTCGTGAAGGAGTTCTTGTAG
XmaI_Kozak_Emx2-f	CCCCCGGGCCACCATGTTTCAGCCGGCGCCCAAGCGC
MLuI_Emx2-r	CGACGCGTAATCGTCTGAGGTCACATCTATTTCC
MLuI_Emx2-f	CGACGCGTCTAATCGTGAAAGATGGACTTAAG
BglII_Prox1-f	AGTTCGAGTGTGGAGATCTTCAAG

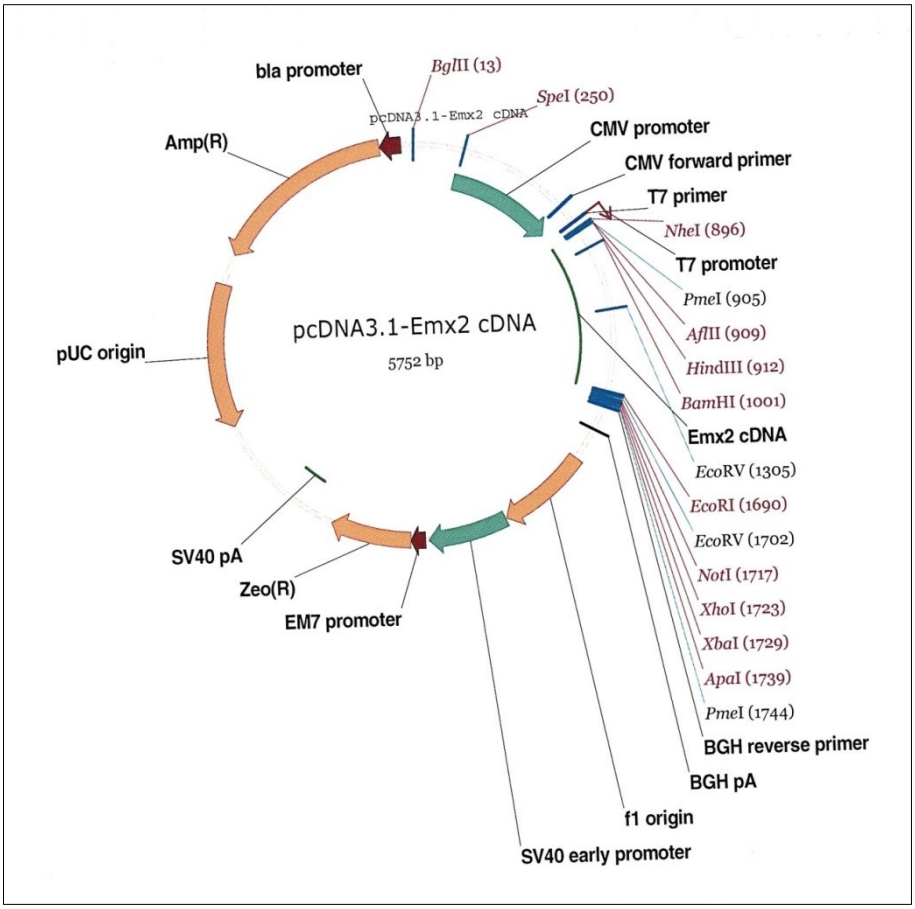

Fig. 2.5: pcDNA3.1 Emx2 Plasmid Construction Map

2.3.1.6 Bacterial Transformation

The obtained DNA plasmids mentioned above were transformed in One Shot® Stbl3TM chemically competent E-coli strains. Then, five individual colonies were picked up and inoculated in a LB medium overnight, containing 50 µg/mL Ampicillin, at 31° C, while being shaken.

Afterwards, the DNA plasmid extraction was performed with Qiagen mini kits. At the end, the DNA concentrations were estimated by measuring absorption at 260 nm using the spectrophotometer and analyzed by double restriction digestion and DNA sequencing.

To check the correct orientation and length of the inserted DNA, a sample of 0.5 µg/µL plasmid DNA was digested with 5 units of restriction enzyme (purchased from New England Biolabs). The digests were normally incubated in an appropriate buffer (Table 2.25) at 37° C for 1-1.5 hours. Afterwards, the digested DNA fragments were analyzed by 0.8% Agarose gel electrophoresis.

Table 2.25: The Overview of Tet-O-FUW-Prox1 and Tet-O-FUW–Emx2 Double restriction

	Tet-O-fuw-Prox1		**Tet-O-fuw-Emx2**		
RE	Cutting site 5′ to 3′	Fragment Size (bp)	RE	Cutting site 5′ to 3′	Fragment Size (bp)
MulI	**7769**	**5536, 5073**	**MulI**	**6352**	**2820, 6345**
XbaI	**2227**		**NheI**	**70**	

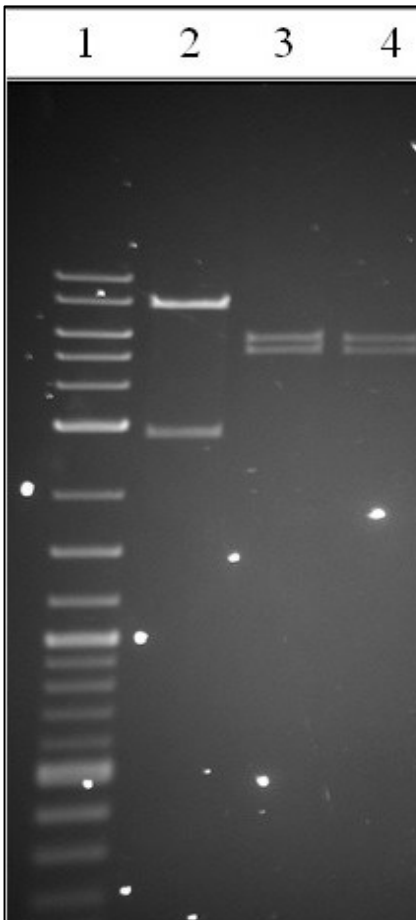

Fig. 2.6a The Result of Tet-O-FUW-Prox1 (10906 bp) and Tet-O-FUW-Emx2 (9165bp), Double Digestion with MulI+Xba (Lane 3, 4) and MulI + NheI (Lane 2), log2DNAladder (Lane 1).

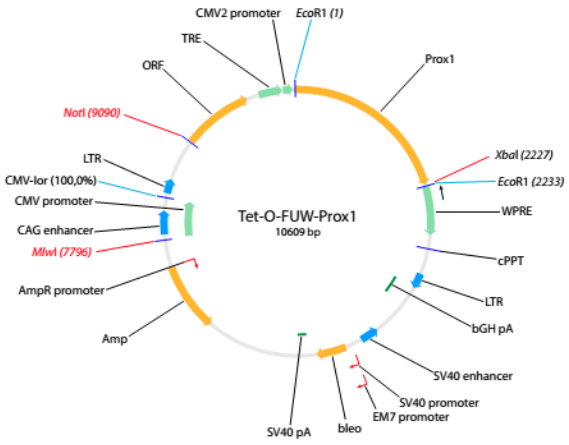

Fig. 2.6b Tet-O-FUW-Prox1 Plasmid Construction Map.

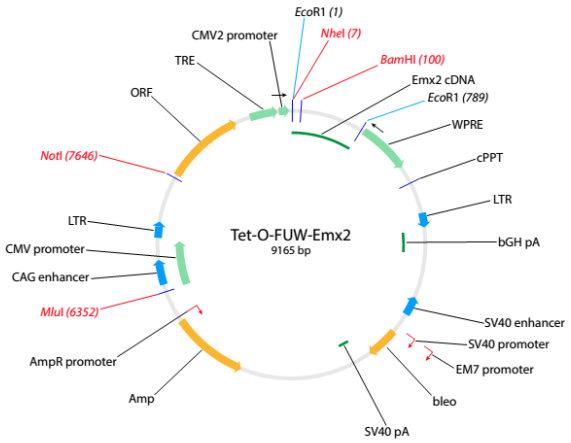

Fig. 2.7 Tet-O-FUW-Emx2 Plasmid Construction Map.

The Eurofins MWG Operon performed all sequencing analyses using the primers mentioned in Table 2.26. The sequencing results were aligned with ClastalW2 database are shown below.

Table 2.26: The Primers for DNA Sequencing

Primer	Sense (5′-to-3′)
CMVb-F	AGC TCG TTT AGT GAA CCG TC
WPRE-R	CAT ACG GGA AGC AAT AGC ATG
Prox1-SF1	GGG TTG AGA ATA TCA TTC GG
Prox1-SF3	TCA GAG TCC ACT AGG TGC TC
Prox1-SR2	GAA GAT CTC CAC ACT CAG AC

2.3.1.8 Gene Sequencing Alignment Data

Prox1

Tet-O-FUW-Prox1 Clone 4 Sequence Alignment

```
Prox1_ORF       ------------------------------------------------------------
Tet-Prox1       TCACGCTGTTTTGACCTCCATAGAAGACACCGGGACCGATCCAGCCTCCGCGGCCCCGAA 60

Prox1_ORF       ---------ATGCCTGACCATGACAGCACAGCCCTCTTAAGCCGGCAAACCAAGAGGAGA 51
Tet-Prox1       TTCGCCACCATGCCTGACCATGACAGCACAGCCCTCTTAAGCCGGCAAACCAAGAGGAGA 120
                         **************************************************

Prox1_ORF       AGGGTTGACATTGGAGTGAAAAGGACGGTAGGGACAGCATCTGCATTTTTTGCTAAGGCA 111
Tet-Prox1       AGGGTTGACATTGGAGTGAAAAGGACGGTAGGGACAGCATCTGCATTTTTTGCTAAGGCA 180
                ************************************************************

Prox1_ORF       AGGGCAACATTTTTCAGTGCCATGAATCCCCAAGGTTCAGAGCAGGATGTTGAATATTCT 171
Tet-Prox1       AGGGCAACATTTTTCAGTGCCATGAATCCCCAAGGTTCAGAGCAGGATGTTGAATATTCT 240
                ************************************************************

Prox1_ORF       GTGGTGCAACACGCAGATGGGGAAAAGTCGAACGTACTCCGCAAGCTGCTGAAGAGGGCG 231
Tet-Prox1       GTGGTGCAACACGCAGATGGGGAAAAGTCGAACGTACTCCGCAAGCTGCTGAAGAGGGCG 300
                ************************************************************

Prox1_ORF       AACTCGTATGAAGATGCCATGATGCCTTTTCCAGGAGCAACTATAATTTCCCAGCTGTTG 291
Tet-Prox1       AACTCGTATGAAGATGCCATGATGCCTTTTCCAGGAGCAACTATAATTTCCCAGCTGTTG 360
                ************************************************************

Prox1_ORF       AAAAATAACATGAACAAAAACGGTGGCACCGAGCCCAGTTTCCAAGCCAGCGGACTCTCT 351
Tet-Prox1       AAAAATAACATGAACAAAAACGGTGGCACCGAGCCCAGTTTCCAAGCCAGCGGACTCTCT 420
                ************************************************************

Prox1_ORF       AGCACAGGCTCCGAAGTACATCAGGAGGATATATGTAGCAACTCTTCAAGAGACAGCCCC 411
Tet-Prox1       AGCACAGGCTCCGAAGTACATCAGGAGGATATATGTAGCAACTCTTCAAGAGACAGCCCC 480
                ************************************************************

Prox1_ORF       CCAGAGTGTCTTTCCCCTTTTGGCAGGCCTACTATGAGCCAGTTTGATGTGGATCGCTTA 471
Tet-Prox1       CCAGAGTGTCTTTCCCCTTTTGGCAGGCCTACTATGAGCCAGTTTGATGTGGATCGCTTA 540
                ************************************************************

Prox1_ORF       TGTGATGAGCACCTGAGAGCAAAGCGCGCCCGGGTTGAGAATATCATTCGGGGTATGAGC 531
Tet-Prox1       TGTGATGAGCACCTGAGAGCAAAGCGCGCCCGGGTTGAGAATATCATTCGGGGTATGAGC 600
                ************************************************************

Prox1_ORF       CATTCCCCCAGTGTGGCATTAAGGGGCAATGAAAACGAAAGAGAGATGGCCCCGCAGTCT 591
Tet-Prox1       CATTCCCCCAGTGTGGCATTAAGGGGCAATGAAAACGAAAGAGAGATGGCCCCGCAGTCT 660
                ************************************************************

Prox1_ORF       GTGAGTCCCCGAGAAAGTTACAGAGAAAACAAACGCAAGCAGAAGCTGCCCCAGCAGCAG 651
Tet-Prox1       GTGAGTCCCCGAGAAAGTTACAGAGAAAACAAACGCAAGCAGAAGCTGCCCCAGCAGCAG 720
                ************************************************************

Prox1_ORF       CAACAGAGTTTCCAGCAGCTGGTTTCAGCCCGAAAAGAACAGAAGCGAGAGGAGCGCCGA 711
Tet-Prox1       CAACAGAGTTTCCAGCAGCTGGTTTCAGCCCGAAAAGAACAGAAGCGAGAGGAGCGCCGA 780
                ************************************************************

Prox1_ORF       CAGCTGAAACAGCAGCTGGAAGACATGCAGAAGCAGCTGCGCCAGCTGCAGGAGAAGTTC 771
Tet-Prox1       CAGCTGAAACAGCAGCTGGAAGACATGCAGAAGCAGCTGCGCCAGCTGCAGGAGAAGTTC 840
                ************************************************************

Prox1_ORF       TACCAGGTCTATGACAGCACAGACTCCGAAAATGATGAAGATGGCGACCTGTCTGAAGAC 831
Tet-Prox1       TACCAGGTCTATGACAGCACAGACTCCGAAAATGATGAAGATGGCGACCTGTCTGAAGAC 900
                ************************************************************

Prox1_ORF       AGCATGCGCTCGGAGATCCTGGATGCACGGGCCCAGGACTCGGTGGGGCGCTCAGACAAT 891
Tet-Prox1       AGCATGCGCTCGGAGATCCTGGATGCACGGGCCCAGGACTCGGTGGGGCGCTCAGACAAT 960
                ************************************************************

Prox1_ORF       GAGATGTGTGAGCTGGACCCAGGGCAGTTCATCGACAGGGCCCGAGCCCTAATCAGGGAG 951
Tet-Prox1       GAGATGTGTGAGCTGGACCCAGGGCAGTTCATCGACAGGGCCCGAGCCCTAATCAGGGAG 1020
                ************************************************************
```

```
Prox1_ORF       CAGGAGATGGCTGAGAACAAGCCTAAGCGAGAAGGCAGCAACAAAGAAAGAGACCACGGG 1011
Tet-Prox1       CAGGAGATGGCTGAGAACAAGCCTAAGCGAGAAGGCAGCAACAAAGAAAGAGACCACGGG 1080
                ************************************************************

Prox1_ORF       CCAAACTCCTTGCAGCCAGAAGGCAAGCATCTGGCAGAGACCTTAAAACAGGAGCTGAAC 1071
Tet-Prox1       CCAAACTCCTTGCAGCCAGAAGGCAAGCATCTGGCAGAGACCTTAAAACAGGAGCTGAAC 1140
                ************************************************************

Prox1_ORF       ACGGCCATGTCGCAGGTTGTGGACACGGTGGTCAAAGTCTTCTCAGCCAAACCCTCTCGC 1131
Tet-Prox1       ACGGCCATGTCGCAGGTTGTGGACACGGTGGTCAAAGTCTTCTCAGCCAAACCCTCTCGC 1200
                ************************************************************

Prox1_ORF       CAGGTTCCTCAGGTCTTCCCACCTCTCCAGATCCCCCAGGCCAGATTCGCAGTCAACGGG 1191
Tet-Prox1       CAGGTTCCTCAGGTCTTCCCACCTCTCCAGATCCCCCAGGCCAGATTCGCAGTCAACGGG 1260
                ************************************************************

Prox1_ORF       GAAAACCACAATTTCCACACGGCCAACCAGCGCCTGCAATGCTTTGGTGATGTCATCATT 1251
Tet-Prox1       GAAAACCACAATTTCCACACGGCCAACCAGCGCCTGCAATGCTTTGGTGATGTCATCATT 1320
                ************************************************************

Prox1_ORF       CCGAACCCCTTGGACACCTTTGGCAGTGTGCAGATGCCTAGTTCCACAGACCAGACGGAA 1311
Tet-Prox1       CCGAACCCCTTGGACACCTTTGGCAGTGTGCAGATGCCTAGTTCCACAGACCAGACGGAA 1380
                ************************************************************

Prox1_ORF       GCCCTTCCCCTGGTGGTCCGAAAAAACTCATCCGAGCAATCTGCCTCTGGCCCGGCCACT 1371
Tet-Prox1       GCCCTTCCCCTGGTGGTCCGAAAAAACTCATCCGAGCAATCTGCCTCTGGCCCGGCCACT 1440
                ************************************************************

Prox1_ORF       GGCGGCCACCACCAGCCCCTGCACCAGTCACCCCTCTCCGCCACTGCAGGCTTCACCACC 1431
Tet-Prox1       GGCGGCCACCACCAGCCCCTGCACCAGTCACCCCTCTCCGCCACTGCAGGCTTCACCACC 1500
                ************************************************************

Prox1_ORF       CCTAGCTTCCGCCATCCCTTTCCCCTGCCCTTGATGGCTTATCCATTTCAGAGTCCACTA 1491
Tet-Prox1       CCTAGCTTCCGCCATCCCTTTCCCCTGCCCTTGATGGCTTATCCATTTCAGAGTCCACTA 1560
                ************************************************************

Prox1_ORF       GGTGCTCCCTCCGGCTCCTTCTCGGGGAAGGACAGAGCCTCTCCTGAGTCCTTAGACTTG 1551
Tet-Prox1       GGTGCTCCCTCCGGCTCCTTCTCGGGGAAGGACAGAGCCTCTCCTGAGTCCTTAGACTTG 1620
                ************************************************************

Prox1_ORF       ACTCGGGACACAACAAGTCTGAGGACCAAGATGTCATCACACCATCTGAGCCACCACCCC 1611
Tet-Prox1       ACTCGGGACACAACAAGTCTGAGGACCAAGATGTCATCACACCATCTGAGCCACCACCCC 1680
                ************************************************************

Prox1_ORF       TGTTCACCAGCACACCCACCCAGCACCGCAGAAGGACTCTCTTTGTCACTCATAAAGTCT 1671
Tet-Prox1       TGTTCACCAGCACACCCACCCAGCACCGCAGAAGGACTCTCTTTGTCACTCATAAAGTCT 1740
                ************************************************************

Prox1_ORF       GAGTGTGGAGATCTTCAAGATATGTCCGACATCTCACCTTATTCAGGAAGCGCAATGCAG 1731
Tet-Prox1       GAGTGTGGAGATCTTCAAGATATGTCCGACATCTCACCTTATTCAGGAAGCGCAATGCAG 1800
                ************************************************************

Prox1_ORF       GAAGGGCTATCACCCAATCACTTGAAAAAGGCAAAACTCATGTTCTTTTACACCCGCTAC 1791
Tet-Prox1       GAAGGGCTATCACCCAATCACTTGAAAAAGGCAAAACTCATGTTCTTTTACACCCGCTAC 1860
                ************************************************************

Prox1_ORF       CCCAGCTCCAACATGCTGAAGACCTACTTCTCGGACGTGAAGTTCAACAGATGCATTACC 1851
Tet-Prox1       CCCAGCTCCAACATGCTGAAGACCTACTTCTCGGACGTGAAGTTCAACAGATGCATTACC 1920
                ************************************************************

Prox1_ORF       TCGCAGCTCATCAAGTGGTTCAGCAATTTCCGTGAGTTTTACTATATCCAGATGGAGAAG 1911
Tet-Prox1       TCGCAGCTCATCAAGTGGTTCAGCAATTTCCGTGAGTTTTACTATATCCAGATGGAGAAG 1980
                ************************************************************

Prox1_ORF       TATGCGCGTCAAGCCATCAATGATGGAGTCACCAGTACAGAAGAGCTCTCCATCACCAGG 1971
Tet-Prox1       TATGCGCGTCAAGCCATCAATGATGGAGTCACCAGTACAGAAGAGCTCTCCATCACCAGG 2040
                *************************************************************

Prox1_ORF       GATTGTGAGCTATACCGAGCCCTCAACATGCACTACAACAAAGCAAATGACTTTGAGGTT 2031
Tet-Prox1       GATTGTGAGCTATACCGAGCCCTCAACATGCACTACAACAAAGCAAATGACTTTGAGGTT 2100
                ************************************************************

Prox1_ORF       CCAGAGAGATTCCTGGAAGTTGCGCAGATCACGTTACGGGAGTTTTTCAATGCCATCATC 2091
Tet-Prox1       CCAGAGAGATTCCTGGAAGTTGCGCAGATCACGTTACGGGAGTTTTTCAATGCCATCATC 2160
                ************************************************************

Prox1_ORF       GCGGGCAAAGATGTTGATCCTTCCTGGAAGAAGGCCATTTACAAGGTCATCTGCAAGCTG 2151
```

```
Tet-Prox1       GCGGGCAAAGATGTTGATCCTTCCTGGAAGAAGGCCATTTACAAGGTCATCTGCAAGCTG 2220
                ************************************************************

Prox1_ORF       GATAGTGAAGTTCCTGAGATTTTCAAATCCCCTAACTGCCTACAAGAACTCCTTCACGAG 2211
Tet-Prox1       GATAGTGAAGTTCCTGAGATTTTCAAATCCCCTAACTGCCTACAAGAACTCCTTCACGAG 2280
                ************************************************************

Prox1_ORF       TAG------------------------------------------------------- 2214
Tet-Prox1       TAGTCTAGAGAATTCGATATCAAGCTTATCGATAATCAACCTCTGGATTACAAAATTTGT 2340
                ***

Prox1_ORF       ------------------------------------------------------------
Tet-Prox1       GAAAGATTGACTGGTATTCTTAACTATGTTGCTCCTTTTACGCTATGTGGATACGCTGCT 2400


Prox1_ORF       ------------------------------------------------------------
Tet-Prox1       TTAATGCCTTTGTATCATGCTATTGCTTCCCGTATGGCTTTCATTTTCTCCTCCTTGTAT 2460


Prox1_ORF       ---------------------------------------------
Tet-Prox1       AATCCTGGTTGCTGTCTCTTTATGAGGAGTTGTGGCCCGTTGTCAGC 2507
```

Emx2

Emx2 Clone 13 Sequence Alignment

```
Emx2            CACGCTGTTTTGACCTCCATAGAAGACACCGGGACCGATCCAGCCTCCGCGGCCCCGAAT 60
gene            ------------------------------------------------------------


Emx2            TCGCTAGCCACCATGTTTCAGCCGGCGCCCAAGCGCTGCTTCACCATCGAGTCGCTGGTG 120
gene            ------------ATGTTTCAGCCGGCGCCCAAGCGCTGCTTCACCATCGAGTCGCTGGTG 48
                            ********************************************

Emx2            GCCAAGGACAGTCCCCTGCCTGCCTCGCGCTCCGAGGATCCCATCCGTCCCGCGGCACTC 180
gene            GCCAAGGACAGTCCCCTGCCTGCCTCGCGCTCCGAGGATCCCATCCGTCCCGCGGCACTC 108
                ************************************************************

Emx2            AGCTACGCCAATTCCAGTCCCATAAATCCGTTCCTCAACGGCTTCCACTCGGCCGCCGCC 240
gene            AGCTACGCCAATTCCAGTCCCATAAATCCGTTCCTCAACGGCTTCCACTCGGCCGCCGCC 168
                ************************************************************

Emx2            GCCGCCGCCGCCGGCAGGGGCGTCTACTCCAACCCGGACTTGGTGTTCGCCGAGGCGGTC 300
gene            GCCGCCGCCGCCGGCAGGGGCGTCTACTCCAACCCGGACTTGGTGTTCGCCGAGGCGGTC 228
                ************************************************************

Emx2            TCGCACCCGCCCAACCCCGCCGTGCCGGTGCACCCGGTGCCGCCGCCGCACGCCCTGGCC 360
gene            TCGCACCCGCCCAACCCCGCCGTGCCGGTGCACCCGGTGCCGCCGCCGCACGCCCTGGCC 288
                ************************************************************

Emx2            GCCCACCCCCTGCCCTCCTCGCATTCGCCACACCCCCTCTTCGCCTCGCAGCAGCGGGAC 420
gene            GCCCACCCCCTGCCCTCCTCGCATTCGCCACACCCCCTCTTCGCCTCGCAGCAGCGGGAC 348
                ************************************************************

Emx2            CCGTCCACCTTCTACCCCTGGCTCATCCACCGCTACCGATATCTGGGTCATCGCTTCCAA 480
gene            CCGTCCACCTTCTACCCCTGGCTCATCCACCGCTACCGATATCTGGGTCATCGCTTCCAA 408
                ************************************************************

Emx2            GGGAACGACACAAGTCCCGAGAGTTTCCTTTTGCACAACGCTCTGGCCAGAAAGCCAAAG 540
gene            GGGAACGACACAAGTCCCGAGAGTTTCCTTTTGCACAACGCTCTGGCCAGAAAGCCAAAG 468
                ************************************************************

Emx2            CGGATTCGAACCGCCTTCTCGCCGTCCCAGCTTTTAAGGCTAGAGCACGCTTTTGAGAAG 600
gene            CGGATTCGAACCGCCTTCTCGCCGTCCCAGCTTTTAAGGCTAGAGCACGCTTTTGAGAAG 528
                ************************************************************

Emx2            AACCATTACGTGGTGGGAGCGGAAAGGAAGCAGCTGGCTCACAGTCTCAGTCTTACGGAA 660
gene            AACCATTACGTGGTGGGAGCGGAAAGGAAGCAGCTGGCTCACAGTCTCAGTCTTACGGAA 588
                ************************************************************

Emx2            ACTCAGGTAAAAGTATGGTTTCAGAACCGGAGAACGAAATTCAAAAGGCAAAAGCTAGAG 720
gene            ACTCAGGTAAAAGTATGGTTTCAGAACCGGAGAACGAAATTCAAAAGGCAAAAGCTAGAG 648
                ************************************************************

Emx2            GAAGAAGGCTCAGATTCTCAACAGAAGAAAAAAGGGACACACCACATTAACCGGTGGAGA 780
gene            GAAGAAGGCTCAGATTCTCAACAGAAGAAAAAAGGGACACACCACATTAACCGGTGGAGA 708
                ************************************************************

Emx2            ATTGCTACCAAGCAG-CGAGTCCGGAGGAAATAGATGTGACCTCAGACGATTAA TCTAAA 839
gene            ATTGCTACCAAGCAGGCGAGTCCGGAGGAAATAGATGTGACCTCAGACGATTAA------ 762
                ***************  ***********************************

Emx2            GGGCGAATTCGATATCAAGCTTATCGATAATCAACCTCTGGATTA 884
gene            ---------------------------------------------
```

2.3.1.9 Plasmid Mini & Maxi Preparation

Following the sequencing alignment, the selected colonies were used as a reference point for the initial cultures (5 mL mini-prep plasmids in large scale production).
The small- and large-scale plasmid preparations were carried out utilizing Qiagen mini kits and endotoxin-free Qiagen maxi kits.

2.4 Cell Culture Methods

In general, the cell culture was performed under sterile conditions in two steps; first, the pseudo lenti-virus particle production, and second, the ESC transduction and differentiation.

2.4.1 Lentivirus Preparation, Titration and Usage

In this study, the use of lentiviral vectors was in accordance with the guidelines of the Ethical Committee of Heidelberg University, Graduate School of Medicine. The lentiviruses were prepared and tittered as described by Verma, IM et al. (Abeldano, Tiscornia et al. 2006) and (Anderson, Cohen et al. 2009) with minor modifications.

2.4.1.1 Lentiviral Plasmids and Packaging Constructs

The plasmids pMDL g/pRRE, pRSV-Rev, and pMD2.G were purchased from Addgene.
To obtain enough lentiviral packaging plasmid DNA for the viral vector productions, the bacteria were cultivated overnight, as a streak culture on an Agar medium containing 50 µg/mL Ampicillin (50 µg/mL) at 37°C. The next day, the single bacteria colonies were picked up and inoculated in 5 mL LB medium supplemented with Ampicillin (50 µg/mL) whilst shaking overnight at 37°C.
After 24 hours, the plasmids were isolated from 1 mL of bacterial culture using the mini kit (Qiagen mini kits) and analyzed by restriction digestion.
The rest of the bacterial culture was utilized for large scale production of plasmids and inoculated in a 400 mL LB medium supplemented with Ampicillin (50 µg/mL) whilst shaking overnight at 37°C. Subsequently, plasmids were isolated with an endotoxin-free maxi kit (Qiagen kits) as specified by the manufacturer.

Table 2.27: The Overview of Packaging Plasmid restriction digestion

Packaging Plasmid					
pMDLg/pRRE (8890bp) (Plasmid #12251)			Prsv-Rev (4180bp) (Plasmid #12253)		
RE	**Cutting Site 5' to 3'**	**Fragment Size (bp)**	**RE**	**Cutting Site 5' to 3'**	**Fragment Size (pb)**
Pst 1	1928-3351 3352-1927	1424 7466	**EoRI**	2024-2334 2335-2023	311 3869
EcoRI	1277-5611 5612-6012 6013-1276	4335 401 4154			
HindIII	697-1593 1594-2220 2221-6001 6002-696	897 627 3781 3585	**AseI**	606-1840 1841-1899 1900-605	1235 59 2886

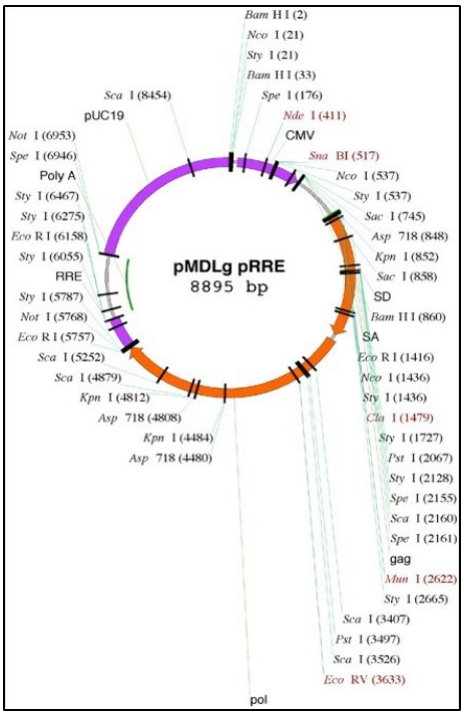

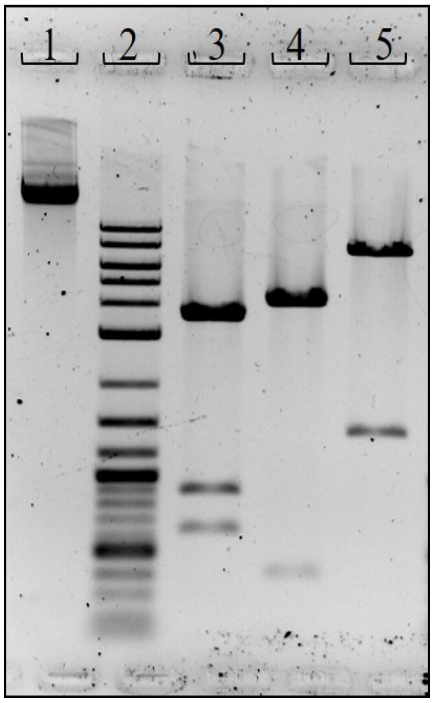

Fig. 2.8a pMDLg-pRRE Plasmid Construction Map.

Fig.2.8b pMDLg-pRRE (8895 bp) digested with HindIII (Lane 3), EcoRI (Lane 4), Pst1 (Lane 5), Uncut (Lane 1).

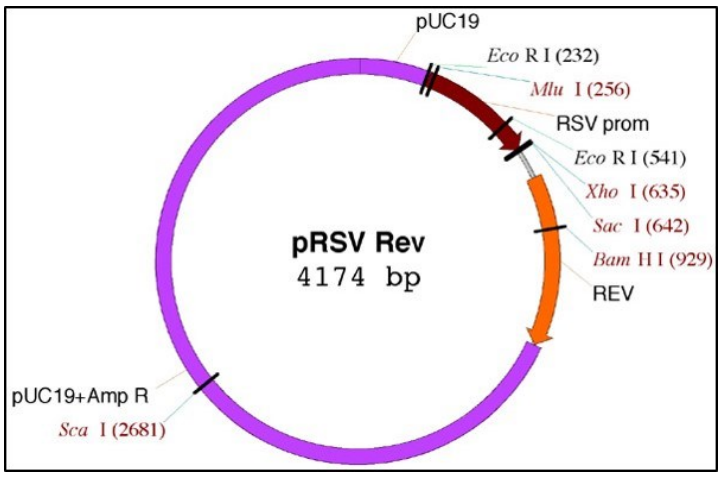

Fig. 2.8c pRSV Rev Plasmid Construction Map

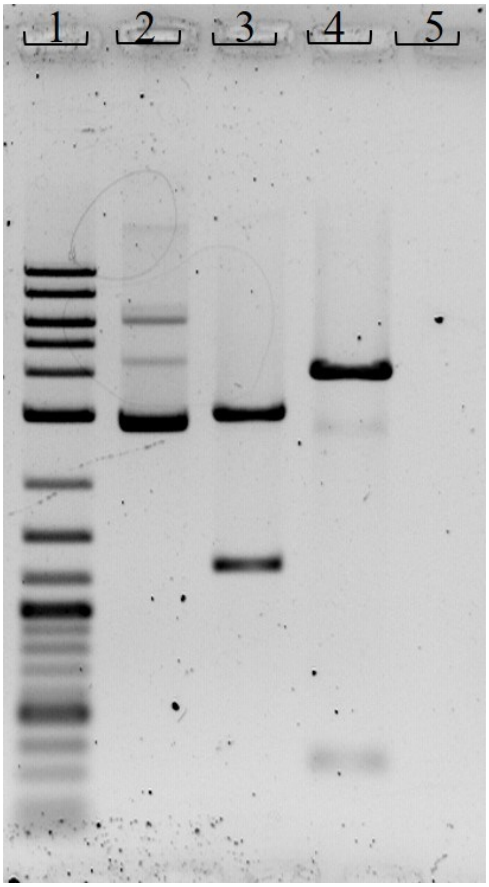

Fig. 2.8d pRSV Rev digested with AseI (Lane 3), EcoRI (Lane 4). Uncut (Lane 2), 2log DNA Marker (Lane 1)

Table 2.28: The Overview of pMD2.G

RE	pMD2.G (5822 bp) (Plasmid # 12259)	
	Cutting Site 5' to 3'	Fragment Size (bp)
SwaI	1192-5270 5271-1191	4079 1743
BglII	1771-5115 5116-1770	3345 2477
AseI	2957-3889 3890-2956	933 4889
EcoRI	968-5121 5122-967	4154 1668

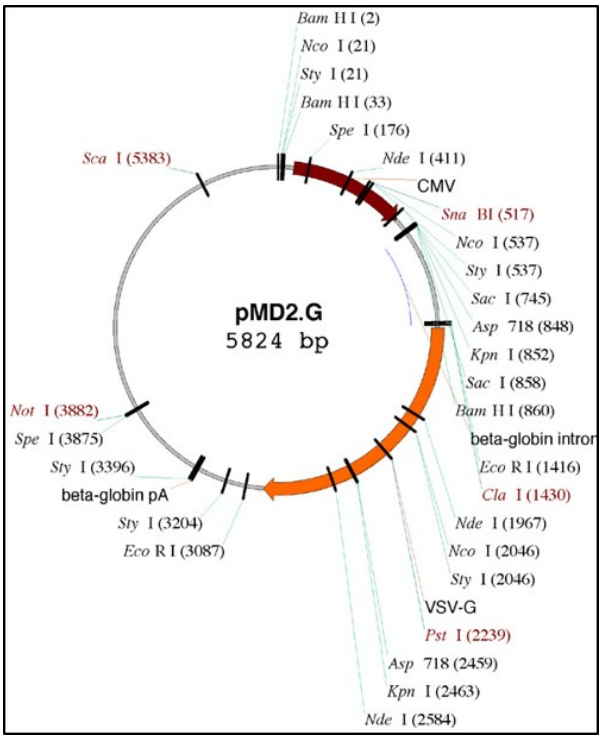

Fig. 2.9a The structure of pMD2.G DNA Plasmid

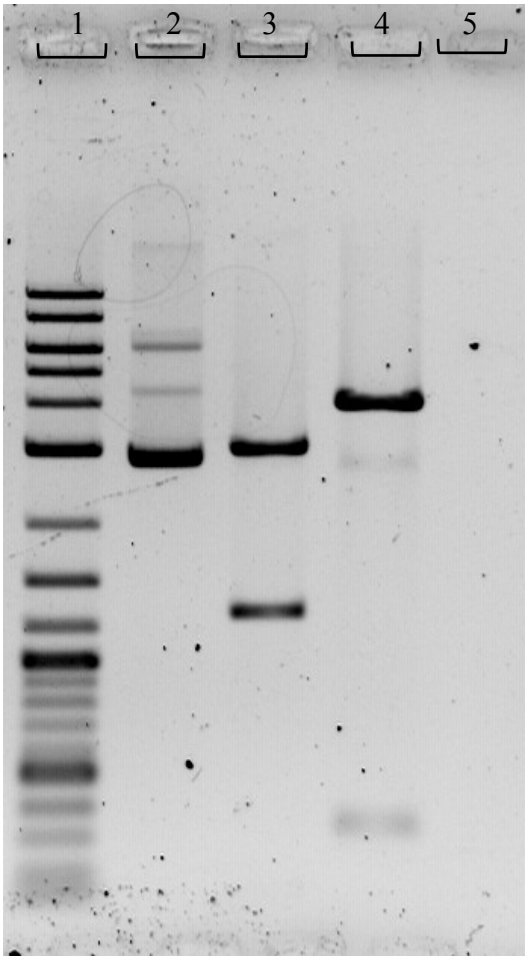

Fig. 2.9b The result of pMD2.G digestion with SwaI (Lane 2), BglII (Lane 3), AseI (Lane 4), EcoRI (Lane 5)

2.4.1.2 HEK293 TN Cell Transfection

For the production of recombinant lentiviral vectors, HEK 293TN (SBI) cells were used as virus packaging cells. A number of $1.8 - 2 \times 10^6$ HEK cells with low passage number (P5-P8) were seeded and grown in 10 mL HEK medium inside a T75 flask just 48 hours before transfection.

The HEK 293NT cells were split from one confluent T75 flask to the 6 × T75 flask. After 12-16 hours, HEK 239TN cells had 50-70 % confluency. The transfection mixture was prepared in a 15 mL falcon tube by mixing 20 µg of the targeted lentiviral plasmids separately, as well as 22.5 µg packaging plasmid (3rd generation plasmids: pMDL g/pRRE-15µg+pRSV-Rev-7.5 µg) and envelop plasmid (pMD2.G-9 µg) (Table 2.28).

Afterwards, the complex mixture was added to OptiMEM very carefully and mixed by finger taps for a minute. Then, Lipofectamine reagent 2000 which had already been mixed with Opti-MEM, was added to the first mixture and then incubated for 15 minutes in RT. The transfection mixture was applied gently to each T75 flask with HEK cells and was swirled for a homogeneous distribution of mixture. The cells were incubated at 37° C, 3 % CO_2 overnight (12-15 hours). At this point, the cells were cultured in DMEM high glucose supplemented with 10 % (Vol/Vol) Heat Inactivated FBS (Tet-free), 2Mm L-glutamine without antibiotics to allow an increased cell growth and viral production. By the next morning, the medium was replaced with 10 mL of fresh HEK medium, supplemented with 10 % Tet-free as well as antibiotic (1% Pen/Strep) and incubated at 37° C, 5 % CO_2 for 2 days (48-50 hours). Afterwards, the viral supernatants were collected and concentrated by ultracentrifugation.

To remove cell debris, the viral supernatants were collected and centrifuged (Eppendorf centrifuge 5804R) for 5 min at 1500 rpm and 4° C. Afterwards, the rest of cell debris were removed by passing the supernatants through the 0.45 µm (TPP, 99745) low–protein–banding filter.

Each SW32 centrifuge tube (Beranek Laborgeräte seton, 7052) was sterilized by 70 % alcohol, and then dried under "biosafety level2 tissue culture cabinet". Afterwards, the tube was filled with filtrated vector–containing cell culture supernatant and adjusted very carefully to reach 34 grams.

The tubes were placed into a pre-cooled Beckman SW32 ultracentrifuge rotor. Then, the ultracentrifugation was performed at 4° C for 2 hours at 22.000 rpm Ultracentrifuge. Next, the tubes were removed carefully from the rotor, and the supernatants were aspirated by vacuum pumps. An amount of 120 µL PBS without Ca^{+2}/Mg^{+2} was added to each tube, in which a min

A pellet was visible at its bottom. The tubes were sealed and incubated on ice for 2 hours. Then the virus plates were broken very carefully by finger tips. To avoid bubble formation, 80 µL of extra PBS without Ca^{+2}/Mg^{+2} was added to each tube, and then the pellet was re-suspended by gently pipetting up and down. A liquid from all re-suspended pellets was combined in a single tube. Then, it was aliquoted in 0.5 mL Eppendorf microfuge tubes in 25-50 µL portions, and immediately was snap-frozen in a liquid nitrogen bath stored at –80°C.

Table 2.28: Transfection Mixture per Each T75 Flask

Lenti-Virus -3rd generation plasmids	DNA(µg/T75 flask)
PMplg/RRE	15
Prsv-Rev	7,5
Envelop.MGD2	9
Transfer vector	20
Lipofectamine 2000	1µL /1 µg DNA
Opti-MEM	1mL

2.4.1.3 Determining Pseudo-Viral Titration by Real-time PCR

After the lentiviral particle preparation, it is necessary to titer the infectivity of the virus particles. This can be determined in vitro by infecting HE2K 293 and target cells, which in the experiment were ES (E14). Consequently, 5×10^4 of the HEK293 cells and ES were seeded in two 24-well plates separately just 24 hours prior to viral infection (Each plates were pre-coated with 0.1 % gelatin for 2 hours at 37° C). For each well, 0.5 mL of DMEM-high glucose was supplemented with 10 % heat-inactivated fetal bovine serum (Tet-free) and penicillin-streptomycin, and incubated at 37° C with 5 % CO_2 overnight. The culture medium was removed from each well, and 0.2 mL of fresh medium including Polyene at 0.6 µg/mL was replaced. The medium was concentrated with the virus particles at serially prepared dilution ratios of 1:10, 1:100, and 1:1000. Each dilution was repeated once more. After 24 hours, the old medium was replaced by the fresh medium and cultured for an extra 48 hours.
Finally, the samples were collected for the virus titration by Lenti-X Provirus Quantitation Kit (Clonetech). The quantification process is described briefly in the following.

2.5.1.3.1 Provirus Quantification

DNA-Extraction

Kit: GenElute Mammalian Genomic DNA Miniprep Kit (Sigma, Cat. # G1N70)
Extraction according to the manufacture's protocol.
Elution: 200 µL Elution Buffer pre-warmed to 55°C, incubated for 5 min at RT prior centrifugation.

Concentration Measurement

DNA concentration was measured on Spectrophotometer NanoDrop 2000c (Thermo Scientific).
Concentrations were in the range of 62 to 161 ng/µL. Ratio A260/280 was in the range of 1,77 to 1,96.

Determination of integrated Provirus Copies

Kit: Lenti-X Provirus Quantification Kit (Clonetech, Cat. # 631239)
Determination was done according to manufacturer's protocol.
Using the provided control template, a dilution series with a defined copy number for a standard curve was prepared. Samples were diluted with EASY buffer to a final concentration in the range of 50 ng/µL.

2 µL of samples and standards were assembled in duplicates on a 96-well fast qPCR plate together with reaction mix. The mix contained Lenti-X provirus forward and reverse primer, ROX Reference Dye LMP and SYBR Advantage qPCR premix in a total reaction volume of 20 µL. Run was performed on a Thermo Fisher StepOne Plus qPCR system. Cycling conditions were:
Initial denaturation: 95°C, 30 sec
40 cycles: 95°C 5 sec
Dissociation curve

According to the user manual, the true provirus copy number per cell (MOI) was calculated. For transfection of mouse ES cells, a MOI of 50 – 100 is optimal as known from the literature.

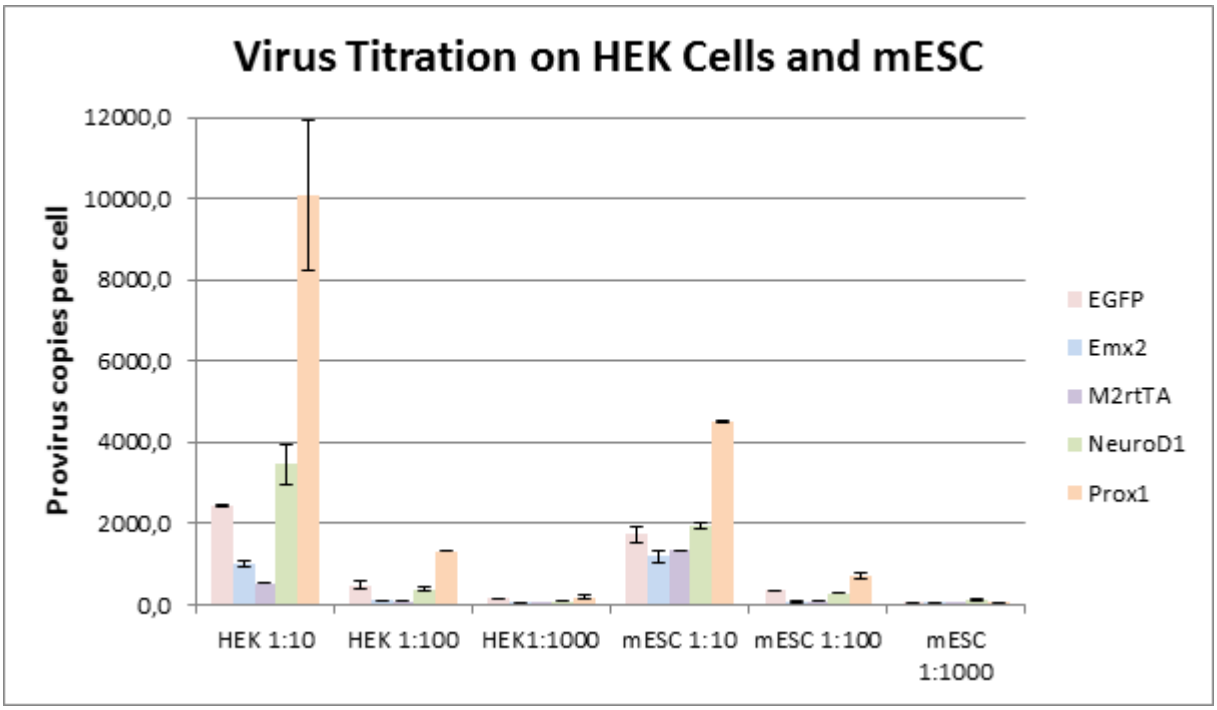

Fig. 2.10 The viral titration qPCR analyses of HEK293 cell and mESCs

2.4.1.4 Functional Titration

For calculating the ratio of the transactivator virus particles to the target lenti-virus gene and investigating the expression of transcription factors, the functional titration was performed. For this purpose, the co-transduction mixture was performed with the combination of the transactivator and target lentivirus genes (Prox1, Emx2, and NeuroD1). This mixture was applied to the HEK 293 cells with three different serial virus particle dilutions of 1:10, 1:100, and 1:1000 as described earlier. Finally, the cells were fixed by using the 4% paraformaldehyde and the immunocytochemistry was performed (Fig. 12-14).

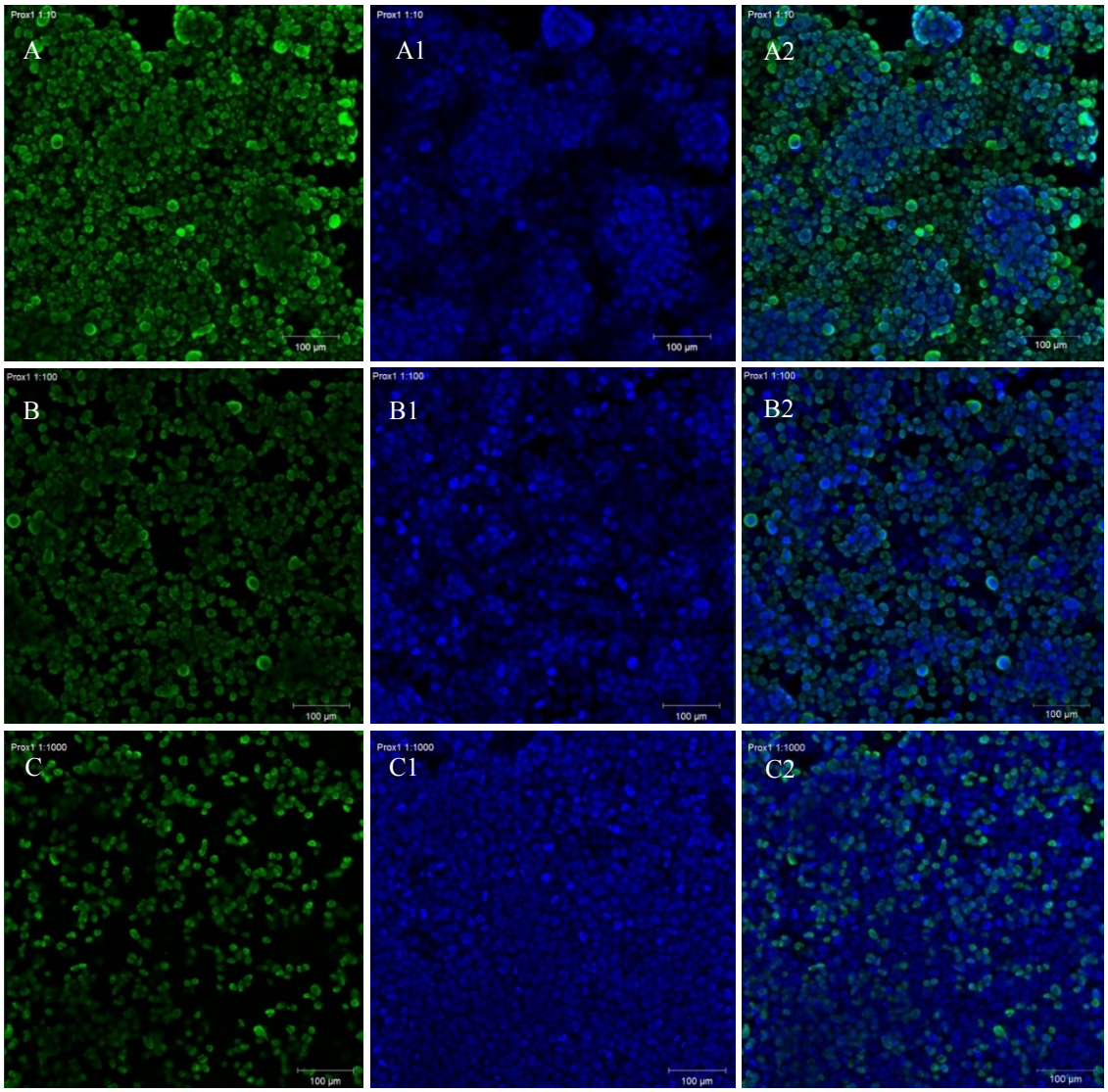

Fig. 2.11 The Tet-O-FUW-Prox1 Lentiviral Functional Titration. The infection efficiency was determined by obtaining the percentage of Prox1 immunocytochemistry in the infected culture with different supernatant dilutions: 1:10 (A), 1:100 (B), and 1:1000 (C) (Scale bar: 100µm).

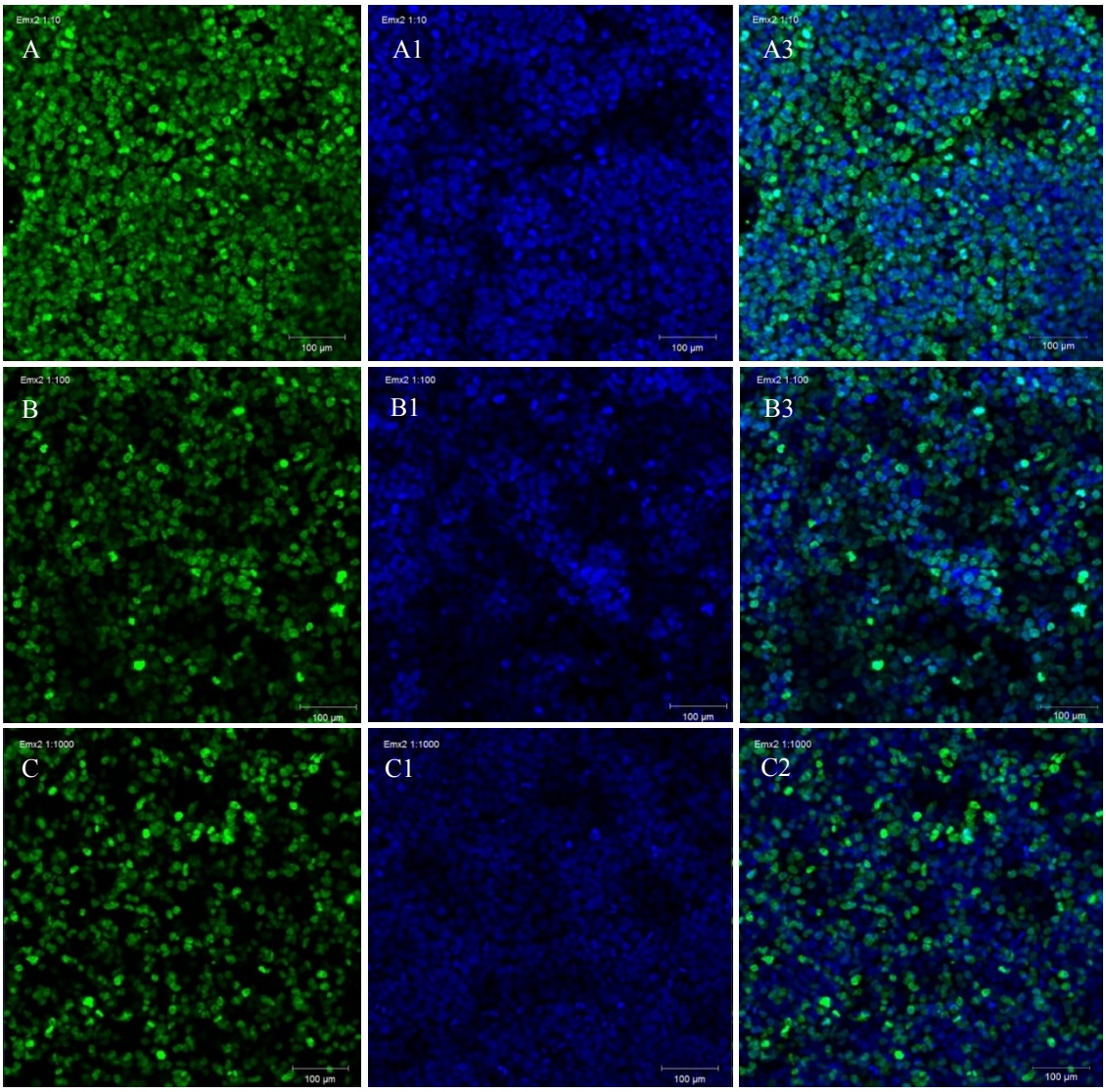

Fig. 2.12 The Tet-O-FUW-Emx2 Lentiviral Functional Titration. The infection efficiency was determined by obtaining the percentage of Prox1 immunocytochemistry in the infected culture with different supernatant dilutions: 1:10 (A), 1:100 (B), and 1:1000 (C) (Scale bar: 100µm).

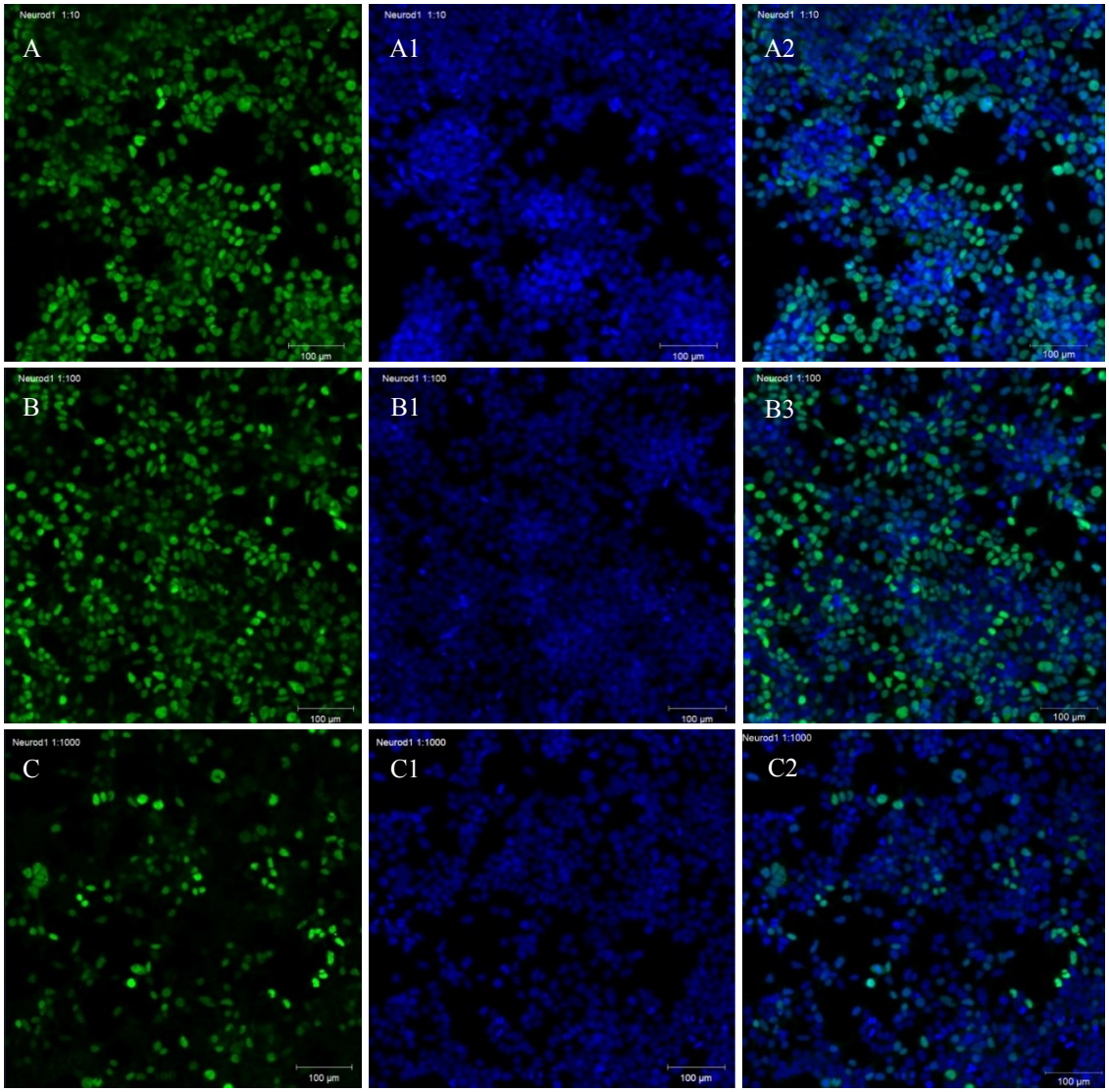

Fig. 2.13 The Tet-O-FUW-NeuroD1 Lentiviral Functional Titration. The infection efficiency was determined by obtaining the percentage of Prox1 immunocytochemistry in the infected culture with different supernatant dilutions: 1:10 (A), 1:100 (B), and 1:1000 (C) (Scale bar: 100µm).

2.4.2 Mouse Feeder Embryonic Cells

2.4.2.1 MEF derivation and irradiation

MEFs were utilized as feeder cells to maintain the mouse embryonic stem cells in an undifferentiated state. They were developed from dissociated ZP mouse embryos (13.5–14 d gestation). This mouse line had genetic manipulation and carried Zeocin antibiotic resistance gene.

To isolate MEFs from mouse embryos, a pregnant mouse at a time was scarified by using CO_2 gas, placed on her back on autoclaved paper towels. After spraying the mouse with 75% ethanol peritoneal, the cavity was opened with a Y-incision. The uterine horns were dissected out, and washed with PBS - containing 1 % penicillin/streptomycin (Life Technologies). The uterine horns were placed on the culture plates and transferred to the sterile bench. The embryos from the uterus were dissected out, and all tissue surrounding each embryo, such as the placenta and the embryonic sac, was removed by using sterile forceps. Afterwards, head, tail, hind limbs, front limbs and internal organs were dissected out. Then, each embryo was transferred into a bacterial 6 mm dish and washed with PBS - containing 1 % penicillin/streptomycin -, and was cut into several pieces with a sterile razor blade. In order to collect a Neomycin resistance embryo, lacZ staining was done on each embryo tail individually.

The tissue clumps were collected in a 60 mm bacterial culture plate, disassociated into cell-suspension using a syringe 18G and pipetted up and down thrice. Afterwards, the cell suspension was incubated with 2 - 5 mL 0.25% Trypsin/EDTA (depending on the number of embryos; 0.5 - 1 mL Trypsin/EDTA per each embryo) (Life Technologies) for 15 minutes at 37° C. After each 5 minutes of incubation, the cells were dissociated by pipetting up and down thoroughly. The trypsin was inactivated by adding a fresh MEF medium. The cell suspension was centrifuged at 300 g for 5 min, then the supernatant was taken off carefully, and the cell pellet re-suspended in a fresh and warm MEF medium. A number of cells equivalent to one embryo were plated onto T150 tissue culture flasks, pre-coated with 0.1 % gelatin. During this time, tail X-Gal staining was done, as described below. The fibroblast outgrowths were visible 24 hours after culture. When the cells were 80 – 90 % confluent, they were expanded 1:3.

After three passages, MEFs were collected and inactivated by γ-radiation 80G in the Heidelberg DKFZ facility.

Inactivation by γ-irradiation:

MEFs were harvested as above, combined into one 15 mL tube and were irradiated with a dose of 80G in the Heidelberg DKFZ facility. The exposure time was 11 - 12 min. The inactivated MEFs were frozen in 10% DMSO/90%FBS at $1.6x10^6$ per cryovial and stored in –80° C for 48 hours for long term storage. For subsequent use, the vials were transferred into a nitrogen liquid tank.

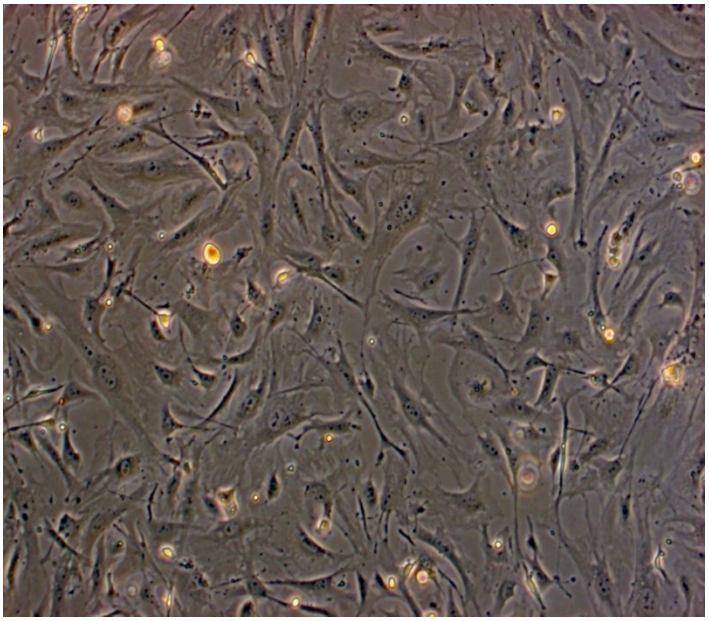

Fig. 2.14 Mouse Embryonic Feeder (MEF) Cells after 48 h Culture. Phase- contrast microscopy image (magnification 10x)

2.4.2.1.1 Genotyping by X-gal staining

The mouse embryos' tails were washed in cold PBS separately and cut into small pieces. A small piece from each embryo was transferred into a 0.5 micro tube (wrapped in foil) and incubated at 37° C for 30 - 60 minutes with freshly prepared X-gal staining solution. For a firmer confirmation of the resistance of the MEF to Neomycin, the X-gal staining was performed for the feeder cells taken from the mouse embryo (E13.5) by using standard protocol.

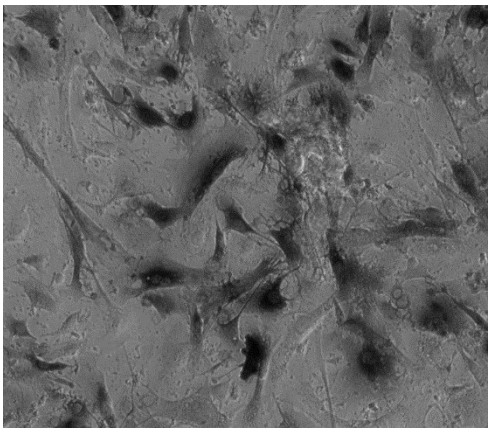

Fig. 2.15 X-Gal Staining of MEF Cells (ZP mouse line) after 48 h Culture

as indicated by blue perinuclear Phase contrast microscopy (magnification 10x)

2.4.2.1.2 Mycoplasma Detection

The mycoplasma contamination is a major problem in cell culture lab. Animal products and primary cell culture are two important source leading to mycoplasma contamination.
Therefore, the MEF cells were checked for mycoplasma infection before applying them for ES cell culture and any purposes.

2.4.2.1.3 Templates for PCR Analysis

To detect mycoplasma contamination, 1 mL of cell culture supernatants were collected from cell culture after 48 and 72 hours in 1.5 mL centrifuge tubes and were stored at +2° - +8° C. 500 µl of the supernatant of cell cultures were transferred to a micro centrifuge tube. Samples were incubated at 95° C for 10 minutes. Afterwards, the samples were centrifuged at 13,000 rpm to pellet cellular debris, and 2 µl of each supernatant were transferred to 0.2 µl Eppendorf micro tubes directly for PCR by Venor® GeM kit.

2.4.2.1.4 Antibiotic Selection in mouse ESC Line

To generate stable homogenous ESC cell lines, un-transfected cells should be removed from the cell culture. Before generating a stable cell line which expresses the transcription factor from an expression construct, it is necessary to determine the minimum antibiotic concentration required to kill all un-transfected ESCs. For this purpose, all transcription factor constructs carry the Zeocin antibiotic resistant gene.

Zeocin, belongs to the bleomycin/phleomycin family of antibiotics isolated from Streptomyces. The Zeocin gene encodes amino-glycoside 3'-phosphotransferase, an enzyme which admits resistance to G418 disulfate and neomycin.

Zeocin is a routinely used antibiotic, which is administered for successful antibiotic selection of transfected mammalian cells. In fact, the transfected cells express a Zeocin resistance gene in addition to the gene of interest during the cell culture. Different cell lines have varying antibiotic sensitivity from 20 - 1000 μg/mL to Zeocin.

To determine the optimal concentration, a prior experiment was performed for the killing of un-transfected ESCs by implementing a serial concentration of 10 to 500 μg/ mL for 5 days. The optimal concentration is suitable for the selection of resistant mammalian clones and depends on cell lines, ionic strength, and growth rate. It is necessary to perform a kill curve for every new cell type and every new batch of Zeocin based on the following protocol:

1. 1000-6000 ESCs were seeded in each well of the 96-well plate for 24 hours.
2. After 24 hours, the medium was removed, and then a fresh medium with varying concentrations of Zeocin™ was added to the wells in a group of 11 concentrations ranging from 50 to 550 μg/mL in linear increments (50, 100, …, 550 μg/mL).
3. The selective medium was replenished every second day, and the percentage of surviving cells was observed over time. Afterwards, the optimal concentration for killing the majority of cells in the desired number of days (within 5 days) was selected. For more clarity in distinguishing viable cells by observation, we employed counting the number of viable cells by standard WST-1 assay.

2.4.2.1.5 WST-1 Assay

The WST-1 Assay was performed to check the antibiotic toxicity based on mitochondrial activity. To determine the optimal antibiotic concentration, we utilized the WST-1 assay and checked the cell proliferation rate during five days of cell culture. For this purpose, ESCs at day one, were seeded at the number of 1000, 2000, 3000, 4000, and 6000 cells in the 96 well plate and cultured for 48 hours. Thereafter, the cells were treated with different antibiotic concentrations. Each experiment was performed and triplicated for a group of 11 concentrations ranging from 50 to 550 µg/mL in linear increments. The cells were exposed to the same concentration and incubated in standard condition for four days. Over this period, the treatment was repeated every second day. Accordingly, the cell viability was analyzed with WST-1 assay by ELISA reader Sunrise™ at wavelength 480 nm, as outlined by the manufacturer.
The obtained data was analyzed by Excel and we concluded that the optimal concentration for ESCs was varying between 80 and 100 µg/ml. This result was consistent with the microscopic observation.

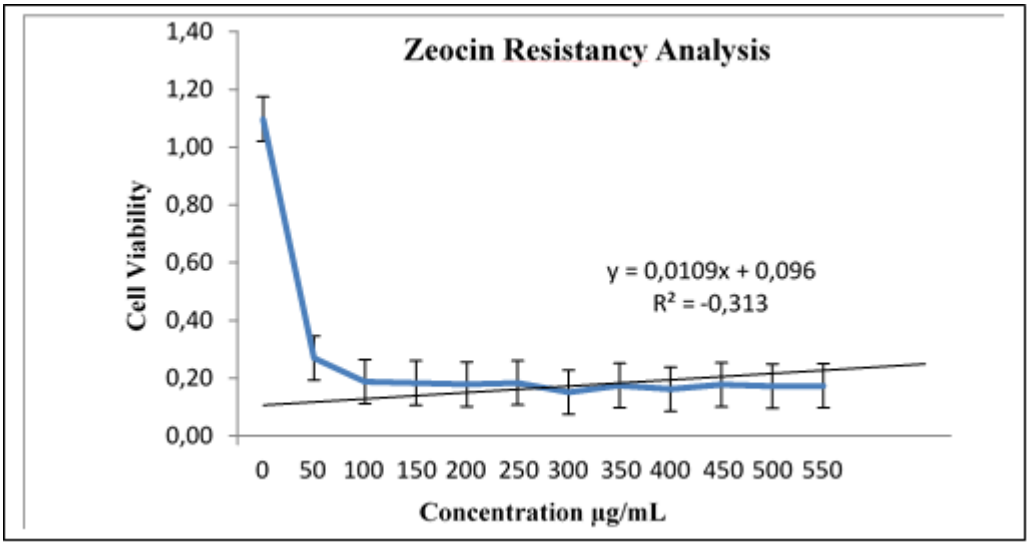

Fig. 2.16 WST Assay Analysis to identify Killing Optimal Zeocin Concentration.

2.4.3 ESC transduction

As emphasized earlier, all of the steps for the utilization of pseudo lentivirus and ESC transduction in biosafety S2-level performed in accordance with the guidelines of the Ethical Committee of Heidelberg University, Graduate School of Medicine.

ESC culture: ESCs are cultured according to standard procedures. The mESCs used in this study were derived from E14 IVC mice (from Austin Smith lab (P20)) and cultured, Zeocin resistant mouse fibroblasts. The mESCs were cultured in ESC medium containing 20 % Tet–free fetal bovine serum (FBS), 1 % nonessential amino acid (NEAA), 100 µM 2-mercaptomethanol (ß-ME), 1 % penicillin-streptomycin, and 1000 U/mL leukemia inhibitory factor (Melander and Olsson).The ES culture medium was changed every day and ES cells were passaged every third day (Fig.18)

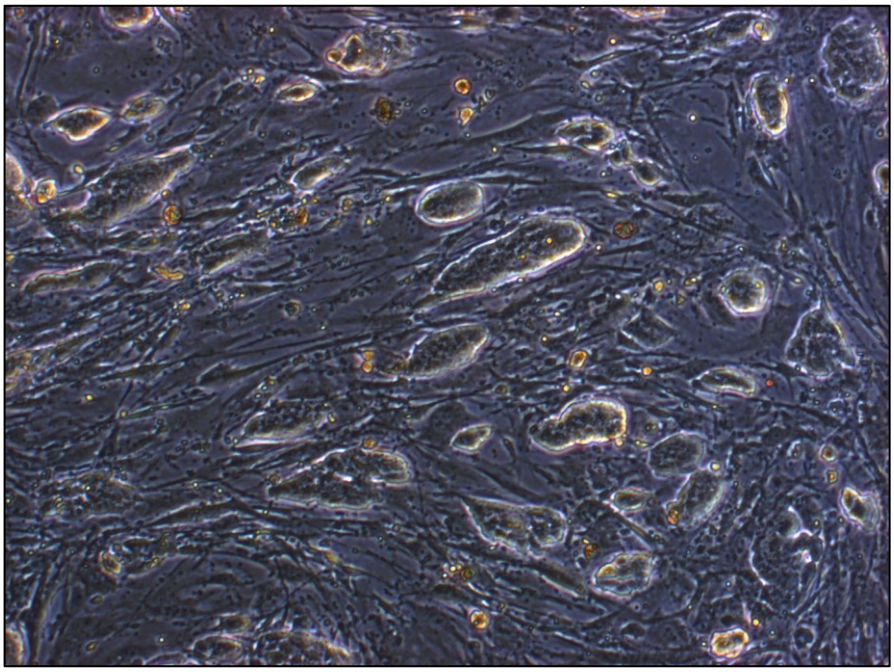

Fig. 2.17 Embryonic Stem Cells E14 IVC; P20. Phase contrast microscopy (magnification 10x).

2.4.3.1 Transduction

ES cells from using two or three wells of a 6-well-plate were trypsinized in 0.25 % trypsin for 3 minutes at 37° C. The colonies were broken up by pipetting the cell suspension up and down for several times. The cells were spun down at 300 g for 3 minutes and re-suspended in 15 mL fresh ES cell media. The cells were then plated onto a gelatinized dish (100 mm) and placed in an incubator for 45 minutes to allow the feeder cells to settle and adhere. After 45 minutes, the media (with ESCs) was removed and the cells were counted. The number of seeded cells is critical, because it should be possible to maintain individual colonies for picking up after 7 - 10 days of antibiotic treatment. An unbalanced number of seeded cells reduce the chances of

identifying a good clone in either way: Too many cells are hard to pick up, while, very few of them would not grow desirably. An approximate number of 5 x 10^4 ESCs were used per each transduction well of a 6-well-plate. The lentivirus co-transduction was performed with virus particles of M2rTtA (trans-activator) and Tet-EGFP at MOIs of 50 – 100 in 1mL of ESC medium was frequently set up. The ESCs' transduction was performed in a medium including polybrene at 8 µg/mL which incubated overnight at 37° C, 5 % CO2.
After nearly 18 hours, 5 x 10^5 feeder cells resistant against Zeocin were added to each infected well. After 24 hours, the cell cultures were washed three times accurately to remove the excess of lentivirus particles and dead cells with warm phosphate buffered saline with Ca^{+2} and Mg^{+2} (PBS^{+}) The cell cultures were continued for 4 days in presence of Zeocin 100 mg/ml.

2.4.3.1.1 Picking up

Colonies were picked up by using standard techniques. Ninety-six colonies were picked "blindly" and transferred onto a 96-well-plate pre-coated with irradiated feeders cell separately. After 24 hours, the colonies were trypsinized in 30 - 50 µL of 0.25 Trypsin for 3 - 5minutes at 37° C and then broken up by pipetting up and down 10 times with 200µL. This single cell suspension was kept and cultured in the same well for 10 - 12 hours, and then the media was changed to remove all traces of trypsin.

2.4.3.1.2 Clone Maintenance/Selection

The media was changed at least once a day for actively growing clones. After 3 - 5 days (depending on the growth rate), clones were split into two 96-well-plates, one filled with feeders and one free of it (but coated with gelatin). Cells grown on the feeders were expanded and frozen down. Cells grown without feeders were expanded and screened by adding tetracycline 500 ng/mL, in order to observe the EGFP expression after 19 – 24 hours. This expression is an indicator of a successful transduction of both plasmids.

2.4.3.1.3 Cryopreservation of Lt-Tet-EGFP-transduced ES Cell Clones

Undifferentiated Lt-Tet-EGFP-transduced ESC clones were frozen after 3 days of culture. The feeding of ES cells before cryopreservation is very important for their maintenance and prevention from post re-thawing differentiation. Meanwhile, the ES medium of Lt-Tet-EGFP-

transduced ES cells clones were renewed 2 - 6 hours before cryopreservation by a fresh medium. Afterwards, Lt-Tet-EGFP ESC cultures were disassociated using 0.05 % trypsin/EDTA and re-suspended in the culture medium. Then, the cell suspension was centrifuged (300 x g, 3 min at RT). After centrifuging, the cell plate was re-suspended with 1 mL fresh ESC medium. Its viability was determined by the trypan blue exclusion method using a 0.1 % (v/v) solution prepared in PBS and the cells counted in a Fuchs-Rosenthal hemocytometer (Brand, Wertheim, Germany). The viability was more than 90 %, to ensure that the cells were healthy enough for freezing. The cells were once more re-suspended in the culture medium; the volume had a cell concentration of 1×10^6cells/mL.

The pre-cooled cryovials were manually filled with 1mL of pre-cooled cryoprotective solutions and mixed gently with cell suspension solution (1:1). The cryovials were placed into a Freezing Container (Nalgene Nunc International) and were stored in a –80º C freezer overnight, then they were transferred in a nitrogen liquid tank for long-term storage until thawing.

2.4.3.1.4 Fluorescence Activated Cell Sorting (FACS)

To remove the some ES cell which had leaky expression and prevent the ES cells clone from differentiation during second or third transduction, FACS analysis was applied.

FACS analysis was performed on BD LSR II (Becton Dickinson), BD Fortessa (Becton Dickinson) by Central Services - Flow Cytometry & FACS Core Facility (FFCF) in Heidelberg University (ZMBH). Cell sorting was performed with BD FACS Aria III (Becton Dickinson) cell sorter. The analysis of FACS data was done with FlowJo software (Tree Star Inc.).

The ESC clone Lt-Tet-EGFP was dissociated with 0.25% Trypsin-EDTA and isolated from MEFs by standard protocol. The single cell suspension was sorted into artificial fractions (low, mid, and high) based on EGFP fluorescent signal intensity.

After cell sorting, all cells expressing EGFP were removed and the rest of the cells were washed and re-cultured on MEF cells. In this experiment unmodified ES cells was applied as control group.

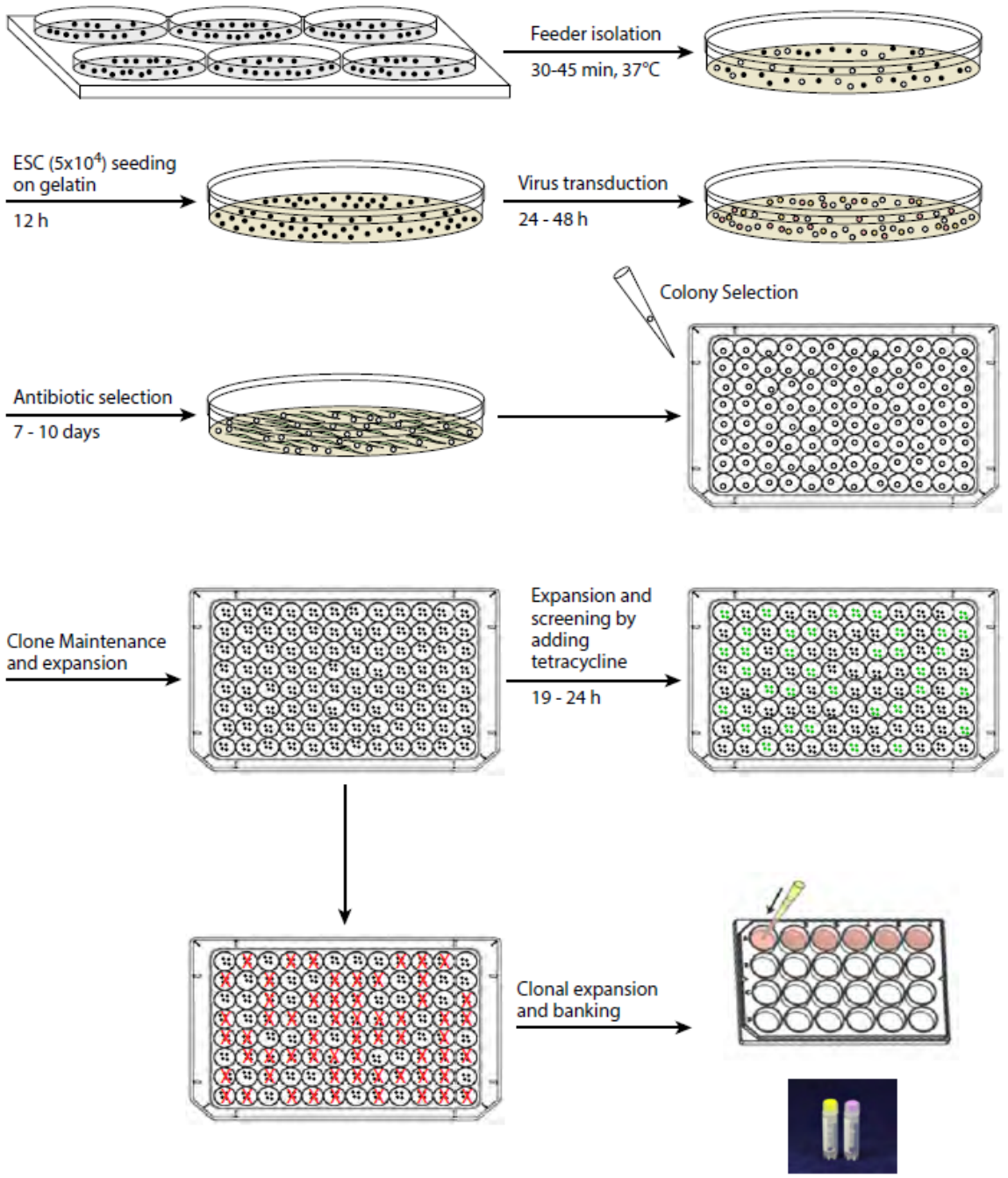

Fig. 2.18 Schematic illustration of transduction procedure of clonal expansion and banking of mESCs under antibiotic resistance

2.4.3.2 Second transduction

After screening and clone banking, the Lt-Tet-EGFP clone G1 was selected randomly and re-transduced by the following Lt-particles separately: Lt-Tet-Prox1, Lt-Tet-Emx2, and Lt-Tet-NeuroD1. As in the case of abovementioned transduction, Lt-Tet-EGFP clone G1 (5×10^4 cells) was seeded and cultured on 0.1% gelatin with the ESC culture medium excluding antibiotic about 12 hours before the second re-transduction.

The colony selection was performed like before, except for the clone screening which, the methods of immunocytochemistry and PCR were employed after treatment by Doxycycline. The cell cultures were continued for 4 days in the presence of Zeocin 100 µg/mL.

The outcome of this procedure was the generation of clones as listed below:

Lt-Tet-Prox1-EGFP

Lt-Tet-Emx2-EGFP

Lt-Tet-NeuroD1-EGFP

2.4.3.3 Third transduction:

A third re-transduction of Lt-Tet-Prox1-EGFP with the pseudo-viral Lt-NeuroD1 particles was performed for the generation of Lt-Tet-Prox1-NeuroD1-EGFP.

The whole process of transduction, clone banking and screening was performed based on the steps described in the last section.

2.4.3.4 PCR:

The integration of transcription factors and inducible stable cell line generation was confirmed by PCR analysis with the following primers.

PCR Reagents and Primers

Total DNA was extracted from all ESC clones after colony expansion by using the mammalian DNA extraction kit according to manufacturer instructions.

The composition of the PCR-reaction was as follows:

2 µl DNA;
0.5 µl dNTPs
2.5µl PCR-buffer (10X)
0.5 µl for each forward and reverse primer
0.25 µl Taq polymerase
18.75 ddH2O

The PCR-reaction was performed in 0.25 mL-reaction tubes and a thermocycler with the same annealing temperature. The negative and positive control templates were included in each PCR-reaction.

After the PCR-reaction, 4 µl loading buffer (6x) was added to each tube. The samples were electrophoretically separated on an agarose-gel (1% agarose in TAE-buffer, at 120 V for approximately 40 – 50 min). The Agarose gels were stained in 10 µl ethidium bromide (10mg/mL) in 500 mL water and remained for 15 min and rinsed in water bath for an extra 15 min. Then the gel was exposed to UV-light in a gel documentation system to visualize DNA-bands.

Table 2.29: Primer sequence and products

Gene	**Primer sequence (5′ - 3′)**	**Length (bp)**
Emx2	Emx2-F1: ACA GTC TCA GTC TTA CGG AAA CTC; WPRE-R1: AGC CAT ACG GGA AGC AAT AGC ATG	354
NeuroD1	NeuroD1-F1: TGC CTT TAC CAT GCA CTA CCC TGC; WPRE-R1: AGC CAT ACG GGA AGC AAT AGC ATG	333
Prox1	Prox1-F1: CAA GCC ATC AAT GAT GGA GTC ACC; WPRE-R1: AGC CAT ACG GGA AGC AAT AGC ATG	447
M2rtTA	M2rtTA-F1: ACT TAG ACA TGC TCC CAG CCG ATG; WPRE-R1: AGC CAT ACG GGA AGC AAT AGC ATG	250

Product	Company	Cat. Number
Taq polymares	Applied Biosystem	M05768
Pcr buffer	Applied Biosystem	M13037
dNTP	Applied Biosystem	N8080260
Agarose	Sigma	A9539

Caption: The PCR components

2.4.3.5 Immunocytochemistry

The immunocytochemistry analysis was a second method used for a firmer confirmation of the expression and functionality of the transcription factors. For this purpose, the cell cultures were fixed in 4 % paraformaldehyde for 15 min. and. subsequently washed several times in PBS. The cells were then blocked for 10 min in a blocking solution containing 10 % goat serum and incubated with primary antibodies diluted overnight at 4° C. The primary antibodies were washed 3 times with PBS. The secondary antibodies were diluted in a blocking solution (with 0.1 % Triton-X-100) and incubated for 30-45 min at RT. The cells were washed in PBS and subsequently stained with DAPI and washed twice in PBS for a total of 20 min. The nuclei were visualized by DAPI staining (1:10.000 in $NaHCO_3$, 4 min incubation).

2.4.3.6 Pilot studies

At the beginning, several protocols for ES neural differentiation were investigated. These experiments revealed that ESCs were not only differentiated into pure neural precursors, but also into several types of cell populations, including all types of embryonic lineages. For example, they were containing beating cardiomyocyte cells of mesodermal origin, flattened epithelium-like cells but not a strong differentiation of neural homogenous precursor cells.
The protocols suggested by Sasai and Gage (Watanabe, Kamiya et al. 2005, Yu, Di Giorgio et al. 2014) appeared more promising in relation with the neural differentiation conditions. The duration of the specific steps in differentiation and media constituents were modified and set up in our lab as a new protocol.
The establishment of an EB protocol for the neural differentiation of ESCs in SFEB culture was a remarkable step in obtaining the neural homogenous precursor cells.
Our study follows the EB formations, because we believe that the EBs as three dimensional structures are the reminiscent of the embryonic development.
Considering the critical role of astrocyte cells in the neural differentiation and maintenance, the adherent co-culture was performed in parallel with our experiment.

2.5 Astrocyte primary cell culture

The astrocyte primary cell culture was prepared from cultures of cortical astrocytes.

A mouse pup (P1 - P4) was sacrificed (one at a time) by decapitation. The head was held with a laboratory tissue and washed with 70 % ethanol. The skin was cut longitudinally with scissors to expose the whole superior surface of the skull. The skull was carefully cut longitudinally with the scissors, then the brain was removed from the skull with a spatula and placed into a 60 mm bacterial dish containing ice-cold L-15 medium.

Inside of the hemispheres were scooped with the spatula. The surface of the cortical halves was cleaned of meninges by using small scissors and fine forceps. The cerebral cortex was dissected out and cut into pieces after incubation with 0.1 % trypsin and 0.01 % deoxyribonuclease I (DNase I). The whole procedure was performed at 37˚ C for about 10 min in water bath while being shaken every 3 min.

The cell digestion was stopped with MEM including 20 % FBS, and were mechanically dissociated by being passed through a 5 mL pipette for 10 – 12 times. After trituration, the cell suspension was passed through Cell Strainer (70 µm) to remove cell clumps.

The suspension was centrifuged at 300 x g for 10 min, and the pellet was re-suspended in an Eagle's medium.

The suspension was diluted to the optimal concentration, and the cells were plated on 75 cm^2 culture flasks pre-coated on poly-L-ornithine (5 µg/mL) at a density of 6.0 x 10^5 cells/cm^2, and then cultivated at 37˚C in 5 % CO_2. The dead cells were removed by changing the medium on the next day. The medium was exchanged with a complete medium every three days. The growth of the astrocyte culture was monitored by phase-contrast microscopy until it reached 80 - 90 % confluency.

At that day of confluency, the cell cultures were split 1:3 and incubated at 37° C for one week. Finally, the cultures freezed at -80°C for short-term- and kept in a liquid Nitrogen tank for long-term storage.

2.5.1 The astrocyte freezing process

The astrocyte cell proliferation was done up to three passages. For a long-term storage, the cells were fed with astrocyte fresh medium 6-8 hours before freezing. Then the cells were trypsinized for 3-5 min based on standard protocol and centrifuged at 300 x g for 3 min. Afterwards, the cells were counted at 2×10^6 and quickly re-suspend by adding 1mL of freezing (cold Cryostem) media per cryovial. The cryovials were placed in Mr. Frosty freezing container and

kept at -80°C for 48 hours. At the end, the vials were placed in the liquid Nitrogen tank for a long-term storage.

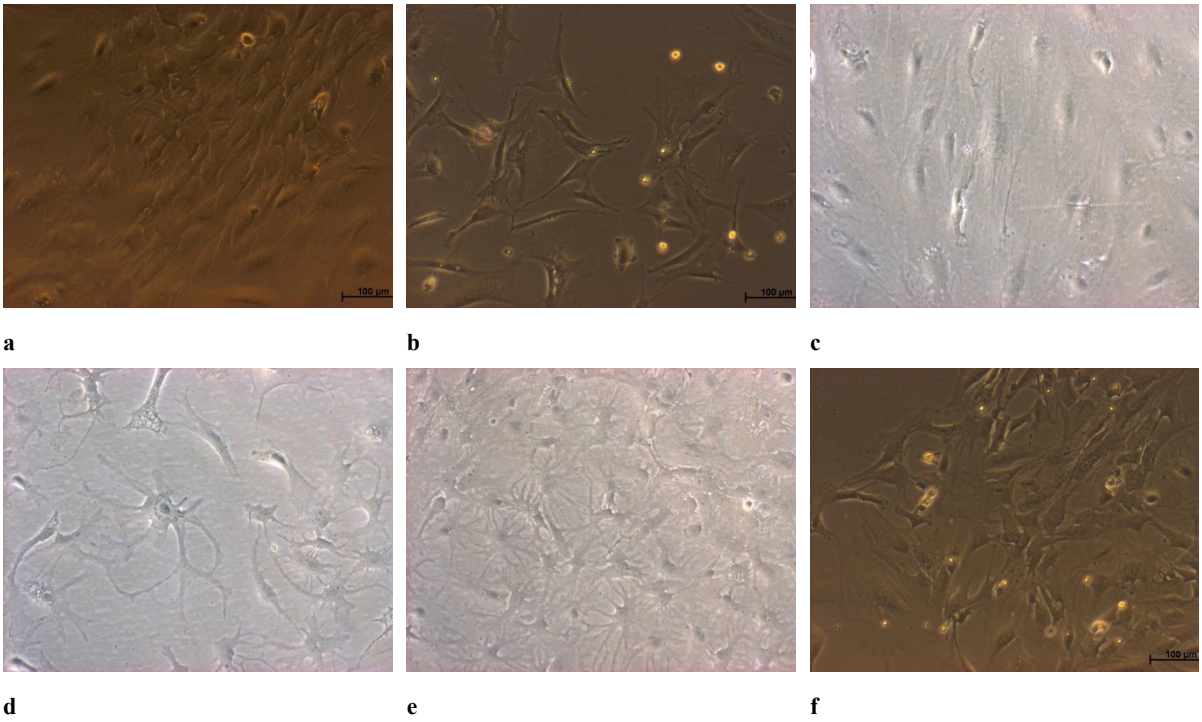

Fig. 2.19 a-f: Light microscope pictures of primary astrocyte culture. Letters A-F demonstrate the variety of morphologies observed using phase contrast microscopy (magnification 10x)

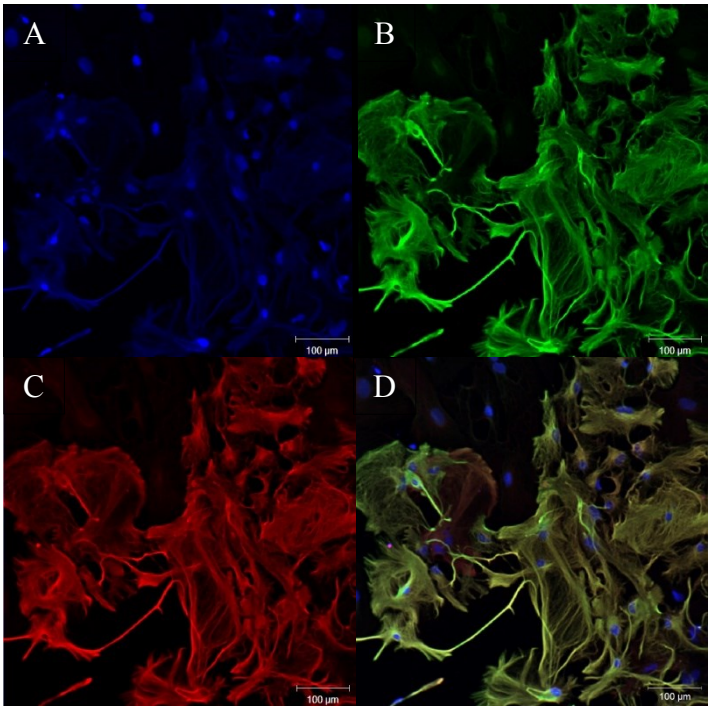

Fig. 2.20 Co-staining of pure primary mouse astrocyte culture with the DAPI (A), GFAP (B), Nestin and (C), Merged (D): Scale bar=100µm.

2.6 Differentiation

The differentiation mechanism was accomplished in two general steps, first, the three dimensional (3D) culture, which is in turn divided into the EB formation and the EB induction, and second, the two dimensional (2D) culture which includes the adherent and astrocyte co-cultures. In the following, we explain each step in more detail.

2.6.1 Embryoid body (EB) formation

The EB formation is a principle step in the differentiation of ESCs. In this study, the EBs culture is used to examine the neural differentiation potential of the genetically modified ESC clones. The term EB has been extensively addressed to describe the PSC aggregates induced to differentiate using a variety of different formation and culture methods, such as the suspension culture or the hanging drop technique. The EBs were capable of forming derivatives of all three germ lineages' layers (ectoderm, mesoderm and endoderm) (Bratt-Leal, Carpenedo et al. 2009). By varying the culture media or growth factors, the EBs are desirably guided towards one of the abovementioned germ lineages' layers. For instance, it has been recognized that relatively homogeneous EBs could be generated as a result of the serum-free culture responsible for ectodermal lineages, such as neural progenitors or neurogenic fate.

Fig. 2.21 The outermost layer (blue): Ectoderm Intermediate Layer (red): Endoderm Inner Layer (yellow).

The physical characteristics of EBs such as shape, size, and homogeneity are some of the typical reference points for differentiation. The size of EBs (cells aggregate) which depends on the number of ESCs (the constituent elements of EBs) is believed to be a critical factor which influences the proportion of differentiating cells turning into different lineages. Moreover, the size of EBs impacts other environmental parameters affecting differentiation such as the

diffusion of soluble molecules, the extent of ECM-cell, and cell–cell adhesive interactions (Bratt-Leal, Carpenedo et al. 2009).

Our strategy was to generate an array of homogeneous and equal size EBs for neuronal differentiation. For this purpose, we implemented AggreWell™400 plate (Stemcell Technologies) in our study. The EBs were allowed to grow for several days or weeks and treated with the set of growth factors, tetracycline or both. Tetracycline was used to switch on the genetic expression of the different transcription factors. At different points in time, the samples had to be taken for genetic expression analysis by Fluidigm Real-Time PCR or immunohistochemistry.

2.6.1.1 Generation of EBs Using AggreWell™:

The details about generating homogeneous EBs for the telencephalic differentiation are provided in the manufacturer's user guide of AggreWell™ plates (Stemcell Technologies). The tough cohesion between the EBs and the surface of microwells could result in the breakdown of EBs while picking up. To overcome this drawback, the AggreWell Rinsing Solution was applied in the amount of 0.5 mL and kept for one minute. Next, the plates were centrifuged at 200 x g for 5 minutes in a swinging bucket rotor that was fitted with a plate holder to eliminate any small air bubbles. Then, the solution was removed from the wells and washed with 2 mL of DMEM/F-12 prior to adding to the cells. Afterwards DMEM/F-12 was gently removed and 0.5 mL dosage from the differentiation medium (1) was placed into each microwell.

Once again, the plates were centrifuged at 200 x g for 5 minutes at the same condition mentioned above.

The ESCs were isolated from the MEFs by using 0.1% gelatin pre-coated dish and incubated for 45 minutes at 37° C, and then the supernatant collected and centrifuged at 300 x g for 3 minutes. Then the cell plates were broken in 1 mL dosage of the differentiation medium (1) and added to each well at the concentration of 6×10^5 cells/mL, generating EBs with 500 cells. The plates were centrifuged once more at 100 x g for 3 minutes to capture the cells in the microwells. The aggregates were harvested 48 hours after adding the ESCs to the plates and at the end, the EBs were transferred to the suspension differentiation culture medium.

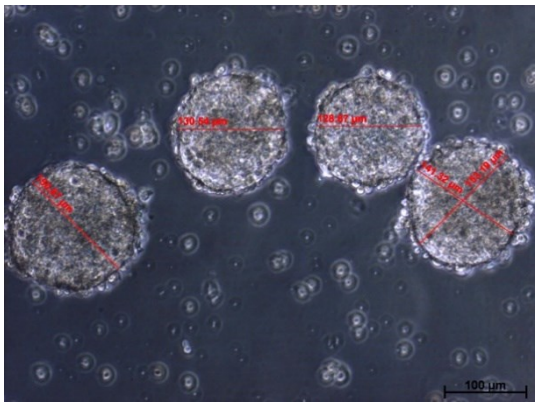

Fig. 2.22 Homogeneous 2- day old EBs.10x magnification. Phase contrast microscopy image.

3D and 2D differentiation of ESC to DG neuroprogenitor cell

Gage modified protocol

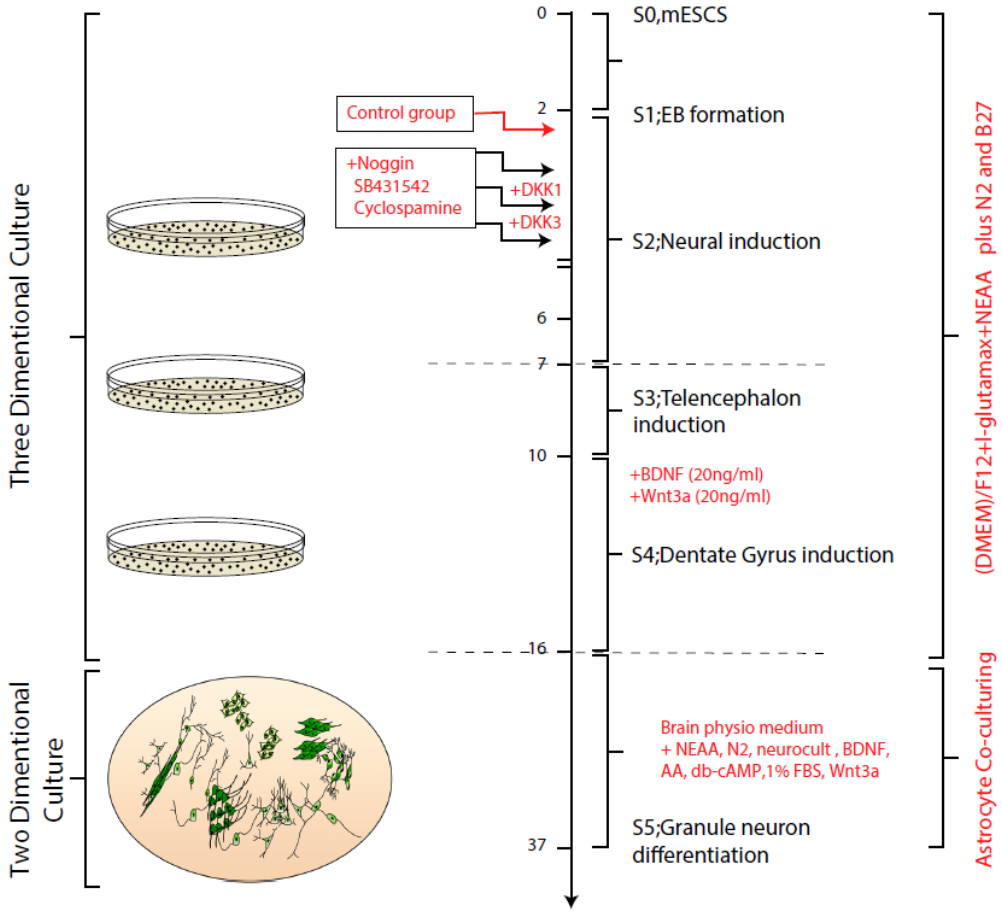

Fig. 2.23 The schematic representation of the differentiation protocols for DG granule cells

We established a new protocol by slight modification of Sasai and Gage protocols (Watanabe, Kamiya et al. 2005); (Sakaguchi, Kadoshima et al. 2015); (Yu, Di Giorgio et al. 2014) for the differentiation of ESCs in vitro into hippocampus-DG granule neurons.
Our protocol is divided into five main stages, following the embryonic development of mice:

Stage 1: Ectodermal induction
Stage 2: Neuro-ectodermal induction
Stage 3: Telencephalon induction
Stage 4: Dentate gyrus induction
Stage 5: Granule neurons full differentiation

2.6.1.2. Ectodermal Induction:

In vivo ectodermal formation is the first step for the generation and development of nervous system. To induce the ectodermal lineage, it is substantial for the cells to be cultivated in a serum-free environment. To this purpose, the serum-free EB (SFEB) culture medium was applied during the EB formation. This condition resulted in the elimination of endodermal and mesodermal cell lineage layers. As a result, we obtained a rich population of the earliest neuroectodermal cell lineages (see the "Results" section).

2.6.1.3 Neuroectodermal Induction

Basically, the ectodermal and neuro-ectodermal inductions in vivo occur almost synchronously. For the induction of ectodermal to earliest neuro-ectodermal differentiation, four principal signaling pathways are involved: FGF2, BMP, WNT-βcatenin, and Notch pathways. Under these circumstances, the first stage of induction is neuroectodermal differentiation, in which the supplement factors such as N2 and B27 in SFEB are utilized. This medium was named the differentiation medium I which included some generic neuro-ectodermal inductive factors such as insulin, apotransferrin, progesterone, and putrescin. To conduct the progress of the neuroectodermal differentiation towards the telencephalon progenitor cells, the model of brain signaling development in vivo is mimicked by inhibiting WNT-βcatenin, Nodal-Activin signaling pathways, BMP, and Shh pathway.

Thus we initially treated EBs with a cocktail of anti-caudalizing factors such as Dkk1 (100ng/mL), Dkk3 (100ng/mL), Noggin (0.5µg/mL), and SB431542 (10mM) SB431542 is an Activin/BMP/TGF-β pathway inhibitor. On the day 7 of differentiation, the majority of EBs were positive for the neuroectodermal markers such as Sox1 and Pax6, and Nestin-GFAP. At the same day, the majority of EBs were also positive for FOXG1, the main marker for telencephalic progenitor cells.

Table Overview of experimental groups used in this study

Group Name	**Treatment**
Group1	The Basal Medium of Differentiation Medium I
Group2	The Differentiation Medium I plus Noggin , SB431542, and Cyclopamine
Group3	The Differentiation Medium I plus Noggin , SB431542, Cyclopamine, and Dkk1
Group4	The Differentiation Medium I plus Noggin , SB431542, Cyclopamine, and Dkk3

2.6.1.4 Telencephalon induction

This step is essentially related to the last one. In fact, whenever we used the cocktail of anti-caudalization, the anterior forebrain fate was induced; and with the inhibition of ventralization (Shh pathway inhibition), the dorsal fate with FOXG1 expression was induced as well. Moreover, after the day 7, we switched on the inducible tetracycline system in modified transcription factor clones by adding tetracycline (500 ng/mL) to induce the transcription factors Emx2, NeuroD1, and Prox1, which are critical to direct telencephalic progenitor cells towards the hippocampus DG granule neurons.

2.6.1.5 DG induction:

Next, the telencephalic neural progenitor EBs were induced by WNT3a (20 ng/mL) and BDNF (20 ng/mL) treatment. These two main growth factors have key roles in DG formation.
During embryonic development, WNT3a is secreted by the CH, which has a source of WNT and BMP signaling in the dorsomedial telencephalon.

2.6.1.6 The full differentiation of DG neurons:

In this stage, 50 individual EBs were collected in a bacterial dish (35 cm in diameter) and pre-treated for 1 h with Y-27632 (5 µM). Then, EBs were placed in an enzymatic cocktail containing DNaseI (80U), Collagenase V (0.5mg/mL), and Accutase while being shaken and kept for15- 20 minutes in the incubator. Subsequently, the EBs were observed after about 10 minutes to make sure that the cells are at the beginning of separation and release from their outermost layers in the cocktail. Afterwards, the cocktail was collected very gently, since the released cells in the cocktail were outermost layer cells (e.g., neurons or neuro-progenitor cells) which are very sensitive to mechanical trituration. Then, the rest of EB bodies were triturated immediately for 5-10 times in order to obtain fully dissociated EBs. The whole suspension was centrifuged at 300 x g for 3 min at 4˚C. At the end, the cell plate was re-suspended in a full differentiation medium and seeded on the poly-ornithine (5 µg) and Laminin (5 µg) 24-well plate.

The co-culture with astrocytes was performed sequentially within 10-12 hours after seeding the suspension cell. In the co-culture sequential process, the astrocytes were pre-cultured inside of the thin filters only 3 days prior to use.

During the culture, the differentiation medium III was applied and every three days, about one third of medium was replaced by a completely fresh medium. The process continued for 21 days. At the final day, some cells were collected for RNA analysis by the Fluidigm system. The rest of the cells were analyzed for DG marker expression by immunofluorescence.

2.6.1.7 Immunofluorescence technique

For immunocytochemical analyses after 37 days of directed telencephalic and DG development, the cell cultures were fixed in 4 % PFA for 20 min at RT and washed with PBS at once. Cells were then blocked and permeabilized for 1 h with blocking solution containing 10 % goat serum for 1 hat RT. Subsequently, the cells were incubated over night with primary antibodies (Table 2.30) diluted in blocking solution at 4° C. The cells were washed in PBS, subsequently stained

with DAPI and again washed twice in PBS for a total of 20 min.

Afterwards, cells were washed two times with PBS. Secondary antibodies were diluted in blocking solution and incubated for 1h at room temperature. The nuclei were visualized by DAPI staining (1:10.000 in $NaHCO_3$, 4 min incubation) with 0.05 % Triton-X-100 and 1% BSA.

.

Table 2.30: Antibody list

Ms = mouse, Rb = rabbit, GP = guinea pig

	Product	Host		Company	Cat. No	S.Ab.	Dilution
1	Oct-4	Rb	polyclonal	abcam	19857		1-5 µg/mL
2	Nanog	Rb	polyclonal	abcam	80892		1:150-1-700
3	Sox2	Rb	polyclonal	abcam	15830		3µg/mL
4	Pax6	Ms	monoclonal	milipore	MAB5552		1:100
5	Nestin	Rb	polyclonal	Sigma	SAB4200394		1:100
6	GFAP	Rb	polyclonal	DAKO	20334		1:50-1:100
7	BLBP	Rb	polyclonal	abcam	ab32423		5 µg/mL
8	Sox1	Rb	polyclonal	abcam	ab87775		1:500
9	Emx2	Rb	polyclonal	abcam	ab11849-50		1:50-1:100
10	Prox1	Ms	monoclonal	Novubiol	NBP1-30045		1:500
11	NeuroD1	Ms	monoclonal	abcam	ab60704		1:500
12	NeuN	Rb	monoclonal	abcam	ab177487		1:80
13	Calretinin	Rb	monoclonal	abcam	ab16694		1:10
16	DCX	GP	polyclonal	Chemicon	Ab5910		1:3000
17	βIII-tubulin	Ms	monoclonal	Sigma	T8660		1:500
19	Map2(2a+2b)	Ms	monoclonal	Sigma	M1406		1:500
22	Calbindin	Rb	polyclonal	abcam	ab11426		1:500
23	Foxg1	Rb	polyclonal	Thermofisher Scientific	PA5-26794		1:10-1:50
24	Tbr2	Rb	polyclonal	milipore	AB2283		1:250
25	Prox1	Rb	polyclonal	abcam	AB5475		1:500
26	Nestin	Ch	polyclonal	Biolegend Novusbio	NB100-1604		1:1000
27	βIII-tubulin	Rb	monoclonal	Biolegend Convence	802001 PRB-435p		1:500
28	βIII-tubulin	Ms	monoclonal	Biolegend Convence	801201 MMS-435P		1:1000
29	NeuroD1	Ms	monoclonal	SantaCruz	Sc46684		1:200

2.6.1.8 DG Differentiation of mESCs by transcription factors induction

For investigating the role of transcription factors in DG induction and differentiation, the same protocol mentioned above-except for the growth factor cocktails-was applied.

2.7 DNA preparation and PCR analysis

Sample Preparation (total RNA Extraction) for Fluidigm analysis

- Cells: collected by trypsinization
- EBs: collected by aspirating with pipette
- Kit: RNeasy Mini-Kit (Qiagen)
- Centrifugation 2 min at 1400 rpm (250 x g)
- Removal of as much medium as possible
- Disturbing the pellet by flicking
- Addition of 100 µl RLT-Lysis buffer with ß-ME, mixing by flipping
- Freezing of samples at -80°C until the sample set is complete

- Samples were thawed
- Addition of 250 µl RLT-buffer with ß-ME to a final volume of 350 µl
- Homogenization by passing lysate 7 times through a 20G needle fitted to a 1 mL syringe
- Extraction according to the manual including optional centrifugation step
- Elution: 35 µl RNase free water
- Concentration measurement with Spectrophotometer NanoDrop 2000c (Thermo Scientific)
- Adjustment to a final RNA concentration of 20 ng/µl with RNase free water

2.8 Gene expression analyses by Fluidigm Biomark system

The gene expression analysis of cells was performed using the Biomark Real-Time quantitative PCR (qPCR) system (Fluidigm) as described before in Conrad et al., 2016. In all cell samples the expression of the following genes was analyzed by TaqMan assays:
Pluripotency genes: POU5F1, NANOG, SOX2
Glial markers: GFAP, MBP, OLIG2
Neural precursor and proliferation markers: NESTIN, KI67, PCNA
Neuronal differentiation markers: NEUN, TUBB3, NCAM1, SYP, GABA, SLC1A3
Markers of telencephalic induction: SOX1, HES5, PAX6, REST1, MASH1, NEUROG2, TBR2, SOX11
Dentate gyrus induction and granule neuron differentiation: NEUROD1, FOXG1, EMX1, EMX2, GLI3, CREB, TBR1, NEUROD2, DCX, PROX1, ID3, FABP7, CALB1, CALB2, BMPR1A, NFIX, CCND2, NR2E1, LHX1, LHX2, LEF1, LRP6
and the housekeeping genes GAPDH, HMBS and normalized with all housekeeping genes TBP. The inventoried TaqMan assays (Applied Biosystem) were pooled to a final concentration of 0.2× for each of the assays. Cells to be analyzed were harvested directly into 9 µl RT-PreAmp Master Mix consisted of 5.0 µl CellsDirect 2× Reaction Mix (Invitrogen), 2.5 µl 0.2× assay pool, 0.2 µl RT/Taq Superscript III (Invitrogen) and 1.3 µl TE buffer. The harvested cells were immediately frozen and stored at −80°C. Cell lysis and sequence-specific reverse transcription was performed at 50°C for 15 min. The reverse transcriptase was inactivated by heating to 95° C for 2 minutes. In the same tube cDNA subsequently underwent through limited sequence-specific amplification by denaturing at 95° C for 15 seconds, and 14 cycle-annealing and amplification at 60° C for 4 minutes. These pre-amplified products were 5-fold diluted prior to analysis with Universal PCR Master Mix and inventoried TaqMan gene expression assays (ABI) in 96.96 Dynamic Arrays on a BioMark System.

GenEx statistical analysis

Ct values obtained from the BioMark System were transferred to the GenEx software (MultiD) for analysis. Missing data in the Biomark system were assigned a Ct of 999 by the instrument software. These were removed in GenEx. Also Ct's larger than a cut-off of 25 were removed, since high Ct's in the Biomark 96.96 microfluidic card were expected to be false positives due to base-line drift or formation of aberrant products, since a sample with a single template molecule is expected to generate a lower Ct. The effect of setting cut-off to 25 was tested by

repeating the analysis with a slightly different cut-off and was found to have negligible effect on the analysis results. Technical repeats were then averaged and any remaining missing data were replaced by the highest Cq measured + an offset of 1 for each gene separately. Managing missing data is primarily required for downstream multivariate classification of the data. An offset of 1 corresponds to assigning a concentration to the samples with off-scale Cq values that is half of the lowest concentration measured for a truly positive sample. The magnitude of the offset does not influence p-values calculated with non-parametric methods, which were preferred when there were off-scale data, but it has small influence on p-values calculated by t-test and on multivariate classification. In essence, the offset is tunes the weight of the off-scale measurement compared to the positive reading, larger offset gives higher weight to the off-scale measurement. We tested the importance of the offset by repeating the analysis using a higher offset up to +4, which corresponds to a concentration of 6% of a truly positive sample, and found negligible effect on the multivariate results. Linear quantities were calculated relative to the sample having lowest expression and data were then converted to log2 scale for analysis. Because of the very large and uncorrelated cell to cell variation of genes´ expressions normalization to the housekeeping genes is not meaningful. Instead, expression levels were presented "per 50 cell" average expression of the genes in different groups was calculated including .95% confidence interval and groups were compared using 1-way ANOVA (Tukey-Kramer's pairwise comparison) and unpaired 2-tailed T-Test. Expression of genes with multiple off-scale readings was compared with non-parametric Mann-Whitney's test. For multivariate analysis to classify the samples based on the combined expression of all the genes data were either mean centered, i.e., subtracting the average expression of each gene, or autoscaled, which is mean centre data also divided by the standard deviation (so called z-score). Autoscaling gives all the genes equal weight in the classification algorithms making them equally essential. Hierarchical clustering (Ward's Algorithm, Euclidean Distance Measure) including heatmap and principal component analysis (PCA) were performed.

Table 2.31: Details of the TaqMan primers used in this study with gene, gene name, species and assay ID

Gene	Gene name	Species	Assay ID
Pou5f1 or Oct4	POU domain, class 5, transcription factor 1	mouse	Mm03053917_g1
Nanog	Nanog homeobox	mouse	Mm02384862_g1
Sox2	SRY (sex determining region Y)-box 2	mouse	Mm00488369_s1
GFAP	glial fibrillary acidic protein	mouse	Mm01253033_m1
MBP	myelin basic protein	mouse	Mm01266402_m1
OLIG2	oligodendrocyte transcription factor 2	mouse	Mm01210556_m1
NESTIN	nestin	mouse	Mm00450205_m1
KI67	antigen identified by monoclonal antibody Ki 67	mouse	Mm01278617_m1
PCNA	proliferating cell nuclear antigen	Mouse	Mm00448100_g1
NEUN	RNA binding protein, fox-1 homolog (C. elegans) 3	Mouse	Mm01248771_m1
TUBB3	tubulin, beta 3 class III	Mouse	Mm00727586_s1
NCAM1	neural cell adhesion molecule 1	Mouse	Mm01149710_m1
SYP	synaptophysin	Mouse	Mm00436850_m1
GABA	gamma-aminobutyric acid (Hamrahian, Ioachimescu et al.) A receptor, subunit alpha 6	Mouse	Mm01227754_m1

SLC1A3	solute carrier family 1 (glial high affinity glutamate transporter), member 3	mouse	Mm00600697_m1
SOX1	SRY (sex determining region Y)-box 1	Mouse	Mm00486299_s1
HES5	hairy and enhancer of split 5 (Drosophila)	Mouse	Mm00439311_g1
PAX6	paired box 6	Mouse	Mm00443081_m1
REST1	RE1-silencing transcription factor	Mouse	Mm00803268_m1
MASH1	achaete-scute complex homolog 1 (Drosophila)	Mouse	Mm03058063_m1
NEUROG2	neurogenin 2	Mouse	Mm00437603_g1
TBR2	eomesodermin homolog (Xenopus laevis)	Mouse	Mm01351984_m1
SOX11	SRY (sex determining region Y)-box 11	Mouse	Mm01281943_s1
NEUROD1	neurogenic differentiation 1	Mouse	Mm01946604_s1
FOXG1	forkhead box G1	Mouse	Mm02059886_s1
EMX1	empty spiracles homeobox 1	Mouse	Mm01182609_m1
EMX2	empty spiracles homeobox 2	Mouse	Mm00550241_m1
GLI3	GLI-Kruppel family member GLI3	Mouse	Mm00492337_m1
CREB	CREB/ATF bZIP transcription factor	Mouse	Mm02525218_s1
TBR1	T-box brain gene 1	Mouse	Mm00493433_m1
NEUROD2	neurogenic differentiation 2	Mouse	Mm00440465_g1
DCX	doublecortin	Mouse	Mm00438400_m1
PROX1	prospero homeobox 1	Mouse	Mm00435969_m1

ID3	inhibitor of DNA binding 3	Mouse	Mm00492575_m1
FABP7	fatty acid binding protein 7, brain	Mouse	Mm00445225_m1
CALB1	calbindin 1	Mouse	Mm00486647_m1
CALB2	calbindin 2	Mouse	Mm00801461_m1
BMPR1A	bone morphogenetic protein receptor, type 1A	Mouse	Mm00477650_m1
NFIX	nuclear factor I/X	Mouse	Mm00477791_m1
CCDN2	cyclin D2	Mouse	Mm00438070_m1
NR2E1	nuclear receptor subfamily 2, group E, member 1	Mouse	Mm00455855_m1
LHX1	LIM homeobox protein 1	Mouse	Mm01297482_m1
LHX2	LIM homeobox protein 2	Mouse	Mm00839783_m1
LEF1	lymphoid enhancer binding factor 1	Mouse	Mm00550265_m1
LRP6	low density lipoprotein receptor-related protein 6	Mouse	Mm00999795_m1
GAPDH	glyceraldehyde-3-phosphate dehydrogenase	Mouse	Mm99999915_g1
HMBS	hydroxymethylbilane synthase	Mouse	Mm01143545_m1
TBP	TATA box binding protein	Mouse	Mm01277042_m1

3. Results

3.1 Preparatory work

Before the establishment of a new strategy for the directed differentiation of mouse ES cells into DG neural precursor and completely differentiated cells, preparatory work had to be performed.

By the use of mouse ES cell culture techniques and the application of molecular cloning techniques at the beginning of this work a tetracycline inducible EGFP expression system in *mouse* ES cells was generated in our lab (Fig. 3.1). We were able to generate stable mouse ES cell lines for tetracycline regulated gene expression with minimal leakiness and a high degree of tetracycline responsivity. These mouse ES cell lines were further engineered for the generation of a double and triple stable cell line, expressing central dentate gyrus transcription factors in an inducible manner. Importantly, the selected cell lines retained their inherent morphology, responded to differentiation signals and exhibited persistent and highly tunable tetracycline inducibility upon continuous culturing.

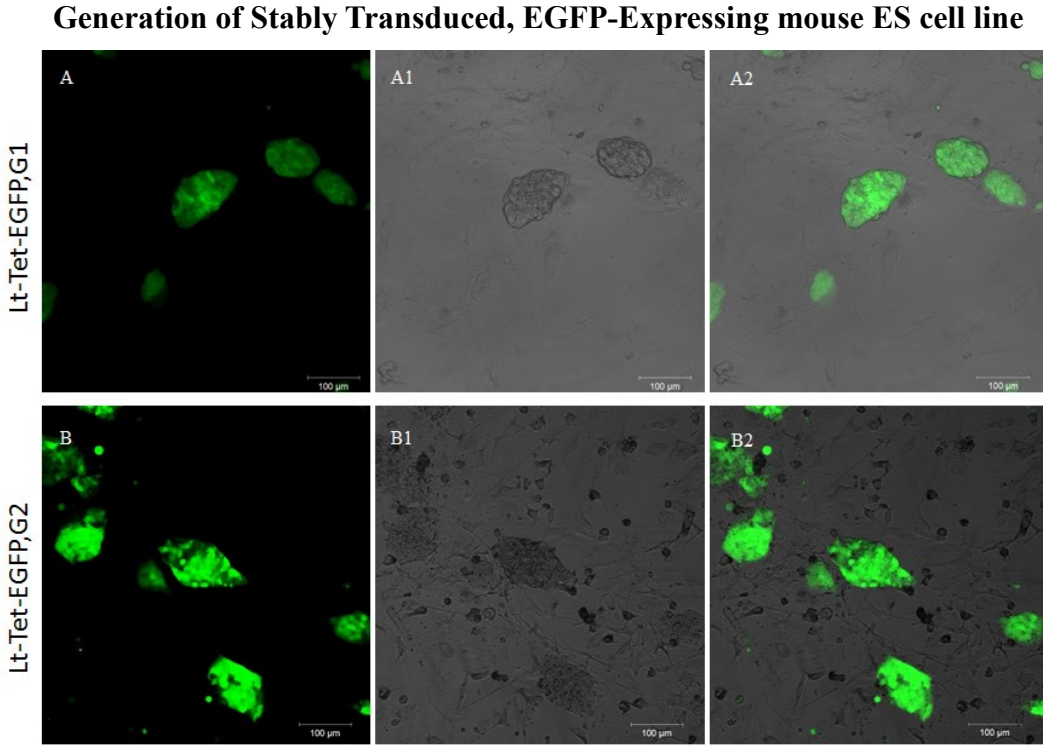

Fig. 3.1 Representative confocal images of generated mouse ES cells lines with inducible EGFP (left column, EGFP; medial column, phase-contrast; right column, merged. EGFP was turned on when treated with 500 ng/mL Dox for 12-19 hours. Scale bar: 100 µm.

The expression of pluripotency factors such as Nanog and Sox2 in the generated cell lines Lt-Tet-EGFP (G1 and G2) revealed their pluripotency (see Fig.3.2) which is a striking evidence of their capability to run through the full spectrum of neural differentiation ranging from neuroectodermal induction towards the dorsal telencephalic differentiation signaling roads. The telencephalic differentiation capacity of the generated cell lines was examined in pilot experiments (data not shown).

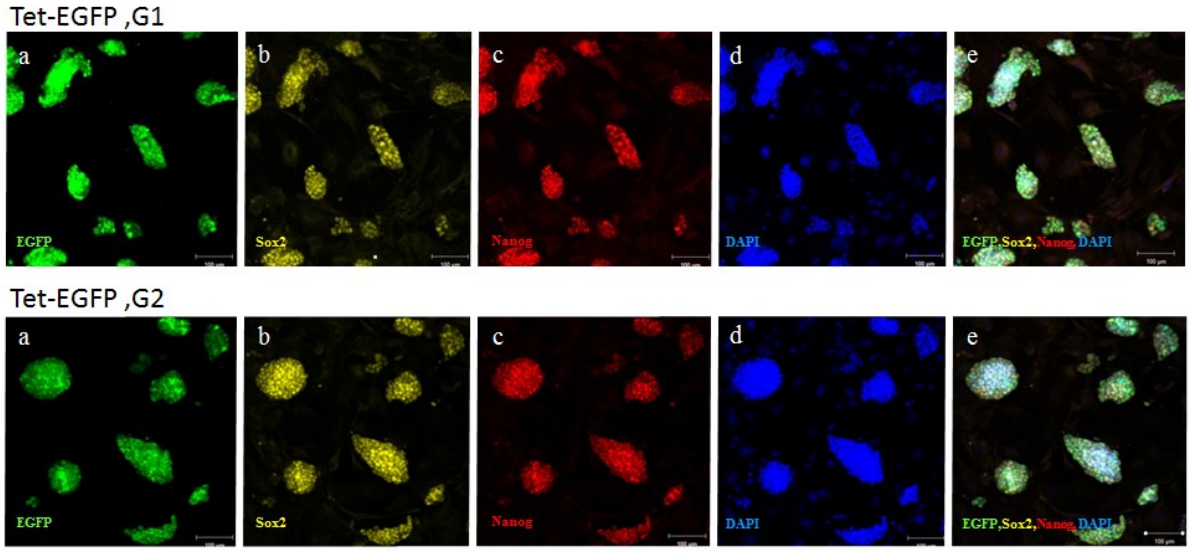

Fig. 3.2 ES:Lt-Tet-EGFP characterization by visualization of pluripotency transcription factors. Homogeneous expression of pluripotency factors is observable in ES cells. (a) EGFP signal and immunofluorescence staining for (b) Sox2, (c) Nanog, (d) staining with DAPI and (e) merge of EGFP clone G1 and G2. Scale bar: 100 µm.

In detail, the mouse ES cell line was established and propagated for multiple passages to ensure homogeneity and robustness among the cells. The ES cells were first examined for their sensitivity to the selection antibiotic Zeocin, by antibiotic killing curve assay. The optimal concentrations required for selection was 100 mg/ml Zeocin.

Mouse ES cells were co-transduced with the M2rtTA and Tet-FUW- EGFP virus particles and then selected with Zeocin. The use of very low antibiotic concentrations accommodates for the sensitivity and slow growing nature of mouse ES cells, thereby allowing for efficient selection of transduced cells. The cells were examined for EGFP expression and as expected, all the clones were positive. Though the clones varied in the degree of EGFP expression, within a single clone there was a uniform intensity of EGFP fluorescence suggesting homogeneity among clonal populations.

Two representative clones ES;Lt-Tet-EGFP G1 and G2 were chosen for further analysis. These clones were selected based on the criterion that they expressed uniform and high levels of EGFP throughout the cell population (Fig. 3.1 and 3.2). In addition, they displayed normal morphological characteristics and growth behavior similar to their parent not transduced ES cell line.

3.2 Neuronal Differentiation of Mouse ES Cells via EB Formation

The mouse ES cells have so far been noteworthy for their pluripotency, easy handling, and high differentiation capacity, along with the study of different molecular mechanisms which are responsible for the directed cellular differentiation.

Several techniques have been proposed for the direct cellular differentiation of ES cells, trying to incorporate several elements such as enrichment, homogenization, and the progressively accurate specification of the differentiating cells.

A well-known method in this category is the EB formation which has been primarily introduced by Ana Wobus (Strubing, Ahnert-Hilger et al. 1995) and D.G Mackey (Okabe, Forsberg-Nilsson et al. 1996) for the generation of enriched neuronal progenitor cells.

This method became popular over the years among numerous research groups around the world, including the research team led by Prof. Sasai which implemented this method along with a defined medium culture and they succeeded for the first time in the differentiation of mouse ES cells to the telencephalic progenitor cells (Watanabe, Kamiya et al. 2005).

Gage and Colleagues in 2013 modified the Sasai's approach to differentiate the hIPS cells towards hippocampus neuronal progenitor cells (Yu, Di Giorgio et al. 2014).

In this study, we applied the homogeneous EB formation technique used for the inducible cocktail of growth factors and transcription factors contributing to the generation of DG during embryonic development. We investigated the effects of these factors in differentiation and the continuous enrichment of the mouse ES cells towards the development of DG progenitor and fully differentiated granule cells.

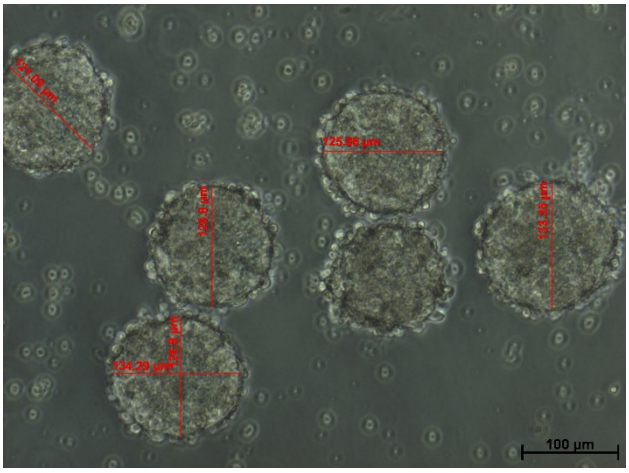

Fig. 3.3 Generation of EBs that are homogeneous in size and shape. Scale bar: 100 µm.

3.3 Differentiation of mouse ES cell into DG precursors in a two-step culture method

3.3.1 Three-dimensional culture of neuroectodermal and telencephalic induction with growth factors treatment

The 3D culture procedure was applied to simulate aspects of early and pre-gastrulation which has been optimized by applying several growth factors which have critical influence during DG development. The elimination of FBS Serum and KO/SR from the culture environment and the simultaneous application of N2 and B27 supplements induced a homogeneous population of neuro-ectodermal progenitor cells expressing Nestin and GFAP markers in all four treatment groups. Nestin and GFAP were located on cellular structures and radial processes in the EBs along an inside- outside gradient (Fig. 3.4).

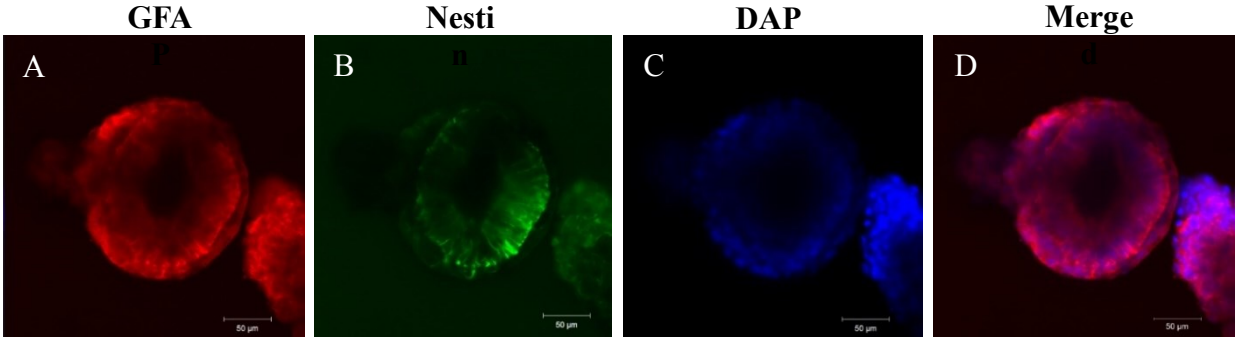

Fig. 3.4 Expression of neuroectodermal markers in 6 day-old EBs treated with a cocktail of growth factors and DKK1(group3). Scale bar: 50 µm.

The simultaneous treatment of EBs by anti-caudalization and anti-ventralization factors Noggin, SB431542, and cyclopamine (growth factors cocktail) induced the neural telencephalic progenitor marker Sox 1 in the treatment group (group 2, 3, 4).

To achieve the pure telencephalic progenitor cell, the EBs were treated with the Wnt signaling inhibitors Dkk1 and Dkk3 separately. The dorsomedial telencephalic markers Pax6 and Nestin were observed during this treatment. The results showed that the EBs which were treated with the growth factors cocktail and Dkk1 expressed the telencephalic marker Foxg1 more strongly than another the groups on day 10 (Fig. 3.5).

During the study of these EBs, it seemed that the configuration of the Foxg1 positive cells followed a distinct specific being located in the middle layers of EBs, while earlier markers such as Sox1 and BLBP were more configured in the interior layers. These markers could not be observed in control groups at the same day.

Expression of neural telencephalic progenitor markers in 10 day-old EBs treated with DKK1 (group3)

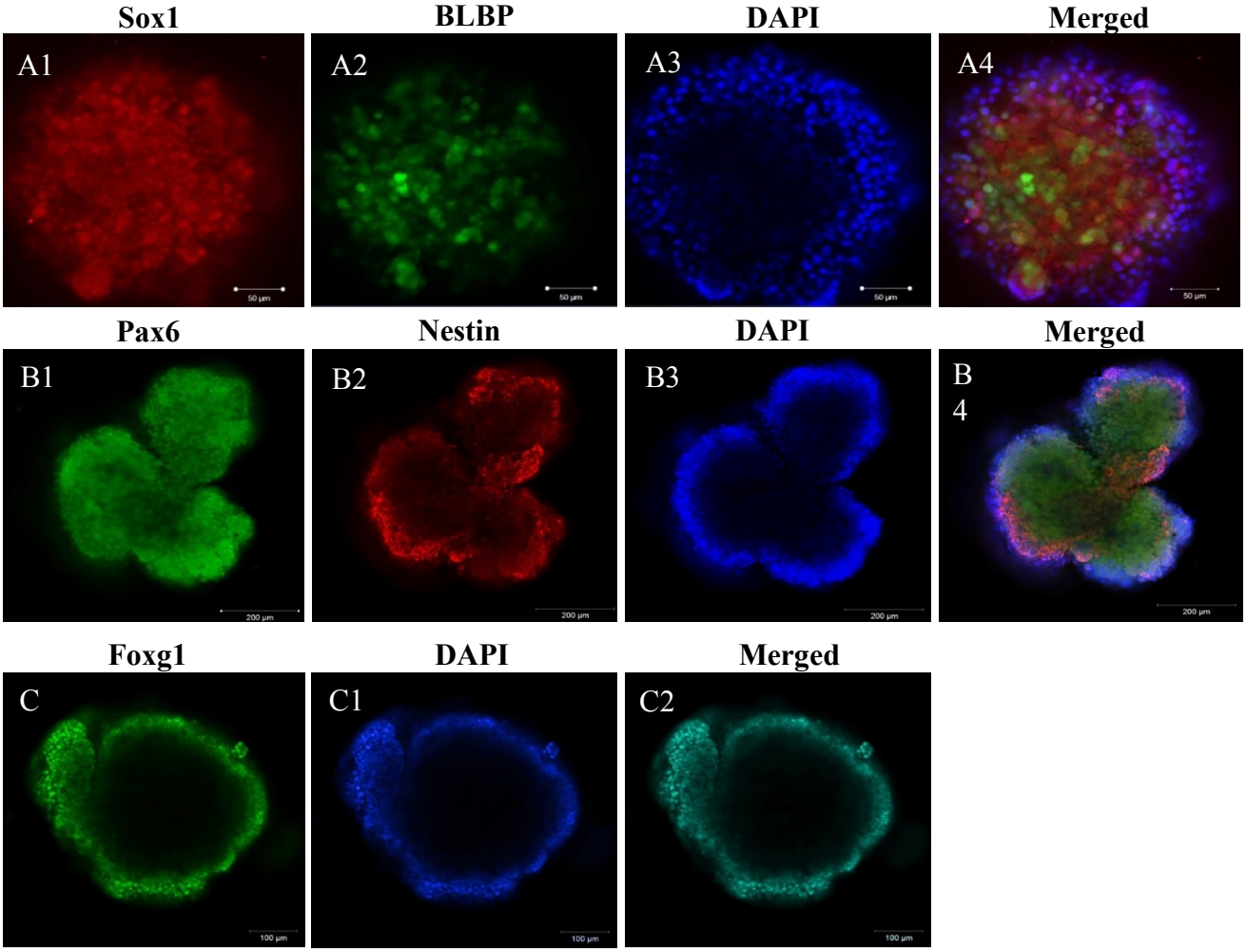

Fig. 3.5 Expression of telencephalic neural marker in 10 days old EBs treated with DKK1. Immunofluorescence analyses of 10-day old mouse ES cell-derived EBs with telencephalic progenitor markers Sox1, BLBP, Pax6 and Foxg1. Nuclei were visualized by DAPI-staining. Scale bar: 100 µm.

3.3.2 Two dimensional culture of telencephalon progenitor cells astrocyte co-culture system

After 16 days, the neurospheres were triturated to a single cell suspension and re-plated on poly-L-Ornithine/laminin and co-cultured with astrocytes. Within 4 to 5days (on 20 to 21 of culture) a small putative neural progenitor cell (NPC) population was observed in the growth factors treatment groups. In these groups, the neuronal progenitor cells markedly exhibit colony-like structures. It seemed that introduction of these growth factors resulted in a specific grouping of NPC on the culture surface. The NPC population started to proliferate and formed distinct borders. From around day 27, the colony-like structures were distinctively recognizable.

The remarkable point about these NPC colony-like structures was that they had specified boundaries---which for the most part---during differentiation and even proliferation, the cells showed no tendency for migrating out from the colony-like structures and still remained in these coherent forms. The number of these structures in the treatment group by Dkk1 were higher than in the other treatment groups (Fig 3.6). On day 37, the morphological observation of NPC colonies under light phase-contrast showed that the NPC colonies *features* in the control group were obviously different than in the treatment groups. In the control, most of the neuro-progenitor cells were sparsely distributed across the cell culture plate in comparison to the groups treated with anti-caudalization and anti- ventralization factors (Noggin, SB431542 and cyclopamine) (Fig. 3.6). The NPC markedly exhibited colony-like structures. It seemed that introduction of these growth factors resulted in a specific grouping of the neuro-progenitor cells in the culture.

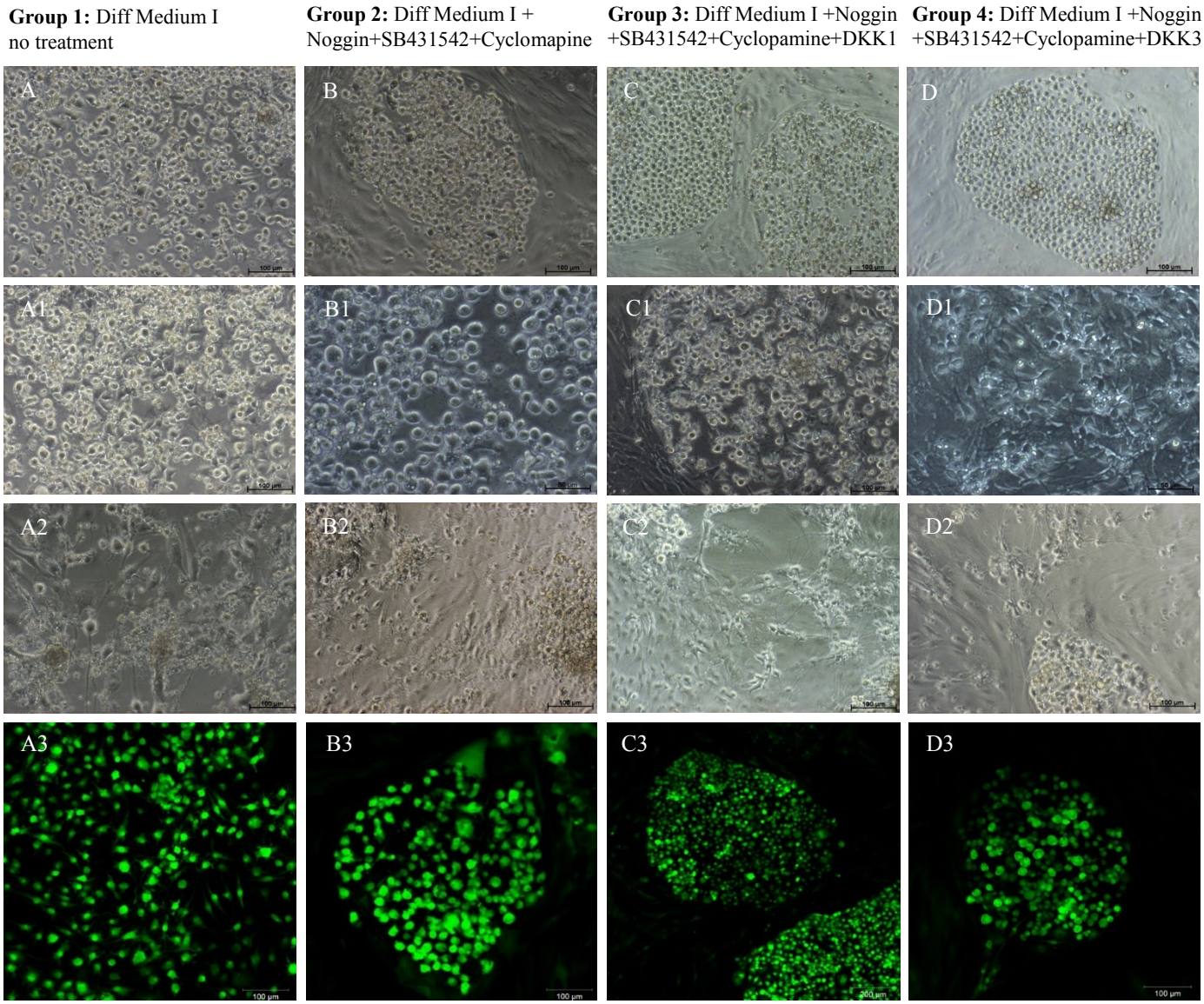

Fig. 3.6 Evaluation of phase contrast and confocal microscopy of four different growth factor treatments in ES:Lt-Tet-EGFP. The first three rows demonstrate the phase contrast (A-A2, B-B2, C-C2, D-D2), and the last row shows the confocal microscope images (A3-D3). Scale bar: 100 µm.
Group1: (Differentiation medium I, no treatment): sparse distribution of NPC.
Group2: (Differentiation medium I+ Noggin+SB431542+Cyclopamine treatment) towards to NPC colony aggregation.
Group3: (Differentiation medium I+ Noggin+SB431542+Cyclopamine treatment+DKK1) the emergence of limited NPC colony aggregation and neural differentiation.
Group4: (Differentiation medium I+ Noggin+SB431542+Cyclopamine treatment+DKK3) colonies morphologically similar to that of group3 were partially observed, but demonstrate considerably more heterogeneity.

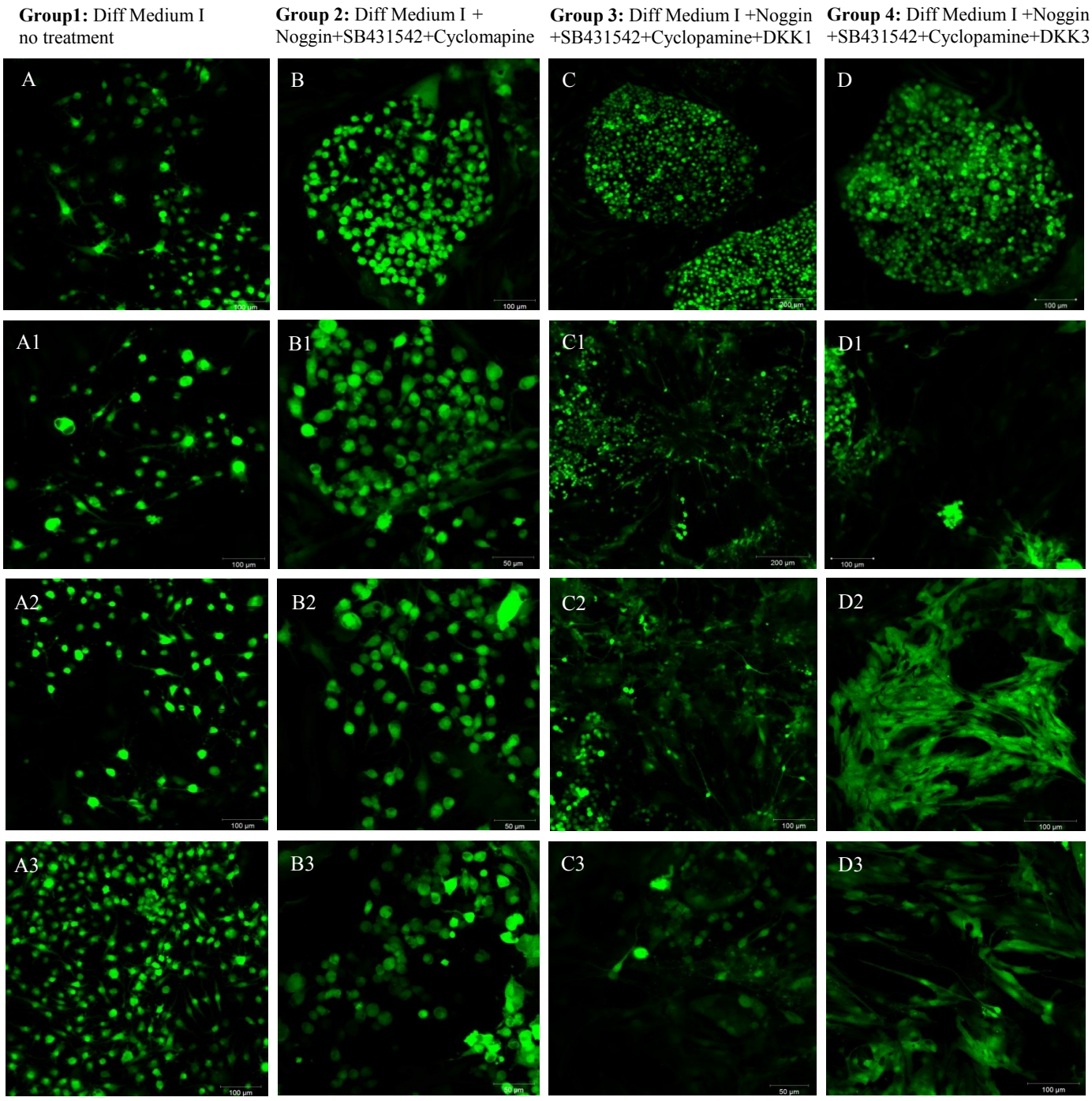

Fig. 3.7 The EGFP expression of NPC derived ES:Lt-Tet-EGFP. The cells were treated with cocktail of growth factors. Group1: sparse distribution of NPCs. Group2: towards NPC colony aggregation. Group3: the emergence of limited NPC colony aggregation and neural differentiation. Group4: colonies morphologically similar to that of group3 were partially observed, but demonstrate considerably more heterogeneity. Scale bar: 100 µm.

The obtained results by immunofluorescent technique showed that most of the cells in the control group expressed only Nestin and GFAP. But telencephalic markers or DG differentiation markers were absolutely not expressed. The immunofluorescent technique revealed that in the growth factors group these structures potentially expressed the specific markers of the DG such as Prox1, NeuroD1 and Tbr2 (see Table 3.1). We named these structures the DG progenitor-like colonies. The notable landmark in the study of these structures is that, for the most part, these structures did not proceed towards the neuronal-like structures with axon, dendrite formation and branching and remained at the stage of DG progenitors.

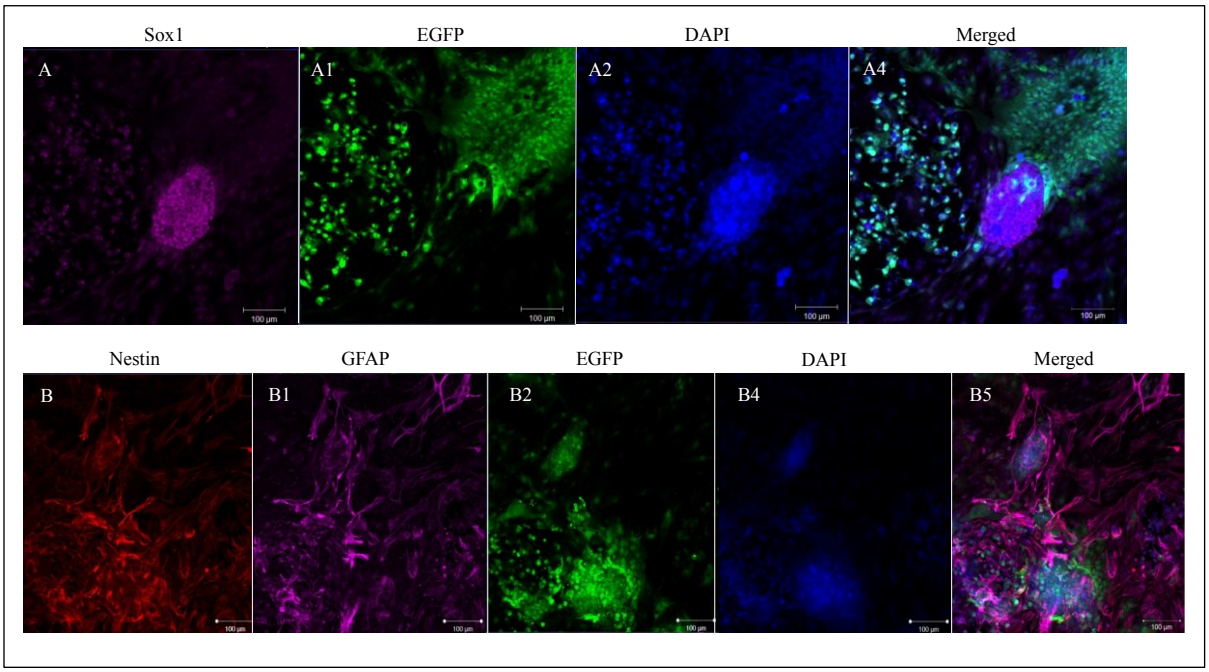

Fig. 3.8 Expression of neuroectodermal markers in 37 day-old adherent cell culture, DKK1 treated (group3). A-A4 Sox1; B-B4 Nestin-GFAP. Nuclear staining with DAPI. Scale bar: 100 µm.

The comparison of different DG markers on day 37 demonstrated that Dkk1 was more effective in the induction and production of ES cell to the DG progenitors (Fig. 3.6-3.10, Table 3.1). Specifically, Dkk1 caused an increased expression of the telencephalic neuronal progenitor markers including Foxg1, BLBP and Tbr-2. Emx2 expressing cells were rarely found. In comparison with other groups, the growth factors cocktail with Dkk1treatment had an inductive effect on the expression of several of the DG markers, like NeuN, NeuroD1, Prox1, Calretinin and Calbindin. But most of these cells were not fully differentiated. The limited differentiation was only observed inside the colonies.

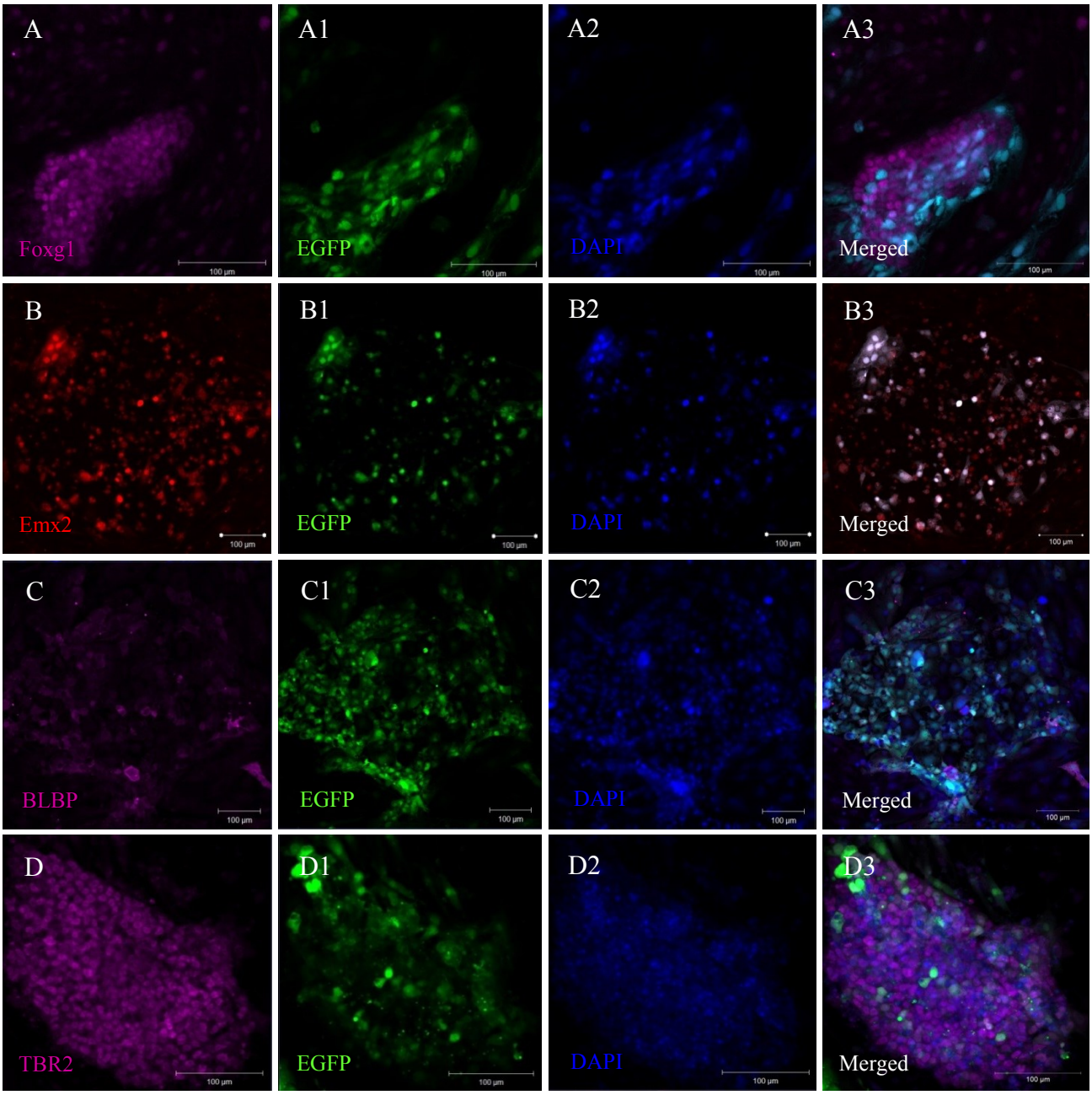

Fig. 3.9 Expression of Telencephalic Neural Progenitor markers in 37 days old adherent cell culture, DKK1 treated (group3). A-A3 Foxg1, B-B3 Emx2, C-C3 BLBP, D-D3 TBR2. Scale bar: 100µm.

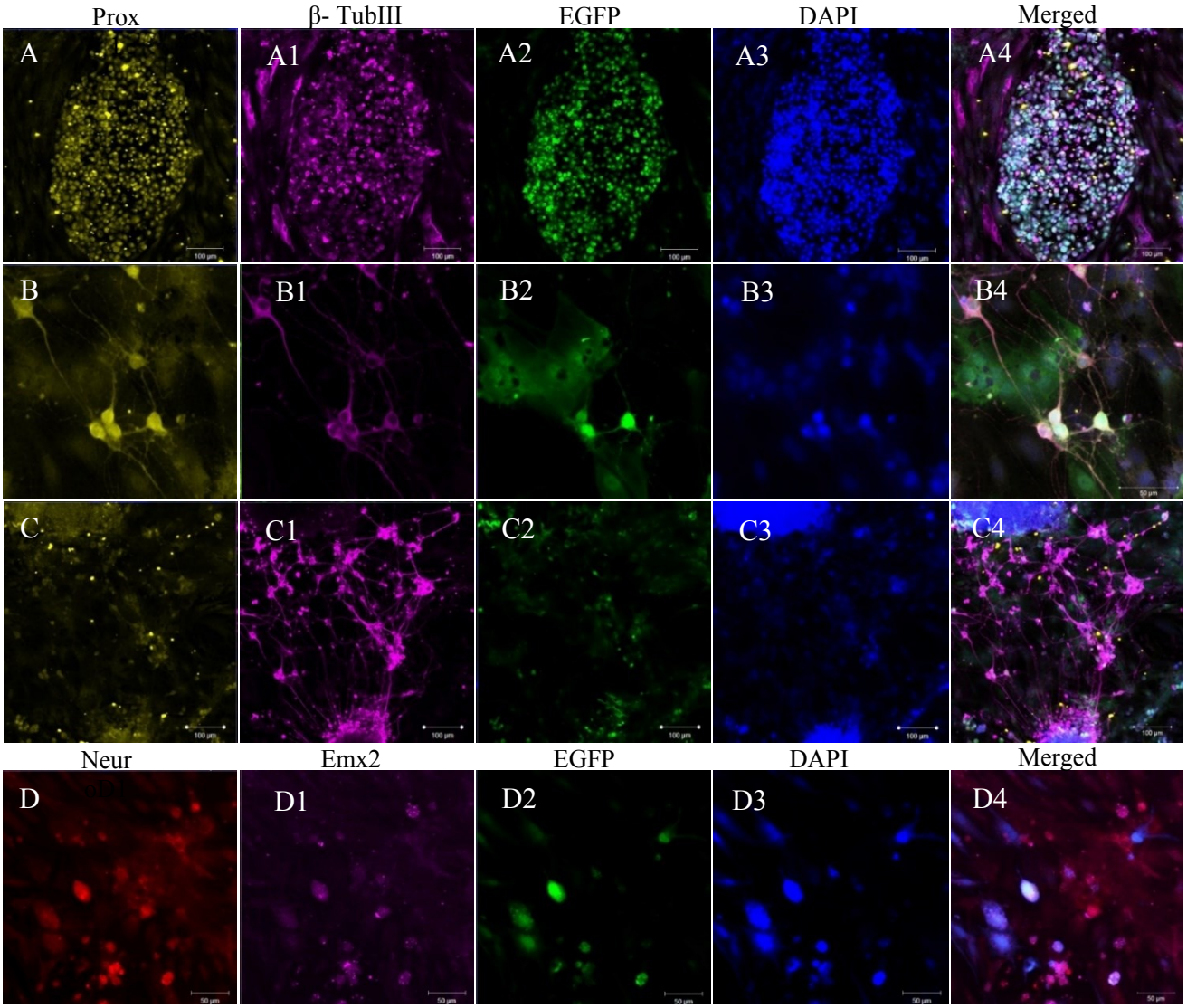

Fig. 3.10 Expression of DG Markers on treated cells with DKK1 on 37 days old astrocyte adherent co-culture. A-A4, B-B4, C-C4 Prox1/βIII-tubulin; D-D4 NeuroD1-Emx2. Nuclear co-staining with DAPI. Scale bar: 100 µm.

In the treatment groups # 1 and # 2, most of the cells were stage of the Sox1 negative progenitor cell phenotype, remained or differentiated towards gliogenesis.

In comparison with Dkk1, the treatment by Dkk3 did not appear to be much effective. This treatment in the early stages of cell culture had a similar role in the induction of markers like BLBP, GFAP, Nestin, and Sox1, but had no significant effect in the induction of specific DG markers such as NeuN, Prox1, Calretinin, Calbindin. None of the other treatment groups had any effects on the induction of Emx2. The neurotransmitter glutamate specific for differentiated DG neurons was not expressed under any of these growth factor conditions.

Different marker expression of DG patterning in ES: Lt-Tet-EGFP, cloneG1 under 4 different growth factor treatments on 37 differentiation day

D37	Neuroectodermal Marker			Telencephalic Neural Progenitor Marker				Dentate Gyrus Markers							
	Sox1	Nestin	GFAP	Foxg1	Emx2	Blbp	Tbr2	NeuN	NeuroD1	DCX	Prox1	Calretinin	Calbindin	βIII-tubulin	Glutamte
G1	-	++	++	-	-	-	-	-	-	-	-	-	-	+	-
G2	+	++	++	+	-	-	-	-	-	-	-	-	-	+	-
G3	++	++	++	++	+	++	+	+	+	+	++	+	+	+	-
G4	++	++	++	+	-	++	++	-	+	++	-	-	-	+	-

Table 3.1: Comparative analysis of the expression of neuroectodermal, telencephalic progenitor and DG marker on 4 different growth factor treatment cell culture conditions. All results are expressed as percentages of the whole population: 0%–5%, negative (−); 6%–39%, low level of marker expression (+); 40%–79%, moderate level of marker expression (++); 80%–100%, high level of marker expression (+++).

3.4 The hippocampal transcription factor induction and DG differentiation

Several studies had shown so far that growth factors---in most cases---due to the induction of neural differentiation genes and by affecting certain transcription factors associated with those genes can play a role in the differentiation and development of neuronal structures (Wilson and Rubenstein 2000); (Wilson and Houart 2004).

Developmental biological research has shown the significant effect of transcription factors during differentiation and development. Because of this fundamental role, a variety of research models have so far investigated the transcription factors during the process of telencephalic and hippocampal development (Eiraku, Watanabe et al. 2008); (Hanashima, Fernandes et al. 2007).

At this stage, we studied the role of the transcription factors Emx2, Prox1 and NeuroD1 separately on the production and induction of the DG granule neurons.

The mouse ES cell lines were further engineered for the generation of a double and triple stable cell line, expressing central DG transcription factors (Emx2, Prox1 and NeuroD1) in an inducible manner. In this regards, the ES; Lt-Tet-EGFP clone G1 was engineered for the

generation of a double and triple stable cell line, expressing central DG transcription factors (Emx2, Prox1 and NeuroD1) in an inducible manner (Fig.3.11).

Generation of stably transduce, transcription factors -EGFP-Expressing mouse ES cell Line

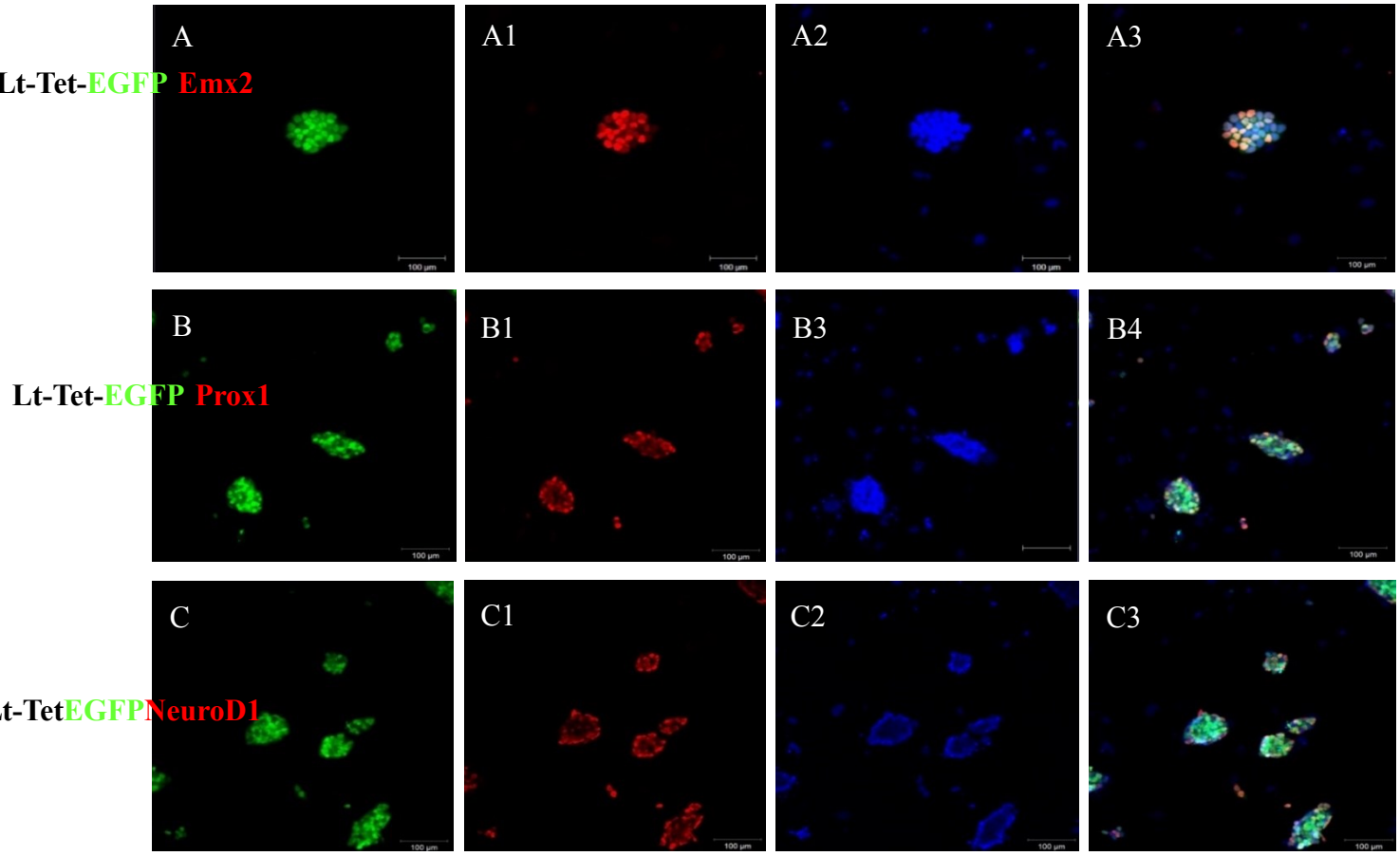

Fig. 3.11 Immunocytochemistry of re-transduced clones. Retransduction of ES: Lt-Tet-EGFP with transcription factors (Emx2, Prox1 and NeuroD1). EGFP was negative without Dox treatment, and was turned on when treated with 500 ng/mL Dox for 12-19 hours. Scale bar: 100 μm.

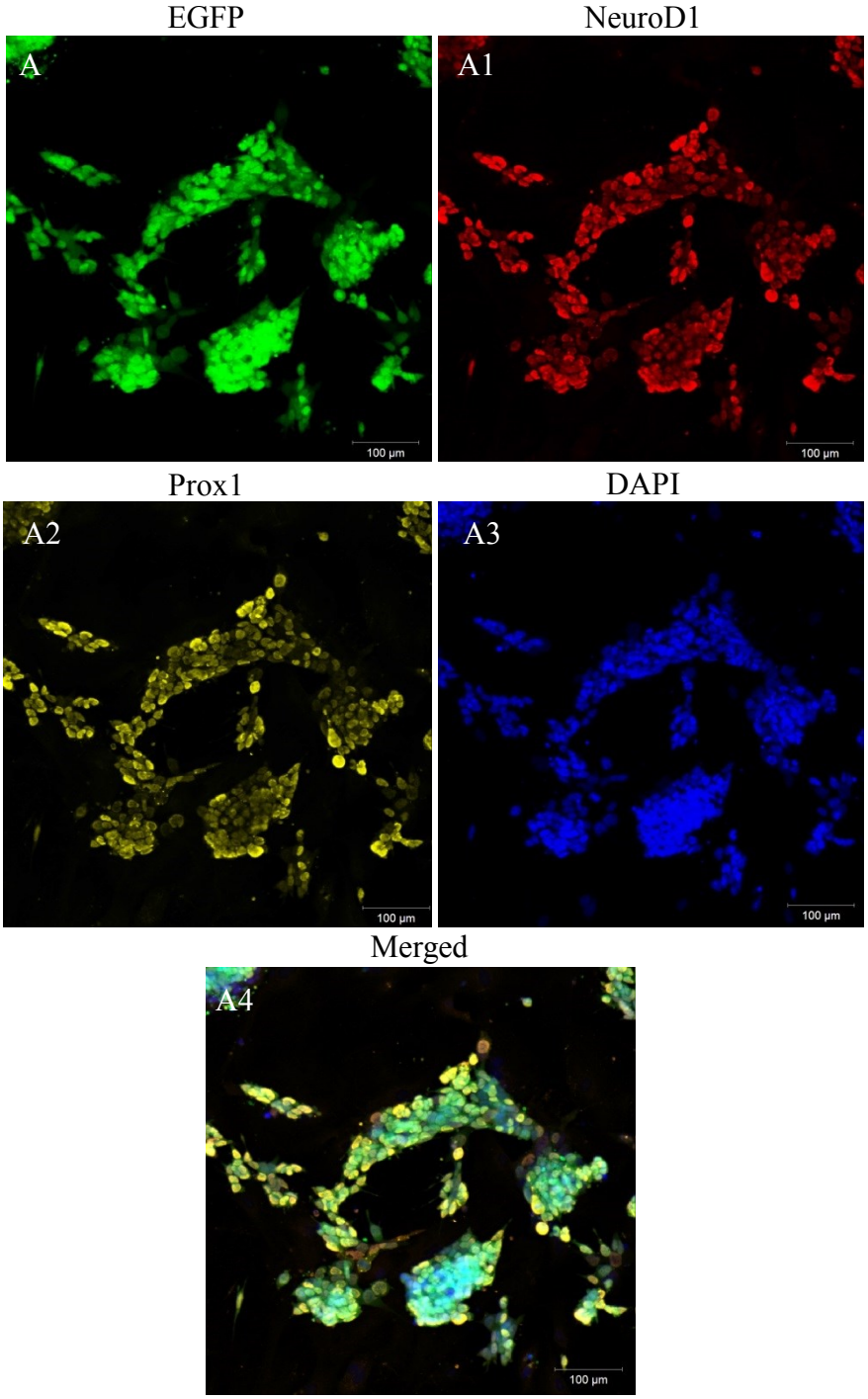

Fig. 3.12 Immunocytochemistry of ES: Lt-Tet-EGFP-NeuroD1-Prox1. Re-transduction of ES;Lt-Tet-EGFP-NeuroD1 with Prox1.EGFP was turned on when treated with 500 ng/mL Dox for 12-19 hours. Scale bar: 100 µm.

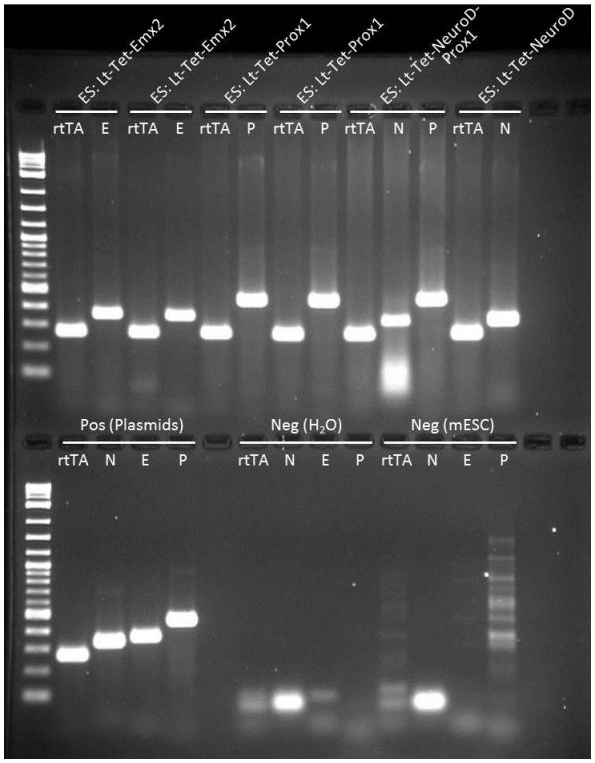

Fig. 3.13 PCR analyses for plasmid integration in genomic DNA from the ES cell line ES: Lt-Tet-Emx2 Clones (lane 1-4), ES:Lt-Tet- Prox1 Clones (lane 6,8,10), ES:Lt-Tet-NeuroD1-Prox1 Colon (lane 9,10, 11), ES:Lt-Tet- NeuroD1 Clone (Lane12,13); Controls (+): Bacterial DNA plasmids: fuw-M2rTtA, Tet-o-FUW-NeuroD1, Tet-o-FUW-Emx2, Tet-o-FUW-Prox1, Control (-), Water, Control (-), ESC (E14).

In this part of the study, the role of exogenous transcription factor expression leading to differentiation towards the induction and generation of DG progenitor cells and DG granule neurons in the absence/presence of Dox was investigated.

The microscopic observations on the day 8 showed that the EB structures at the stage of telencephalic induction by the addition of Dox revealed a strong EGFP expression (Fig. 3.14).

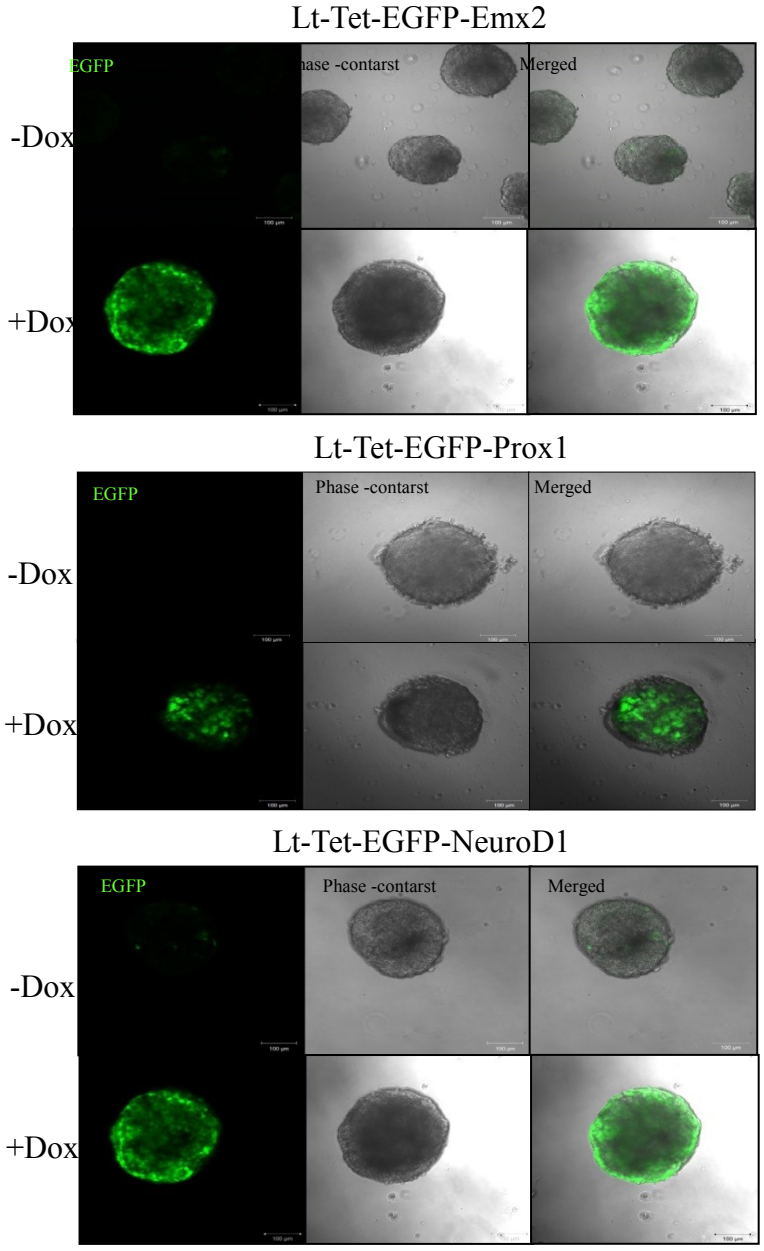

Fig. 3.14 Evaluation of EGFP expression on 8dayold EBs of transgenic clones. Representative confocal images (left column, EGFP; medial column, phase-contrast; right column, merged. 12 -19 h after Dox (500 ng/ml) and without treatment. Scale bar: 100 µm.

ES: Lt-Tet-EGFP-Emx2

By the end of day 37, the cellular differentiation in different clones by the induction of Dox showed that a persistent and vigorous expression of Emx2 in LT-Tet-EGFP-Emx2 prohibited the induction of DG progenitor cells and neurogenesis. In fact, it seems that the high expression of Emx2 by the inducible tetracycline system as described above, suppressed the

differentiation of telencephalic neuronal progenitor cells to DG progenitor cells and DG granule neurons in comparison with other ES cell transcriptional inducible cell lines like Prox1 and NeuroD1 (Fig. 3.15 -3.16; Table 3.2).

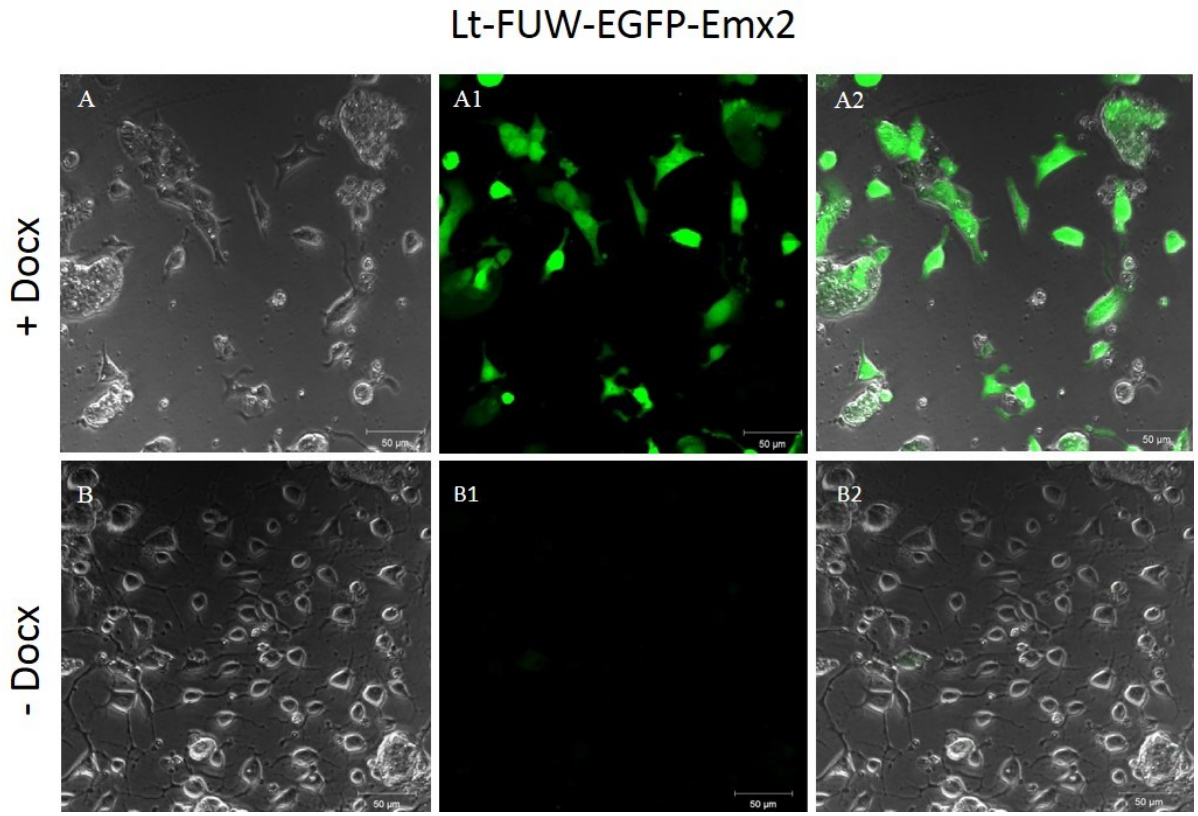

Fig. 3.15 DG differentiation of ES: Lt-Tet-EGFP-Emx2 on day37. Representative confocal images with Lt-FUW-EGFP-Emx2, the left column (A,B) phase-contrast, middle column (A1,B1) EGFP, and right column (A2,B2) merged. Scale bar: 100 µm.

ES:Lt-Tet-EGFP-NeuroD1 clones

The treatment of ES: Lt-EGFP-NeuroD1 clones resulted in the expression of Nestin and GFAP along with the telencephalic neuronal progenitor marker FoxG1. The observation of DG markers such as NeuN, NeuroD1, Prox1, βIII-tubulin, and Map(2a+2b) showed the existence of neurogenesis and gliogenesis. These results also showed that the transcription factor NeuroD1 alone was not capable for final DG differentiation.

Lt-Tet-EGFP-NeuroD1

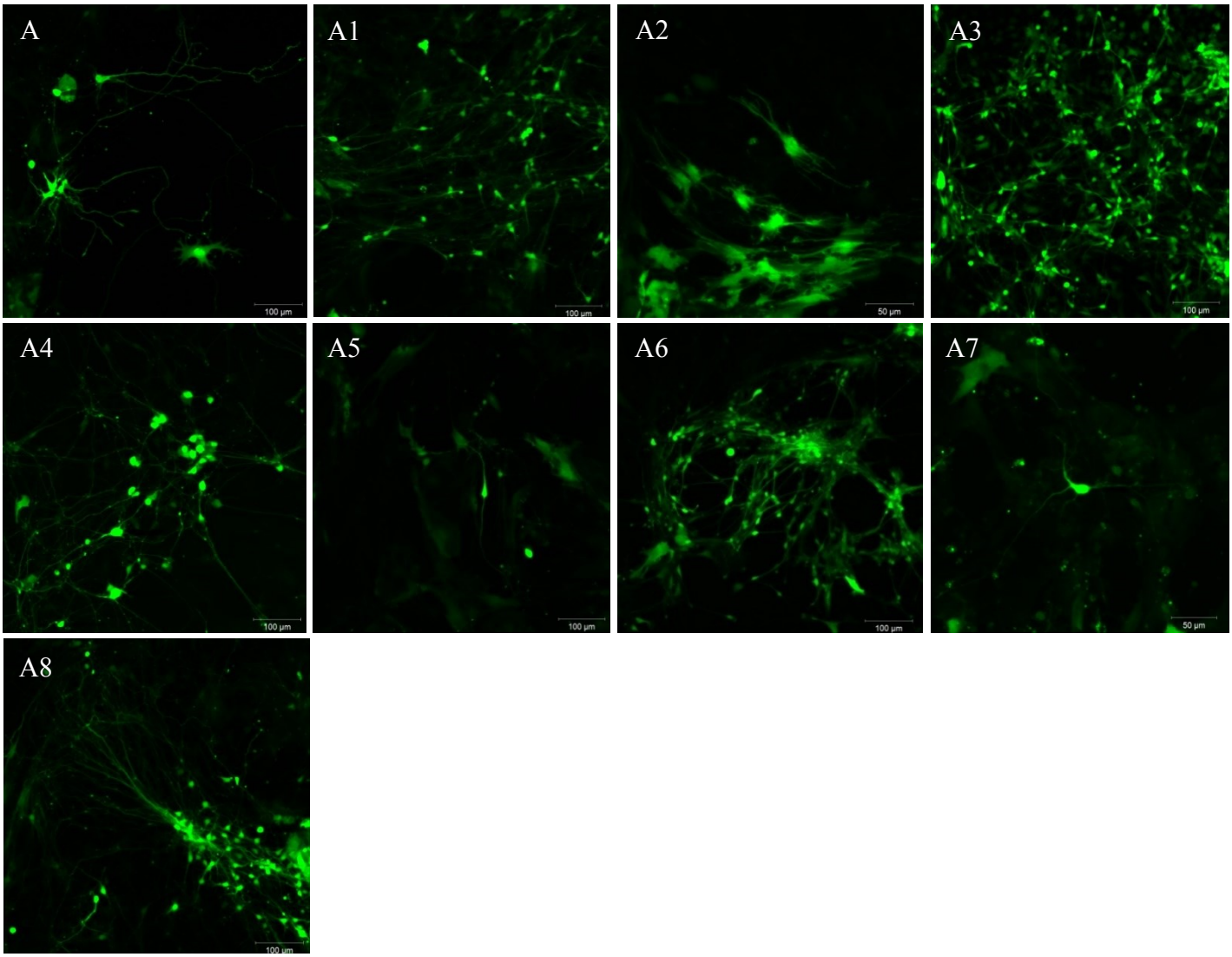

Fig. 3.16 Dentate gyrus differentiation of ES: Lt- Tet-EGFP -NeuroD1 on day 37.
Representative confocal images with Lt- Tet-EGFP-NeuroD1 on astrocyte co-culture.
Scale bar: 100 μm.

ES: Lt-Tet-EGFP-Prox1

The treatment of the clone ES: Lt-Tet-EGFP-Prox1 on day 37 resulted in the expression of the markers Nestin and GFAP. It seems that the existence of these markers resembled the astrocyte rather than neuroectodermal cellular phenotype. Moreover, the expression of the telencephalic neuronal marker FoxG1 was positive. Also the DG marker NeuN, Prox1, Calretinin, βIII-tubulin, Synaptophysin and Map (2a+2b) were expressed. In contrast in this group, the expression of NeuroD1, Calbindin, Glutamate, and Emx2 was not observed.

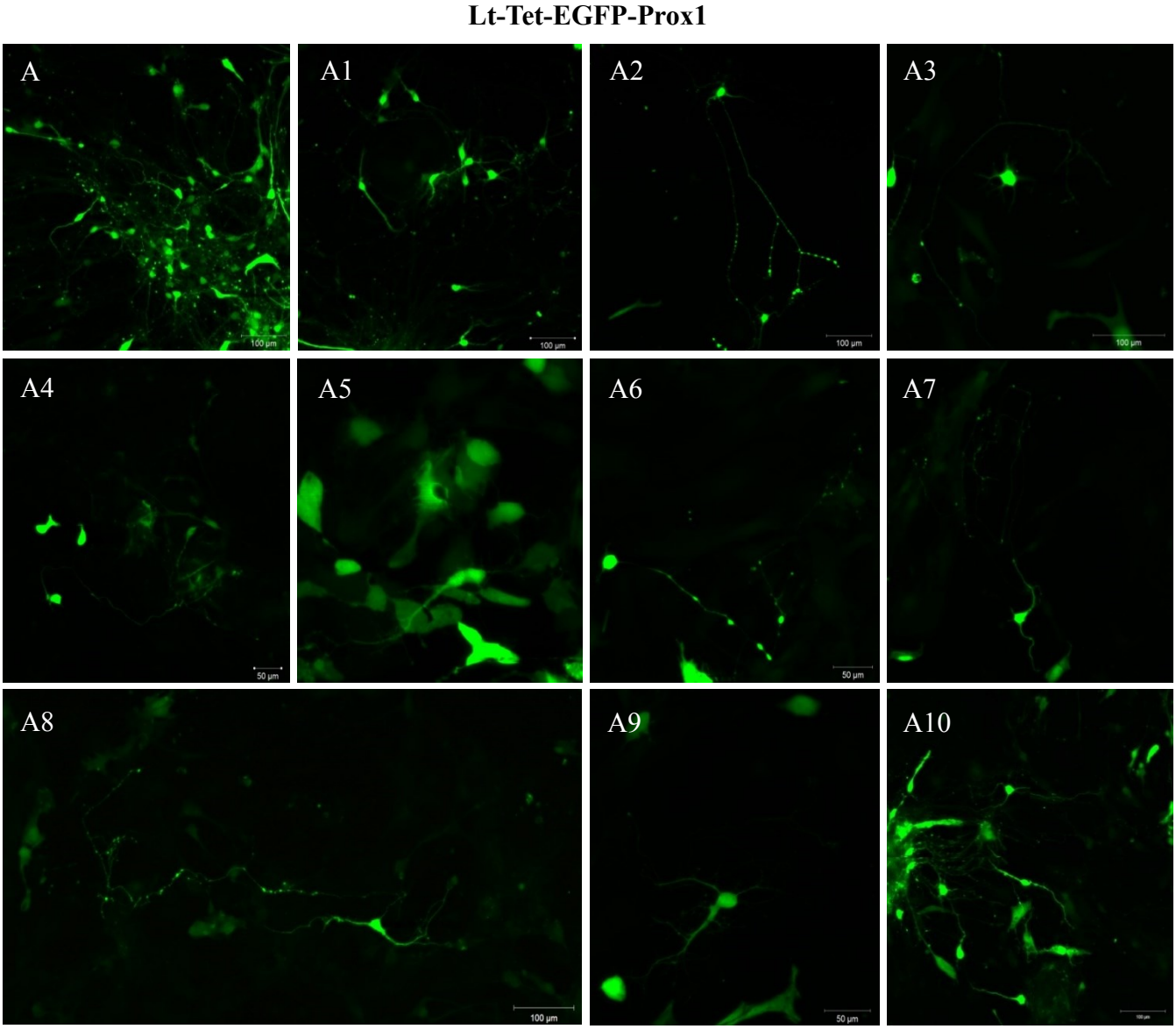

Fig. 3.17 Dentate gyrus differentiation of ES: Lt-Tet-EGFP –Prox1 on day 37 adherent astrocyte co-culture. Representative confocal images with the EGFP. Scale bar: 100 μm.

ES:Lt-Tet-EGFP-Prox1-NeuroD1

On day 37, the activation of ES: Lt-Tet-EGFP-Porx1-NeuroD1 resulted in a considerable increase in the expression of markers Prox1, NeuroD1, NeuN and βIII-tubulin compared with the growth factor and transcription factor alone groups. In fact, it seems that the combined overexpression of these transcription factors had also a synergic role in the induction of calbindin and calretinin. The morphological observations also clearly demonstrated a considerable increase in neurogenesis compared with other the groups, as well.

Lt-Tet-EGFP-NeuroD1 +Prox1

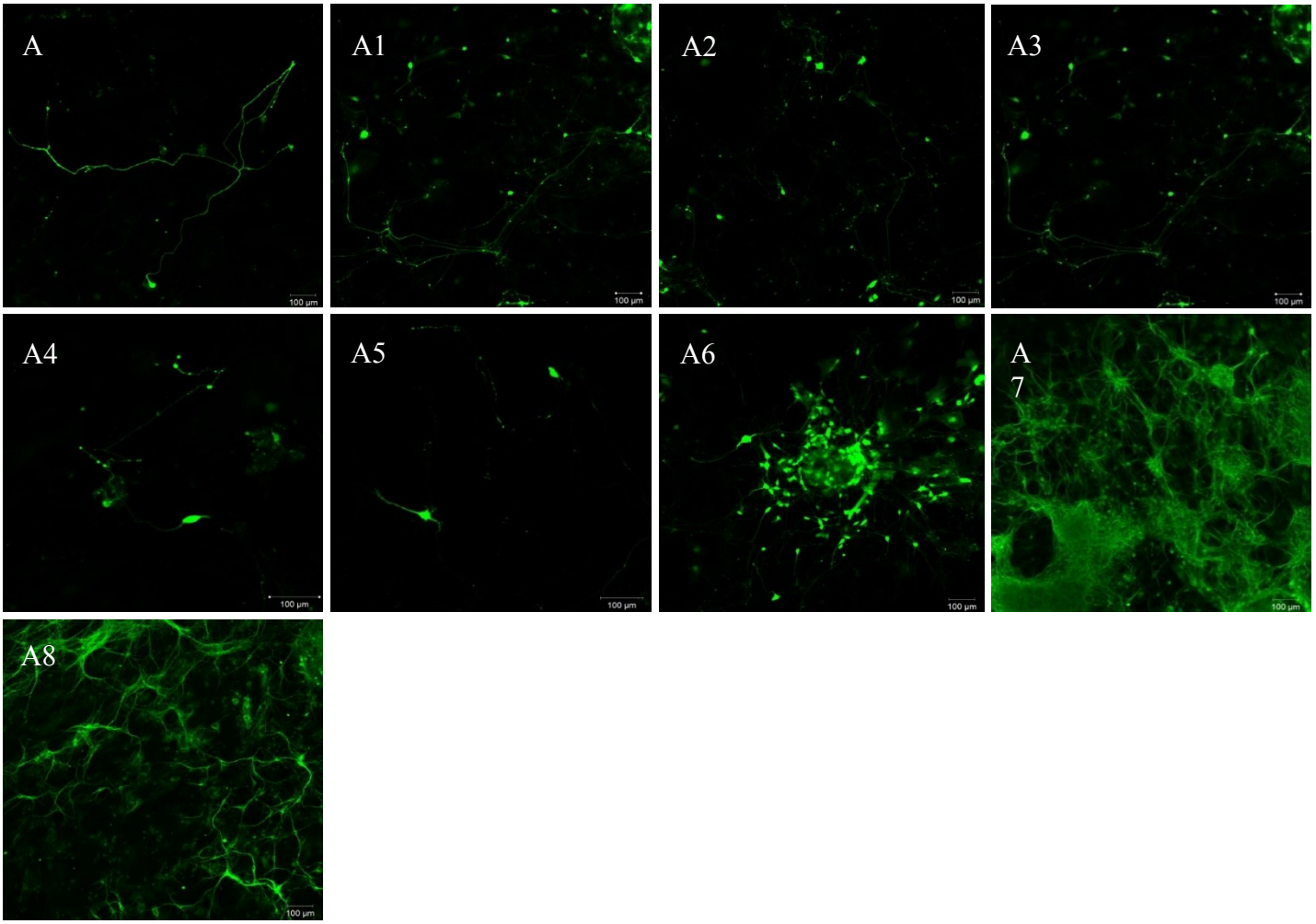

Fig. 3.18 Dentate gyrus differentiation of Lt-Tet-EGFP–NeuroD1-Prox1 on 37 days old adherent astrocyte co-culture. Representative confocal images with EGFP. Scale bar: 100 μm.

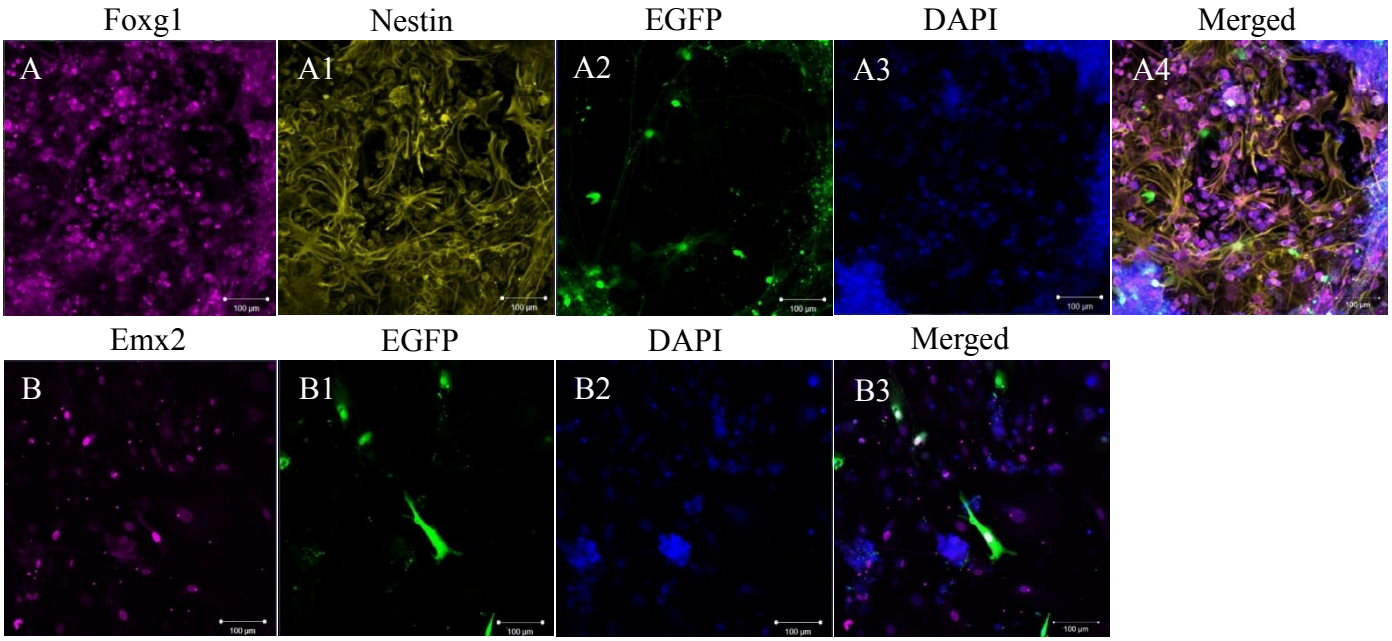

Fig. 3.19 Expression of telencephalic marker in 37 days old adherent cell culture in Lt-Tet-EGFP-NeuroD1-Prox1 cell line. (A-A4) Foxg1/Nestin, (B-B3) Emx2/EGFP. DAPI co staining was used. Scale bar: 100µm.

Lt-Tet-EGFP-NeuroD1+Prox1

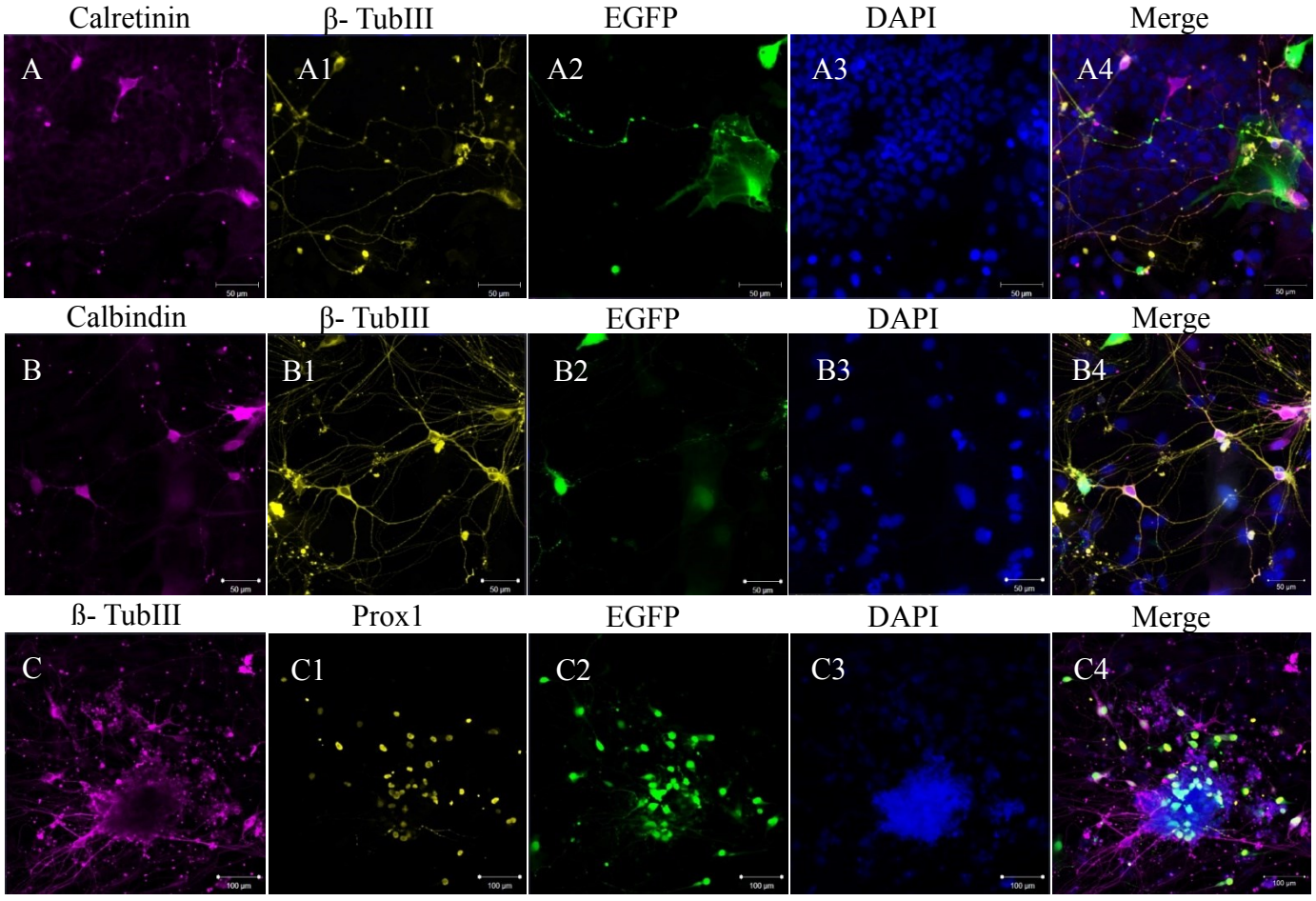

Fig. 3.20 Expression of dentate gyrus markers in 37 days old adherent cell culture. A-A4 Calretinin/ βIII-tubulin, B-B4 Calbindin/ βIII-tubulin, C-C4 βIII-tubulin /Prox1. DAPI co-staining. Scale bar: 100 µm.

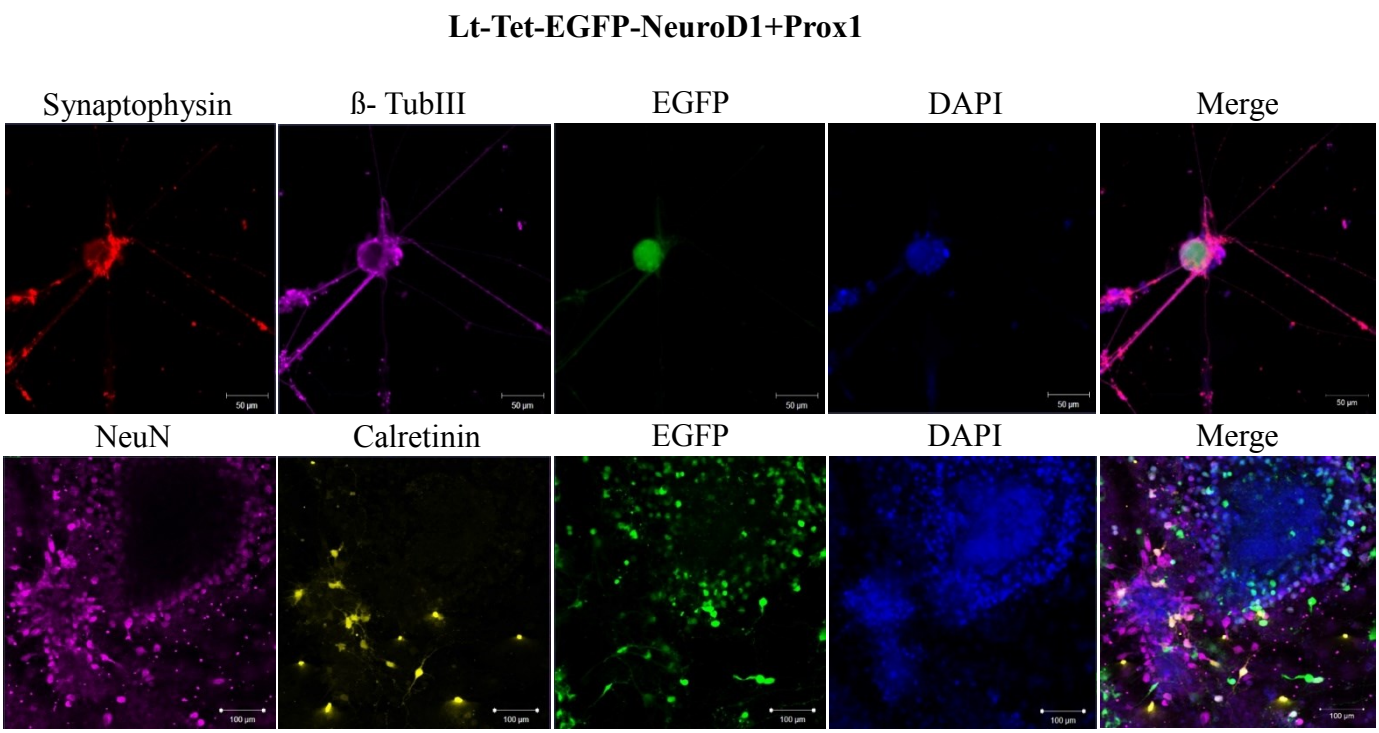

Fig. 3.21 Expression of Dentate Gyrus Marker in ES:Lt-Tet-EGFP-NeuroD1-Prox1 cell line on 37 days old astrocyte adherent co-culture. DAPI co-staining. Scale bar: 100 µm.

Furthermore, in this group, the expression of synaptic and neurotransmitter marker synaptophysin and glutamate increased (Fig. 3.21, Table3.2).

The length of the axons and dendrites in this group in comparison with other groups showed also a profound increase, the processes become amazingly long and branched. In other groups such a general development of these distinctive structures was not recognized.in the growth factor group the cells stayed mainly in progenitor state and only developed on the Dkk1 treated group partially.

The results of the effects of the growth factors and comparing them with the transcription factors have shown that the growth factors will more lead to the induction of neuro-progenitor cells than the transcription factors. In vise versa the transcription factor and especially the combined overexpression of Prox1 and NeuroD1 pushed the cells to a neuronal phenotype. The colony-like structures inducted by the growth factors were no longer observed in the transcription factor groups at all.

d37	Neuroectodermal Marker		Telencephalic Neural Progenitor Marker		Dentate Gyrus Markers								
	Nestin	GFAP	Foxg1	Emx2	NeuN	NeuroD1	Prox1	Calretinin	Calbindin	βIII-tubulin	Glutamte	synaptophysin	Map2 (a+b)
Emx2	+	+	+	+++	-	-	-	-	-	-	-	-	-
Prox1	++	++	+	-	+	-	+++	+	-	+	-	+	+
NeuroD1	++	++	+	-	+	+++	+	--	-	+	-	+	+
Prox1 +NeuroD1	++	++	++	+	+	+++	+++	+	+	+++	+	+++	+++

Table 3.2 Comparative analysis of the expression of neuroectodermal, telencephalic progenitor and dentate gyrus markers on transcription factors treatment cell culture condition . All results are expressed as percentages of the whole population: 0%–5%, negative (−); 6%–39%, low level of marker expression (+); 40%–79%, moderate level of marker expression (++); 80%–100%, high level of marker expression (+++).

3.5 Overall transcriptional profiling by nano-fluidic real–time PCR

The set of markers for characterizing genes enriched in different stages of directed neuronal differentiation of mouse ES cells towards hippocampal-DG phenocytes included glial markers (GFAP, MBP, OLIG2), neural precursor and proliferation markers (NESTIN, KI67, PCNA), neuronal differentiation markers (NEUN, TUBB3, NCAM1, SYP, GABA, SLC1A3), markers of telencephalic induction (SOX1, HES5, PAX6, REST1, MASH1, NEUROG2, TBR2, SOX11), and genes typical for DG induction and granule neuron differentiation (NEUROD1, FOXG1, EMX1, EMX2, GLI3, CREB, TBR1, NEUROD2, DCX, PROX1, ID3, FABP7, CALB1, CALB2, BMPR1A, NFIX, CCND2, NR2E1 , LHX1, LHX2, LEF1, LRP6).

These experimental groups with approx. 8000 data points obtained from Real-time PCR reactions in a Fluidigm system were readily compared and visualized in dendograms, heatmaps, bar graphs using descriptive statistics and statistical comparison were made using in the case of two groups, with either t-test, ANOVA and correlation analysis. The difference between the groups is shown in logarithmic scale and the confidence interval is indicated.

Overall comparisons of experimental groups with growth factors, transcription factors and control groups

When comparing the gene expression profiling of all different groups, it was revealed that in the dentogram and heatmap analysis, the different stages of neural in vitro development can be clearly separated. It became obvious that while at d0 and d2 most of the genes analyzed were missing from d7 onwards, the neuronal differentiation profile increased and reached its maximum during EB formation at d16, in single cell culture from d23 - d37 the hippocampal DG profiles increased again. The strongest profiles were achieved by the overexpression of the transcription factors, while with the only application of growth factors, including Dkk1 the degree of a DG specific expression profile of differentiation was reduced (see Fig 3.22).

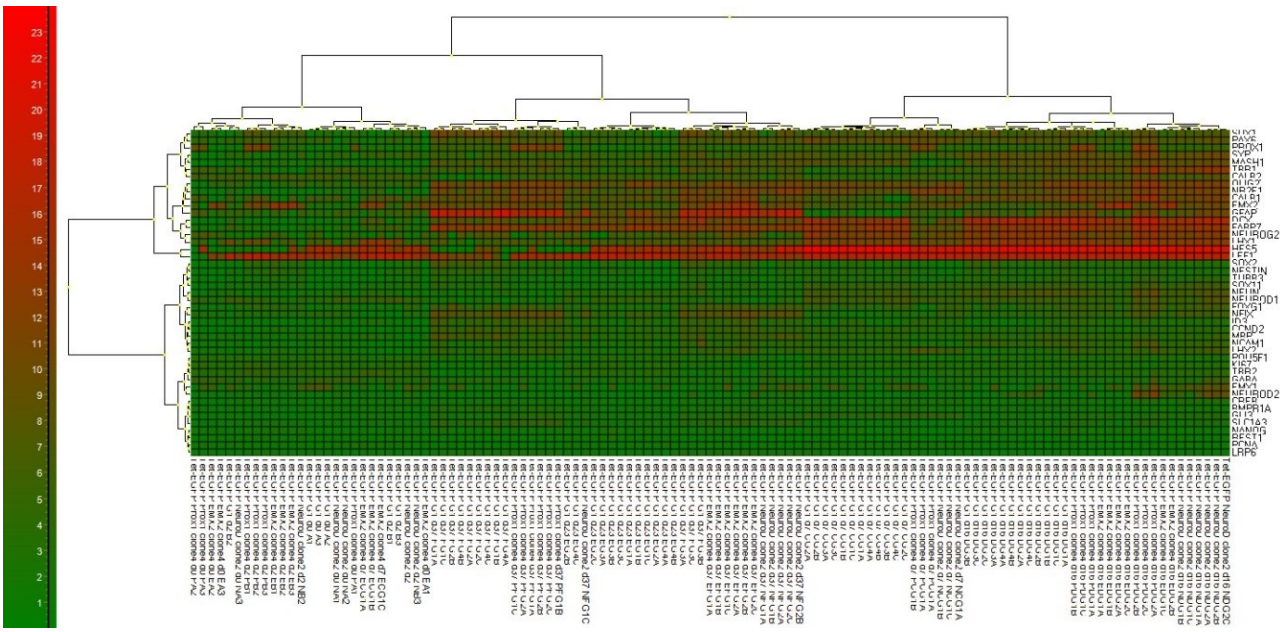

Fig. 3.22 Gene expression profiling of all experimental groups with single applications of growth or transcriptions factors and control groups. Heat map showing array of neural differentiation associated genes with each column representing the experimental groups. Note that NeuroD show the strongest difference to all other groups. A clustering algorithm is used to group rows (samples) and columns (Sha, Zhou et al.) to produce two cluster trees. The samples and genes are arranged in the order given in the tree so that each data row in the data file corresponds to a column in the heat map and vice versa. The color of a cell in the heatmap relates to the expression of the gene in the sample that the cell corresponds to.

Correlation Analysis at d16

In the comparison of the control groups, Tet EGFP G1 d16+ and Tet EGFP G1 d16- the expression profiles are very similar, most of the genes cluster inside the area of significance measured as distance from center 1.

At d16, Tet-EGFP Emx2 clone 4 has a low impact on the expression profile of the analyzed genes, although Emx2 is strongly overexpressed. Many of the genes analyzed tend to minimally move towards the control group, however, no strong expression profile is shown by the Tet-EGFP d16 control-group.

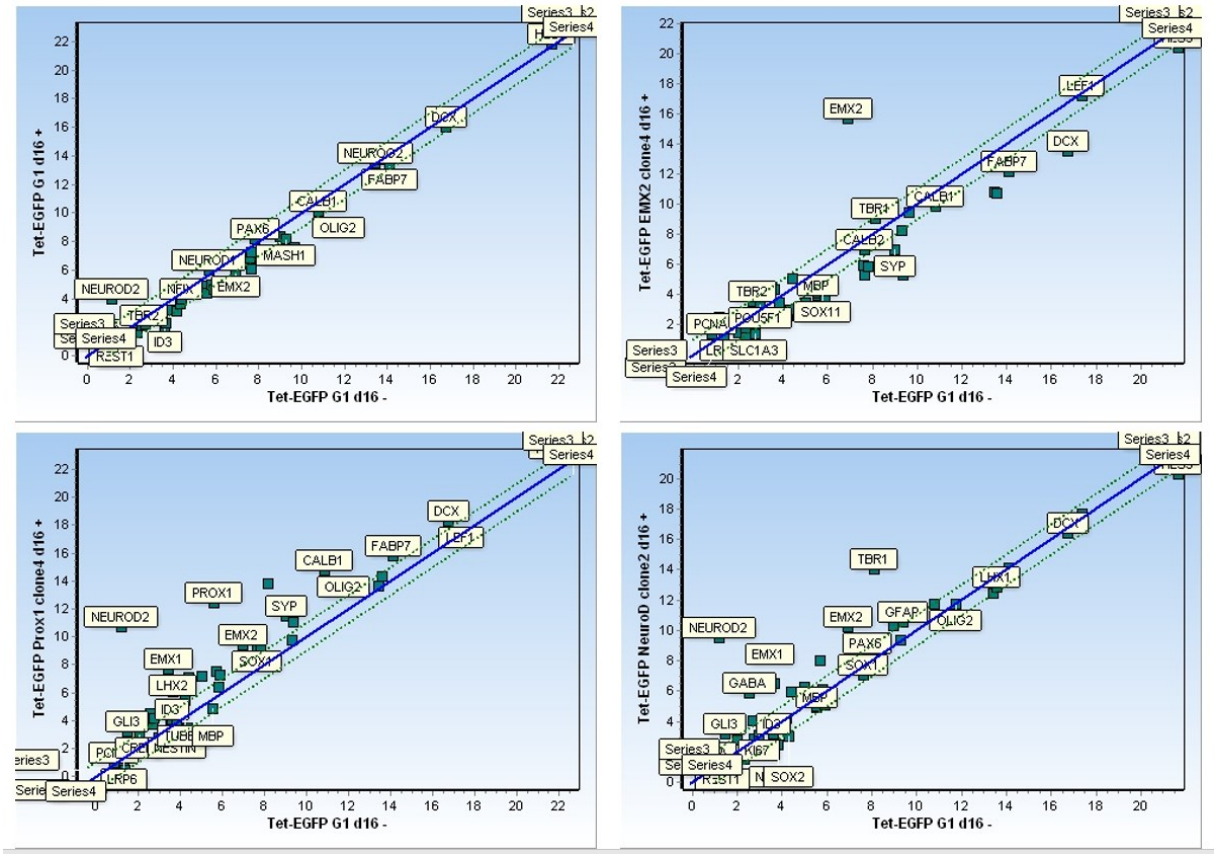

Over-expressed genes				Under-expressed genes			
	Tet-EGFP G1 d16 - (X)	Tet-EGFP EMX2 clone4 d16 +(Y)	Diff(Y-X)		Tet-EGFP G1 d16 - (X)	Tet-EGFP EMX2 clone4 d16 +(Y)	Diff(Y-X)
EMX2	6,92208	15,66169	8,73961	GFAP	9,37479	5,28833	-4,08646
NEUROD2	1,1715	2,53422	1,36273	DCX	16,7472	13,50936	-3,23784
				LHX1	13,56933	10,71034	-2,85899
				NEUROG2	13,43388	10,82763	-2,60625
				NEUN	7,64084	5,31228	-2,32856
				NCAM1	5,88597	3,72356	-2,1624
				SYP	8,99156	6,96892	-2,02264
				FABP7	14,10843	12,1802	-1,92822
				PAX6	7,79905	5,88792	-1,91113
				SOX1	7,61068	5,97818	-1,6325
				MBP	5,54355	3,956	-1,58755
				TUBB3	4,18879	2,60929	-1,5795
				FOXG1	5,02497	3,48647	-1,53849
				OLIG2	11,76277	10,22795	-1,53483
				SOX11	5,78763	4,27423	-1,5134
				PROX1	5,55633	4,08221	-1,47412
				SLC1A3	2,73876	1,42672	-1,31203
				SOX2	4,3124	3,00278	-1,30962
				HES5	21,67083	20,403	-1,26783
				ID3	3,5864	2,3659	-1,2205
				BMPR1A	2,33334	1,2094	-1,12394
				NEUROD1	5,68066	4,59032	-1,09034
				MASH1	9,29438	8,2661	-1,02827

Over-expressed genes				Under-expressed genes			
	Tet-EGFP G1 d16 -(X)	Tet-EGFP NeuroD clone2 d16 +(Y)	Diff(Y-X)		Tet-EGFP G1 d16 - (X)	Tet-EGFP NeuroD clone2 d16 +(Y)	Diff(Y-X)
NEUROD2	1,1715	9,51473	8,34323	HES5	21,67083	20,3104	-1,36043
TBR1	8,13333	14,06268	5,92936	NESTIN	3,8137	2,47406	-1,33964
EMX1	3,43129	8,54996	5,11867	SOX2	4,3124	2,99577	-1,31663
GABA	2,53718	5,89485	3,35768				
EMX2	6,92208	10,20973	3,28765				
LHX2	3,63901	6,53897	2,89995				
NEUROD1	5,68066	8,04375	2,36309				
GLI3	1,48318	3,19	1,70681				
NFIX	4,40112	5,91934	1,51822				
NR2E1	9,65339	11,05944	1,40604				
TBR2	2,67877	4,03096	1,35219				
SYP	8,99156	10,2818	1,29024				
FOXG1	5,02497	6,29841	1,27344				
PAX6	7,79905	9,03946	1,24041				
GFAP	9,37479	10,55486	1,18007				

Over-expressed genes				Under-expressed genes			
	Tet-EGFP G1 d16 - (X)	Tet-EGFP Prox1 clone4 d16 -(Y)	Diff(Y-X)		Tet-EGFP G1 d16 - (X)	Tet-EGFP Prox1 clone4 d16 -(Y)	Diff(Y-X)
PROX1	5,55633	12,07194	6,51561	NEUROG2	13,43388	10,19712	-3,23676
TBR1	8,13333	9,83435	1,70102	PAX6	7,79905	6,01706	-1,78199
LHX2	3,63901	5,27896	1,63995				
CALB1	10,81114	12,43988	1,62874				
GFAP	9,37479	10,97059	1,5958				
GLI3	1,48318	2,86378	1,3806				
TBR2	2,67877	3,96501	1,28624				
NEUROD2	1,1715	2,37975	1,20825				
FABP7	14,10843	15,2365	1,12807				

Fig. 3.23 Correlation analysis and data of transcription factors at d16. EMX2, Prox1 and NeuroD1 versus EGFP control. Both Prox1 and NeuroD1 overexpression reinforce dorsal telencephalic differentiation expression profiling.

(Tet-EGFP G1 d16 -) vs (Tet-EGFP EMX2 clone4 d16 +)	Fold change	Difference (A-B log scale)	P-Value
EMX2	-427,45087	-8,73961	0,000007104
MBP	3,00538	1,58755	0,000712497
GFAP	16,98823	4,08646	0,000858036
NCAM1	4,4766	2,1624	0,001001903
TUBB3	2,98867	1,5795	0,002697566
BMPR1A	2,17941	1,12394	0,003824599
TBR2	-1,85102	-0,88832	0,005041253
DCX	9,43379	3,23784	0,006481781
SLC1A3	2,48291	1,31203	0,009777375
ID3	2,33028	1,2205	0,010086786
SYP	4,06326	2,02264	0,01066079
MASH1	2,03958	1,02827	0,011495697
PROX1	2,77813	1,47412	0,0129118
NEUN	5,02305	2,32856	0,014289138
SOX11	2,85482	1,5134	0,015378714
LHX1	7,25506	2,85899	0,023785252
PCNA	-1,46701	-0,55288	0,026176835
FABP7	3,80586	1,92822	0,028228864
OLIG2	2,89754	1,53483	0,032488365
CCND2	1,78199	0,83349	0,033972893
GLI3	-1,7673	-0,82155	0,042782926
NFIX	-1,54971	-0,632	0,056017046
NEUROG2	6,08919	2,60625	0,065842079
LRP6	1,41893	0,50481	0,069503449
NEUROD1	2,12924	1,09034	0,069713796
PAX6	3,76104	1,91113	0,076211821
CALB2	1,60338	0,68112	0,080325271
SOX1	3,1005	1,6325	0,093476368
HES5	2,40799	1,26783	0,117666226
SOX2	2,47877	1,30962	0,120201134
CREB	1,48254	0,56807	0,127703982
LHX2	-1,64458	-0,71772	0,153257041
FOXG1	2,90491	1,53849	0,180604329
KI67	1,13946	0,18835	0,249895644
CALB1	1,98761	0,99104	0,273400078
LEF1	1,14887	0,20021	0,300791493
NEUROD2	-2,57171	-1,36273	0,315793191
TBR1	-1,87691	-0,90836	0,321567154
POU5F1	-1,26931	-0,34405	0,401166868
NANOG	1,41384	0,49962	0,457755504
NESTIN	1,29185	0,36944	0,523666399
REST1	1,12781	0,17353	0,596726331
NR2E1	1,13597	0,18392	0,674480363
EMX1	-1,70271	-0,76783	0,675993416
GABA	1,05362	0,07536	0,832243133

(Tet-EGFP G1 d16 -) vs (Tet-EGFP Prox1 clone4 d16 +)	Fold change	Difference (A-B log scale)	P-Value
PROX1	-118,6613	-6,89071	0,000018636
NFIX	-6,30838	-2,65727	0,00027921
SYP	-5,57574	-2,47916	0,000461483
NEUROD2	-726,67881	-9,50498	0,0009186
CALB1	-15,1484	-3,92109	0,0009581
KI67	1,75315	0,80995	0,002088116
SLC1A3	-2,59938	-1,37816	0,002563725
DCX	-2,96712	-1,56907	0,003165611
OLIG2	-4,36936	-2,12742	0,003303055
GFAP	-3,18196	-1,66991	0,004123828
FABP7	-3,16344	-1,66149	0,004881984
PAX6	-2,58249	-1,36876	0,004894662
HES5	-2,16271	-1,11284	0,004956172
TUBB3	-2,39507	-1,26007	0,008815917
NR2E1	-6,0535	-2,59777	0,01094055
BMPR1A	1,58932	0,66841	0,01265146
TBR1	-51,27927	-5,6803	0,013988729
NEUROD1	-3,55309	-1,82907	0,017686925
NCAM1	-2,59026	-1,3731	0,019530296
GLI3	-3,2988	-1,72194	0,021937305
CREB	-1,84452	-0,88324	0,023392626
MBP	1,5873	0,66658	0,026366095
CALB2	-3,10698	-1,63551	0,027715438
EMX2	-5,66403	-2,50183	0,02784916
LHX1	-1,71977	-0,78221	0,037300956
EMX1	-19,01576	-4,24912	0,052897852
REST1	1,94871	0,96252	0,054568673
NEUN	-2,71398	-1,44041	0,063611361
FOXG1	-4,35114	-2,12139	0,06490166
LHX2	-5,36915	-2,42469	0,071647555
MASH1	-1,36855	-0,45265	0,112506211
LRP6	1,29806	0,37636	0,142676037
GABA	-3,94431	-1,97977	0,189811885
SOX11	-1,50516	-0,58991	0,198319215
TBR2	-2,00854	-1,00615	0,221028198
LEF1	-1,1327	-0,17976	0,25290606
SOX2	1,7748	0,82766	0,301912398
ID3	-1,37372	-0,45809	0,364951298
NANOG	1,52692	0,61062	0,367167525
PCNA	-1,07158	-0,09975	0,367251459
SOX1	-1,53294	-0,6163	0,405387919
POU5F1	1,16877	0,22499	0,69354472
CCND2	-1,08167	-0,11326	0,74354992
NEUROG2	-1,12799	-0,17375	0,753050142
NESTIN	1,07028	0,09799	0,862630983

(Tet-EGFP G1 d16 -) vs (Tet-EGFP NeuroD clone2 d16 +)	Fold change	Difference (A-B log scale)	P-Value
NEUROD2	-324,76035	-8,34323	0,000002383
GABA	-10,25087	-3,35768	0,000008503
NEUROD1	-5,14471	-2,36309	0,000058733
LHX2	-7,46403	-2,89995	0,000261455
NR2E1	-2,65009	-1,40604	0,000312905
TBR1	-60,94159	-5,92936	0,00034084
NFIX	-2,86437	-1,51822	0,000378172
EMX2	-9,7652	-3,28765	0,000385668
TBR2	-2,55299	-1,35219	0,000892133
SYP	-2,44569	-1,29024	0,003568254
HES5	2,56762	1,36043	0,003753094
GLI3	-3,26439	-1,70681	0,003940705
NEUROG2	1,98324	0,98786	0,005880745
GFAP	-2,26588	-1,18007	0,006823616
EMX1	-34,74351	-5,11867	0,007776859
PAX6	-2,36265	-1,24041	0,011462411
NCAM1	1,73536	0,79523	0,012435477
BMPR1A	1,4869	0,57231	0,014301304
PROX1	1,4586	0,54458	0,015385384
CREB	-1,69592	-0,76207	0,016663499
PCNA	-1,35392	-0,43714	0,018493404
CALB1	-1,85779	-0,89359	0,031974071
NESTIN	2,53088	1,33964	0,051582747
LHX1	1,63731	0,71133	0,076057694
SOX2	2,49084	1,31663	0,097344579
CALB2	-1,31816	-0,39852	0,108802373
MBP	1,55089	0,6331	0,127448808
FOXG1	-2,41738	-1,27344	0,141089069
LEF1	-1,19733	-0,25982	0,185808211
DCX	1,28681	0,3638	0,202700979
NANOG	1,79991	0,84792	0,203938933
LRP6	1,17946	0,23813	0,253813987
ID3	1,32967	0,41107	0,274456141
SOX11	-1,27469	-0,35015	0,300502317
KI67	-1,10554	-0,14475	0,357152535
SOX1	1,50131	0,58622	0,45465218
POU5F1	1,2257	0,2936	0,473156491
SLC1A3	-1,10782	-0,14773	0,482176892
MASH1	-1,06482	-0,09062	0,608399078
CCND2	-1,02546	-0,03627	0,795953492
REST1	1,05082	0,07152	0,828573531
TUBB3	-1,03095	-0,04398	0,848698797
FABP7	-1,02435	-0,03471	0,861729978
NEUN	1,0289	0,0411	0,90188059
OLIG2	1,02663	0,03792	0,923283957

Fig. 3.24: t-test analysis of transcription factors at d16: EMX2, Prox1 and NeuroD1 in comparison to TET EGFP.

At d16, the Prox1 over-expression strongly upregulates NeuroD2 (strongest expression), followed by TBR1, CALB1. Also NFIX, SYP, NR2E1 are upregulated. Interestingly, Prox1 overexpression also lead to an increase of the expression of Emx2 and NeuroD1. NeuroD1 strongly upregulated NeuroD2, TBR1 and Emx1. Furthermore, LHX2 and Emx2 were increased. Prox1 was negatively regulated by NeuroD1. In comparing the overexpressions of Emx2 and Prox1, all genes were shifted to the side of Prox1. The strongest overexpression of NeuroD2 was followed by GFEP, DCX, TBR1, SYP, FABP7, NEUN, LHX1, FoxG1, NCAM1, TUBB3, SLC1A3 and NR2E1. In the comparison with Emx2, NeuroD1 strongly upregulated NeuroD2, GFAP, TBR1, Emx1, GABA, SYP and PAX6. No genes were upregulated by Emx2.

While NeuroD1 and Prox1 overexpression lead to a strong regulation of hippocampal progenitor markers, an overexpression of Emx2 showed no influence. The regulation of Prox1 and NeuroD1 similarly and strongly upregulated NeuroD2 and Emx1, Emx2. The comparison of Prox1, NeuroD1 und Emx2 showed that the most of hippocampal progenitors and differentiation genes were regulated by Prox1 and NeuroD1. The expression profiles of NeuroD1 and Prox1 were quite similar.

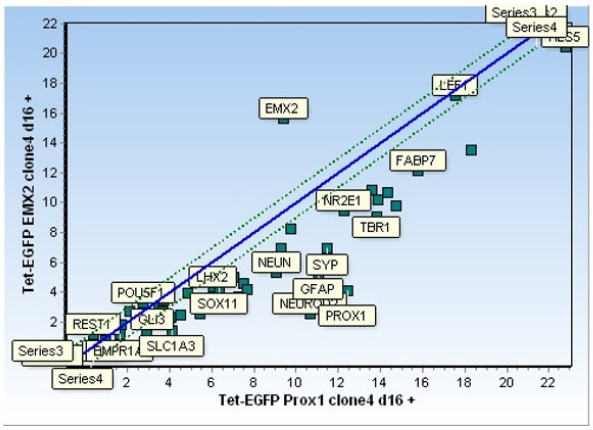

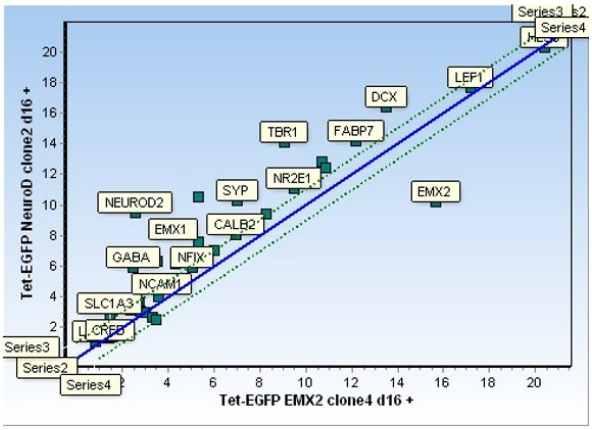

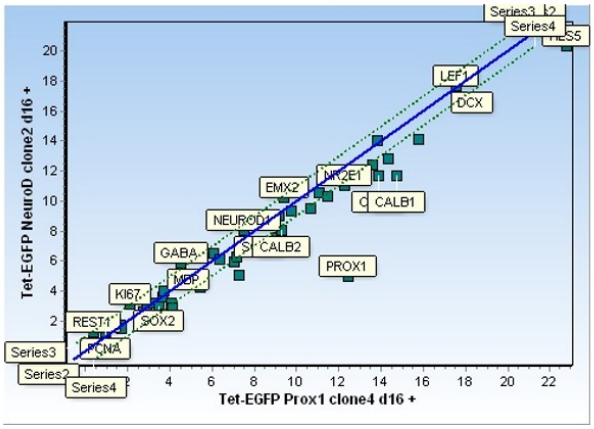

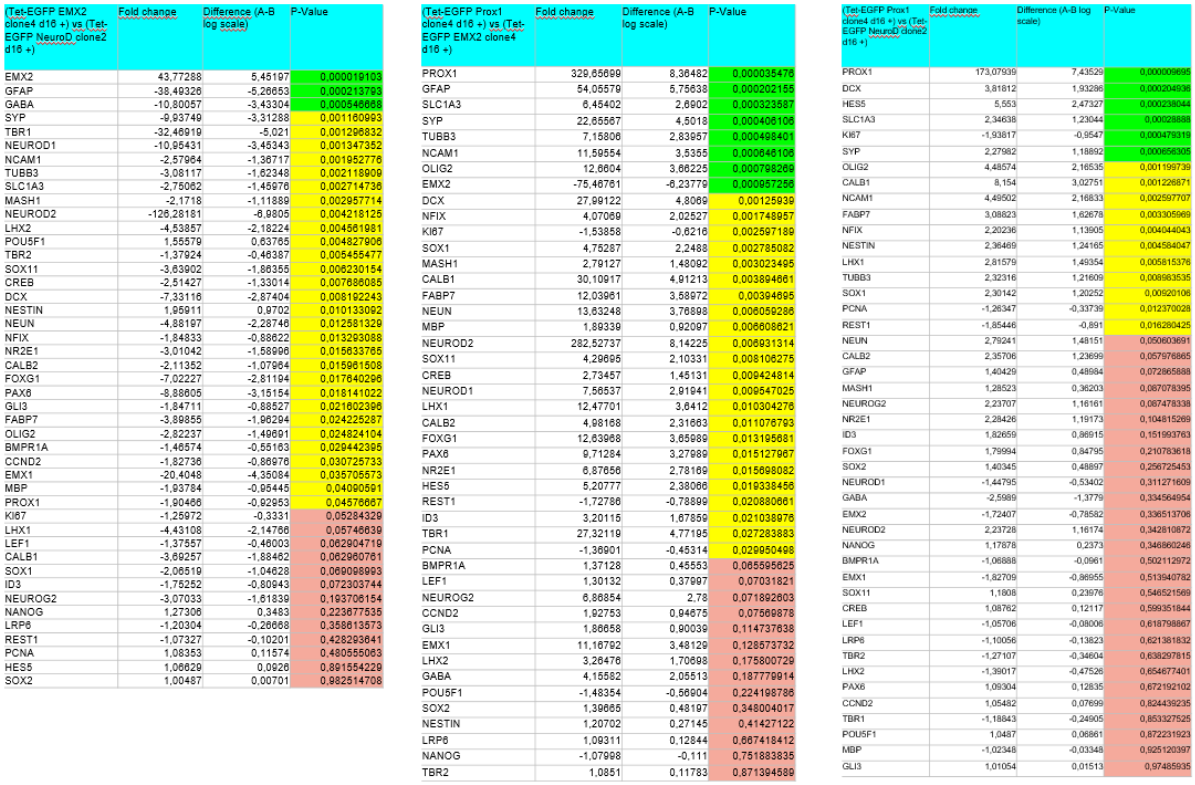

(Tet-EGFP EMX2 clone4 d16 +) vs (Tet-EGFP NeuroD clone2 d16 +)	Fold change	Difference (A-B log scale)	P-Value
EMX2	43,77288	5,45197	0,000019103
GFAP	-38,49326	-5,26653	0,000213793
GABA	-10,80057	-3,43304	0,000546668
SYP	-9,93749	-3,31288	0,001160993
TBR1	-32,46919	-5,021	0,001296832
NEUROD1	-10,95431	-3,45343	0,001347352
NCAM1	-2,57964	-1,36717	0,001952776
TUBB3	-3,08117	-1,62348	0,002118909
SLC1A3	-2,75062	-1,45976	0,002714736
MASH1	-2,1718	-1,11889	0,002957714
NEUROD2	-126,28181	-6,9805	0,004218125
LHX2	-4,53857	-2,18224	0,004561981
POU5F1	1,55579	0,63765	0,004827906
TBR2	-1,37924	-0,46387	0,005455477
SOX11	-3,63902	-1,86355	0,006230154
CREB	-2,51427	-1,33014	0,007686085
DCX	-7,33116	-2,87404	0,008192243
NESTIN	1,95911	0,9702	0,010133092
NEUN	-4,88197	-2,28746	0,012581329
NFIX	-1,84833	-0,88622	0,013293088
NR2E1	-3,01042	-1,58996	0,015833765
CALB2	-2,11352	-1,07964	0,015961508
FOXG1	-7,02227	-2,81194	0,017640296
PAX6	-8,88605	-3,15154	0,018141022
GLI3	-1,84711	-0,88527	0,021602396
FABP7	-3,89855	-1,96294	0,024225287
OLIG2	-2,82237	-1,49691	0,024824104
BMPR1A	-1,46574	-0,55163	0,029442395
CCND2	-1,82736	-0,86976	0,030725733
EMX1	-20,4048	-4,35084	0,035705573
MBP	-1,93784	-0,95445	0,04090591
PROX1	-1,90466	-0,92953	0,04576667
KI67	-1,25972	-0,3331	0,05284329
LHX1	-4,43108	-2,14766	0,05746639
LEF1	-1,37557	-0,46003	0,062904719
CALB1	-3,69257	-1,88462	0,062960761
SOX1	-2,06519	-1,04628	0,069098993
ID3	-1,75252	-0,80943	0,072303744
NEUROG2	-3,07033	-1,61839	0,193706154
NANOG	1,27306	0,3483	0,223677535
LRP6	-1,20304	-0,26668	0,358613573
REST1	-1,07327	-0,10201	0,428293641
PCNA	1,08353	0,11574	0,480555063
HES5	1,06629	0,0926	0,891554229
SOX2	1,00487	0,00701	0,982514708

(Tet-EGFP Prox1 clone4 d16 +) vs (Tet-EGFP EMX2 clone4 d16 +)	Fold change	Difference (A-B log scale)	P-Value
PROX1	329,65699	8,36482	0,000035478
GFAP	54,05579	5,75638	0,000202155
SLC1A3	6,45402	2,6902	0,000323587
SYP	22,65567	4,5018	0,000406106
TUBB3	7,15806	2,83957	0,000498401
NCAM1	11,59554	3,5355	0,000646106
OLIG2	12,6604	3,66225	0,000798269
EMX2	-75,46761	-6,23779	0,000957256
DCX	27,99122	4,8069	0,00125939
NFIX	4,07069	2,02527	0,001748957
KI67	-1,53858	-0,6216	0,002597189
SOX1	4,75287	2,2488	0,002785082
MASH1	2,79127	1,48092	0,003023495
CALB1	30,10917	4,91213	0,003894661
FABP7	12,03961	3,58972	0,00394695
NEUN	13,63248	3,76898	0,006059286
MBP	1,89339	0,92097	0,006608621
NEUROD2	282,52737	8,14225	0,006931314
SOX11	4,29695	2,10331	0,008106275
CREB	2,73457	1,45131	0,009424814
NEUROD1	7,56537	2,91941	0,009547025
LHX1	12,47701	3,6412	0,010304276
CALB2	4,98168	2,31663	0,011076793
FOXG1	12,63968	3,65989	0,013195681
PAX6	9,71284	3,27989	0,015127967
NR2E1	6,87656	2,78169	0,015698082
HES5	5,20777	2,38066	0,019338456
REST1	-1,72786	-0,78899	0,020880861
ID3	3,20115	1,67859	0,021038976
TBR1	27,32119	4,77195	0,027283883
PCNA	-1,36901	-0,45314	0,029950498
BMPR1A	1,37128	0,45553	0,065595625
LEF1	1,30132	0,37997	0,07031821
NEUROG2	6,88854	2,78	0,071892603
CCND2	1,92753	0,94675	0,07569878
GLI3	1,86658	0,90039	0,114737638
EMX1	11,16792	3,48129	0,128573732
LHX2	3,26476	1,70698	0,175800729
GABA	4,15582	2,05513	0,187779914
POU5F1	-1,48354	-0,56904	0,224198786
SOX2	1,39665	0,48197	0,348004017
NESTIN	1,20702	0,27145	0,41427122
LRP6	1,09311	0,12844	0,667418412
NANOG	-1,07998	-0,111	0,751883835
TBR2	1,0851	0,11783	0,871394589

(Tet-EGFP Prox1 clone4 d16 +) vs (Tet-EGFP NeuroD clone2 d16 +)	Fold change	Difference (A-B log scale)	P-Value
PROX1	173,07939	7,43529	0,000009695
DCX	3,81812	1,93286	0,000204936
HES5	5,553	2,47327	0,000238044
SLC1A3	2,34638	1,23044	0,00028888
KI67	-1,93817	-0,9547	0,000479319
SYP	2,27982	1,18892	0,000656305
OLIG2	4,48574	2,16535	0,001199739
CALB1	8,154	3,02751	0,001226871
NCAM1	4,49502	2,16833	0,002597707
FABP7	3,08823	1,62678	0,003305969
NFIX	2,20236	1,13905	0,004044043
NESTIN	2,36469	1,24165	0,004584047
LHX1	2,81579	1,49354	0,005815376
TUBB3	2,32316	1,21609	0,008983535
SOX1	2,30142	1,20252	0,00920106
PCNA	-1,26347	-0,33739	0,012370028
REST1	-1,85446	-0,891	0,016280425
NEUN	2,79241	1,48151	0,050603691
CALB2	2,35706	1,23699	0,057976865
GFAP	1,40429	0,48984	0,072865888
MASH1	1,28523	0,36203	0,087078395
NEUROG2	2,23707	1,16161	0,087478338
NR2E1	2,28426	1,19173	0,104815269
ID3	1,82659	0,86915	0,151993763
FOXG1	1,79994	0,84795	0,210783618
SOX2	1,40345	0,48897	0,256725453
NEUROD1	-1,44795	-0,53402	0,311271609
GABA	-2,5989	-1,3779	0,334564954
EMX2	-1,72407	-0,78582	0,336513706
NEUROD2	2,23728	1,16174	0,342810872
NANOG	1,17878	0,2373	0,346860246
BMPR1A	-1,06888	-0,0961	0,502112972
EMX1	-1,82709	-0,86955	0,513940782
SOX11	1,1808	0,23976	0,546521569
CREB	1,08762	0,12117	0,599351844
LEF1	-1,05706	-0,08006	0,618798867
LRP6	-1,10056	-0,13823	0,621381832
TBR2	-1,27107	-0,34604	0,638297815
LHX2	-1,39017	-0,47526	0,654677401
PAX6	1,09304	0,12835	0,672192102
CCND2	1,05482	0,07699	0,824439235
TBR1	-1,18843	-0,24905	0,853327525
POU5F1	1,0487	0,06861	0,872231923
MBP	-1,02348	-0,03348	0,925120397
GLI3	1,01054	0,01513	0,97485935

Fig. 3.25 Correlation analysis and t-tests of transcription factors at d16: EMX2/Prox1; Prox1/NeuroD1; EMX2/NeuroD1

Comparison at d37

In the comparison of growth factors and differentiation it became obvious, that DKK1 has the strongest influence on accomplishing a partial dorsal telencephalic phenotype. At d37, DKK1 in comparison to DKK3 strongly regulated HES5, DCX and CALB2. TBR1, SYP, NeuN, LEF1, and CALB1 were weakly upregulated by DKK1. In contrast, DKK3 did not influence the differentiation pattern at all. At d37, Emx2 overexpression strongly upregulated HES5, moderately upregulated CALB2 and weakly NEUROG2, LEF1 and CALB1. SOX1 and 2, OLIG2, MBP and GFAP were negatively regulated by EMX2. The central gene regulated by EMX2 was HES5. HES5 is a negative regulator of neurogenesis. Prox1 moderately upregulated MASH1 and weakly CALB1, 2 and TBR1. Moderately downregulated were SOX1, 2, MBP and SOX11, weakly GFAP, NEUROG2, DCX and TUBB3. NeuroD1 strongly upregulated HES5, and moderately CALB2 and EMX1. SOX1, 2 and ID3 were weakly downregulated. In the direct comparison of Prox11 and EMX2 at d37, EMX2 overexpression overwrote Prox1. The strongest upregulated gene by EMX2 was HES5, followed by NEUROG2. In comparison

of NEUROD1 and PROX1 at d37, it appears that NEUROD1 strongly regulated HES5, also EMX1,2 were stronger influenced by NEUROD1. NEUROD1 overrode Prox1. Weakly upregulated by NEUROD1 were NR2E1 and SYP. PROX1 was only stronger regulating CALB1.

The dentate granule cell is defined by the expression of a specific class of genes. None of the single experimental groups could reach the complete expression profile of the granule cell differentiation.

The strongest regulated genes were GFAP, SOX1, HES5, EMX2, ECX, FABP7, and NR2E1. With the exception of HES5, which was also strongly regulated by EMX2 and NeuroD1, all other strongly regulated genes were achieved in the control group and with addition of DKK1 or DKK3 respectively. DKK3 and Prox1 were strong negative regulators of HES5, and Prox1 and EMX2 of EMX1.

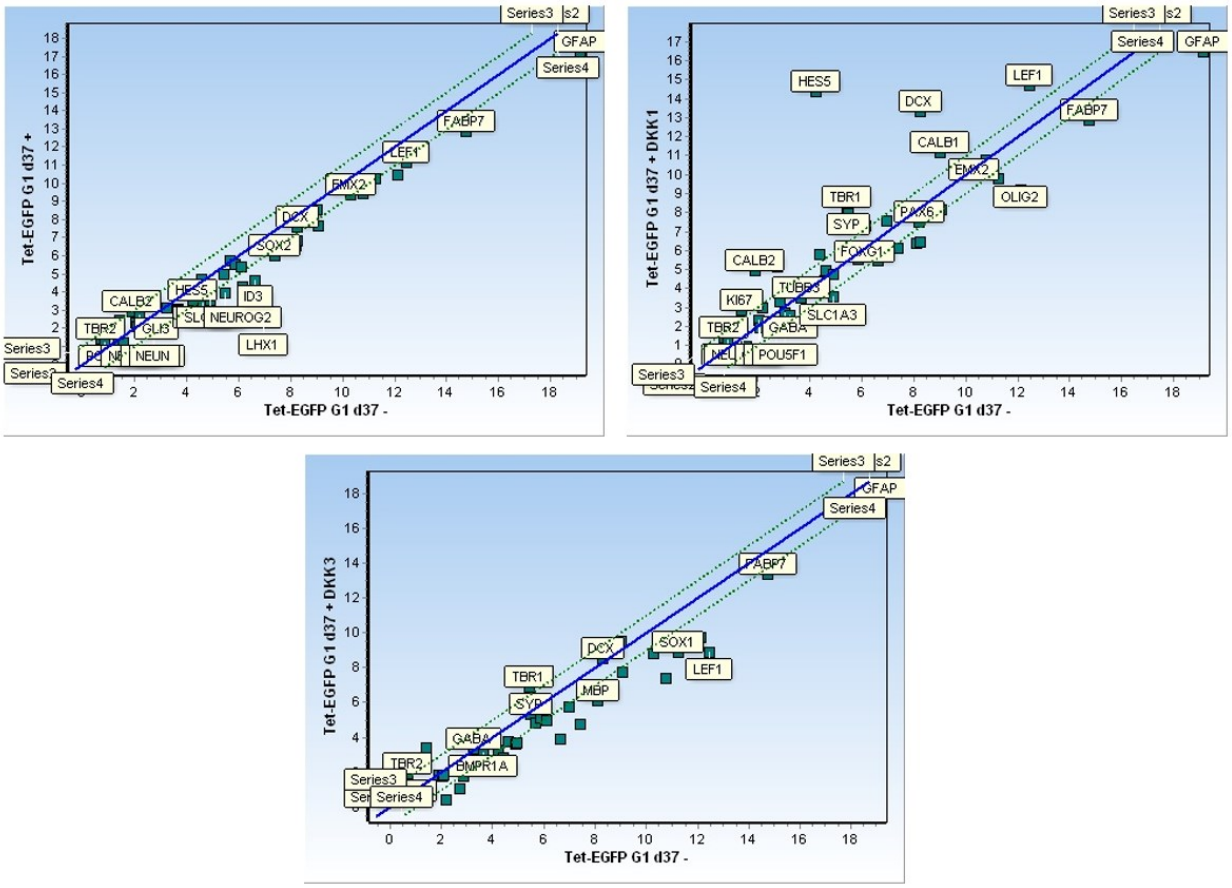

Over-expressed genes	Tet-EGFP G1 d37 -(X)	Tet-EGFP G1 d37 + DKK1(Y)	Diff(Y-X)	Under-expressed genes	Tet-EGFP G1 d37 -(X)	Tet-EGFP G1 d37 + DKK1(Y)	Diff(Y-X)
HES5	4,23504	14,36222	10,12718	OLIG2	12,09454	9,19767	-2,89687
DCX	8,27075	13,32299	5,05224	GFAP	19,13922	16,45125	-2,68797
CALB2	1,91352	4,96341	3,04989	FABP7	14,73964	12,87529	-1,86436
TBR1	5,41112	8,30083	2,8897	MASH1	8,26994	6,47128	-1,79866
SYP	5,49731	7,95051	2,4532	MBP	8,09298	6,39451	-1,69847
NEUN	2,7471	5,11918	2,37207	BMPR1A	3,64492	2,0441	-1,60081
LEF1	12,46487	14,70687	2,242	SOX1	11,26352	9,78949	-1,47403
CALB1	9,02311	11,15727	2,13417	SLC1A3	4,92144	3,54893	-1,37251
KI67	1,37673	2,83032	1,45359	SOX2	7,39729	6,12564	-1,27165
NCAM1	4,39202	5,8157	1,42369	ID3	6,63466	5,46787	-1,16679
NEUROG2	6,16617	7,31376	1,14759	NANOG	2,71871	1,66907	-1,04964

Over-expressed genes	Tet-EGFP G1 d37 -(X)	Tet-EGFP G1 d37 + DKK3(Y)	Diff(Y-X)	Under-expressed genes	Tet-EGFP G1 d37 -(X)	Tet-EGFP G1 d37 + DKK3(Y)	Diff(Y-X)
EMX1	1,41947	3,3919	1,97243	LEF1	12,46487	8,889	-3,57587
NEUROG2	6,16617	7,79612	1,62995	NR2E1	10,77568	7,40513	-3,37055
TBR1	5,41112	6,87584	1,46471	ID3	6,63466	3,86575	-2,76891
KI67	1,37673	2,75877	1,38204	SOX2	7,39729	4,76347	-2,63382
TBR2	0,69902	1,88947	1,19045	SOX1	11,26352	8,8429	-2,42061
				OLIG2	12,09454	9,72604	-2,3685
				SOX11	4,63951	2,64911	-1,99041
				MBP	8,09298	6,10753	-1,98546
				NEUROD1	2,17155	0,42265	-1,74891
				NANOG	2,71871	1,07139	-1,64733
				NCAM1	4,39202	2,83426	-1,55776
				EMX2	10,28394	8,77611	-1,50783
				MASH1	8,26994	6,80056	-1,46939
				PAX6	8,22133	6,75456	-1,46677
				GFAP	19,13922	17,68182	-1,4574
				FABP7	14,73964	13,38033	-1,35932
				NFIX	9,04185	7,74934	-1,2925
				SLC1A3	4,92144	3,65303	-1,26841
				LHX2	4,8874	3,62273	-1,26467
				LHX1	6,9789	5,7235	-1,25539
				TUBB3	3,67673	2,56681	-1,10993
				GLI3	2,85552	1,75027	-1,10525
				FOXG1	6,09164	4,99928	-1,09237

Fig. 3.26 Correlation analysis with data of growth factors at d37: *Dkk1* and *Dkk3* versus TET EGFP-.

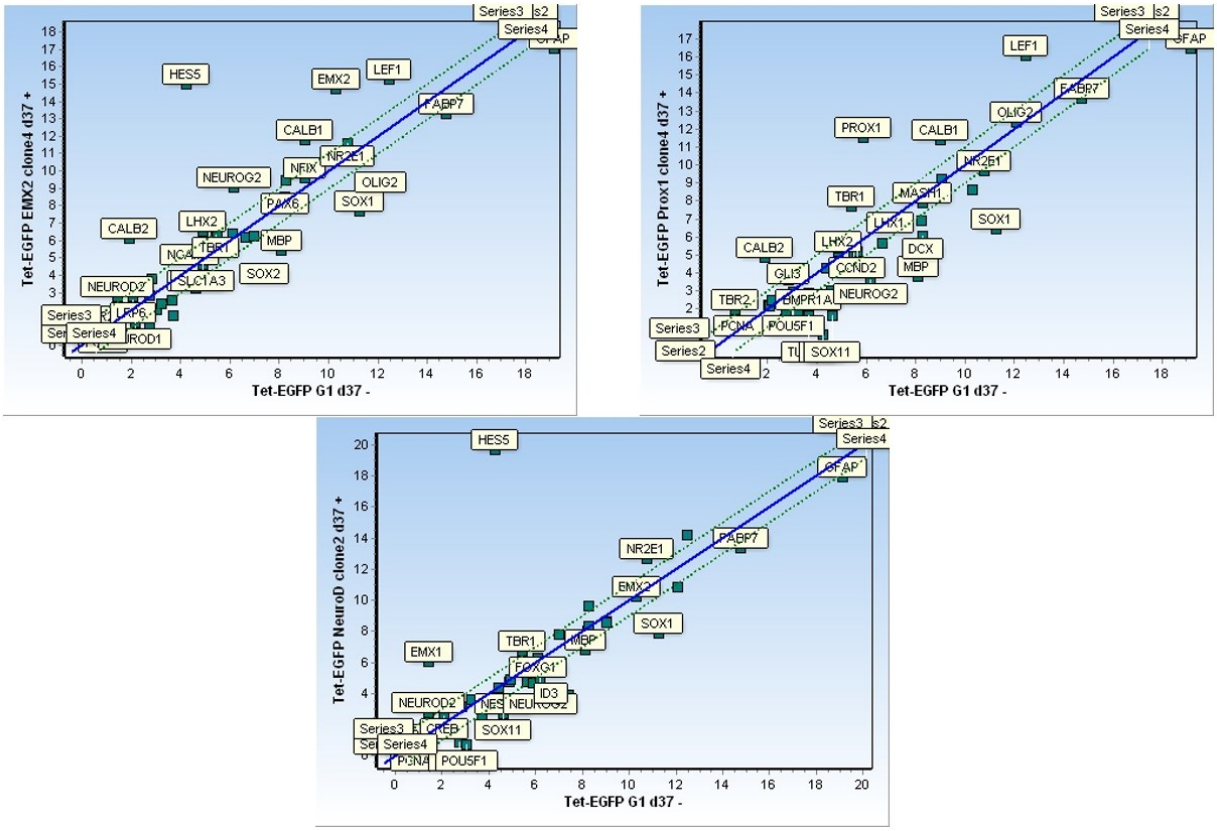

Over-expressed genes	Tet-EGFP G1 d37 - (X)	Tet-EGFP Prox1 clone4 d37 +(Y)	Diff(Y-X)	Under-expressed genes	Tet-EGFP G1 d37 - (X)	Tet-EGFP Prox1 clone4 d37 +(Y)	Diff(Y-X)
PROX1	5,8673	11,52511	5,65781	SOX2	7,39729	2,58508	-4,81221
LEF1	12,46487	16,09807	3,6332	SOX1	11,26352	6,45333	-4,81019
CALB2	1,91352	4,8428	2,92927	MBP	8,09298	3,77775	-4,31523
CALB1	9,02311	11,42282	2,39971	HES5	4,23504	0,58319	-3,65185
TBR1	5,41112	7,69154	2,28042	SOX11	4,63951	1,6179	-3,02161
TBR2	0,69902	1,97768	1,27866	GFAP	19,13922	16,46005	-2,67917
EMX1	1,41947	2,46667	1,04721	NEUROG2	6,16617	3,59166	-2,57451
				DCX	8,27075	6,032	-2,23875
				TUBB3	3,67673	1,63433	-2,0424
				FOXG1	6,09164	4,21489	-1,87675
				EMX2	10,28394	8,62845	-1,65549
				NESTIN	4,59113	3,00733	-1,58381
				GABA	3,23854	1,89811	-1,34044
				NANOG	2,71871	1,40464	-1,31407
				PAX6	8,22133	6,92014	-1,30119
				NR2E1	10,77568	9,69173	-1,08395
				NEUN	2,7471	1,71205	-1,03506
				FABP7	14,73964	13,70667	-1,03297

	Tet-EGFP G1 d37 - (X)	Tet-EGFP EMX2 clone4 d37 +(Y)	Diff(Y-X)		Tet-EGFP G1 d37 - (X)	Tet-EGFP EMX2 clone4 d37 +(Y)	Diff(Y-X)
HES5	4,23504	15,02032	10,78529	SOX1	11,26352	7,70676	-3,55676
EMX2	10,28394	14,70971	4,42577	SOX2	7,39729	4,08107	-3,31622
CALB2	1,91352	6,1116	4,19808	OLIG2	12,09454	9,35421	-2,74033
NEUROG2	6,16617	9,02335	2,85718	MBP	8,09298	5,44138	-2,6516
LEF1	12,46487	15,26316	2,79829	GFAP	19,13922	17,0656	-2,07362
CALB1	9,02311	11,77458	2,75147	TUBB3	3,67673	1,6762	-2,00053
LHX2	4,8874	6,49754	1,61014	PROX1	5,8673	3,95619	-1,91111
NEUROD2	1,41947	2,77979	1,36032	NANOG	2,71871	0,99665	-1,72206
DCX	8,27075	9,43569	1,16494	FABP7	14,73964	13,28841	-1,45123
				NESTIN	4,59113	3,25325	-1,33789
				SOX11	4,63951	3,51131	-1,12821
				BMPR1A	3,64492	2,55213	-1,09279
				POU5F1	3,04452	2,02151	-1,023

Over-expressed genes	Tet-EGFP G1 d37 - (X)	Tet-EGFP NeuroD clone2 d37 +(Y)	Diff(Y-X)	Under-expressed genes	Tet-EGFP G1 d37 - (X)	Tet-EGFP NeuroD clone2 d37 +(Y)	Diff(Y-X)
HES5	4,23504	19,66844	15,4334	SOX2	7,39729	3,88673	-3,51057
CALB2	1,91352	6,79074	4,87721	SOX1	11,26352	7,89401	-3,36951
EMX1	1,41947	6,01548	4,59602	POU5F1	3,04452	0,71962	-2,3249
SYP	5,49731	7,43614	1,93883	ID3	6,63466	4,38383	-2,25083
NR2E1	10,77568	12,69606	1,92038	BMPR1A	3,64492	1,67951	-1,96541
LEF1	12,46487	14,20149	1,73662	SOX11	4,63951	2,70128	-1,93824
DCX	8,27075	9,6424	1,37166	NANOG	2,71871	0,86935	-1,84936
NEUROD2	1,41947	2,77692	1,35745	FABP7	14,73964	13,37496	-1,36469
TBR1	5,41112	6,75284	1,34171	MBP	8,09298	6,81639	-1,2766
				OLIG2	12,09454	10,84676	-1,24778
				NEUROG2	6,16617	4,94503	-1,22113
				GFAP	19,13922	17,94967	-1,18955
				NESTIN	4,59113	3,42048	-1,17065
				PROX1	5,8673	4,70209	-1,16521
				TUBB3	3,67673	2,57766	-1,09907

Fig. 3.27 Correlation analysis and data of EMX2, Prox1 and NeuroD1 transcription factor overexpression at d37: EMX2, Prox1 and NeuroD1 versus EGFP control.

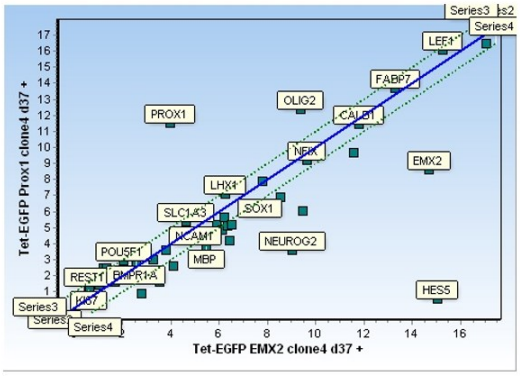

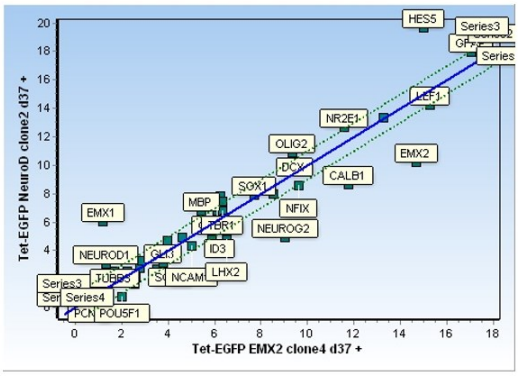

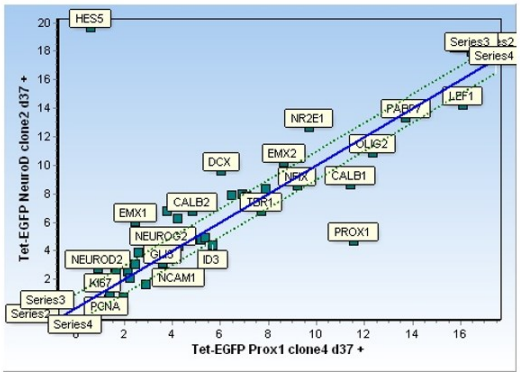

Over-expressed genes	Tet-EGFP EMX2 clone4 d37 +(X)	Tet-EGFP Prox1 clone4 d37 +(Y)	Diff(Y-X)	Under-expressed genes	Tet-EGFP EMX2 clone4 d37 +(X)	Tet-EGFP Prox1 clone4 d37 +(Y)	Diff(Y-X)
PROX1	3,95619	11,52511	7,56892	HES5	15,02032	0,58319	-14,43713
OLIG2	9,35421	12,35814	3,00393	EMX2	14,70971	8,62845	-6,08126
TBR1	6,32738	7,69154	1,36415	NEUROG2	9,02335	3,59166	-5,43169
EMX1	1,1769	2,46667	1,28978	DCX	9,43569	6,032	-3,40369
NEUROD1	1,30066	2,45446	1,1538	FOXG1	6,41565	4,21489	-2,20075
				SOX11	3,51131	1,6179	-1,8934
				NR2E1	11,56983	9,69173	-1,8781
				NEUROD2	2,77979	0,90319	-1,8766
				MBP	5,44138	3,77775	-1,66363
				PAX6	8,51275	6,92014	-1,59261
				SOX2	4,08107	2,58508	-1,49598
				LHX2	6,49754	5,19142	-1,30612
				CALB2	6,1116	4,8428	-1,2688
				SOX1	7,70676	6,45333	-1,25343
				SYP	6,31405	5,11996	-1,19409
				NEUN	2,84463	1,71205	-1,13259

Over-expressed genes	Tet-EGFP EMX2 clone4 d37 +(X)	Tet-EGFP NeuroD clone2 d37 +(Y)	Diff(Y-X)	Under-expressed genes	Tet-EGFP EMX2 clone4 d37 +(X)	Tet-EGFP NeuroD clone2 d37 +(Y)	Diff(Y-X)
EMX1	1,1769	6,01548	4,83859	EMX2	14,70971	10,207	-4,50271
HES5	15,02032	19,66844	4,64811	NEUROG2	9,02335	4,94503	-4,07831
NEUROD1	1,30066	3,09617	1,79551	CALB1	11,77458	8,61483	-3,15975
LHX1	6,23884	7,82701	1,58816	ID3	6,18709	4,38383	-1,80326
OLIG2	9,35421	10,84676	1,49255	LHX2	6,49754	4,74232	-1,75523
MBP	5,44138	6,81639	1,375	POU5F1	2,02151	0,71962	-1,30189
KI67	0,57364	1,86573	1,2921	CCND2	5,90121	4,74289	-1,15832
GABA	2,34135	3,59809	1,25674	LEF1	15,26316	14,20149	-1,06167
NR2E1	11,56983	12,69606	1,12623	NFIX	9,61345	8,56309	-1,05036
SYP	6,31405	7,43614	1,12209				

Over-expressed genes	Tet-EGFP Prox1 clone4 d37 +(X)	Tet-EGFP NeuroD clone2 d37 +(Y)	Diff(Y-X)	Under-expressed genes	Tet-EGFP Prox1 clone4 d37 +(X)	Tet-EGFP NeuroD clone2 d37 +(Y)	Diff(Y-X)
HES5	0,58319	19,66844	19,08525	PROX1	11,52511	4,70209	-6,82302
DCX	6,032	9,6424	3,6104	CALB1	11,42282	8,61483	-2,80799
EMX1	2,46667	6,01548	3,54881	LEF1	16,09807	14,20149	-1,89658
MBP	3,77775	6,81639	3,03863	OLIG2	12,35814	10,84676	-1,51138
NR2E1	9,69173	12,69606	3,00433	ID3	5,65568	4,38383	-1,27185
SYP	5,11996	7,43614	2,31618	TBR2	1,97768	0,72843	-1,24925
FOXG1	4,21489	6,28297	2,06808	BMPR1A	2,88036	1,67951	-1,20085
CALB2	4,8428	6,79074	1,94794				
NEUROD2	0,90319	2,77692	1,87373				
GABA	1,89811	3,59809	1,69998				
EMX2	8,62845	10,207	1,57855				
NEUN	1,71205	3,26176	1,54972				
GFAP	16,46005	17,94967	1,48962				
SOX1	6,45333	7,89401	1,44068				
NEUROG2	3,59166	4,94503	1,35338				
SOX2	2,58508	3,88673	1,30164				
SOX11	1,6179	2,70128	1,08337				
PAX6	6,92014	8,00304	1,0829				

Fig. 3.28 Correlation analysis and data of EMX2, Prox1 and NeuroD1 transcription factors overexpression at d37: direct comparisons of EMX2/Prox1; Prox1/NeuroD1; EMX2/NeuroD1

The strongest granule cell differentiation expression profile was reached with the combined overexpression of PROX1 and NEUROD1.

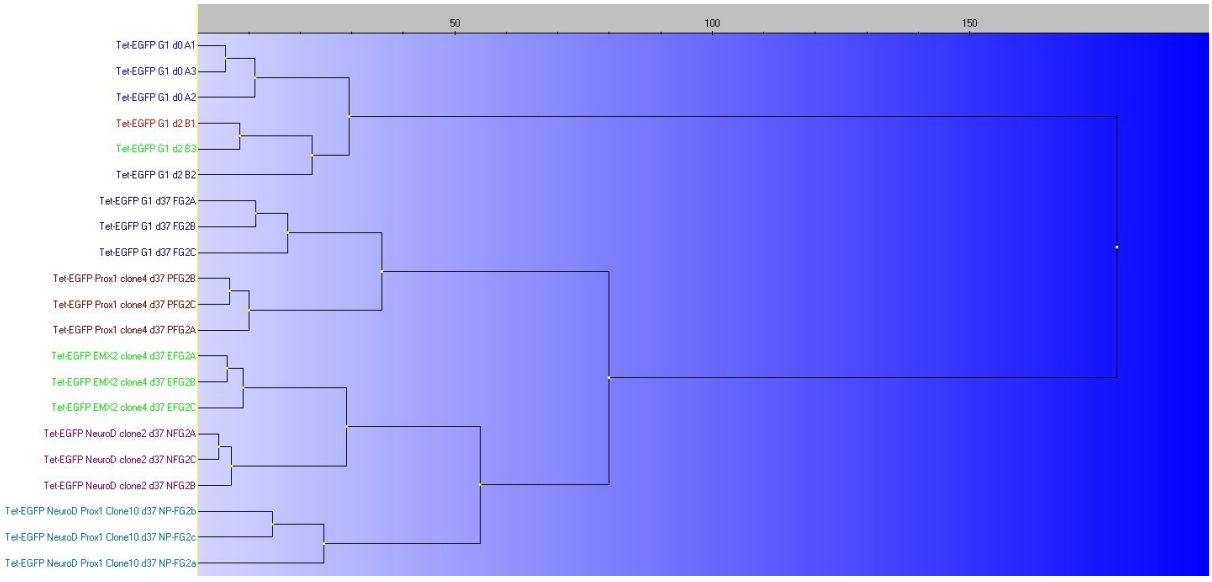

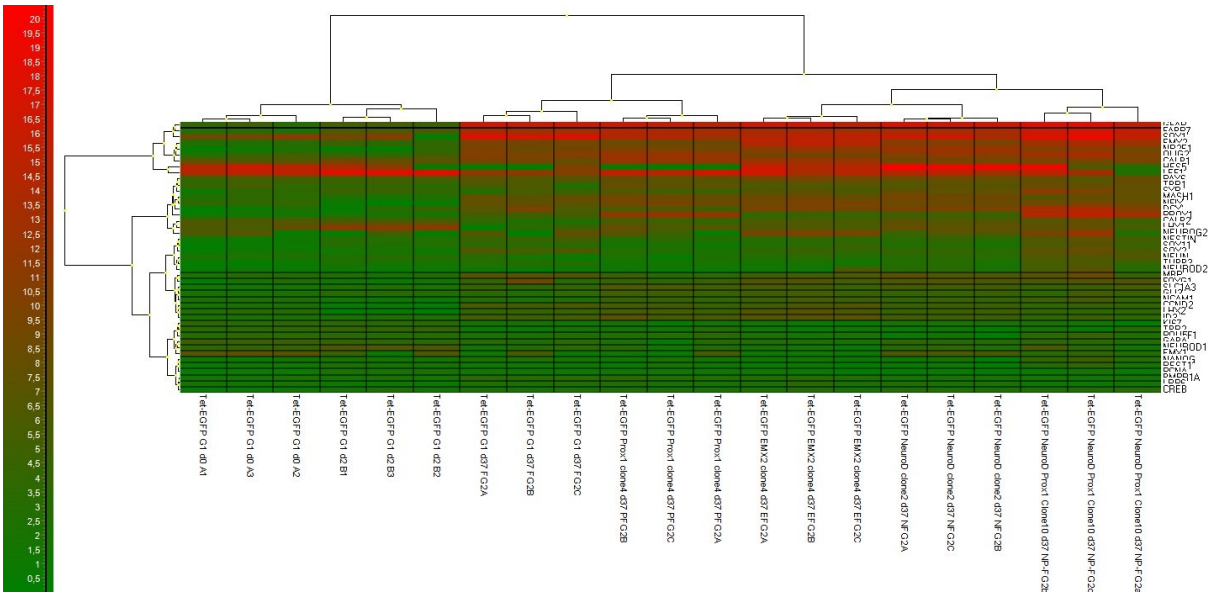

Fig. 3.29 Gene expression profiling of NeuroD1/Prox1 with NeuroD1, Prox1, Emx2, and EGFP control groups. (A) Hierarchical clustering of NeuroD1/Prox1 with NeuroD1, Prox1, Emx2, and EGFP control groups and (B) Heat map showing array of neural differentiation associated genes with each column representing the experimental groups. Note that NeuroD1/Prox1 showed the strongest difference to all other groups.

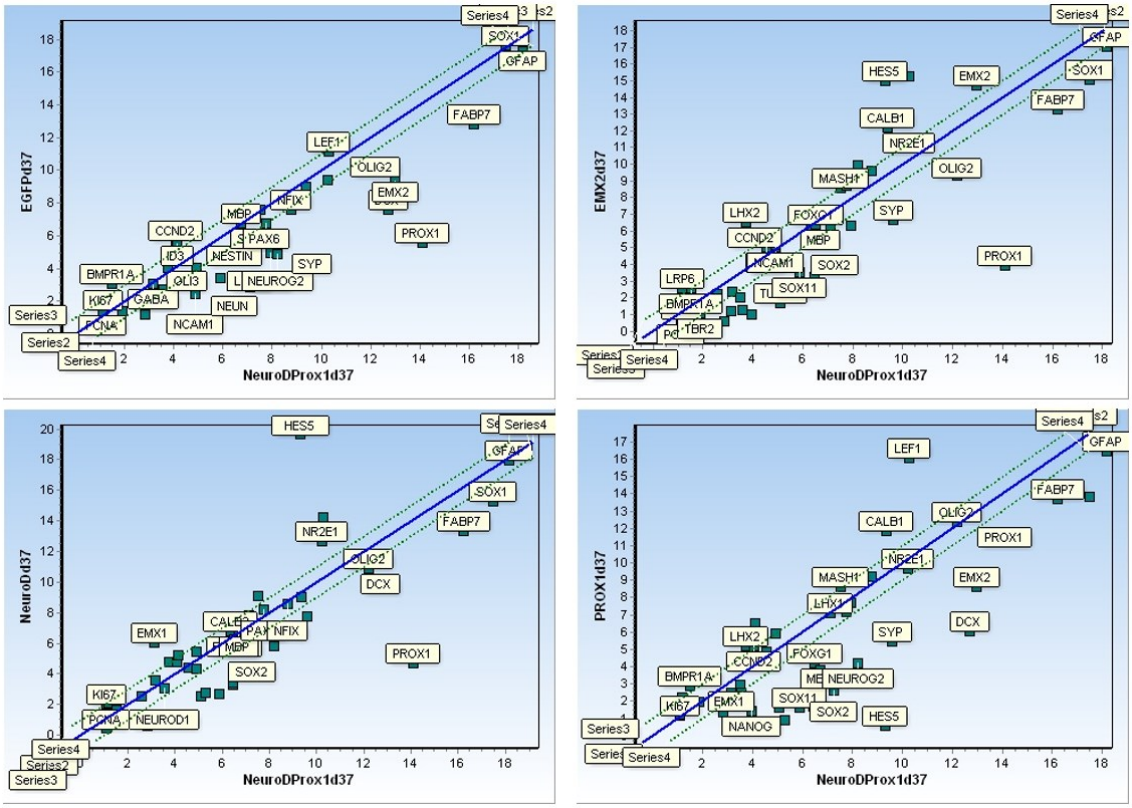

(NeuroDProx1d37) vs (NeuroDd37)	Fold change	Difference (A-B log scale)	P-Value
NEUN	9,09496	3,18507	0,000070759
PROX1	670,32556	9,38872	0,000137137
EMX1	-7,34417	-2,8766	0,000554286
FABP7	7,08828	2,82544	0,000733388
EMX2	6,77599	2,76043	0,003651629
LRP6	-1,90806	-0,93211	0,006489637
NESTIN	8,27015	3,04791	0,008155489
MASH1	-2,992	-1,58111	0,010921401
SOX11	9,08086	3,18283	0,012044088
NR2E1	-5,49316	-2,45764	0,015038811
REST1	4,66446	2,22171	0,017704769
LHX2	-2,00556	-1,00401	0,021160608
TUBB3	5,65821	2,50035	0,028706013
TBR1	2,25379	1,17235	0,034571972
DCX	8,37446	3,066	0,051742052
CCND2	-1,59204	-0,67087	0,066632966
ID3	-2,16837	-1,11661	0,069140629
PCNA	1,53174	0,61517	0,100902152
HES5	-1330,22908	-10,37746	0,105936124

(NeuroDProx1d37) vs (EGFPd37)	Fold change	Difference (A-B log scale)	P-Value
BMPR1A	-2,98045	-1,57553	0,000025048
PROX1	371,64018	8,53776	0,000170195
LRP6	-2,16393	-1,11365	0,000976226
EMX2	12,43341	3,63615	0,001183616
FABP7	10,26467	3,35961	0,001482856
NEUN	23,1704	4,53421	0,001654586
NCAM1	5,403	2,43376	0,003967952
NFIX	2,22335	1,15274	0,005072491
CCND2	-3,17694	-1,66764	0,005347257
SYP	39,76425	5,3134	0,012999311
CALB2	10,69729	3,41917	0,021073049
SOX11	5,48829	2,45636	0,022695547
NEUROD2	23,49229	4,55412	0,023029126
TUBB3	4,18223	2,06427	0,034522497
DCX	34,39931	5,10431	0,034619462
REST1	3,08656	1,626	0,037365455
ID3	-2,63174	-1,39602	0,045007926
NESTIN	3,38734	1,76015	0,045145626

(NeuroDProx1d37) vs (PROX1d37)	Fold change	Difference (A-B log scale)	P-Value
EMX2	20,23782	4,33898	0,000636769
CALB1	-5,60021	-2,48548	0,000811735
NEUN	26,62636	4,73478	0,000958007
FABP7	5,63228	2,49372	0,002775866
SOX11	19,24218	4,2662	0,004276196
NESTIN	11,0125	3,46107	0,004413271
DCX	102,2815	6,6764	0,004747049
LHX2	-2,73798	-1,45311	0,005343826
BMPR1A	-2,5882	-1,37195	0,006063593
TUBB3	10,88051	3,44367	0,006838022
FOXG1	4,8399	2,27498	0,007949619
LRP6	-2,06825	-1,04841	0,011477761
SYP	17,72462	4,14768	0,012388546
PROX1	5,9204	2,5657	0,019580062
ID3	-5,23597	-2,38846	0,023924909
NEUROD2	20,74096	4,37441	0,026265918
SOX1	12,877	3,68672	0,032068101
MASH1	-2,16301	-1,11304	0,039306125
CCND2	-2,1546	-1,10742	0,041210909
REST1	2,80111	1,486	0,061012849
MBP	7,67181	2,93957	0,081031977
SLC1A3	-1,96545	-0,97486	0,11556673
HES5	418,12397	8,70779	0,154797686

(NeuroDProx1d37) vs (EMX2d37)	Fold change	Difference (A-B log scale)	P-Value
PROX1	1124,1455	10,13461	0,000091766
NEUN	12,14421	3,6022	0,000097302
BMPR1A	-2,06153	-1,04371	0,000234058
CALB1	-7,14652	-2,83724	0,0002746
LHX2	-6,77036	-2,75923	0,000812185
FABP7	7,52649	2,91198	0,001016736
EMX1	3,89598	1,96199	0,001265462
TBR1	3,02683	1,59781	0,001933671
ID3	-7,56776	-2,91987	0,003038838
NESTIN	9,28658	3,21515	0,004346806
TUBB3	10,56932	3,40181	0,006954153
CCND2	-3,55337	-1,82919	0,016720095
REST1	4,82753	2,27129	0,017580407
EMX2	-3,34563	-1,74228	0,020844598
LRP6	-2,64033	-1,40072	0,023915042
SYP	7,74674	2,95359	0,032147384
SOX11	5,17945	2,3728	0,041410142
DCX	9,66461	3,27271	0,046446484

Fig. 3.30 correlation and t-test analysis comparing NeuroD1/Prox1 with NeuroD1, Prox1, Emx2, and EGFP control. Fold-change differences in log scale and p- values are shown comparisons with $p < 0.05$ are significant.

The combined overexpression of NeuroD1 and Prox1 initiated an overexpression of neuronal differentiation markers and dentate gyrus specific genes including synaptophysin, DCX, NeuroD2, NeuN, Emx2, CALB2, FABP7, NCAM1 and βIII-Tubulin.

4. Discussion

The brain cortex consists of a highly complex network of different subtypes of specialized neurons and glial cells controlled by growth factors, transcription factors and guidance molecules. The neurons are localized in nuclei which contain functional intrinsic circuits connected to other brain regions within extrinsic circuits via axonal pathways. In the development of this complex differentiated network, the neuronal and glial cell type specification, patterning, arealization, and axonal and dendritic pathfinding constitute major constructional components.
The pluripotent stem cells including ESCs and iPSCs make it possible to build up these neuronal networks in order to analyze the specification of neurons in the brain and their functional networks under normal and neuropathological conditions.
Recent research in developmental neuroscience and in stem cells has witnessed a considerable progress in the differentiation of pluripotent stem cells (PSCs) to regionally and functionally specialized subtypes of neurons and glial cells. The manipulation and simulation of developmental processes in vitro enables the production of enriched neural precursor cells and differentiated neurons resembling those in the brain. The production of neurons based on the PSC could lay the foundation for the in vitro modeling of pathological processes including the identification of drugs and therapeutics for neurological malfunctions and defects in the cortex.

The DG is the most primitive brain cortex area that develops most dorsally in the telencephalon. The principal neurons of the DG are the glutamatergic granular cells with a dendritic tree extending into the molecular layer and an axon building up the Mossy fiber tract which connects the DG to pyramidal cells of the CA.

The neuronal differentiation in specific brain areas is controlled by coordinated morphogenetic processes, which involve the temporal and spatial axial distribution of growth factors along gradients. It has been postulated that the gradients of morphogenes define the transcriptional code and thereby the identity of the neural precursors in the adjacent areas.

The DG development of is controlled by a growth factor gradient of Wnt3a, BNDF, and Dkk1 signaling combined with low SHH. The major transcription factors of the developing DG include EMX2, Prox1 and NeuroD1.

In this research, we aimed at stimulating parts of the developmental program of DG neurons by establishing a new protocol with slight modifications of the protocols designed by Watanabe, Yu and Sakaguchi (Watanabe, Kamiya et al. 2005); (Yu, Di Giorgio et al. 2014); (Sakaguchi, Kadoshima et al. 2015). Our protocol follows the embryonic development of mice for the differentiation of ESCs in vitro into DG granule neurons. It can be divided into the following five main stages: the ectodermal, neuro-ectodermal, telencephalic, DG induction, and fully-differentiated granule neuron stage.
By reanalyzing the expression profiles of all known growth factors in DG development, we came to the conclusion that, in addition to Wnt3a and BDNF and blocking SHH signaling, the main key players are the growth factors DKK1 and DKK3, and the transcription factors EMX2, Prox1 and NeuroD1.

The Growth Factors

Dkk1

Within gastrulating embryonic cells, the DKK1 expression is observable on day E6.5, a region in which the conjunction between anterior visceral endoderm and epiblast takes place (Glinka, Wu et al. 1998); (Pearce, Penny et al. 1999); (Zakin, Reversade et al. 2000).
During the neural induction process, the posterior-positioned cells are particularly disposed to patterning factors like WNTs and RA, and then progress towards the caudal pattern. Yet, the cells which are placed in the anterior sector of the neural plate are less affected by factors influencing caudal patterning. They maintain their anterior feature ,due to the endogenous expression of their inhibitors, such as Dkk1 as a WNT inhibitor signal (Glinka, Wu et al. 1998); (Wilson and Houart 2004).
Shortly after the formation of the neural tube, a substantial portion of the anterior region extends to form the telencephalon. In turn, the telencephalon region is segregated into two separate areas by the gradients of dorso-ventral patterning factors: the dorsal and the ventral telencephalon (Wilson and Rubenstein 2000).

Dkk1 is a member of the dickkopf family and encodes a secreted protein with two cysteine rich regions. It is involved in embryonic development by the inhibition of the Wnt signaling pathway.

In fact, the dickkopf protein encoded by DKK1 is an antagonistic inhibitor of the WNT signaling pathway that isolates the LRP6 co-receptor (Bafico, Liu et al. 2001); (Mao, Wu et al. 2001); (Semenov, Tamai et al. 2001) and Kremen. It thus constitutes a triplet complex which stimulates fast internalization and diminution of the cell-surface LRP6, so that it cannot help inactivating the WNT signaling pathway (Lewis, Khoo et al. 2008). The WNT signaling has proven to play a key role in stem cell differentiation and embryogenesis. The pluripotency of human and mouse ESCs has been discovered by the activation of WNT signaling by a pharmacological inhibitor of GSK-3 (Sato, Meijer et al. 2004).

In *Dkk1* knockout mice, the forebrain development is impaired (Mukhopadhyay, Shtrom et al. 2001). The extensive contribution of WNT and DKK family genes in the differentiation of multiple cell lineages during embryonic development is an indication that DKK is possibly involved in turning on the differentiation of mouse ESCs into primary germ layers.

Kong et al. investigated the roles of Dkk1 in ESC differentiation. They have shown that the over-expression of DKK1 in ESCs pushes the differentiation of mouse ESCs and EBs towards the neuroectodermal lineage (Kong and Zhang 2009).

Dkk1 has been identified for having a patterning role and increasing the expression of Foxg1, which is an important regulator of telencephalic cell cycles (Manuel, Martynoga et al. 2011).

The Foxg1 knockout causes premature prolongation of telencephalic progenitor cell cycles and increased neurogenic divisions, leading to severe hypoplasia of the telencephalon (Martynoga, Morrison et al. 2005).

By the addition of DKK1, we observed NPC colony-like structures with specified boundaries during differentiation and even proliferation. We named these structures the DG progenitor-like colonies. The landmark of these structures is that they did not proceed towards the neuronal-like structures with axon, dendrite formation, and branching-while remaining at the stage of DG precursors. The observation of Kong and colleagues also confirmed that DKK1 treatment did not result in further neural differentiation (Kong and Zhang 2009). They have suggested that this may be due to the need for additional factors for differentiation in this direction. In other words, the effect of a single growth factor or an overexpression of one transcription factor may not be sufficient for further differentiation.

In fact, the ICC data has shown that growth factor cocktails with DKK1 on day 10 induced the ESC differentiation towards an early specified neuroectodermal stage with co-expression of

Foxg1, Blbp, Pax6, and other generic neuroectodermal markers such as Nestin, GFAP, and Sox1.

The proliferation of telencephalic progenitors is controlled by Foxg1. Foxg1 regulates Pax6 activity, which in turn regulates the cell proliferation autonomously in a regional manner. There is strong evidence that one of the primary functions of the transcription factors Foxg1 and Pax6 is to regulate telencephalic cell cycles (Martynoga, Morrison et al. 2005); (Estivill-Torrus, Pearson et al. 2002); (Quinn, Molinek et al. 2007); (Manuel, Georgala et al. 2007); (Xuan, Baptista et al. 1995).

The colony formation in the DKK1 treatment group proved that WNT signaling pathways are not sufficiently suppressed by DKK1; there the neuronal progenitor cells could pass this stage and become fully-differentiated neurons.

As a consequence, the growth factor treatment with DKK1on d37 might have induced DG neuronal progenitor cells which remained morphologically in the same status, yet a full differentiation was suppressed.

The upregulation of HES5 on d37 demonstrated that DG progenitors could not differentiate completely. Other studies have shown that the over-expression of HES5 in the hippocampus down-regulates the expression of some pro-neuronal genes and delays cell differentiation. In fact, the up-regulation of HES5 had an influence on the notch-signaling pathways to the point that neurogenesis was inhibited, but the differentiation of neuronal stem cells and progenitor cells was continued (Mendes-da-Silva, Lemes et al. 2015).In addition, HES5 marks putative NSCs in granule neuron lineages and DCX neuronal precursors (type 2-b and type 3 cells) (Lugert, Basak et al. 2010).

The NPC colony-like structures on d37 were positive in ICC for Nestin, βIII-tubulin, GFAP, NeuN, Neurod1, Prox1, Calretinin and Calbindin, but most of these cells were not fully differentiated. The neurotransmitter glutamate specific for differentiated DG neurons was not expressed under DKK1 supplementation. The genetic data analysis showed that the treatment with DKK1 resulted in the up regulation of HES5, DCX, CALB2, LEF1, TBR1, SYP, NEUN and CALB1.

Dkk3

Dkk3 is another member of the DKK family which is a putative WNT inhibitor. During the mouse embryogenesis, the expression of DKK3 is detectable in the hippocampus at E15.5 developmental stage. The expression level of DKK3 is high in the CA1–CA3 region of the hippocampus and low in the DG. Moreover, the high level of DKK3 expression observed in the

cortex, hippocampus, and brain stem has suggested a role of DKK3 neuroplasticity in cortex and hippocampus (Krupnik, Sharp et al. 1999); (Zhang, Moseley et al. 2004).

During adult neurogenesis, the expression of DKK3 is restricted to NPCs in the SVZ and was absent in the SGZ. In contrast, DKK1 initially expressed in the SGZ and granule neurons and at a low level in the SVZ region (Seib, Corsini et al. 2013). This different expression patterning emphasizes the regional specification of mechanisms controlling neurogenesis.

The DKK3 knockout mouse analysis has remarkably proven a particular role of DKK3 in neurogenesis in vivo, namely a regulation of neuronal commitment, but no proliferation or self-renewal of NPCs. This function of DKK3 is entirely consistent with the role of Wnt signaling in the neuronal fate commitment (Song, Stevens et al. 2002); (Lie, Colamarino et al. 2005).

In comparison with DKK1, the treatment by DKK3 did not appear to be much effective in our studies. This treatment in the early stages of cell culture had a similar role in the induction of markers like BLBP, GFAP, Nestin, and Sox1 (neuroectodermal induction), but ICC analysis did not reveal any significant effect in the induction of specific DG markers such as NeuN, Prox1, Calretinin or Calbindin at day 37 of differentiation.

Zhang et al. also showed that the DKK3- EGFP–positive cells were able to form primary neurospheres merely in vitro. Indeed, the neurogenesis was attenuated by DKK3 expression. In accordance with this observation, DKK3 treatment did not have significant influence on ESCs differentiation to DG neurons.

The Transcription Factors

Emx2

During the mouse embryonic development, the Emx2 expression was detectable in telencephalon at E11.5 and at early stages of hippocampus development *at* E13.5.

In vivo studies have revealed that in Emx2 knockout mice, the hippocampus fails to form a normal DG as well as the normal layering of principal neurons in the hippocampus proper (Tole, Goudreau et al. 2000). At the same time in Emx2 overexpressing mice, the progenitors induce the production of granule neurons of the DG (Hamasaki, Leingartner et al. 2004).

In this study, the overexpression of Emx2 by the inducible tetracycline system suppressed the differentiation of telencephalic neuronal progenitor cells towards DG progenitor cells and DG granule neurons.

The gene expression analysis illustrated that EMX2 overexpression induced a strong upregulation of HES5. During mouse development, HES5 expression covers almost all regions

of the developing nervous system of mouse embryos around embryonic day 10.5 (E10.5) (Hatakeyama, Bessho et al. 2004). Later on, HES5 expression becomes restricted to the ventricular zone, which contains the neural precursor cells and cell bodies of radial glia (Akazawa, Sasai et al. 1992); (Sasai, Kageyama et al. 1992).

It has been demonstrated that overexpression of HES genes in mouse embryos inhibits neurogenesis and maintains neural stem cell pools (Ishibashi, Moriyoshi et al. 1994); (Ohtsuka, Sakamoto et al. 2001).

HES genes are downstream targets of the Notch pathway. They encode transcriptional repressors that predominantly control the proneural basic helix-loop-helix genes and thus regulate the maintenance of undifferentiated cells (Ohtsuka, Sakamoto et al. 2001); (Kageyama and Ohtsuka 1999).The characterization of the SGZ in Hes5 GFP reporter mice revealed that Hes5 GFP is expressed in cells which have both radial (54%) and horizontal (46%) morphologies. However, only 60% of Hes5 GFP+ cells overlapped with Sox2, BLBP and GFAP, thus indicating that Hes5 GFP labels are only a subset of the NSC population (Lugert, Basak et al. 2010).

Furthermore, it has been shown that Emx2 overexpression in cortical stem cells inhibits the astrocyte progenitor proliferation by repressing EgfR and Fgf9 (Falcone, Filippis et al. 2015).

In our study, the Emx2 overexpression decreased the expression of Nestin and GFAP known as astrocyte markers on d37. It seems that the overexpression of Emx2 suppressed cell proliferation and inhibited neurogenesis and gliogenesis, leading to a quiescent stage by a high expression of HES5.

In fact, considering the role of Emx2 in DG development during embryogenesis, we initially supposed that the upregulation of this gene may lead to DG neuroepithelial differentiation. Surprisingly, despite of our expectation, not only DG differentiation was absent, but also, both neurogenesis and gliogenesis were suppressed. This requires a more accurate investigation in the future.

The overexpression of Emx2, induced the expression of Neurog2, LHX2, which are expressed in intermediate progenitor cells (IPCs) type 2a and 3a, while most of the neurogenesis and neuroectodermal markers such as βIII-tubulin, Gfap, Sox1 were suppressed. It seems that the overexpression of Emx2 causes the IPCs to enter a quiescent phase.

In fact, the expression level and time interval of Emx2 expression both have a critical effect on DG induction during embryonic development. By using the Tet-inducible system, the sequential and transient expression of Emx2 can therefore regulate the induction of IPCs into DG differentiation.

Prox1

During the mouse embryonic development at E13.5, the Prox1 expression is detectable in the DG, regulated by canonical WNT signaling and has a stage-specified role in embryonic and adult hippocampal neurogenesis. Prox1 expression is highly restricted to DG during embryonic (dentate neuroepithelium) and adult hippocampus development (Galichet, Guillemot et al. 2008); (Lavado and Oliver 2007). Therefore, Prox1 was identified as a suitable marker to recognize the migration and targeting of DG granular neurons during development.

Lavado and colleagues have shown that Prox1 is necessary for the maturation of granule cells in the DG during development and for the maintenance of intermediate progenitors during adult neurogenesis. But it has been proven that ectopic expression of Prox1 can induce premature differentiation of neural stem cells (Lavado, Lagutin et al. 2010).

This group has also verified that Prox1 is expressed in the DG stem cells up to the fully differentiated granular cells. However, Prox1 expression is not restricted to granular cells in the DG. Therefore, it is only possible to characterize the granule cells in combination with other markers such as NeuroD1, Calretinin, Calbindin, and Glutamate.

The overexpression of Prox1 resulted in the expression of the markers Nestin and GFAP. Moreover, the expression of the telencephalic neuronal marker Foxg1 was positive by ICC. Foxg1, formerly BF-1, is expressed continuously in the postnatal and adult DG. This transcription factor is involved in the Rett syndrome, which is characterized by a reduced hippocampus size, indicating its important role in hippocampal development. Conditional ablation of Foxg1 resulted in the loss of the subgranular zone and a severely disrupted secondary radial glial scaffold, leading to the impaired migration of granule cells (Tian and Macdonald 2012, Tian, Xu et al. 2012). Moreover, a detailed characterization of these mutants revealed that Foxg1 may be necessary for the maintenance of the DG progenitor pool, and that the lack of Foxg1 promotes both gliogenesis and neurogenesis. Prox1 overexpression leads NPCs to neuronal differentiation and increased neuron-like structures in vitro. Moreover, our gene expression analysis showed that Prox1 overexpression had a positive feedback on Lef1, TBR1, CALB1 and CALB2 expression. When the data was aligned side-by-side with the Allen Brain Atlas, it was confirmed that the genes mentioned above are active during the development of the DG. Moreover, the data showed that the overexpression of Prox1 had a negative regulation on HES5 and did not activate a Notch signaling pathway contrary to the Emx2 overexpression that conducted the cells to enter the quiescent state. The ICC analysis revealed that the overexpression of Prox1 induced the expression of DG markers NeuN, Prox1, Calretinin, βIII-tubulin, synaptophysin, and Map (2a+2b). In contrast, the expression of Emx2,

NeuroD1, Calbindin, and glutamate was not observed. The in vitro observation thus indicated, that the overexpression of Prox1 alone is not sufficient to induce mESCs to fully-differentiated granule neurons.

NeuroD1

During the mouse embryonic development, the NeuroD1 expression is detectable in the hippocampus at E14.5.

NEUROD1 is a bHLH transcription factor required for the survival and maturation of adult-born granule cell neurons. The data showed that NeuroD1 has a transient and dynamic expression profile which is restricted to progenitors/neuroblasts (type 2b and type 3 cells) which are transient from immature to mature granule neurons.

The gene analysis indicated that the overexpression of NeuroD1 repressed the expression of Sox2 three-folded. Some evidence suggests that the suppression of Sox2 is also required for granule neuron differentiation, which is mediated by WNT/β-catenin transcriptional activation of NeuroD1 and the removal of Sox2 repression on the NeuroD1 promoter (Kuwabara, Hsieh et al. 2009). This Sox2-dependent repression of NeuroD1 must be eliminated in order that neurogenesis can progress (Ehm, Goritz et al. 2010). In this regard, the overexpression of NeuroD1 resulted in an increase of the neurogenesis, while the expression of glial markers such as Nestin and GFAP were decreased in comparison with the control group. In the same way, it seems that the overexpression of NeuroD1 and the suppression of Sox2 as a result of neurogenesis were both born by a decrease in gliogenesis.

The co-expression of NeuroD1 and DCX revealed that these cells are committed to the neuronal fate. On d37, the overexpression of NeuroD1 upregulated some genes, including HES5, CALB2, EMX1, SYP, NR2E1, LEF1, DCX, NueroD2, and TBR1. Once again when the data was aligned side-by-side with the Allen Brain Atlas, it was confirmed that the genes mentioned above are responsible for the development of the hippocampus during embryogenesis. Interestingly, given the role of NeuroD1 in immature precursor/neuroblasts, we expected that the overexpression of NeuroD1 can merely induce the immature transient precursor cells to mature granule neurons which express Prox1. Our data, however, indicated that the in vitro treatment of ES: Lt-EGFP-NeuroD1 clones resulted in the expression of DG markers such as NeuN, NeuroD1, Prox1, βIII-tubulin, and Map (2a+2b). But, in this group, the co-expressions of Prox1 with Calbindin, Calretinin, and glutamate/ βIII-tubulin were not observed. In conclusion, the overexpression of the NeuroD1 transcription factor alone was not sufficient to induce fully-differentiated DG neurons.

Combined overexpression of Prox1 and NeuroD1

The conditional activation of Prox1-NeuroD1 in ESCs resulted in a considerable increase in the expression of the markers Prox1, NeuroD1, NeuN, and βIII-tubulin, compared with the growth factor and transcription factor groups. In fact, it seemed that the combined overexpression of these transcription factors had also a synergic role in the induction of calbindin and calretinin. The morphological observations also demonstrated a considerable increase in neurogenesis compared with other groups.

In addition, in this group, the expression of the synaptic and neurotransmitter markers synaptophysin and glutamate increased.

In comparison with other groups the length of the axons and dendrites in this group did equally demonstrate a profound increase, while the processes became amazingly long and branched. In other groups, such a general development of these distinctive structures was not recognized. In the growth factor group, the cells principally remained in a/the progenitor state and only partially developed on the DKK1-treated group.

The results of the effects of growth factors, and comparing them with transcription factors have shown that the growth factors will more lead to the induction of neuro-progenitor cells than the transcription factors. In vice versa, the transcription factor and especially the combined overexpression of Prox1 and NeuroD1 pushed the cells to a neuronal phenotype. The colony-like structures inducted by the growth factors were no longer observed in the transcription factor groups.

The strongest granule cell differentiation expression profile was reached with the combined overexpression of PROX1 and NEUROD1.

The combined overexpression of NeuroD1 and Prox1 initiated an overexpression of neuronal differentiation markers and DG specific genes including, Emx2, FABP7, NCAM1, SYP, TBR1 NeuN, NeuroD2, DCX, CALB2, Synaptophysin and βIII-Tubulin. Moreover, many of the genes substantial for DG development were induced by this programming approach of directed differentiation (see also Appendix, Figs. 10.10, 10.11).

5. Summary

ESCs have the capacity of unlimited self-renewal and pluripotency, which are promising tools ranging from basic research in developmental biology to future therapeutic applications. Following the establishment of basic techniques for ESC cultivation and neuronal differentiation, the main objective was to direct the differentiation towards specific types of neurons. For instance, our goal was to direct the differentiation of ESCs towards the DG granule neurons.

So far, two major reports have been published in regard to the hippocampal induction from ESC and IPS cells (Yu, Di Giorgio et al. 2014); (Sakaguchi, Kadoshima et al. 2015). Both strategies are based on the role of growth factors related to the hippocampus development. Initially, the online platforms GenePaint.org and Allen Brain Atlas as well as previous studies dealing with the cellular localization of both growth factors and transcription factors in the DG and molecular mechanisms contributing to DG differentiation were used as underlying scenario. Resulting from that the question arised which growth factor combination would be of stronger influence to the differentiation into DG granule neurons from mESCs.

The growth factor cocktail with DKK1 has proven to be more inductive in telencephalic neuronal progenitor cells and also more prone to the generation of highly enriched mouse DG progenitor-like colonies - which expressed DG markers such as Prox1, Neurod1 and Tbr2.

In the next part, the role of the transcription factors Emx2, Prox1 and NeuroD1 in the production and induction of DG granule neurons was investigated. A high expression of Emx2 suppresses the differentiation of telencephalic neuronal progenitor cells to DG progenitor cells and DG granule neurons, while NeuroD1 and Prox1 overexpression lead to a strong up-regulation of hippocampal progenitor markers.

The strongest granule cell differentiation expression profile was reached with the combined overexpression of PROX1 and NEUROD1. Morphological observations clearly demonstrate a considerable increase in neurogenesis. This phenomenon can be seen in other groups as well. A comparison of the growth factor effects with those of the transcription factors do show that the growth factors will lead to an increase in the induction of neuro-progenitor cells. By contrast, the transcription factors, and especially the combined prox1 and neurod1, pushed the cells to neuronal phenotype.

In summary, it can be concluded that the combination of central DG transcription factors mainly influences DG granule neuron differentiation in vitro. Furthermore, it became obvious that the combination of a DG specific growth factor cocktail and transcription factors will lead to a significant differentiation of DG granule neurons.

5.1 Zusammenfassung

ESCs haben die Fähigkeit unbegrenzter Selbsterneuerung und Pluripotenz. Es sind vielversprechende Werkzeuge, die von der Grundlagenforschung in der Entwicklungsbiologie bis zu zukünftigen therapeutischen Ansätze reichen. Nach der Etablierung grundlegender Techniken für die Kultivierung und neuronalen Differenzierung der ESC war das Hauptanliegen dieser Arbeit die Differenzierung in spezifische Neuronen des Telencephalons. Und zwar bestand unser Ziel darin, die Differenzierung der ESCs auf die Körnerzellen des Gyrus dentatus auszurichten.

Bislang wurden zwei wichtige Arbeiten über die Hippocampus-Induktion von ES- und IPS-Zellen publiziert (Yu, Di Giorgio et al. 2014) (Sakaguchi, Kadoshima et al. 2015). Beide Methoden basieren auf der Rolle der Wachstumsfaktoren in Bezug auf die Hippocampus-Entwicklung. Zu Beginn der Arbeit wurden sowohl die Online-Plattformen GenePaint und Allen Brain Atlas als auch frühere Studien bezüglich zellulärer Lokalisation von Wachstums- und Transkriptions-Faktoren studiert. Daraus ergab sich die Fragestellung, welche der Wachstumsfaktor- Kombinationen einen größeren Einfluss auf die Differenzierung der Körnerzellen des Gyrus dentatus aus mESCs haben.

Der Wachstumsfaktor-Cocktail mit DKK1 zeigte eine ausgeprägtere Induktion der neuronalen Progenitor-Zellen im Telencephalon. Zudem bewirkte dieser eine stärkere Generierung von Kolonien hochangereicherter Gyrus dentatus-Zellen. Diese zeigen Ähnlichkeit mit Progenitor-Zellen und exprimieren die Gyrus dentatus-Marker Prox1, Neurod1 und Emx1.

Im nächsten Teil wurde die Rolle der Transkriptionsfaktoren Emx2, Prox1 und NeuroD1 im Hinblick auf Produktion und Induktion von Körnerzellen des Gyrus dentatus jeweils separat untersucht. Eine hohe Expression von Emx2 unterdrückt die Differenzierung von telencephalen neuronalen Progenitor-Zellen in Körnerzellen. Eine Überexprimierung von NeuroD1 und Prox1 hingegen führen zu einer starken Hochregulierung hippocampaler Progenitor–Marker.

Die stärkste Differenzierung in Körnerzellen wurde mit einer kombinierten Überexpression von PROX1 und NEUROD1 erreicht. Morphologische Beobachtungen zeigen deutlich einen signifikanten Anstieg der Neurogenese. Dies zeigt sich ebenfalls im Vergleich zu anderen Gruppen. Der Vergleich zwischen den Differenzierungs-Effekten von Wachstums- und Transkriptionsfaktoren zeigt, dass die Wachstumsfaktoren eine stärkere Induktion von Neuro-

Progenitorzellen als Transkriptionsfaktoren herbeiführen. Im Gegensatz dazu führen die Transkriptionsfaktoren, und insbesondere die Kombination von Prox1 und Neurod1, zu einer Ausbildung des neuronalen Phänotyps der Zellen.

Aus all diesen Beobachtungen ergibt sich Folgendes: Die Kombination von zentralen Transkriptionsfaktoren des Gyrus dentatus beeinflussen hauptsächlich die Differenzierung in Körnerzellen in vitro. Weiter zeigte sich, dass ein Gyrus dentatus spezifischer Wachstumsfaktor-Cocktail und Transkriptionsfaktoren zu einer effektiveren Differenzierung der Granula Neurone des Gyrus dentatus führen.

6. References

Abeldano, A. M., J. Tiscornia, L. P. Cendeno, P. Brea and E. N. Chouela (2006). "Basal cell carcinoma in palm and sole." Skinmed **5**(1): 40-42.

Akazawa, C., Y. Sasai, S. Nakanishi and R. Kageyama (1992). "Molecular characterization of a rat negative regulator with a basic helix-loop-helix structure predominantly expressed in the developing nervous system." J Biol Chem **267**(30): 21879-21885.

Altman, J. and S. A. Bayer (1990). "Migration and distribution of two populations of hippocampal granule cell precursors during the perinatal and postnatal periods." J Comp Neurol **301**(3): 365-381.

Andersen, J., N. Urban, A. Achimastou, A. Ito, M. Simic, K. Ullom, B. Martynoga, M. Lebel, C. Goritz, J. Frisen, M. Nakafuku and F. Guillemot (2014). "A transcriptional mechanism integrating inputs from extracellular signals to activate hippocampal stem cells." Neuron **83**(5): 1085-1097.

Anderson, A. H., A. J. Cohen, N. G. Kutner, J. B. Kopp, P. L. Kimmel and P. Muntner (2009). "Missed dialysis sessions and hospitalization in hemodialysis patients after Hurricane Katrina." Kidney Int **75**(11): 1202-1208.

Angevine, J. B., Jr. (1965). "Time of neuron origin in the hippocampal region. An autoradiographic study in the mouse." Exp Neurol Suppl: Suppl 2:1-70.

Ansorg, A., O. W. Witte and A. Urbach (2012). "Age-dependent kinetics of dentate gyrus neurogenesis in the absence of cyclin D2." BMC Neurosci **13**: 46.

Arnold, S. J., G. J. Huang, A. F. Cheung, T. Era, S. Nishikawa, E. K. Bikoff, Z. Molnar, E. J. Robertson and M. Groszer (2008). "The T-box transcription factor Eomes/Tbr2 regulates neurogenesis in the cortical subventricular zone." Genes Dev **22**(18): 2479-2484.

Bafico, A., G. Liu, A. Yaniv, A. Gazit and S. A. Aaronson (2001). "Novel mechanism of Wnt signalling inhibition mediated by Dickkopf-1 interaction with LRP6/Arrow." Nat Cell Biol **3**(7): 683-686.

Bagri, A., T. Gurney, X. He, Y. R. Zou, D. R. Littman, M. Tessier-Lavigne and S. J. Pleasure (2002). "The chemokine SDF1 regulates migration of dentate granule cells." Development **129**(18): 4249-4260.

Bayer, S. A. (1980). "Development of the hippocampal region in the rat. I. Neurogenesis examined with 3H-thymidine autoradiography." J Comp Neurol **190**(1): 87-114.

Bayer, S. A. (1980). "Development of the hippocampal region in the rat. II. Morphogenesis during embryonic and early postnatal life." J Comp Neurol **190**(1): 115-134.

Berninger, B., M. R. Costa, U. Koch, T. Schroeder, B. Sutor, B. Grothe and M. Gotz (2007). "Functional properties of neurons derived from in vitro reprogrammed postnatal astroglia." J Neurosci **27**(32): 8654-8664.

Bertrand, N., D. S. Castro and F. Guillemot (2002). "Proneural genes and the specification of neural cell types." Nat Rev Neurosci **3**(7): 517-530.

Bonaguidi, M. A., T. McGuire, M. Hu, L. Kan, J. Samanta and J. A. Kessler (2005). "LIF and BMP signaling generate separate and discrete types of GFAP-expressing cells." Development **132**(24): 5503-5514.

Bonaguidi, M. A., C. Y. Peng, T. McGuire, G. Falciglia, K. T. Gobeske, C. Czeisler and J. A. Kessler (2008). "Noggin expands neural stem cells in the adult hippocampus." J Neurosci **28**(37): 9194-9204.

Bond, A. M., C. Y. Peng, E. A. Meyers, T. McGuire, O. Ewaleifoh and J. A. Kessler (2014). "BMP signaling regulates the tempo of adult hippocampal progenitor maturation at multiple stages of the lineage." Stem Cells **32**(8): 2201-2214.

Bratt-Leal, A. M., R. L. Carpenedo and T. C. McDevitt (2009). "Engineering the embryoid body microenvironment to direct embryonic stem cell differentiation." Biotechnol Prog **25**(1): 43-51.

Campbell, C. E., M. Piper, C. Plachez, Y. T. Yeh, J. S. Baizer, J. M. Osinski, E. D. Litwack, L. J. Richards and R. M. Gronostajski (2008). "The transcription factor Nfix is essential for normal brain development." BMC Dev Biol **8**: 52.

Caronia, G., J. Wilcoxon, P. Feldman and E. A. Grove (2010). "Bone morphogenetic protein signaling in the developing telencephalon controls formation of the hippocampal dentate gyrus and modifies fear-related behavior." J Neurosci **30**(18): 6291-6301.

Castro, D. S., B. Martynoga, C. Parras, V. Ramesh, E. Pacary, C. Johnston, D. Drechsel, M. Lebel-Potter, L. G. Garcia, C. Hunt, D. Dolle, A. Bithell, L. Ettwiller, N. Buckley and F. Guillemot (2011). "A novel function of the proneural factor Ascl1 in progenitor proliferation identified by genome-wide characterization of its targets." Genes Dev **25**(9): 930-945.

Chae, T., Y. T. Kwon, R. Bronson, P. Dikkes, E. Li and L. H. Tsai (1997). "Mice lacking p35, a neuronal specific activator of Cdk5, display cortical lamination defects, seizures, and adult lethality." Neuron **18**(1): 29-42.

Cheng, X., C. M. Hsu, D. S. Currle, J. S. Hu, A. J. Barkovich and E. S. Monuki (2006). "Central roles of the roof plate in telencephalic development and holoprosencephaly." J Neurosci **26**(29): 7640-7649.

Colak, D., T. Mori, M. S. Brill, A. Pfeifer, S. Falk, C. Deng, R. Monteiro, C. Mummery, L. Sommer and M. Gotz (2008). "Adult neurogenesis requires Smad4-mediated bone morphogenic protein signaling in stem cells." J Neurosci **28**(2): 434-446.

Conzen, C., M. Conzen, N. Rubsamen and R. Mikolajczyk (2016). "Predictors of the patient-centered outcomes of surgical carpal tunnel release - a prospective cohort study." BMC Musculoskelet Disord **17**: 190.

de Wert, G. and C. Mummery (2003). "Human embryonic stem cells: research, ethics and policy." Hum Reprod **18**(4): 672-682.

Del Rio, J. A., B. Heimrich, V. Borrell, E. Forster, A. Drakew, S. Alcantara, K. Nakajima, T. Miyata, M. Ogawa, K. Mikoshiba, P. Derer, M. Frotscher and E. Soriano (1997). "A role for

Cajal-Retzius cells and reelin in the development of hippocampal connections." Nature **385**(6611): 70-74.

Di Giorgio, F. P., G. L. Boulting, S. Bobrowicz and K. C. Eggan (2008). "Human embryonic stem cell-derived motor neurons are sensitive to the toxic effect of glial cells carrying an ALS-causing mutation." Cell Stem Cell **3**(6): 637-648.

Dimos, J. T., K. T. Rodolfa, K. K. Niakan, L. M. Weisenthal, H. Mitsumoto, W. Chung, G. F. Croft, G. Saphier, R. Leibel, R. Goland, H. Wichterle, C. E. Henderson and K. Eggan (2008). "Induced pluripotent stem cells generated from patients with ALS can be differentiated into motor neurons." Science **321**(5893): 1218-1221.

Drakew, A., T. Deller, B. Heimrich, C. Gebhardt, D. Del Turco, A. Tielsch, E. Forster, J. Herz and M. Frotscher (2002). "Dentate granule cells in reeler mutants and VLDLR and ApoER2 knockout mice." Exp Neurol **176**(1): 12-24.

Ehm, O., C. Goritz, M. Covic, I. Schaffner, T. J. Schwarz, E. Karaca, B. Kempkes, E. Kremmer, F. W. Pfrieger, L. Espinosa, A. Bigas, C. Giachino, V. Taylor, J. Frisen and D. C. Lie (2010). "RBPJkappa-dependent signaling is essential for long-term maintenance of neural stem cells in the adult hippocampus." J Neurosci **30**(41): 13794-13807.

Eiraku, M., K. Watanabe, M. Matsuo-Takasaki, M. Kawada, S. Yonemura, M. Matsumura, T. Wataya, A. Nishiyama, K. Muguruma and Y. Sasai (2008). "Self-organized formation of polarized cortical tissues from ESCs and its active manipulation by extrinsic signals." Cell Stem Cell **3**(5): 519-532.

Ekholm, S. V. and S. I. Reed (2000). "Regulation of G(1) cyclin-dependent kinases in the mammalian cell cycle." Curr Opin Cell Biol **12**(6): 676-684.

Elmi, M., Y. Matsumoto, Z. J. Zeng, P. Lakshminarasimhan, W. Yang, A. Uemura, S. Nishikawa, A. Moshiri, N. Tajima, H. Agren and K. Funa (2010). "TLX activates MASH1 for induction of neuronal lineage commitment of adult hippocampal neuroprogenitors." Mol Cell Neurosci **45**(2): 121-131.

Elstner, A., A. Damaschun, A. Kurtz, G. Stacey, B. Aran, A. Veiga and J. Borstlap (2009). "The changing landscape of European and international regulation on embryonic stem cell research." Stem Cell Res **2**(2): 101-107.

Englund, C., A. Fink, C. Lau, D. Pham, R. A. Daza, A. Bulfone, T. Kowalczyk and R. F. Hevner (2005). "Pax6, Tbr2, and Tbr1 are expressed sequentially by radial glia, intermediate progenitor cells, and postmitotic neurons in developing neocortex." J Neurosci **25**(1): 247-251.

Estivill-Torrus, G., H. Pearson, V. van Heyningen, D. J. Price and P. Rashbass (2002). "Pax6 is required to regulate the cell cycle and the rate of progression from symmetrical to asymmetrical division in mammalian cortical progenitors." Development **129**(2): 455-466.

Evans, M. J. and M. H. Kaufman (1981). "Establishment in culture of pluripotential cells from mouse embryos." Nature **292**(5819): 154-156.

Fagerberg, L., B. M. Hallstrom, P. Oksvold, C. Kampf, D. Djureinovic, J. Odeberg, M. Habuka, S. Tahmasebpoor, A. Danielsson, K. Edlund, A. Asplund, E. Sjostedt, E. Lundberg, C. A. Szigyarto, M. Skogs, J. O. Takanen, H. Berling, H. Tegel, J. Mulder, P. Nilsson, J. M.

Schwenk, C. Lindskog, F. Danielsson, A. Mardinoglu, A. Sivertsson, K. von Feilitzen, M. Forsberg, M. Zwahlen, I. Olsson, S. Navani, M. Huss, J. Nielsen, F. Ponten and M. Uhlen (2014). "Analysis of the human tissue-specific expression by genome-wide integration of transcriptomics and antibody-based proteomics." Mol Cell Proteomics **13**(2): 397-406.

Falcone, C., C. Filippis, M. Granzotto and A. Mallamaci (2015). "Emx2 expression levels in NSCs modulate astrogenesis rates by regulating EgfR and Fgf9." Glia **63**(3): 412-422.

Fan, X., H. Xu, W. Cai, Z. Yang and J. Zhang (2003). "Spatial and temporal patterns of expression of Noggin and BMP4 in embryonic and postnatal rat hippocampus." Brain Res Dev Brain Res **146**(1-2): 51-58.

Fernandes, M., G. Gutin, H. Alcorn, S. K. McConnell and J. M. Hebert (2007). "Mutations in the BMP pathway in mice support the existence of two molecular classes of holoprosencephaly." Development **134**(21): 3789-3794.

Forster, E., A. Tielsch, B. Saum, K. H. Weiss, C. Johanssen, D. Graus-Porta, U. Muller and M. Frotscher (2002). "Reelin, Disabled 1, and beta 1 integrins are required for the formation of the radial glial scaffold in the hippocampus." Proc Natl Acad Sci U S A **99**(20): 13178-13183.

Fukuchi-Shimogori, T. and E. A. Grove (2001). "Neocortex patterning by the secreted signaling molecule FGF8." Science **294**(5544): 1071-1074.

Fukuchi-Shimogori, T. and E. A. Grove (2003). "Emx2 patterns the neocortex by regulating FGF positional signaling." Nat Neurosci **6**(8): 825-831.

Furuta, Y., D. W. Piston and B. L. Hogan (1997). "Bone morphogenetic proteins (BMPs) as regulators of dorsal forebrain development." Development **124**(11): 2203-2212.

Galceran, J., I. Farinas, M. J. Depew, H. Clevers and R. Grosschedl (1999). "Wnt3a-/--like phenotype and limb deficiency in Lef1(-/-)Tcf1(-/-) mice." Genes Dev **13**(6): 709-717.

Galceran, J., E. M. Miyashita-Lin, E. Devaney, J. L. Rubenstein and R. Grosschedl (2000). "Hippocampus development and generation of dentate gyrus granule cells is regulated by LEF1." Development **127**(3): 469-482.

Galichet, C., F. Guillemot and C. M. Parras (2008). "Neurogenin 2 has an essential role in development of the dentate gyrus." Development **135**(11): 2031-2041.

Giacomini, M., F. Baylis and J. Robert (2007). "Banking on it: public policy and the ethics of stem cell research and development." Soc Sci Med **65**(7): 1490-1500.

Glinka, A., W. Wu, H. Delius, A. P. Monaghan, C. Blumenstock and C. Niehrs (1998). "Dickkopf-1 is a member of a new family of secreted proteins and functions in head induction." Nature **391**(6665): 357-362.

Gossen, M., S. Freundlieb, G. Bender, G. Muller, W. Hillen and H. Bujard (1995). "Transcriptional activation by tetracyclines in mammalian cells." Science **268**(5218): 1766-1769.

Gross, R. E., M. F. Mehler, P. C. Mabie, Z. Zang, L. Santschi and J. A. Kessler (1996). "Bone morphogenetic proteins promote astroglial lineage commitment by mammalian subventricular zone progenitor cells." Neuron **17**(4): 595-606.

Grove, E. A. and T. Fukuchi-Shimogori (2003). "Generating the cerebral cortical area map." Annu Rev Neurosci **26**: 355-380.

Grove, E. A. and S. Tole (1999). "Patterning events and specification signals in the developing hippocampus." Cereb Cortex **9**(6): 551-561.

Grove, E. A., S. Tole, J. Limon, L. Yip and C. W. Ragsdale (1998). "The hem of the embryonic cerebral cortex is defined by the expression of multiple Wnt genes and is compromised in Gli3-deficient mice." Development **125**(12): 2315-2325.

Guo, W., A. C. Murthy, L. Zhang, E. B. Johnson, E. G. Schaller, A. M. Allan and X. Zhao (2012). "Inhibition of GSK3beta improves hippocampus-dependent learning and rescues neurogenesis in a mouse model of fragile X syndrome." Hum Mol Genet **21**(3): 681-691.

Hamasaki, T., A. Leingartner, T. Ringstedt and D. D. O'Leary (2004). "EMX2 regulates sizes and positioning of the primary sensory and motor areas in neocortex by direct specification of cortical progenitors." Neuron **43**(3): 359-372.

Hamrahian, A. H., A. G. Ioachimescu, E. M. Remer, G. Motta-Ramirez, H. Bogabathina, H. S. Levin, S. Reddy, I. S. Gill, A. Siperstein and E. L. Bravo (2005). "Clinical utility of noncontrast computed tomography attenuation value (hounsfield units) to differentiate adrenal adenomas/hyperplasias from nonadenomas: Cleveland Clinic experience." J Clin Endocrinol Metab **90**(2): 871-877.

Hanashima, C., M. Fernandes, J. M. Hebert and G. Fishell (2007). "The role of Foxg1 and dorsal midline signaling in the generation of Cajal-Retzius subtypes." J Neurosci **27**(41): 11103-11111.

Hatakeyama, J., Y. Bessho, K. Katoh, S. Ookawara, M. Fujioka, F. Guillemot and R. Kageyama (2004). "Hes genes regulate size, shape and histogenesis of the nervous system by control of the timing of neural stem cell differentiation." Development **131**(22): 5539-5550.

Hebert, J. M., Y. Mishina and S. K. McConnell (2002). "BMP signaling is required locally to pattern the dorsal telencephalic midline." Neuron **35**(6): 1029-1041.

Heng, Y. H., R. C. McLeay, T. J. Harvey, A. G. Smith, G. Barry, K. Cato, C. Plachez, E. Little, S. Mason, C. Dixon, R. M. Gronostajski, T. L. Bailey, L. J. Richards and M. Piper (2014). "NFIX regulates neural progenitor cell differentiation during hippocampal morphogenesis." Cereb Cortex **24**(1): 261-279.

Hirabayashi, Y., Y. Itoh, H. Tabata, K. Nakajima, T. Akiyama, N. Masuyama and Y. Gotoh (2004). "The Wnt/beta-catenin pathway directs neuronal differentiation of cortical neural precursor cells." Development **131**(12): 2791-2801.

Hirotsune, S., M. W. Fleck, M. J. Gambello, G. J. Bix, A. Chen, G. D. Clark, D. H. Ledbetter, C. J. McBain and A. Wynshaw-Boris (1998). "Graded reduction of Pafah1b1 (Lis1) activity results in neuronal migration defects and early embryonic lethality." Nat Genet **19**(4): 333-339.

Hodge, R. D., A. J. Garcia, 3rd, G. E. Elsen, B. R. Nelson, K. E. Mussar, S. L. Reiner, J. M. Ramirez and R. F. Hevner (2013). "Tbr2 expression in Cajal-Retzius cells and intermediate neuronal progenitors is required for morphogenesis of the dentate gyrus." J Neurosci **33**(9): 4165-4180.

Hodge, R. D., T. D. Kowalczyk, S. A. Wolf, J. M. Encinas, C. Rippey, G. Enikolopov, G. Kempermann and R. F. Hevner (2008). "Intermediate progenitors in adult hippocampal neurogenesis: Tbr2 expression and coordinate regulation of neuronal output." J Neurosci **28**(14): 3707-3717.

Hodge, R. D., B. R. Nelson, R. J. Kahoud, R. Yang, K. E. Mussar, S. L. Reiner and R. F. Hevner (2012). "Tbr2 is essential for hippocampal lineage progression from neural stem cells to intermediate progenitors and neurons." J Neurosci **32**(18): 6275-6287.

Imayoshi, I. and R. Kageyama (2011). "The role of Notch signaling in adult neurogenesis." Mol Neurobiol **44**(1): 7-12.

Ishibashi, M., K. Moriyoshi, Y. Sasai, K. Shiota, S. Nakanishi and R. Kageyama (1994). "Persistent expression of helix-loop-helix factor HES-1 prevents mammalian neural differentiation in the central nervous system." EMBO J **13**(8): 1799-1805.

Iwano, T., A. Masuda, H. Kiyonari, H. Enomoto and F. Matsuzaki (2012). "Prox1 postmitotically defines dentate gyrus cells by specifying granule cell identity over CA3 pyramidal cell fate in the hippocampus." Development **139**(16): 3051-3062.

Kageyama, R. and T. Ohtsuka (1999). "The Notch-Hes pathway in mammalian neural development." Cell Res **9**(3): 179-188.

Khalaf-Nazzal, R. and F. Francis (2013). "Hippocampal development - old and new findings." Neuroscience **248**: 225-242.

Komada, M., T. Iguchi, T. Takeda, M. Ishibashi and M. Sato (2013). "Smoothened controls cyclin D2 expression and regulates the generation of intermediate progenitors in the developing cortex." Neurosci Lett **547**: 87-91.

Kong, X. B. and C. Zhang (2009). "Dickkopf (Dkk) 1 promotes the differentiation of mouse embryonic stem cells toward neuroectoderm." In Vitro Cell Dev Biol Anim **45**(3-4): 185-193.

Kowalczyk, A., R. K. Filipkowski, M. Rylski, G. M. Wilczynski, F. A. Konopacki, J. Jaworski, M. A. Ciemerych, P. Sicinski and L. Kaczmarek (2004). "The critical role of cyclin D2 in adult neurogenesis." J Cell Biol **167**(2): 209-213.

Kriks, S., J. W. Shim, J. Piao, Y. M. Ganat, D. R. Wakeman, Z. Xie, L. Carrillo-Reid, G. Auyeung, C. Antonacci, A. Buch, L. Yang, M. F. Beal, D. J. Surmeier, J. H. Kordower, V. Tabar and L. Studer (2011). "Dopamine neurons derived from human ES cells efficiently engraft in animal models of Parkinson's disease." Nature **480**(7378): 547-551.

Krupnik, V. E., J. D. Sharp, C. Jiang, K. Robison, T. W. Chickering, L. Amaravadi, D. E. Brown, D. Guyot, G. Mays, K. Leiby, B. Chang, T. Duong, A. D. Goodearl, D. P. Gearing, S. Y. Sokol and S. A. McCarthy (1999). "Functional and structural diversity of the human Dickkopf gene family." Gene **238**(2): 301-313.

Kunze, A., S. Grass, O. W. Witte, M. Yamaguchi, G. Kempermann and C. Redecker (2006). "Proliferative response of distinct hippocampal progenitor cell populations after cortical infarcts in the adult brain." Neurobiol Dis **21**(2): 324-332.

Kuwabara, T., J. Hsieh, A. Muotri, G. Yeo, M. Warashina, D. C. Lie, L. Moore, K. Nakashima, M. Asashima and F. H. Gage (2009). "Wnt-mediated activation of NeuroD1 and retro-elements during adult neurogenesis." Nature Neuroscience **12**(9): 1097-U1096.

Lancaster, M. A., M. Renner, C. A. Martin, D. Wenzel, L. S. Bicknell, M. E. Hurles, T. Homfray, J. M. Penninger, A. P. Jackson and J. A. Knoblich (2013). "Cerebral organoids model human brain development and microcephaly." Nature **501**(7467): 373-379.

Lavado, A., O. V. Lagutin, L. M. Chow, S. J. Baker and G. Oliver (2010). "Prox1 is required for granule cell maturation and intermediate progenitor maintenance during brain neurogenesis." PLoS Biol **8**(8).

Lavado, A. and G. Oliver (2007). "Prox1 expression patterns in the developing and adult murine brain." Dev Dyn **236**(2): 518-524.

Lee, J. E. (1997). "Basic helix-loop-helix genes in neural development." Curr Opin Neurobiol **7**(1): 13-20.

Lee, S. M., S. Tole, E. Grove and A. P. McMahon (2000). "A local Wnt-3a signal is required for development of the mammalian hippocampus." Development **127**(3): 457-467.

Lewis, S. L., P. L. Khoo, R. A. De Young, K. Steiner, C. Wilcock, M. Mukhopadhyay, H. Westphal, R. V. Jamieson, L. Robb and P. P. Tam (2008). "Dkk1 and Wnt3 interact to control head morphogenesis in the mouse." Development **135**(10): 1791-1801.

Li, G., H. Kataoka, S. R. Coughlin and S. J. Pleasure (2009). "Identification of a transient subpial neurogenic zone in the developing dentate gyrus and its regulation by Cxcl12 and reelin signaling." Development **136**(2): 327-335.

Li, G. and S. J. Pleasure (2005). "Morphogenesis of the dentate gyrus: what we are learning from mouse mutants." Dev Neurosci **27**(2-4): 93-99.

Lie, D. C., S. A. Colamarino, H. J. Song, L. Desire, H. Mira, A. Consiglio, E. S. Lein, S. Jessberger, H. Lansford, A. R. Dearie and F. H. Gage (2005). "Wnt signalling regulates adult hippocampal neurogenesis." Nature **437**(7063): 1370-1375.

Ligon, K. L., Y. Echelard, S. Assimacopoulos, P. S. Danielian, S. Kaing, E. A. Grove, A. P. McMahon and D. H. Rowitch (2003). "Loss of Emx2 function leads to ectopic expression of Wnt1 in the developing telencephalon and cortical dysplasia." Development **130**(10): 2275-2287.

Lim, D. A., A. D. Tramontin, J. M. Trevejo, D. G. Herrera, J. M. Garcia-Verdugo and A. Alvarez-Buylla (2000). "Noggin antagonizes BMP signaling to create a niche for adult neurogenesis." Neuron **28**(3): 713-726.

Lu, M., E. A. Grove and R. J. Miller (2002). "Abnormal development of the hippocampal dentate gyrus in mice lacking the CXCR4 chemokine receptor." Proc Natl Acad Sci U S A **99**(10): 7090-7095.

Lugert, S., O. Basak, P. Knuckles, U. Haussler, K. Fabel, M. Gotz, C. A. Haas, G. Kempermann, V. Taylor and C. Giachino (2010). "Quiescent and active hippocampal neural stem cells with distinct morphologies respond selectively to physiological and pathological stimuli and aging." Cell Stem Cell **6**(5): 445-456.

Lukaszewicz, A. I. and D. J. Anderson (2011). "Cyclin D1 promotes neurogenesis in the developing spinal cord in a cell cycle-independent manner." Proc Natl Acad Sci U S A **108**(28): 11632-11637.

Ma, L., Y. Liu and S. C. Zhang (2011). "Directed differentiation of dopamine neurons from human pluripotent stem cells." Methods Mol Biol **767**: 411-418.

Machon, O., M. Backman, O. Machonova, Z. Kozmik, T. Vacik, L. Andersen and S. Krauss (2007). "A dynamic gradient of Wnt signaling controls initiation of neurogenesis in the mammalian cortex and cellular specification in the hippocampus." Dev Biol **311**(1): 223-237.

Mallamaci, A., R. Iannone, P. Briata, L. Pintonello, S. Mercurio, E. Boncinelli and G. Corte (1998). "EMX2 protein in the developing mouse brain and olfactory area." Mech Dev **77**(2): 165-172.

Mallamaci, A., L. Muzio, C. H. Chan, J. Parnavelas and E. Boncinelli (2000). "Area identity shifts in the early cerebral cortex of Emx2-/- mutant mice." Nat Neurosci **3**(7): 679-686.

Mangale, V. S., K. E. Hirokawa, P. R. Satyaki, N. Gokulchandran, S. Chikbire, L. Subramanian, A. S. Shetty, B. Martynoga, J. Paul, M. V. Mai, Y. Li, L. A. Flanagan, S. Tole and E. S. Monuki (2008). "Lhx2 selector activity specifies cortical identity and suppresses hippocampal organizer fate." Science **319**(5861): 304-309.

Manuel, M., P. A. Georgala, C. B. Carr, S. Chanas, D. A. Kleinjan, B. Martynoga, J. O. Mason, M. Molinek, J. Pinson, T. Pratt, J. C. Quinn, T. I. Simpson, D. A. Tyas, V. van Heyningen, J. D. West and D. J. Price (2007). "Controlled overexpression of Pax6 in vivo negatively autoregulates the Pax6 locus, causing cell-autonomous defects of late cortical progenitor proliferation with little effect on cortical arealization." Development **134**(3): 545-555.

Manuel, M. N., B. Martynoga, M. D. Molinek, J. C. Quinn, C. Kroemmer, J. O. Mason and D. J. Price (2011). "The transcription factor Foxg1 regulates telencephalic progenitor proliferation cell autonomously, in part by controlling Pax6 expression levels." Neural Dev **6**: 9.

Mao, B., W. Wu, Y. Li, D. Hoppe, P. Stannek, A. Glinka and C. Niehrs (2001). "LDL-receptor-related protein 6 is a receptor for Dickkopf proteins." Nature **411**(6835): 321-325.

Marchetto, M. C., A. R. Muotri, Y. Mu, A. M. Smith, G. G. Cezar and F. H. Gage (2008). "Non-cell-autonomous effect of human SOD1 G37R astrocytes on motor neurons derived from human embryonic stem cells." Cell Stem Cell **3**(6): 649-657.

Marin-Padilla, M. (1998). "Cajal-Retzius cells and the development of the neocortex." Trends Neurosci **21**(2): 64-71.

Maroof, A. M., S. Keros, J. A. Tyson, S. W. Ying, Y. M. Ganat, F. T. Merkle, B. Liu, A. Goulburn, E. G. Stanley, A. G. Elefanty, H. R. Widmer, K. Eggan, P. A. Goldstein, S. A.

Anderson and L. Studer (2013). "Directed differentiation and functional maturation of cortical interneurons from human embryonic stem cells." Cell Stem Cell **12**(5): 559-572.

Martin, G. R. (1981). "Isolation of a pluripotent cell line from early mouse embryos cultured in medium conditioned by teratocarcinoma stem cells." Proc Natl Acad Sci U S A **78**(12): 7634-7638.

Martynoga, B., J. L. Mateo, B. Zhou, J. Andersen, A. Achimastou, N. Urban, D. van den Berg, D. Georgopoulou, S. Hadjur, J. Wittbrodt, L. Ettwiller, M. Piper, R. M. Gronostajski and F. Guillemot (2013). "Epigenomic enhancer annotation reveals a key role for NFIX in neural stem cell quiescence." Genes Dev **27**(16): 1769-1786.

Martynoga, B., H. Morrison, D. J. Price and J. O. Mason (2005). "Foxg1 is required for specification of ventral telencephalon and region-specific regulation of dorsal telencephalic precursor proliferation and apoptosis." Dev Biol **283**(1): 113-127.

Melander, A. and J. Olsson (1999). "35th Annual Meeting of the European Association for the Study of Diabetes : Brussels, Belgium, 28 September-2 October 1999." Diabetologia **42**(Suppl 1): A1-A330.

Melief, S. M., Zwaginga, J.J., Fibbe, W.E. and Roelofs, H. (2013) Adipose-Derived Multipotent Stromal Cells Have a Higher Immunomodulatory Capacity Than Their Bone Marrow Counterparts. Stem Cells Translational Medicine, 2, 455-463. http://dx.doi.org/10.596.

Mendes-da-Silva, C., S. F. Lemes, S. Baliani Tda, M. D. Versutti and M. A. Torsoni (2015). "Increased expression of Hes5 protein in Notch signaling pathway in the hippocampus of mice offspring of dams fed a high-fat diet during pregnancy and suckling." Int J Dev Neurosci **40**: 35-42.

Mira, H., Z. Andreu, H. Suh, D. C. Lie, S. Jessberger, A. Consiglio, J. San Emeterio, R. Hortiguela, M. A. Marques-Torrejon, K. Nakashima, D. Colak, M. Gotz, I. Farinas and F. H. Gage (2010). "Signaling through BMPR-IA regulates quiescence and long-term activity of neural stem cells in the adult hippocampus." Cell Stem Cell **7**(1): 78-89.

Miyamoto, N., M. Yoshida, S. Kuratani, I. Matsuo and S. Aizawa (1997). "Defects of urogenital development in mice lacking Emx2." Development **124**(9): 1653-1664.

Miyata, T., T. Maeda and J. E. Lee (1999). "NeuroD is required for differentiation of the granule cells in the cerebellum and hippocampus." Genes Dev **13**(13): 1647-1652.

Monaghan, A. P., E. Grau, D. Bock and G. Schutz (1995). "The mouse homolog of the orphan nuclear receptor tailless is expressed in the developing forebrain." Development **121**(3): 839-853.

Mukhopadhyay, M., S. Shtrom, C. Rodriguez-Esteban, L. Chen, T. Tsukui, L. Gomer, D. W. Dorward, A. Glinka, A. Grinberg, S. P. Huang, C. Niehrs, J. C. Izpisua Belmonte and H. Westphal (2001). "Dickkopf1 is required for embryonic head induction and limb morphogenesis in the mouse." Dev Cell **1**(3): 423-434.

Murai, K., Q. Qu, G. Sun, P. Ye, W. Li, G. Asuelime, E. Sun, G. E. Tsai and Y. Shi (2014). "Nuclear receptor TLX stimulates hippocampal neurogenesis and enhances learning and memory in a transgenic mouse model." Proc Natl Acad Sci U S A **111**(25): 9115-9120.

Muzio, L., B. Di Benedetto, A. Stoykova, E. Boncinelli, P. Gruss and A. Mallamaci (2002). "Emx2 and Pax6 control regionalization of the pre-neuronogenic cortical primordium." Cereb Cortex **12**(2): 129-139.

Nicholas, C. R., J. Chen, Y. Tang, D. G. Southwell, N. Chalmers, D. Vogt, C. M. Arnold, Y. J. Chen, E. G. Stanley, A. G. Elefanty, Y. Sasai, A. Alvarez-Buylla, J. L. Rubenstein and A. R. Kriegstein (2013). "Functional maturation of hPSC-derived forebrain interneurons requires an extended timeline and mimics human neural development." Cell Stem Cell **12**(5): 573-586.

Niclis, J., A. O. Trounson, M. Dottori, A. Ellisdon, S. P. Bottomley, Y. Verlinsky and D. Cram (2009). "Human embryonic stem cell models of Huntington disease." Reprod Biomed Online **19**(1): 106-113.

Nieto, M., C. Schuurmans, O. Britz and F. Guillemot (2001). "Neural bHLH genes control the neuronal versus glial fate decision in cortical progenitors." Neuron **29**(2): 401-413.

Niu, W., Y. Zou, C. Shen and C. L. Zhang (2011). "Activation of postnatal neural stem cells requires nuclear receptor TLX." J Neurosci **31**(39): 13816-13828.

Ohshima, T., J. M. Ward, C. G. Huh, G. Longenecker, Veeranna, H. C. Pant, R. O. Brady, L. J. Martin and A. B. Kulkarni (1996). "Targeted disruption of the cyclin-dependent kinase 5 gene results in abnormal corticogenesis, neuronal pathology and perinatal death." Proc Natl Acad Sci U S A **93**(20): 11173-11178.

Ohtsuka, T., M. Sakamoto, F. Guillemot and R. Kageyama (2001). "Roles of the basic helix-loop-helix genes Hes1 and Hes5 in expansion of neural stem cells of the developing brain." J Biol Chem **276**(32): 30467-30474.

Okabe, S., K. Forsberg-Nilsson, A. C. Spiro, M. Segal and R. D. McKay (1996). "Development of neuronal precursor cells and functional postmitotic neurons from embryonic stem cells in vitro." Mech Dev **59**(1): 89-102.

Oliver, G., B. Sosa-Pineda, S. Geisendorf, E. P. Spana, C. Q. Doe and P. Gruss (1993). "Prox 1, a prospero-related homeobox gene expressed during mouse development." Mech Dev **44**(1): 3-16.

Panchision, D. M., J. M. Pickel, L. Studer, S. H. Lee, P. A. Turner, T. G. Hazel and R. D. McKay (2001). "Sequential actions of BMP receptors control neural precursor cell production and fate." Genes Dev **15**(16): 2094-2110.

Pauklin, S. and L. Vallier (2013). "The cell-cycle state of stem cells determines cell fate propensity." Cell **155**(1): 135-147.

Pearce, J. J., G. Penny and J. Rossant (1999). "A mouse cerberus/Dan-related gene family." Dev Biol **209**(1): 98-110.

Pellegrini, M., A. Mansouri, A. Simeone, E. Boncinelli and P. Gruss (1996). "Dentate gyrus formation requires Emx2." Development **122**(12): 3893-3898.

Perrier, A. L., V. Tabar, T. Barberi, M. E. Rubio, J. Bruses, N. Topf, N. L. Harrison and L. Studer (2004). "Derivation of midbrain dopamine neurons from human embryonic stem cells." Proc Natl Acad Sci U S A **101**(34): 12543-12548.

Pleasure, S. J., A. E. Collins and D. H. Lowenstein (2000). "Unique expression patterns of cell fate molecules delineate sequential stages of dentate gyrus development." J Neurosci **20**(16): 6095-6105.

Qin, S., W. Niu, N. Iqbal, D. K. Smith and C. L. Zhang (2014). "Orphan nuclear receptor TLX regulates astrogenesis by modulating BMP signaling." Front Neurosci **8**: 74.

Qu, Q., G. Sun, W. Li, S. Yang, P. Ye, C. Zhao, R. T. Yu, F. H. Gage, R. M. Evans and Y. Shi (2010). "Orphan nuclear receptor TLX activates Wnt/beta-catenin signalling to stimulate neural stem cell proliferation and self-renewal." Nat Cell Biol **12**(1): 31-40; sup pp 31-39.

Quinn, J. C., M. Molinek, B. S. Martynoga, P. A. Zaki, A. Faedo, A. Bulfone, R. F. Hevner, J. D. West and D. J. Price (2007). "Pax6 controls cerebral cortical cell number by regulating exit from the cell cycle and specifies cortical cell identity by a cell autonomous mechanism." Dev Biol **302**(1): 50-65.

Rakic, P. (1995). "A small step for the cell, a giant leap for mankind: a hypothesis of neocortical expansion during evolution." Trends Neurosci **18**(9): 383-388.

Renner, M., M. A. Lancaster, S. Bian, H. Choi, T. Ku, A. Peer, K. Chung and J. A. Knoblich (2017). "Self-organized developmental patterning and differentiation in cerebral organoids." EMBO J.

Reubinoff, B. E., M. F. Pera, C. Y. Fong, A. Trounson and A. Bongso (2000). "Embryonic stem cell lines from human blastocysts: somatic differentiation in vitro." Nat Biotechnol **18**(4): 399-404.

Rickmann, M., D. G. Amaral and W. M. Cowan (1987). "Organization of radial glial cells during the development of the rat dentate gyrus." J Comp Neurol **264**(4): 449-479.

Roy, N. S., C. Cleren, S. K. Singh, L. Yang, M. F. Beal and S. A. Goldman (2006). "Functional engraftment of human ES cell-derived dopaminergic neurons enriched by coculture with telomerase-immortalized midbrain astrocytes." Nat Med **12**(11): 1259-1268.

Rubenstein, J. L. and P. A. Beachy (1998). "Patterning of the embryonic forebrain." Curr Opin Neurobiol **8**(1): 18-26.

Rubin, A. N. and N. Kessaris (2013). "PROX1: a lineage tracer for cortical interneurons originating in the lateral/caudal ganglionic eminence and preoptic area." PLoS One **8**(10): e77339.

Sakaguchi, H., T. Kadoshima, M. Soen, N. Narii, Y. Ishida, M. Ohgushi, J. Takahashi, M. Eiraku and Y. Sasai (2015). "Generation of functional hippocampal neurons from self-organizing human embryonic stem cell-derived dorsomedial telencephalic tissue." Nat Commun **6**: 8896.

Saric, T., L. P. Frenzel and J. Hescheler (2008). "Immunological barriers to embryonic stem cell-derived therapies." Cells Tissues Organs **188**(1-2): 78-90.

Sasai, Y., R. Kageyama, Y. Tagawa, R. Shigemoto and S. Nakanishi (1992). "Two mammalian helix-loop-helix factors structurally related to Drosophila hairy and Enhancer of split." Genes Dev **6**(12B): 2620-2634.

Sato, N., L. Meijer, L. Skaltsounis, P. Greengard and A. H. Brivanlou (2004). "Maintenance of pluripotency in human and mouse embryonic stem cells through activation of Wnt signaling by a pharmacological GSK-3-specific inhibitor." Nat Med **10**(1): 55-63.

Schuurmans, C., O. Armant, M. Nieto, J. M. Stenman, O. Britz, N. Klenin, C. Brown, L. M. Langevin, J. Seibt, H. Tang, J. M. Cunningham, R. Dyck, C. Walsh, K. Campbell, F. Polleux and F. Guillemot (2004). "Sequential phases of cortical specification involve Neurogenin-dependent and -independent pathways." EMBO J **23**(14): 2892-2902.

Scott, I. C., B. M. Steiglitz, T. G. Clark, W. N. Pappano and D. S. Greenspan (2000). "Spatiotemporal expression patterns of mammalian chordin during postgastrulation embryogenesis and in postnatal brain." Dev Dyn **217**(4): 449-456.

Seib, D. R., N. S. Corsini, K. Ellwanger, C. Plaas, A. Mateos, C. Pitzer, C. Niehrs, T. Celikel and A. Martin-Villalba (2013). "Loss of Dickkopf-1 restores neurogenesis in old age and counteracts cognitive decline." Cell Stem Cell **12**(2): 204-214.

Semenov, M. V., K. Tamai, B. K. Brott, M. Kuhl, S. Sokol and X. He (2001). "Head inducer Dickkopf-1 is a ligand for Wnt coreceptor LRP6." Curr Biol **11**(12): 951-961.

Seo, S., J. W. Lim, D. Yellajoshyula, L. W. Chang and K. L. Kroll (2007). "Neurogenin and NeuroD direct transcriptional targets and their regulatory enhancers." EMBO J **26**(24): 5093-5108.

Sessa, A., C. A. Mao, A. K. Hadjantonakis, W. H. Klein and V. Broccoli (2008). "Tbr2 directs conversion of radial glia into basal precursors and guides neuronal amplification by indirect neurogenesis in the developing neocortex." Neuron **60**(1): 56-69.

Sha, J., Z. Zhou, J. Li, L. Yin, H. Yang, G. Hu, M. Luo, H. C. Chan, K. Zhou and g. Spermatogenesis study (2002). "Identification of testis development and spermatogenesis-related genes in human and mouse testes using cDNA arrays." Mol Hum Reprod **8**(6): 511-517.

Sherr, C. J. (1994). "G1 phase progression: cycling on cue." Cell **79**(4): 551-555.

Shi, Y., D. Chichung Lie, P. Taupin, K. Nakashima, J. Ray, R. T. Yu, F. H. Gage and R. M. Evans (2004). "Expression and function of orphan nuclear receptor TLX in adult neural stem cells." Nature **427**(6969): 78-83.

Shi, Y., P. Kirwan and F. J. Livesey (2012). "Directed differentiation of human pluripotent stem cells to cerebral cortex neurons and neural networks." Nat Protoc **7**(10): 1836-1846.

Shimamura, K. and J. L. Rubenstein (1997). "Inductive interactions direct early regionalization of the mouse forebrain." Development **124**(14): 2709-2718.

Shimogori, T., V. Banuchi, H. Y. Ng, J. B. Strauss and E. A. Grove (2004). "Embryonic signaling centers expressing BMP, WNT and FGF proteins interact to pattern the cerebral cortex." Development **131**(22): 5639-5647.

Simeone, A., D. Acampora, M. Gulisano, A. Stornaiuolo and E. Boncinelli (1992). "Nested expression domains of four homeobox genes in developing rostral brain." Nature **358**(6388): 687-690.

Song, H., C. F. Stevens and F. H. Gage (2002). "Astroglia induce neurogenesis from adult neural stem cells." Nature **417**(6884): 39-44.

Strubing, C., G. Ahnert-Hilger, J. Shan, B. Wiedenmann, J. Hescheler and A. M. Wobus (1995). "Differentiation of pluripotent embryonic stem cells into the neuronal lineage in vitro gives rise to mature inhibitory and excitatory neurons." Mech Dev **53**(2): 275-287.

Sugiyama, T., N. Osumi and Y. Katsuyama (2013). "The germinal matrices in the developing dentate gyrus are composed of neuronal progenitors at distinct differentiation stages." Dev Dyn **242**(12): 1442-1453.

Sun, Y., J. Hu, L. Zhou, S. M. Pollard and A. Smith (2011). "Interplay between FGF2 and BMP controls the self-renewal, dormancy and differentiation of rat neural stem cells." J Cell Sci **124**(Pt 11): 1867-1877.

Theil, T., G. Alvarez-Bolado, A. Walter and U. Ruther (1999). "Gli3 is required for Emx gene expression during dorsal telencephalon development." Development **126**(16): 3561-3571.

Thomson, J. A., J. Itskovitz-Eldor, S. S. Shapiro, M. A. Waknitz, J. J. Swiergiel, V. S. Marshall and J. M. Jones (1998). "Embryonic stem cell lines derived from human blastocysts." Science **282**(5391): 1145-1147.

Tian, M. and R. L. Macdonald (2012). "The intronic GABRG2 mutation, IVS6+2T->G, associated with childhood absence epilepsy altered subunit mRNA intron splicing, activated nonsense-mediated decay, and produced a stable truncated gamma2 subunit." J Neurosci **32**(17): 5937-5952.

Tian, M., C. S. Xu, R. Montpetit and R. H. Kramer (2012). "Rab3A mediates vesicle delivery at photoreceptor ribbon synapses." J Neurosci **32**(20): 6931-6936.

Tole, S., C. Christian and E. A. Grove (1997). "Early specification and autonomous development of cortical fields in the mouse hippocampus." Development **124**(24): 4959-4970.

Tole, S., G. Goudreau, S. Assimacopoulos and E. A. Grove (2000). "Emx2 is required for growth of the hippocampus but not for hippocampal field specification." J Neurosci **20**(7): 2618-2625.

Urban, N. and F. Guillemot (2014). "Neurogenesis in the embryonic and adult brain: same regulators, different roles." Front Cell Neurosci **8**: 396.

Vallier, L. and R. A. Pedersen (2005). "Human embryonic stem cells: an in vitro model to study mechanisms controlling pluripotency in early mammalian development." Stem Cell Rev **1**(2): 119-130.

Vanderhaeghen, P. (2012). "Generation of cortical neurons from pluripotent stem cells." Prog Brain Res **201**: 183-195.

Wapinski, O. L., T. Vierbuchen, K. Qu, Q. Y. Lee, S. Chanda, D. R. Fuentes, P. G. Giresi, Y. H. Ng, S. Marro, N. F. Neff, D. Drechsel, B. Martynoga, D. S. Castro, A. E. Webb, T. C. Sudhof, A. Brunet, F. Guillemot, H. Y. Chang and M. Wernig (2013). "Hierarchical mechanisms for direct reprogramming of fibroblasts to neurons." Cell **155**(3): 621-635.

Watanabe, K., D. Kamiya, A. Nishiyama, T. Katayama, S. Nozaki, H. Kawasaki, Y. Watanabe, K. Mizuseki and Y. Sasai (2005). "Directed differentiation of telencephalic precursors from embryonic stem cells." Nat Neurosci **8**(3): 288-296.

Wilkinson, G., D. Dennis and C. Schuurmans (2013). "Proneural genes in neocortical development." Neuroscience **253**: 256-273.

Wilson, S. W. and C. Houart (2004). "Early steps in the development of the forebrain." Dev Cell **6**(2): 167-181.

Wilson, S. W. and J. L. Rubenstein (2000). "Induction and dorsoventral patterning of the telencephalon." Neuron **28**(3): 641-651.

Xuan, S., C. A. Baptista, G. Balas, W. Tao, V. C. Soares and E. Lai (1995). "Winged helix transcription factor BF-1 is essential for the development of the cerebral hemispheres." Neuron **14**(6): 1141-1152.

Yang, N., Y. H. Ng, Z. P. Pang, T. C. Sudhof and M. Wernig (2011). "Induced neuronal cells: how to make and define a neuron." Cell Stem Cell **9**(6): 517-525.

Yoshida, M., S. Assimacopoulos, K. R. Jones and E. A. Grove (2006). "Massive loss of Cajal-Retzius cells does not disrupt neocortical layer order." Development **133**(3): 537-545.

Yoshida, M., Y. Suda, I. Matsuo, N. Miyamoto, N. Takeda, S. Kuratani and S. Aizawa (1997). "Emx1 and Emx2 functions in development of dorsal telencephalon." Development **124**(1): 101-111.

Yu, D. X., F. P. Di Giorgio, J. Yao, M. C. Marchetto, K. Brennand, R. Wright, A. Mei, L. McHenry, D. Lisuk, J. M. Grasmick, P. Silberman, G. Silberman, R. Jappelli and F. H. Gage (2014). "Modeling hippocampal neurogenesis using human pluripotent stem cells." Stem Cell Reports **2**(3): 295-310.

Zakin, L., B. Reversade, B. Virlon, C. Rusniok, P. Glaser, J. M. Elalouf and P. Brulet (2000). "Gene expression profiles in normal and Otx2-/- early gastrulating mouse embryos." Proc Natl Acad Sci U S A **97**(26): 14388-14393.
Zhang, C. L., Y. Zou, W. He, F. H. Gage and R. M. Evans (2008). "A role for adult TLX-positive neural stem cells in learning and behaviour." Nature **451**(7181): 1004-1007.

Zhang, J., A. Moseley, A. G. Jegga, A. Gupta, D. P. Witte, M. Sartor, M. Medvedovic, S. S. Williams, C. Ley-Ebert, L. M. Coolen, G. Egnaczyk, M. B. Genter, M. Lehman, J. Lingrel, J. Maggio, L. Parysek, R. Walsh, M. Xu and B. J. Aronow (2004). "Neural system-enriched gene expression: relationship to biological pathways and neurological diseases." Physiol Genomics **18**(2): 167-183.

Zhao, Y., H. Z. Sheng, R. Amini, A. Grinberg, E. Lee, S. Huang, M. Taira and H. Westphal (1999). "Control of hippocampal morphogenesis and neuronal differentiation by the LIM homeobox gene Lhx5." Science **284**(5417): 1155-1158.

Zhou, C. J., C. Zhao and S. J. Pleasure (2004). "Wnt signaling mutants have decreased dentate granule cell production and radial glial scaffolding abnormalities." J Neurosci **24**(1): 121-126.

Zhou, C. J., C. J. Zhao and S. J. Pleasure (2004). "Wnt signaling mutants have decreased dentate granule cell production and radial glial scaffolding abnormalities." Journal of Neuroscience **24**(1): 121-126.

7. Own Publications

1: Conrad S, Azizi H, Hatami M, Kubista M, Bonin M, Hennenlotter J, Renninger M, Skutella T. Differential gene expression profiling of enriched human spermatogonia after short- and long-term culture. Biomed Res Int. 2014; 2014:138350. doi: 10.1155/2014/138350. PubMed PMID: 24738045; PubMed Central PMCID: PMC3971551.

2: Conrad S, Azizi H, Hatami M, Kubista M, Bonin M, Hennenlotter J, Sievert KD, Skutella T. Expression of Genes Related to Germ Cell Lineage and Pluripotency in Single Cells and Colonies of Human Adult Germ Stem Cells. Stem Cells Int. 2016; 2016:8582526. doi: 10.1155/2016/8582526. PubMed PMID: 26649052; PubMed Central PMCID: PMC4655073.

3: Fathi A, **Hatami** M, Hajihosseini V, Fattahi F, Kiani S, Baharvand H, Salekdeh GH. Comprehensive gene expression analysis of human embryonic stem cells during differentiation into neural cells. PLoS One. 2011;6(7): e22856. doi: 10.1371/journal.pone.0022856. Erratum in: PLoS One. 2011;6(8). doi: 10.1371/annotation/ba9082c9-69ee-43ac-81f0-5d71c3a01028. PubMed PMID: 21829537; PubMed Central PMCID: PMC3145766.

4: Fathi A, **Hatami** M, Vakilian H, Han CL, Chen YJ, Baharvand H, Salekdeh GH. Quantitative proteomics analysis highlights the role of redox hemostasis and energy metabolism in human embryonic stem cell differentiation to neural cells. J Proteomics. 2014 Apr 14; 101:1-16. doi: 10.1016/j.jprot.2014.02.002. PubMed PMID: 24530625.

5: Shahhoseini M, Taghizadeh Z, Hatami M, Baharvand H. Retinoic acid dependent histone 3 demethylation of the clustered HOX genes during neural differentiation of human embryonic stem cells. Biochem Cell Biol. 2013 Apr;91(2):116-22. doi: 10.1139/bcb-2012-0049. PubMed PMID: 23527641.

6: Zare-Mehrjardi N, Khorasani MT, Hemmesi K, Mirzadeh H, Azizi H, Sadatnia B, **Hatami** M, Kiani S, Barzin J, Baharvand H. Differentiation of embryonic stem cells into neural cells on 3D poly (D, L-lactic acid) scaffolds versus 2D cultures. Int J Artif Organs. 2011 Oct;34(Melief):1012-23. doi: 10.5301/ijao.5000002. PubMed PMID: 22161284.

7: Nemati S, **Hatami** M, Kiani S, Hemmesi K, Gourabi H, Masoudi N, Alaei S, Baharvand H. Long-term self-renewable feeder-free human induced pluripotent stem cell-derived neural progenitors. Stem Cells Dev. 2011 Mar;20(3):503-14. doi: 10.1089/scd.2010.0143. PubMed PMID: 20632795.

8: Baharvand H, Mehrjardi NZ, Hatami M, Kiani S, Rao M, Haghighi MM. Neural differentiation from human embryonic stem cells in a defined adherent culture condition. Int J Dev Biol. 2007;51(5):371-8. PubMed PMID: 17616926.

9: Hatami M, Mehrjardi NZ, Kiani S, Hemmesi K, Azizi H, Shahverdi A, Baharvand H. Human embryonic stem cell-derived neural precursor transplants in collagen scaffolds promote recovery in injured rat spinal cord. Cytotherapy. 2009;11(5):618-30. doi: 10.1080/14653240903005802. PubMed PMID: 19548142.

10: Rohani L, Karbalaie K, Vahdati A, Hatami M, Nasr-Esfahani MH, Baharvand H. Embryonic stem cell sphere: a controlled method for production of mouse embryonic stem cell aggregates for differentiation. Int J Artif Organs. 2008 Mar;31(3):258-65. PubMed PMID: 18373320.

11: Najafi F, Zare Mehrjardi N, Hatami M,Baharvand H*.Differentiation of Mouse Embryonic Stem Cells into Dorsal Interneurons of the spinal cord using BMP4 and Activin A.Yakhteh Medical J, (English), 2009, 11 (3), 277-284

12: Moghadasali R, Zeynali B, Soleimani M, Hatami M,Baharvand H*.The effect of astrocyte-conditioned medium, retinoic acid and basic fibroblast growth factor on neural differentiation of mouse embryonic stem cells.Yakhteh Medical Journal, Vol 9, No 3, Autumn 2007, Pages: 176-183

13: Baharvand H*, **Hatami** M, Massumi M.Induction of human embryonic stem cells into neuronal differentiation by increasing cyclic adenosine mono phosphate.Physiology and Pharmacology J. Vol. 10, No. 1, Spring 2006, 11-19.

14: Baharvand H, Taee A, Massumi M, Jafari H, Mollamohammadi S, Hatami M, Zarei Moradi Sh.Effect of mouse strain on establishment of embryonic stem cell lines. J. of Iranian Anatomical Sciences, Vol. 2, No. 3, Autumn 2004, 21-31. (Persian, with English abstract)

15: Baharvand, H., M. **Hatami**, and N. Zare. "THE EFFECT OF RETINOIC ACID HUMAN EMBRYONIC STEM CELLS WITH AND WITHOUT ROSETTE MORPHOLOGY." (2004): 103-109.

16: Narges ZareMe hrjerdi, Hossein Baharvand, Maryam Hatami, Sahar Kiani,Transplantation of human embryonic stem cell derivied neural –like tubes in spinal cord injury model. 4th annual meeting of the international society for stem cell research. June 29- July1, 2006, Toronto, ON, Canada. Poster presentation.

17: Maryam **Hatami**, Hossein Baharvand, Narges Zare Mehrjerdi, Sahar Kiani, haghighi mehdi, Differentiation of Motoneuron from Human Embryonic Stem Cells and their Transplantation into Rat model of Spinal Cord Injury. 4th annual meeting of the international society for stem cell research. June 29- July1, 2006, Toronto, ON, Canada. Poster presentation.

18: Maryam **Hatami**, Hossein Baharvand, Narges Zare Mehrjerdi, Sahar Kiani, haghighi mehdi, Transplantation of embryonic stem cells for promote recovery in injured rat Spinal Cord: precursor or stem cells. Baltic summer school. Kiel. 2006 Poster presentation.

19: Farzaneh Najafi, Hossein Baharvand, Maryam Hatami, Mohammad Massumi, Narges Zare. Specification of diverse cell types of dorsal half of the neural tube from mouse embryonic stem cells by BMP-4. 4th annual meeting of the international society for stem cell research. June 29- July1, 2006, Toronto, ON, Canada. Poster presentation.

20: Farzaneh Najafi , Hossein Baharvand , Maryam Hatami ,Ali Farrokhi , Mohammad Massumi , Narges Zare .Generation of dorsal cell types of the neural tube from mouse embryonic stem cells. 14th international conference society of differentiation. October 7-11, 2006, Innsbruck- Austria. Oral Presentation.

Presentation in international scientific meetings:
Poster Presentation

- 2017 Till & McCulloch Meetings (TMM2017); Mont-Tremblant, Québec, Canada: Dentate gyrus development and transcription factors combination.

- **2015 Till & McCulloch Meetings** (TMM2015) Till & McCulloch Toronto, Canada: Embryonic stem cell and dentate gyrus differention signalling pathways.

- 2013 International Society for Stem Cell Research (13th ISSCR) Annual Meeting, Boston, US: Using mouse embryonic stem cells to identify signalling molecules involved in development of granular Hippocampal neurons.

8. CURRICULUM VITAE

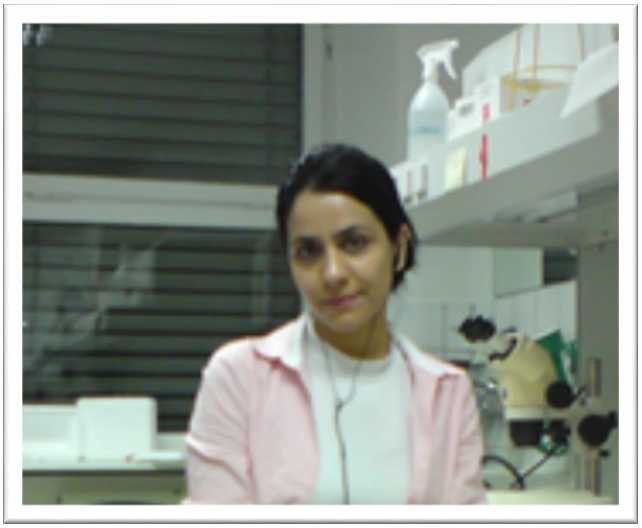

Maryam Hatami, PhD. Candidate
Stem Cell Biology

PERSONAL INFORMATION

Surname: Hatami
First Name: Maryam
Place of Birth: Tehran, Iran
Date of Birth: 19.09.1975
Gender: Female
Marital status: Single
Nationality: Iranian
Cell Phone: +49 170 29378369
Email: hatami@ana.uni-heidelberg.de
Address: Institute for Anatomy and Cell Biology III, Im Neuenheimer Feld 307, 69120 Heidelberg, Germany

LANGUAGE SKILLS

Persian: Native
German: Basic
English: Fluent (writing and speaking)

EDUCATION

Jan.2012 – Present	University of Heidelberg, Heidelberg, Germany Stem Cell Biology, **PhD. Candidate**
Oct.1999 – Dec.2003	Science and Research, Islamic Azad University Tehran, Iran Biology (Cellular and molecular biology), Master of Science G.P.A (Grade point Average): 16.90 out of 20 (A)
Sep.1993 – Feb. 1996	Islamic AZAD University, Tonekabon, Iran Molecular Cell Biology (Microbiology) G.P.A: 17.18 out of 20 (A)

THESIS TITLE

PhD. Thesis

Combination of Prox1/NeuroD1 Transcription Factor Boosts Generation of Dentate Gyrus Granule Neurons from Pluripotent Stem Cells

M.Sc. Sex determination of preimplantation human embryo by Nested PCR

Grade of Thesis: 19.50 out of 20 (A+)

PROFESSIONAL EXPERIENCE

2004-2010	Department of Stem Cells of Royan Institute, Iran Research Assistant in.
July 2011 – Present	Heidelberg University, Institute for Anatomy and Cell Biology III PhD student
2016	Heidelberg University, Institute for Anatomy and Cell Biology III Lecturing in Cell Biology Seminar

Interests

Embryonic Stem Cells and IPS cells
Cellular and molecular aspects of differentiation of stem cells into neuron cells and signaling mechanism.
Organoid culture

Experiences

- General cell and tissue culture techniques (primary culture and established lines)
- Isolation and Culture of spermatogonial and oogonial stem cell culture
- Isolation and Culture of fat mesenchymal stem cells (rat & horse)
- Neural differentiation of mouse and human embryonic stem cells
- Scaffolding culture system for mouse embryonic stem cells
- Cell viability measurement (MTT and WST-1 assay)
- Mouse and Human embryonic stem cell culture
- Enzyme-linked immunosorbent assay (ELISA)
- Culture and maintenance of human IPS cells
- Three dimensional cultures of nerve cells
- mRNA reprogramming of somatic cells
- Schwann cell culture (rat and human)
- Hippocampus slice culture
- Immunocytochemistry
- RT-PCR and qPCR
- Viral Transduction
- Molecular Cloning
- Flow cytometry
- Electroporation
- Transfection

AWARDS

First winner of award 'The Second Biology and Biotechnology Congress for Students' Tonekabon, Azad University, April 2003.
Winner of travel award to attend the Till & McCulloch Meetings 2015

HONORS

Top student of B.Sc. course and Top student of M.Sc. course

9. ACKNOWLEDGEMENTS

First of all, I would like to express my sincere gratitude to my thesis advisor Prof. Dr. Thomas Skutella of the department for Anatomy and Cell Biology for his invaluable guidance, enormous support and great patience. The door to Prof. Skutella office was always open whenever I ran into a trouble spot or had a question about my research or writing. I am gratefully indebted to Dr. Xunlei Zhou and Sabine Conrad for their very valuable comments and help on this thesis.

I am grateful to Priv.-Doz. Dr. med. Klaus Zweckberger for accepting to take on the task of my second supervisor.

I am thankful to Prof. Dr. Paul Schnitzler for the acceptance to be the third referee and Chairman of the defense.

There are many other people I must especially thank for their wonderful friendship or assistance in the preparation and completion of this thesis: my beloved friends Leili, Pooyan, Narges, Adeleh, Laleh, Ursula, Roberta, Hossein A., Yuanfeng, Ilse, Sabrina, Younian and Zhoubin and also my colleagues Steffen, Gerald, Andrea, Johanna, Richard and Mahdi.

I should also mention my foretime professor and mentor Dr. Hossein Baharvand who introduced me to the fascinating field of stem cell and developmental biology.

Finally, I must express my very profound gratitude to my parents and siblings for providing me with unfailing support and continuous encouragement throughout my years of study and through the process of researching and writing this thesis. This accomplishment would not have been possible without them. Thank you.

Maryam Hatami
Heidelberg, 2017

Was immer Du tun

und erträumen kannst,

Du kannst damit beginnen.

Im Mut liegen Schöpferkraft,

Stärke und Zauber.

Johann Wolfgang von Goethe

This thesis is dedicated to my beloved parents.

10. Appendix

Emx2 expression

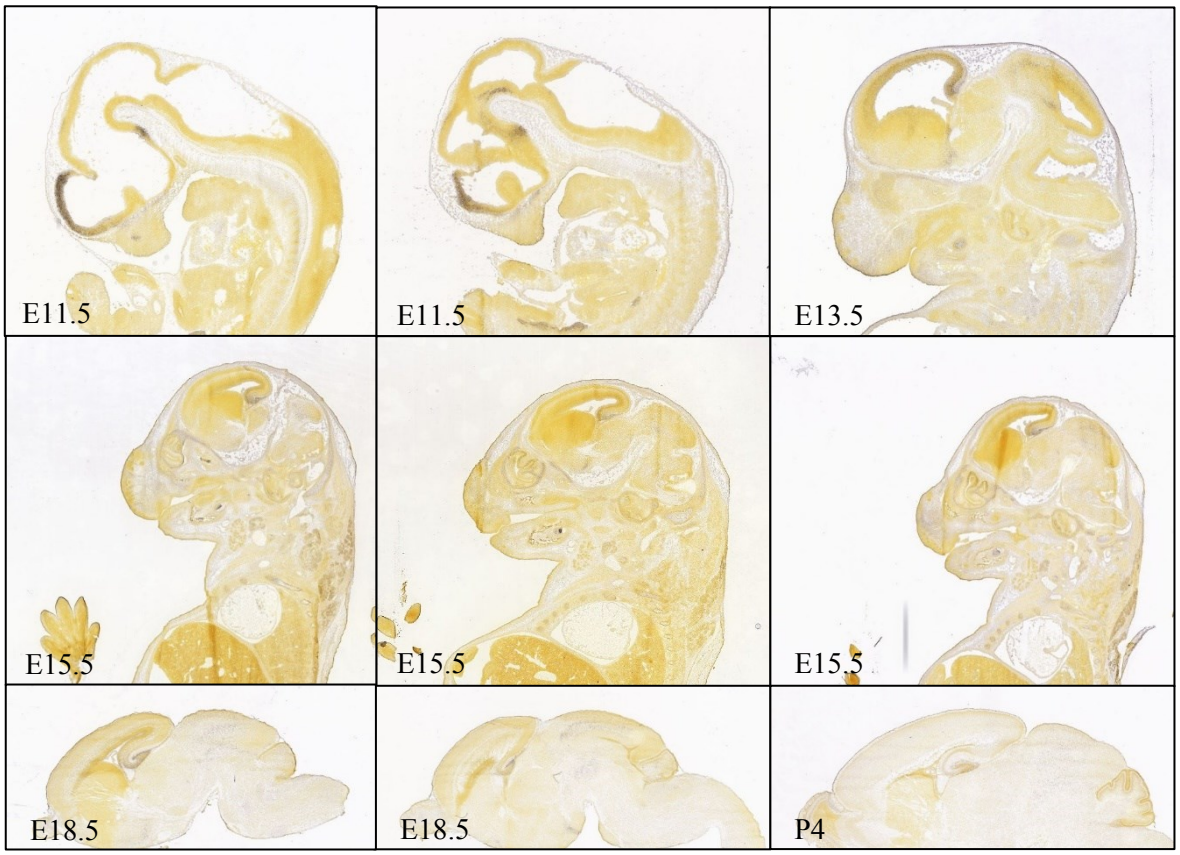

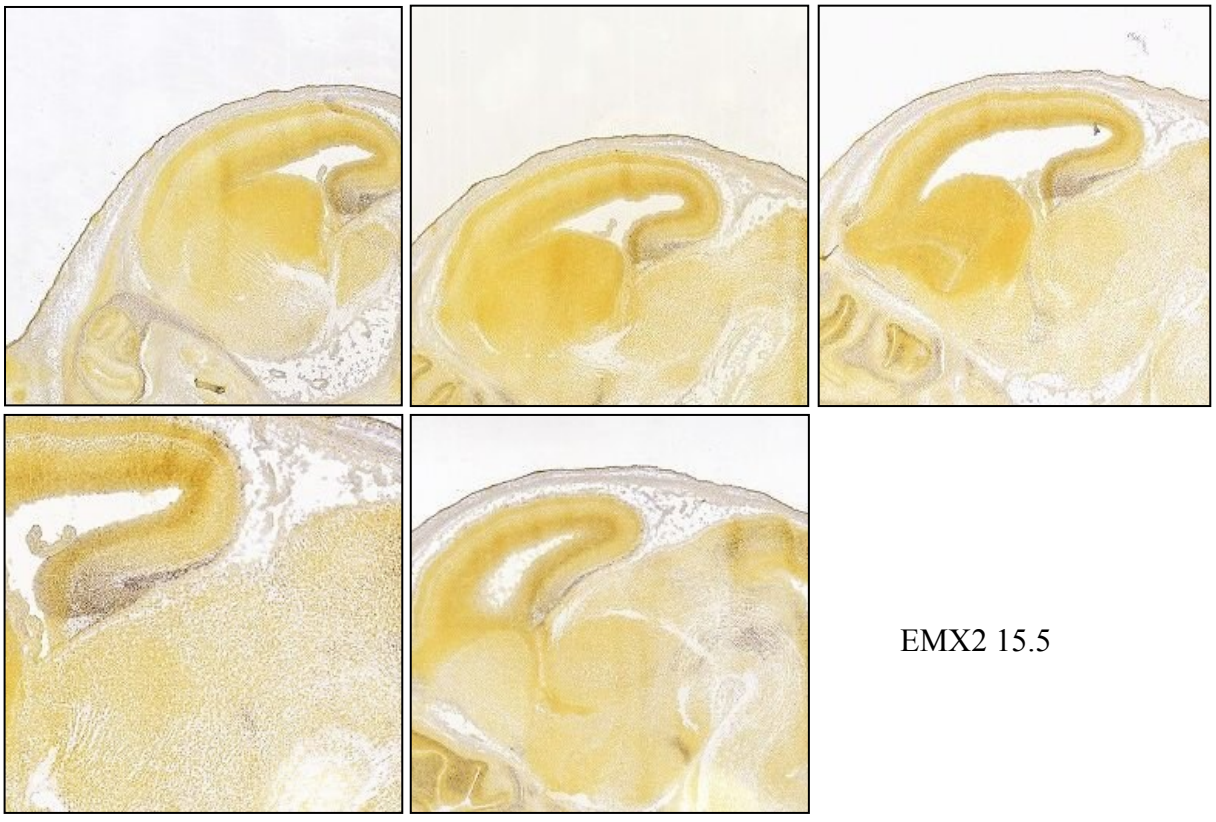

EMX2 15.5

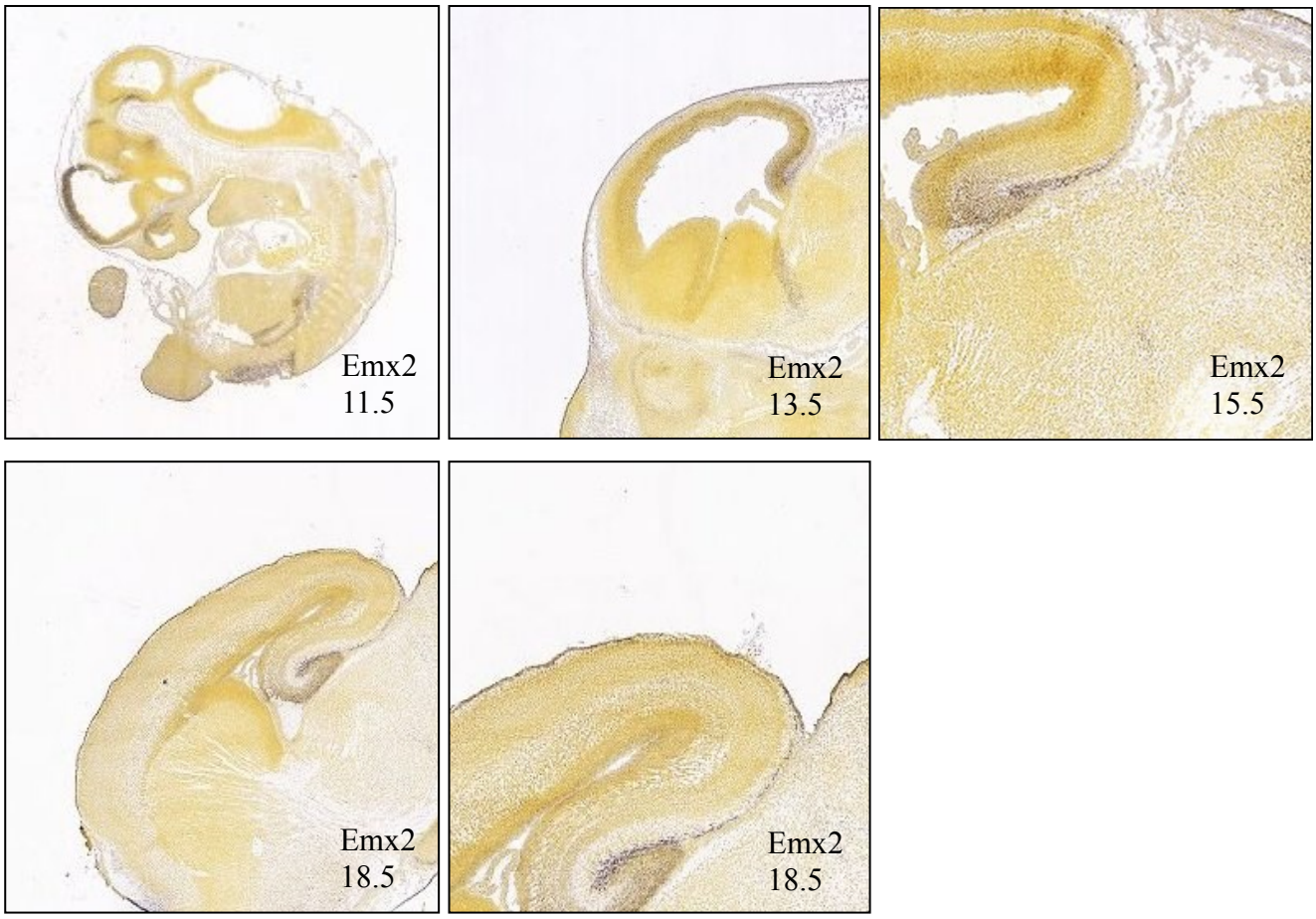

Figs. 10.1 EMX2 cortical area-specific gene expression with an increasing ventral-dorsal gradient along the ventricular zone. Both DG precursor cells and CR cells are labeled.

Prox1 expression

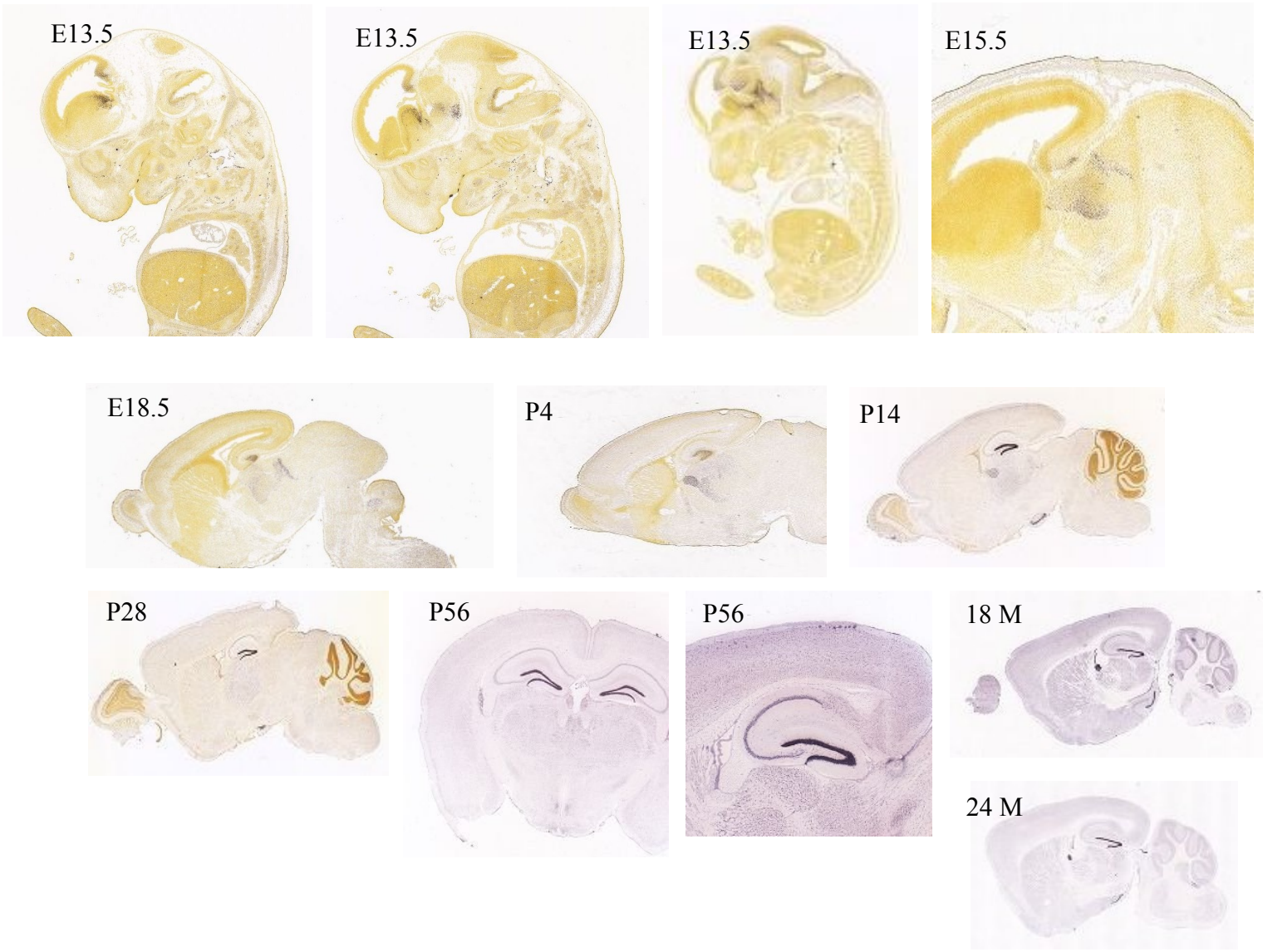

Figs 10.2 During mouse telencephalic development, Prox1 expression is restricted to the DG.

NeuroD1 expression

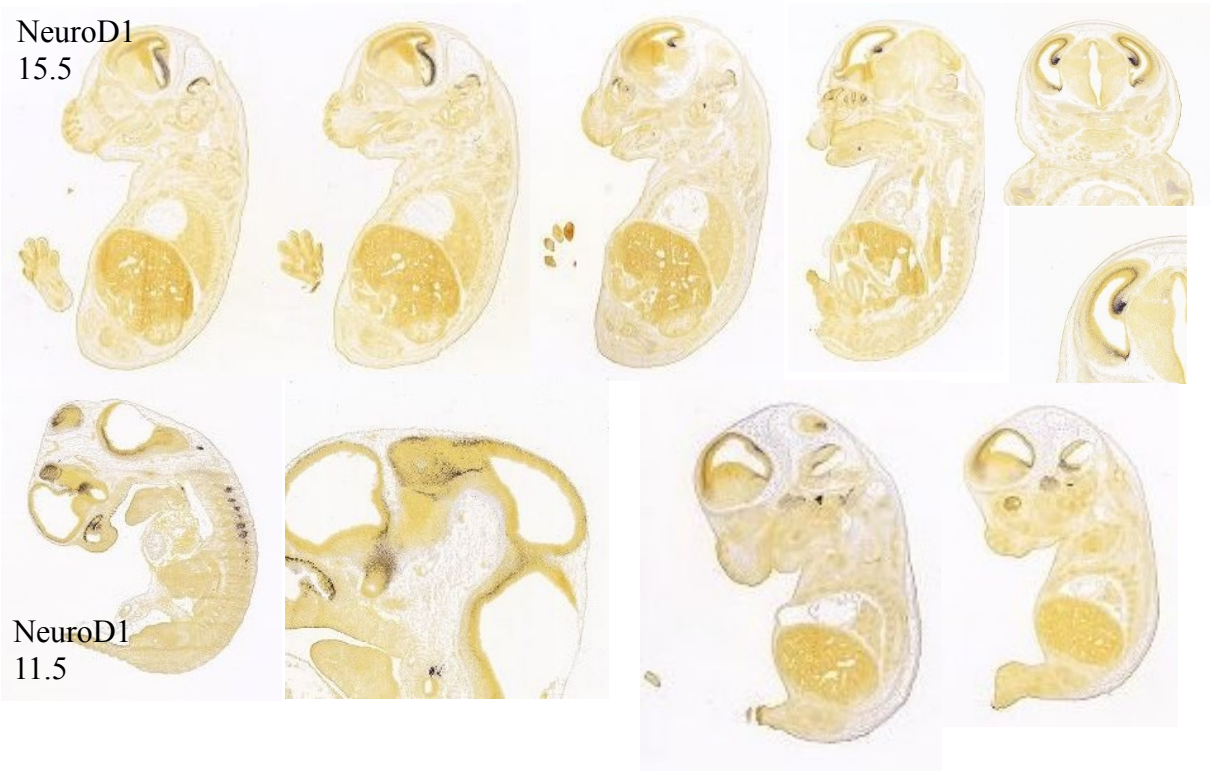

EMX2, Prox1 and NeuroD1 expression

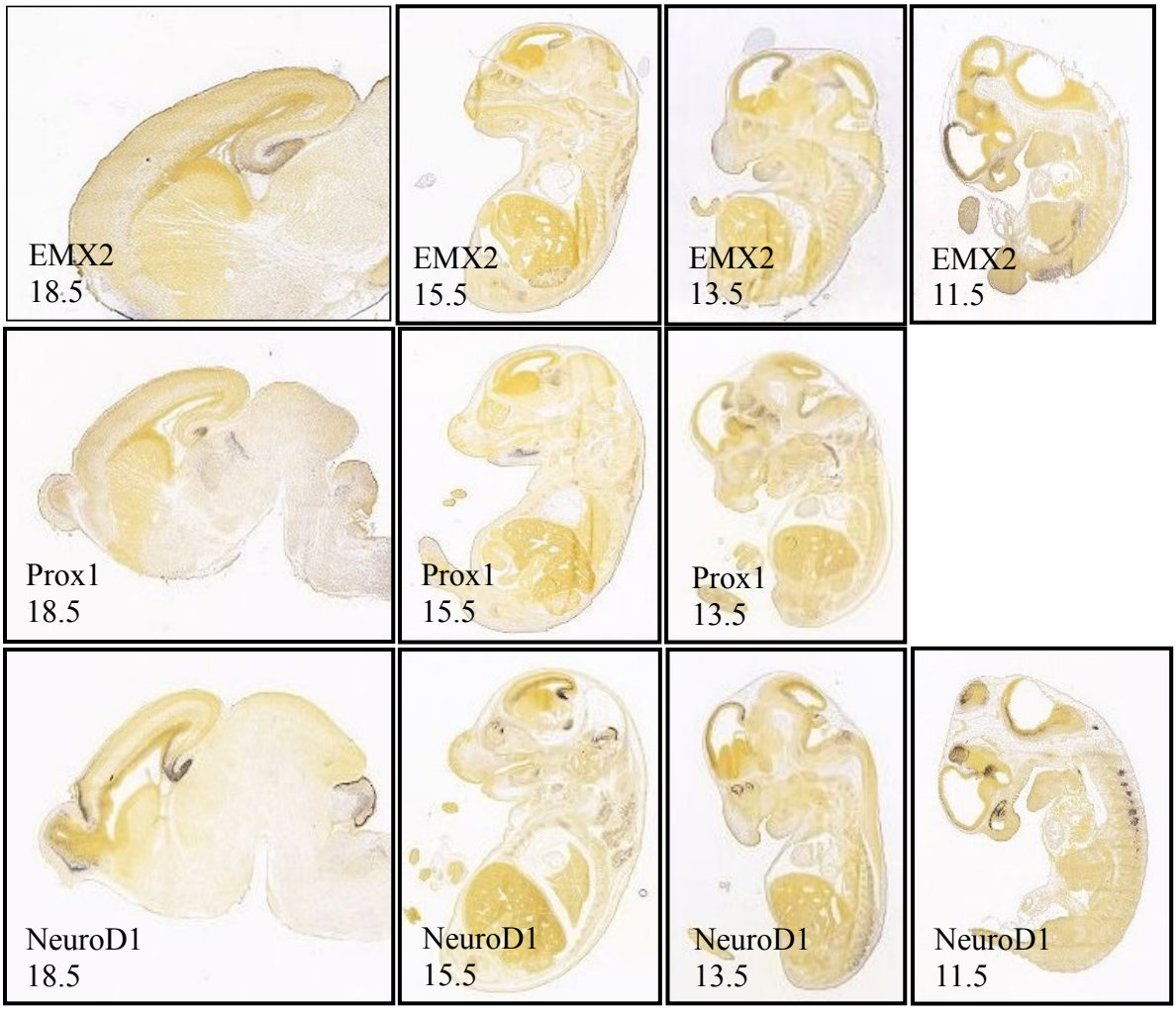

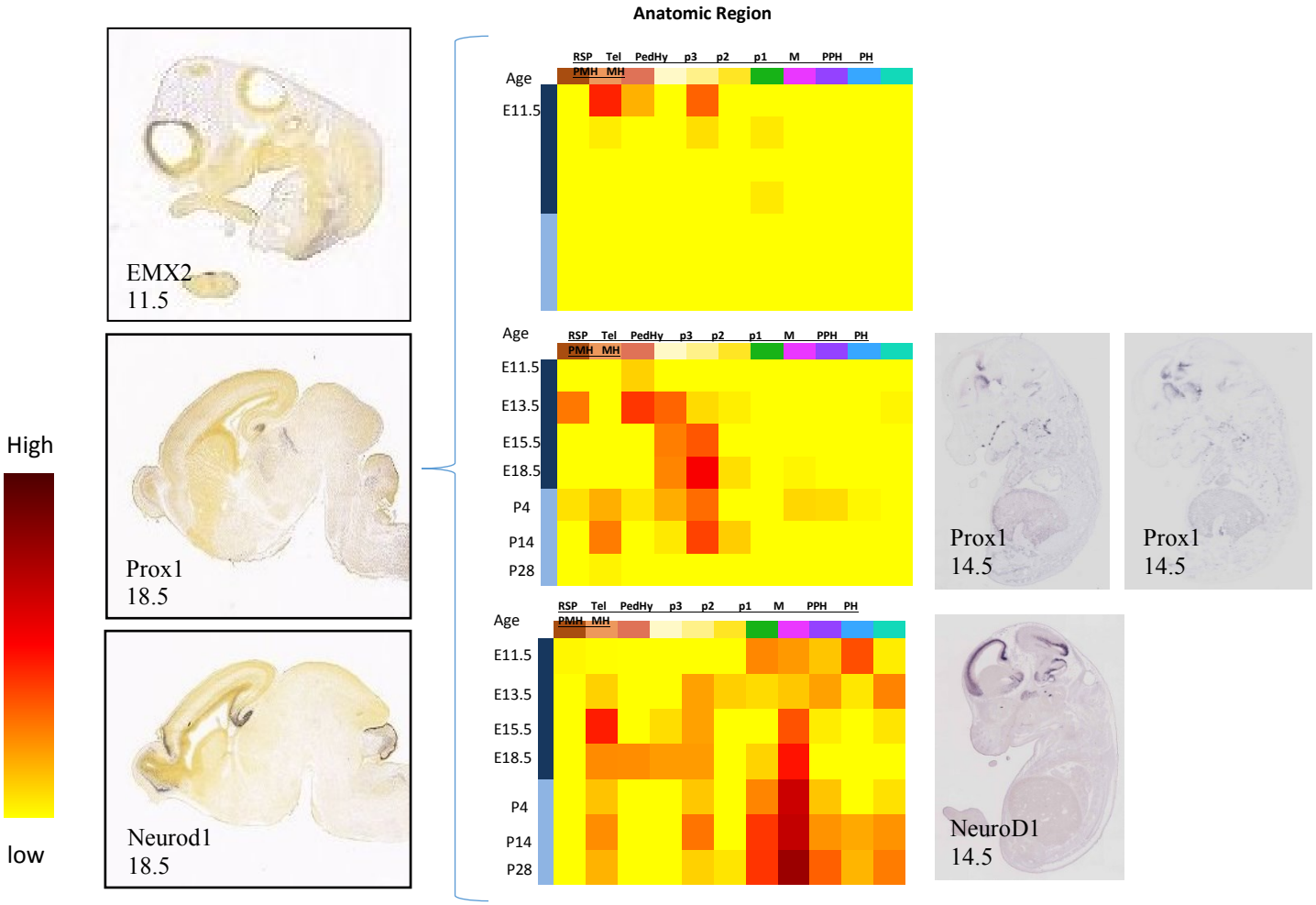

Growth factors

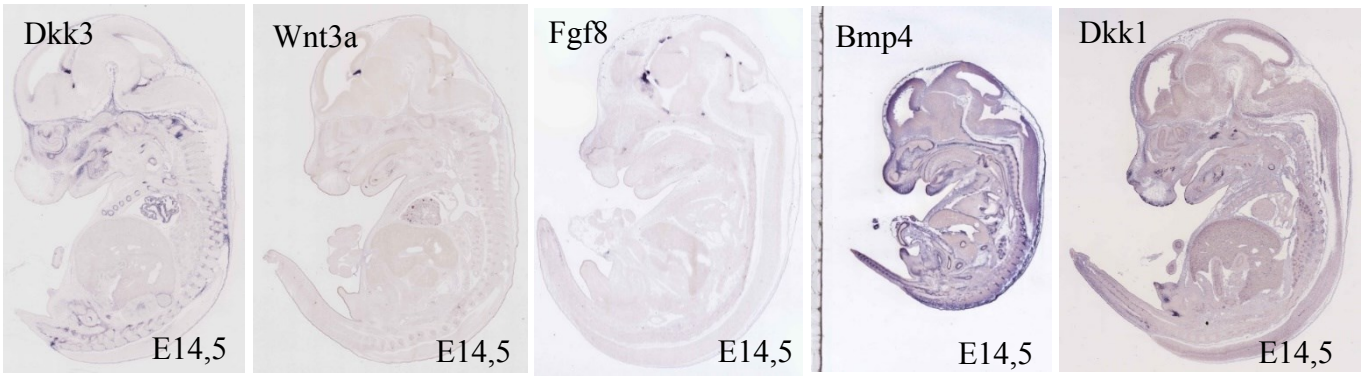

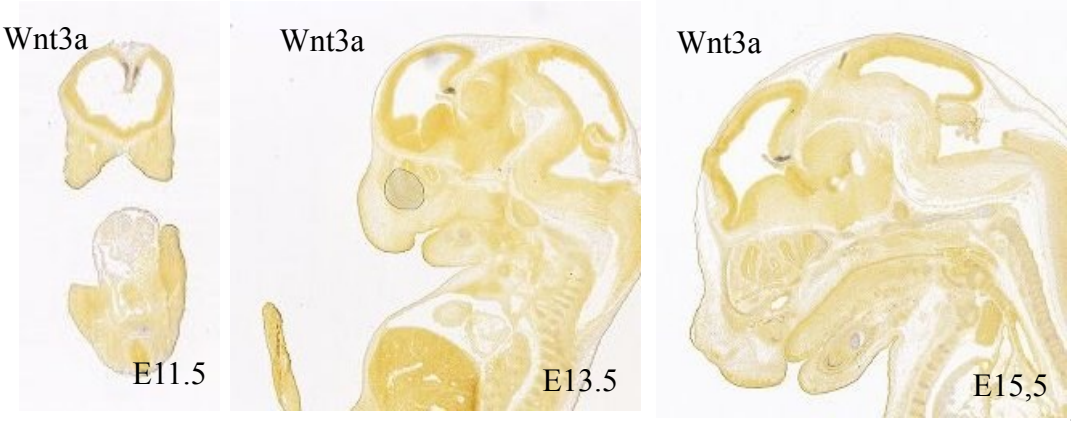

FACS sorting gates for EGFP^{+} cells in Tet-O-FUW-EGFP clone G1 analysis.

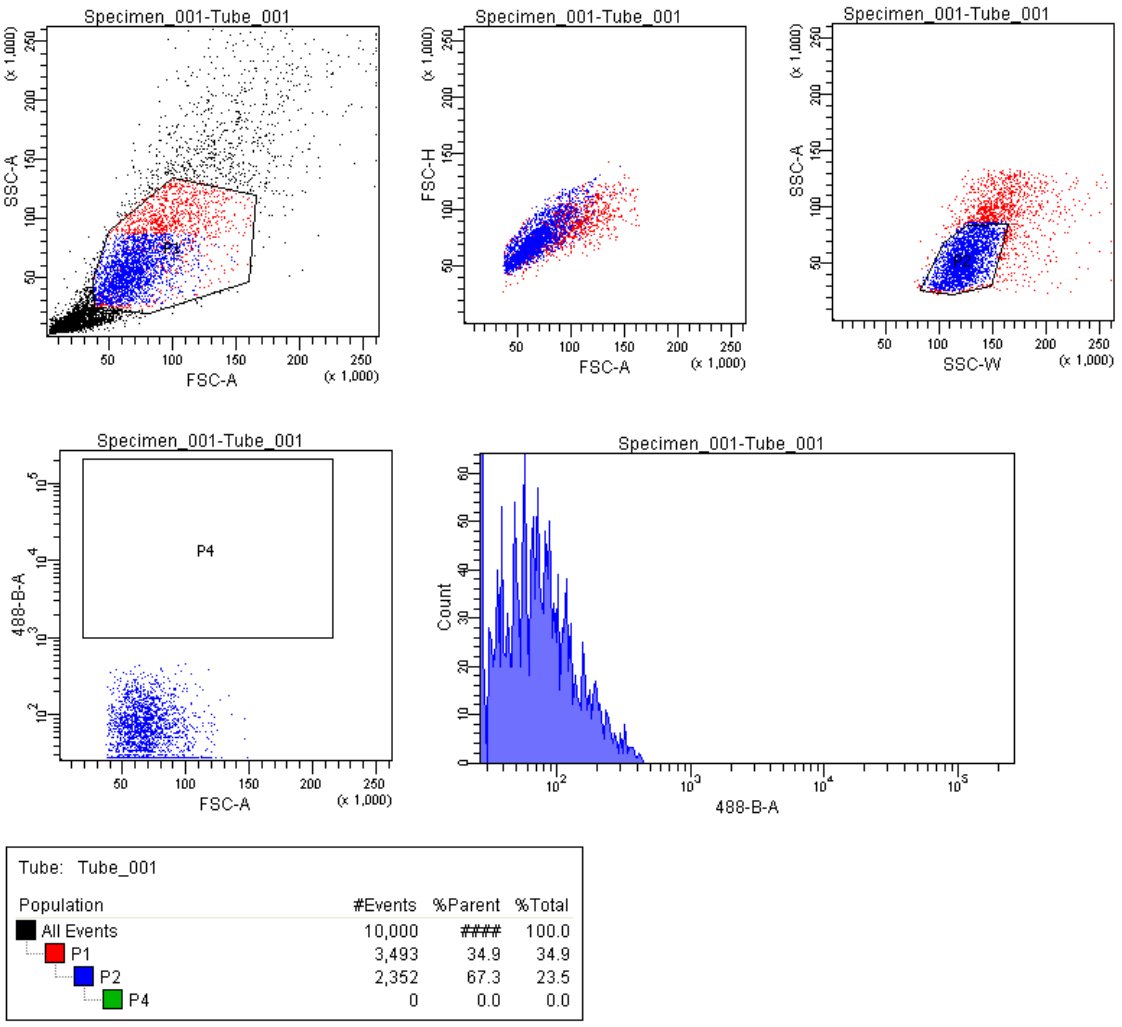

Fig. 10.7 mESc transduced with Lt-Tet-O-Fuw- EGFP and Fuw-M2rtTA were enzymatically dispersed and sorted by FACS to remove of cells with leaky EGFP expression.

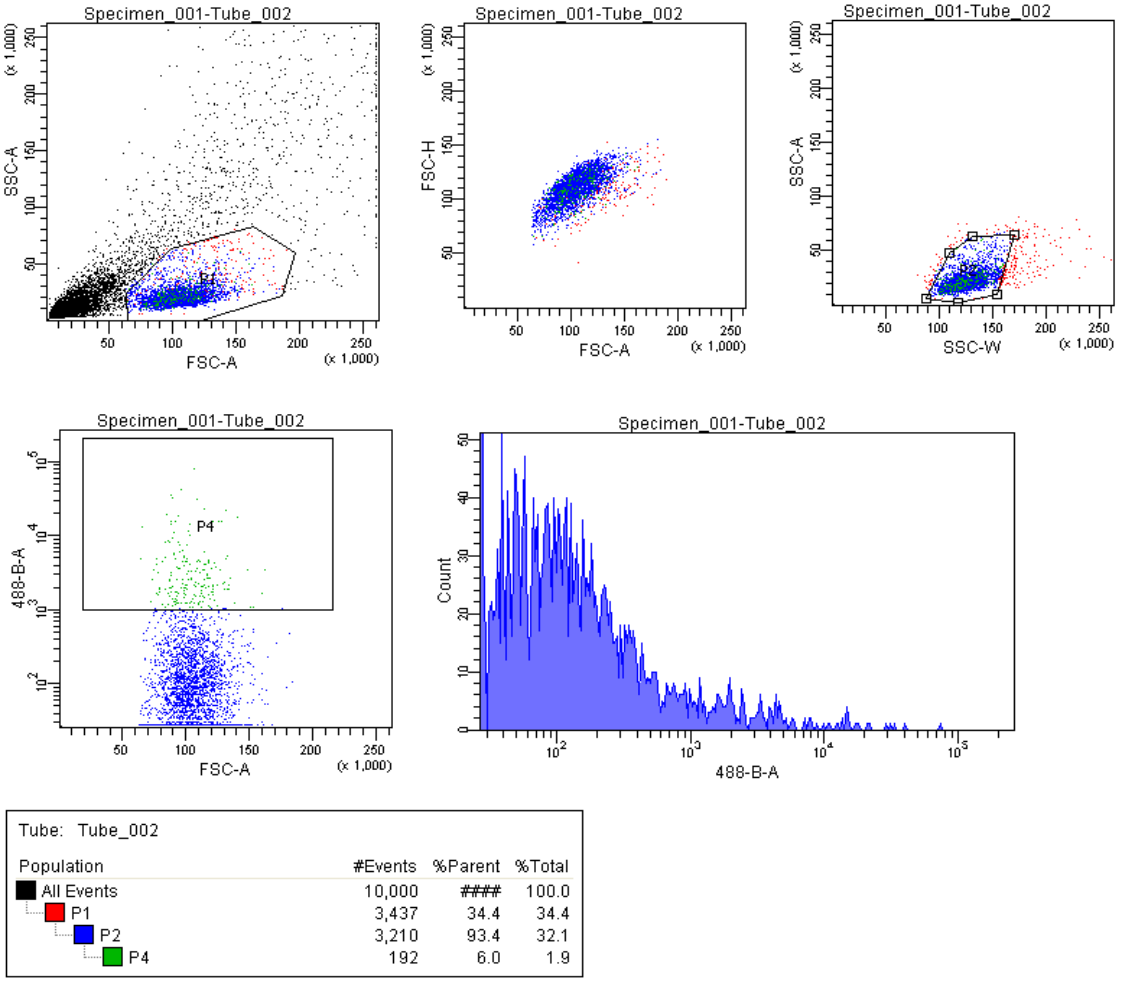

Fig. 10.8 mESc transduced with Lt-Tet-O-Fuw- EGFP and Fuw-M2rtTA were enzymatically dispersed and sorted by FACS to remove of cells with leaky EGFP expression.

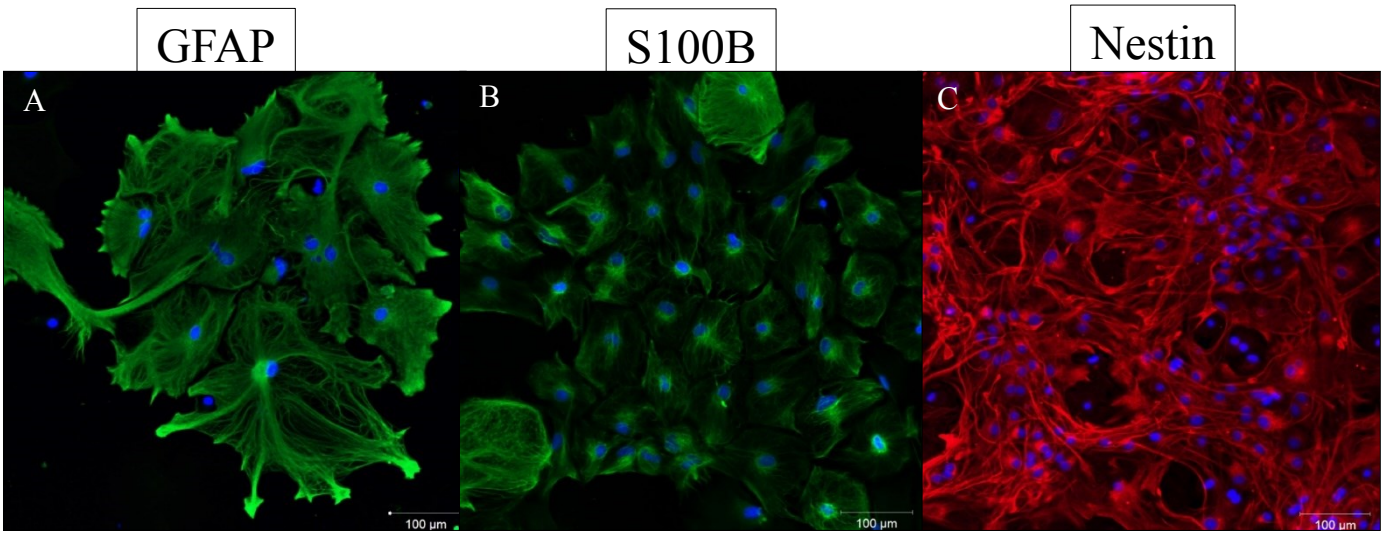

Fig 10.9 Pure primary astrocyte culture. Immunostaining of primary mouse astrocyte cultures with the markers GFAP, S100B (green) and Nestin (red) revealed pure primary astrocyte culture. Nuclei are stained with 4',6'-diamidino-2-phenylindole (DAPI) (blue). Scale bar: 100 µm.

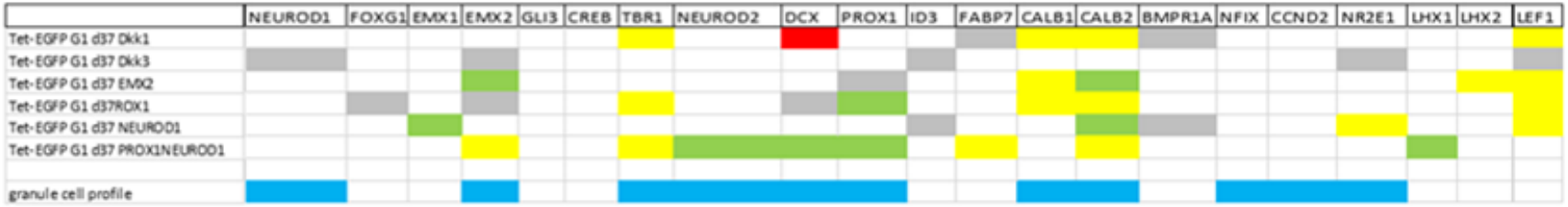

Fig 10.10 The Dentate granule cell is defined by the expression of genes and proteins marked in light blue. None of the single experimental groups can reach the complete expression profile of the granule cell differentiation at d37. The strongest regulated genes are HES5 and DCX, followed by NEUN, SYP, EMX1, EMX2 NEUROD2, PROX1, CALB2 and LHX1. With the exception of HES5, which is also strongly regulated by EMX2 and NEUROD, all other strongly regulated genes are induced in the control group and with addition of DKK1 or DKK3 respectively. DKK3 and PROX1 are strong negative regulators of HES5, and PROX1, and EMX2 and Prox1 overexpression of EMX1. The strongest granule cell differentiation is achieved with the combination of PROX1 and NEUROD.

Growth factor treatment group	Neuroentodermal Marker			Telencephalic Neural Progenitor Marker				Dentate Gyrus Marker							
D37	Sox1	Nestin	GFAP	Foxg1	Emx2	Blbp	Tbr2	NeuN	NeuroD1	DCX	Prox1	Calretinin	Calbidin	β-tubulinIII	Gulatamate
Tet-EGFP G1 d37, Control Group															
Tet-EGFP G1, Growth Factors treatment															
Tet-EGFP G1, Growth Factors treatment + Dkk1															
Tet-EGFP G1 Growth Factors treatment+ Dkk3															

Tanscription factor treatment group, D37	Neuroectodermal Marker		Telencphalic Neural progenitor Marker		Dentate Gyrus Marker								
	Nestin	GFAP	Foxg1	Emx2	NenN	NeuroD1	Prox1	Calretinin	Calbidin	β-tubulinIII	Gulatamate	Synaptophysin	Map(2a+2b)
Tet-EGFP G1,EMX2													
Tet-EGFP G1, PROX1													
Tet-EGFP G1, NEUROD1													
Tet-EGFP G1 PROX1NEUROD1													

Fig 10.11 Immunocytochemical analysis of growth factor and transcriptions factor treatment at day 37 with neuroectodermal, telencephalic progenitor and Dentate gyrus antibody staining.